From the

Institute for Cardiovascular Prevention (IPEK)

of the Ludwig-Maximilians-Universität München

Director: Univ.-Prof. Dr. med. Christian Weber

Ccl17-dependent release of Ccl3 restrains regulatory T cells thereby aggravating atherosclerosis

Dissertation

zum Erwerb des Doctor of Philosophy (Ph.D.)

an der Medizinischen Fakultät der

Ludwig-Maximilians-Universität München

Submitted by

M.Sc. Carlos Neideck

from

Taió in Santa Catarina, Brazil

on

21.03.2018

Supervisor: Prof. Dr. med. Christian Weber

Second evaluator: Prof. Dr. rer. nat. Jürgen Bernhagen

Dean: Prof. Dr. Reinhard Hickel

Date of oral defense: 23.07.2018

Affidavit

Neideck, Carlos

_____

Name, Surname

_____

Street

_____

Zip Code, Town

_____

Country

I hereby declare, that the submitted thesis entitled:

"Ccl17-dependent release of Ccl3 restrains regulatory T cells thereby aggravating atherosclerosis."

is my own work. I have only used the sources indicated and have not made unauthorized use of services of a third party. Where the work of others has been quoted or reproduced, the source is always given.

I further declare that the submitted thesis or parts thereof have not been presented as part of an examination degree to any other university.

Munich, 25.07.2018   Carlos Neideck

Place, date   Signature doctoral candidate

Confirmation of congruency between printed and electronic version of the doctoral thesis

Neideck, Carlos

_____

Name, Surname

_____

Street

_____

Zip Code, Town

_____

Country

I hereby declare that the electronic version of the submitted thesis, entitled:

"Ccl17-dependent release of Ccl3 restrains regulatory T cells thereby aggravating atherosclerosis."

is congruent with the printed version both in content and format.

Munich, 25.07.2018   Carlos Neideck

Place, date   Signature doctoral candidate

The results of this work will be, or are partly published in:

Neideck C, van der Vorst E, Mandl M, Jansen Y , Blanchet X, Faussner A, Megens RT, Drechsler M, Weber C, Döring Y. **"Ccl17-dependent release of Ccl3 restrains regulatory T cells thereby aggravating atherosclerosis."** (in preparation)

von Hundelshausen P, Agten S*, Eckardt V*, Schmitt M*, Blanchet X*, Ippel H*, **Neideck C***, Bidzhekov K*, Wichapong K*, Faussner A, Drechsler M, Grommes J, van Geffen J, Li H, Leberzammer J, Naumann R, Dijkgraaf I, Nicolaes G, Döring Y, Soehnlein O, Lutgens E, Heemskerk J, Koenen R, Mayo K, Hackeng T, Weber C. (2017) **"Chemokine interactome mapping enables tailored intervention in acute and chronic inflammation."** *Science Translational Medicine* 9(384):eaah6650.
* denotes equal contribution

Table of Content

Abbreviations

Ab	antibody
AD	atopic dermatitis
Ag	antigen
AGE	advanced glycation end products
AIDS	Acquired Immune Deficiency Syndrome
APCs	antigen presenting cells
Apoe	Apolipoprotein E
ATP	adenosine triphosphate
BATF	Basic leucine zipper transcriptional factor ATF-like
BCR	B cell receptor
BDCA	blood dendritic cell antigen
BM	bone marrow
BMDCs	bone-marrow derived DCs
BSA	bovine serum albumin
CAD	coronary artery disease
cAMP	cyclic adenosine monophosphate
CD	cluster of differentiation
cDC	conventional DC
cDNA	copy DNA
CDP	common DC precursor
CFA	complete Freuds Adjuvants
CFSE	carboxyfluorescein succinimidyl ester
CLP	common lymphoid progenitor cells
c-Maf	musculoaponeurotic fibrosarcoma oncogene homologue
cMOP	common monocyte progenitor
CMP	common myeloid progenitor cell
CpG	Cytidine – phosphate – Guanosine –rich DNA
CRE	cAMP-responsive element
CTLA-4	cytotoxic T-lymphocyte-associated Protein 4
CVD	Cardio vascular disease
Cy3	cyanine 3
DAG	diacylglycerol
DAPI	4',6-Diamidino-2-phenylindol
DC	dendritic cell
DMSO	dimethylsulfoxide
DN	double negative
DNA	desoxyribonucleic acid
DP	double positive
dsDNA	double stranded DNA
DTR	Diphtheria toxin receptor
e.g.	for example (from Latin: exempli gratia)

EAE	experimental autoimmune encephalopathy
EC	extracellular
EDTA	ethylenediaminetetraacetic acid
ELISA	enzyme-linked immunosorbent assay
ETP	early T cell progenitors
FACS	Fluorescent activated cell sorting
FCS	fetal calf serum
FITC	fluorescein isothiocyannate
FLT	fms like tyrosine kinase
FMO	fluorescence minus one
Foxp3	Forkhead-Box-Protein P3
FRC	fibroblastic reticular cells
GAGs	glycosaminoglycans
GAPDH	glyseraldehyde-3-phosphate dehydrogenase
GATA	GATA binding protein
GEF	guanine nucleotide exchange factor
GM-CSF	Granulocyte-macrophage colony-stimulating factor
GPCR	G-protein coupled receptor
h	hours
HBSS	Hanks' balanced salt solution
HEV	high endothelial venules
HFD	high fat diet
HLA-DR	Human Leukocyte Antigen – antigen D Related
HRP	horse radish peroxidase
HSC	hematopoietic stem cells
HSP	heat shock proteins
IC	intracellular
Id2	inhibitor of DNA binding 2
IEL	intraepithelial lymphocytes
IFN	Interferon
Ig	Immunoglobulin
IL	interleukin
IP_3	inositol 1,4,5-triphosphate
IRF	Interferon regulatory factor
iTregs	induced Tregs
JAK	Janus kinase
LAMP	lysosomal-associated membrane protein
LDL	low-density-lipoprotein
LFA-1	lymphocyte function-associated antigen-1
LN	lymph node
mAb	monoclonal Ab
MCP	mast cell progenitor
M-CSF	macrophage colony-stimulating-factor
MDP	macrophage and DC progenitor

MDS	Molecular dynamic simulation
MEP	megakaryocyte and erythroid progenitor
MFI	mean fluorescence intensity
MHC	major histocompatibility complex
min	minute
MIP1-α	Macrophage inflammatory protein 1 alpha
MMP	matrix metalloproteinase
MPO	Myeloperoxidase
mRNA	messenger ribonucleic acid
mTOR	mechanistic Target of Rapamycin
NC	normal chow diet
NFAT	nuclear factor of activated T-cells
NK	Natural killer
NMR	nuclear magnetic resonance
nTregs	natural Tregs
ON	overnight
OVA	ovalbumin
OVA	ovalbumin
oxLDL	oxidized LDL
pAb	polyclonal Ab
PAMPS	Pathogen associated molecular patterns
PBS	phosphate buffered saline
PCR	polymerase chain reaction
pDC	plasmacytoid DC
pDC	plasmacytoid DC
PDCA-1	plasmacytoid dendritic cell antigen-1
PDCA-1	pDC antigen-1
PFA	paraformaldehyde
PIP2	phosphatidylinositol-4,5-bisphosphate
PKA	protein kinase A
PKC	protein kinase C
PLC	phospholipase C
PMA	phorbol-12-myristate-13-acetate
PRR	Pattern recognition receptor
PSGL-1	P-selectin glycoprotein ligand 1
RANTES	Regulated upon Activation, Normal T cell Expressed, and Secreted
RbpJ	Recombining binding protein suppressor of hairless
RhoA	Ras homolog gene family A
RNA	ribonucleotide acid
ROCK	RhoA kinase
RorγT	RAR-related orphan receptor gamma
RT	room temperature
SD	standard deviation
SDS	sodium-dodecyl sulfate

SEM	standard error of mean
SMC	smooth muscle cell
SP	single positive
SRF	serum response factor
SSC	saline-sodium citrate
STAT	signal transducer and activator of transcription
STAT	signal transducer and activator of transcription
TARC	thymus and activation regulated chemokine
Tbet	T-box expressed in T cells
TCF-4	Transcription factor 4
TCM	central memory T cells
TCR	T cell receptor
TEM	effector memory T cells
TGF	Transforming growth factor
T_H	T helper type
TLO	tertiary lymphoid organ
TLR	Toll-like receptor
TNF	tumor necrosis factor
Treg	regulatory T cells
VCAM-1	vascular cell adhesion molecule 1
VLA-4	Very Late Antigen-4
VLDL	very low–density lipoprotein
VSMC	vascular smooth muscle cells
wt	wild-type
Zbtb	Zinc finger and BTB domain-containing protein

List of Figures

List of Tables

1. Introduction

Over the last 50 years, mortality rates caused by cardiovascular diseases (CVD) dropped by 60 % and thereby faster than any other cause. These outstanding ameliorations in CVD outcomes were mainly due to improvements in the prevention and treatment of CVD.[1] But still, in the year 2012, 17.5 million deaths were associated with CVD, making it the number one cause of death in the world, representing 31 % of all global deaths. Of these fatalities, approximately 7.4 million (42 % of all CVD related deaths) were due to coronary heart disease and 6.7 million (38 % of all CVD related deaths) were due to stroke.[1] CVD include a group of conditions which are mainly related to the heart and vasculature, such as stroke, abdominal aortic aneurysms or coronary artery diseases (CAD). The underlying cause of these disorders is predominantly atherosclerosis. There are a plethora of different risk factors involved in the onset of CVD which can include genetic predispositions and natural aging, but also smoking, obesity, hypertension, diabetes mellitus, and hyperlipidemia.[2] Until today, atherosclerosis has not been considered curable. This is due to a lack of appropriate early diagnosis or successful disease modifying treatments, which aim to either prevent atherosclerotic lesion progression or reduce already existing lesion size. Therefore, understanding key mechanisms in play and the investigation of the pathogenesis of atherosclerosis is crucial to develop and establish more effective therapeutic approaches and novel therapies. Hypertension and hyperlipidemia are well known risk factors for atherosclerosis, but today it is also appreciated that atherosclerosis is a chronic inflammatory disease of the arterial wall, driven and modulated by immune responses.[3] Whereas the role of monocytes/macrophages to the progression of atherosclerosis is well established, the role of other mononuclear cells, namely T cells and dendritic cells (DCs) still needs to be further elucidated.

The following introduction describes the role of the immune system during atherosclerosis. It points out the implications different immune cells - primarily DCs and T cells – have during the onset of this disease. Furthermore, it will give a brief overview of the immune system and additionally on the origin of leukocytes and elucidates their potential roles during atherogenesis.

1.1. The immune system

The main duty of the immune system is to preserve the integrity of an individual by providing protection against attacks from "outside" (e.g. bacteria, viruses, parasites) and from within such as degenerated cells or modified agents like lipids.[4] To fulfill this responsibility effectively the immune system must carry out four main tasks: *First*, the immunological recognition, where the presence of an infection must be detected. *Second*, it has to be contained and *third*, if possible eliminated. As important the elimination of an infection is, an overwhelming immunological response can lead to tissue damage and has to be avoided. Therefore, the immune response must be kept under control, and has to be regulated. The *fourth* task is generating an immunological memory which protects the individual against reappearing pathogens and allows an immediate and stronger response against any subsequent exposure to it.[5] An immune response can be mediated via two differently organized immunological effector systems. First the innate (unspecific) immunity and second the adaptive (specific) immunity.

1.1.1 The innate immune system

The innate immune response serves as the first defense against pathogens. It is formed by a variety of cells and molecules (Figure 1) which are able to mount an immediate innate immune response as soon as microorganisms breach physical and chemical defense barriers such as skin and mucosal epithelia (lining airways or gut). Important components of the innate immune system are phagocytic cells (macrophages and granulocytes), that continuously patrol the body searching for dangerous non-self-components (pathogen–associated molecular patterns (PAMPS) which they can detect with their germ line encoded pattern recognition receptors (PRR), such as Toll-like receptors (TLRs).[6] Stimulated cells then engulf the pathogen and degrade it intracellularly. Together with the complement system, these cells play a pivotal role in fighting extracellular pathogens. Other components of the innate immune system, like natural killer cells (NK-cells) and interferons (IFN), are key mediators in fighting intracellular pathogens like viruses.[7] Often, the innate immune response does not succeed in resolving the infection. Therefore, triggering of an acquired/adaptive immune response becomes necessary.

1.1.2. The adaptive immune system

Next to the innate immune system, the acquired or adaptive immune system is the second immunological effector system and further characterized through its antigen specificity. An adaptive immune response starts when antigen presenting cells (APC), carrying an antigen they picked up at sites of infection, travel to secondary lymphoid organs. DCs (see Chapter Dendritic cells) are highly specialized APCs and, like macrophages and granulocytes, DCs engulf pathogens and process them. However, the main role of DCs is not the clearance of an infection. Their principal duty lies in presenting antigens through the Major Histocompatibility Complex (MHC) to cells of the adaptive immunity, placing them at the border of innate and adaptive immunity. APCs can carry two types of MHC peptide-binding proteins: MHC class I and MHC class II. While intracellular antigens bind to MHC class I and are recognized by cluster of differentiation (CD) 8^+ T cells, extracellular antigens are presented by MHC class II to $CD4^+$ T cells. Besides DCs, other cells, namely activated macrophages and B cells can act as APCs and present antigens via MHC molecules. Nevertheless, among APCs DCs are the most specialized cells, expressing the highest amounts of MHC molecules. Another feature of APCs, next to the expression of MHC molecules, is the expression of costimulatory molecules (e. g. B7 molecules). These molecules provide the co-stimulatory signal, which is characterized by being antigen nonspecific. Co-stimulatory signals are provided for instance through interactions of CD28 (on T cells) and CD80/CD86 (B7 molecules on APCs).[5]

Through antigen presentation, DCs can activate specific antigen-recognition receptors on the surface of lymphocytes. Lymphocytes include natural killer cells, T cells (see Chapter

T cells and B cells. They are the main type of cell found in lymph, which led to the term "lymphocyte".[5] The antigen-recognition receptors on the surface of lymphocytes are termed either B cell receptor (BCR) on B cells or T cell receptor (TCR) on T cells, respectively. The BCR and the TCR are not germ line encoded (as PRR on cells of the innate immunity), but are rather created by somatic V(D)J gene rearrangement.[8] For instance, the T-cell receptor α and β chains each consist of a variable (V) amino-terminal region and a constant (C) region. The TCRα locus contains V and J gene segments (V_α and J_α). The TCRβ locus contains D gene segments in addition to V_β and

J_β gene segments. The T cell receptor gene rearrangement occurs during T-cell development through somatic recombination, to form complete V-domain exons and takes place in the thymus.[5] The processes underlying gene rearrangement in B and T cells are similar. Regarding the α chain, a functional V-region exon is generated, when a Vα gene segment rearranges to a Jα gene segment. Transcription and splicing of the VJα exon to Cα generates the messenger ribonucleic acid (mRNA) that is translated to yield the T-cell receptor α-chain protein.[5] The variable domain of the β chain is encoded in three gene segments denominated, Vβ, Dβ, and Jβ. Rearrangement of these segments results in a functional VDJβ V-region exon. This VDJβ V-region exon is further transcribed and spliced to join to Cβ. The resulting mRNA is translated to yield the T-cell receptor β chain. After their biosynthesis the α and β chains will pair to yield the α:β T-cell receptor heterodimer.[5] This process of somatic V(D)J gene rearrangement allows for an essentially unlimited adaptive immune recognition through antigen receptors, enabling specific immune responses to almost any pathogen. Activated pathogen specific lymphocytes proliferate and are recruited to the site of inflammation to fight the intruder. Activated B cells for example induce a humoral immune response through the production of antibodies, whereas active T cells secrete a specific set of cytokines that are part of a cell-mediated immune response.[9,10] After first contact and successful elimination of an invader some of the antigen-specific lymphocytes are retained and create a memory cell repertoire, that leads to faster and enhanced response to subsequent encounters with the same pathogen.[11]

Nature Reviews | Cancer
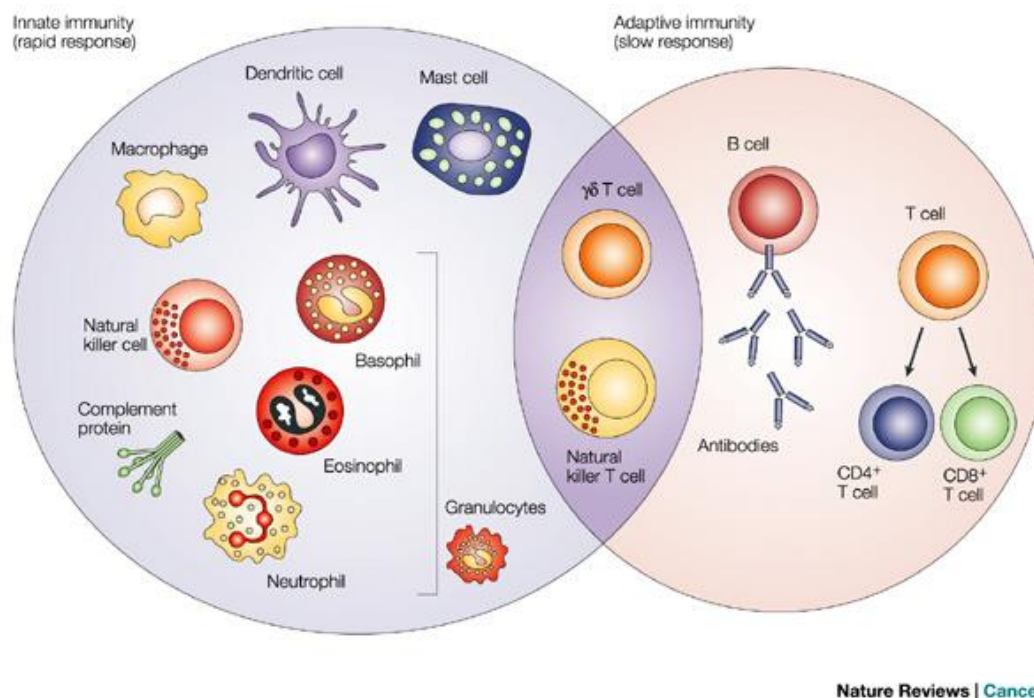
Figure 1. Cells of the innate and adaptive immune system. The innate immune system acts as the first line of defense during an inflammation. It consists of various cell types such as natural killer cells, macrophages, dendritic cells and granulocytes. Granulocytes can be subdivided into basophils, eosinophils and neutrophils. Humoral components of the innate immunity include the complement system and antimicrobial peptides. The innate immune system is build up by B cells and T cells. B cells produce antibodies and T cells can be further grouped into CD4^{+} T helper cells and CD8^{+} cytotoxic T cells. γδ T cells and natural killer cells bridge between innate and adaptive immunity (copied from Dranoff *et al.*).[12]

1.2.   Cells of the immune system

Leukocytes or white blood cells make up the cellular compartment of both the innate and the adaptive immune response. Leukocytes originate in the bone marrow from hematopoietic stem cells (HSC). HSCs can give rise or differentiate into common myeloid (CMP) and lymphoid progenitor cells (CLP). On the one side, macrophages, granulocytes, DCs and megakaryocytes originate all from CMPs and form together the branch of the innate immune system. On the other side, CLPs develop into B cells and T cells, which build up adaptive immunity. DCs can be generated either from CMPs or CLPs underscoring their significant role at the border of innate and adaptive immunity (Figure 2).[13,14]
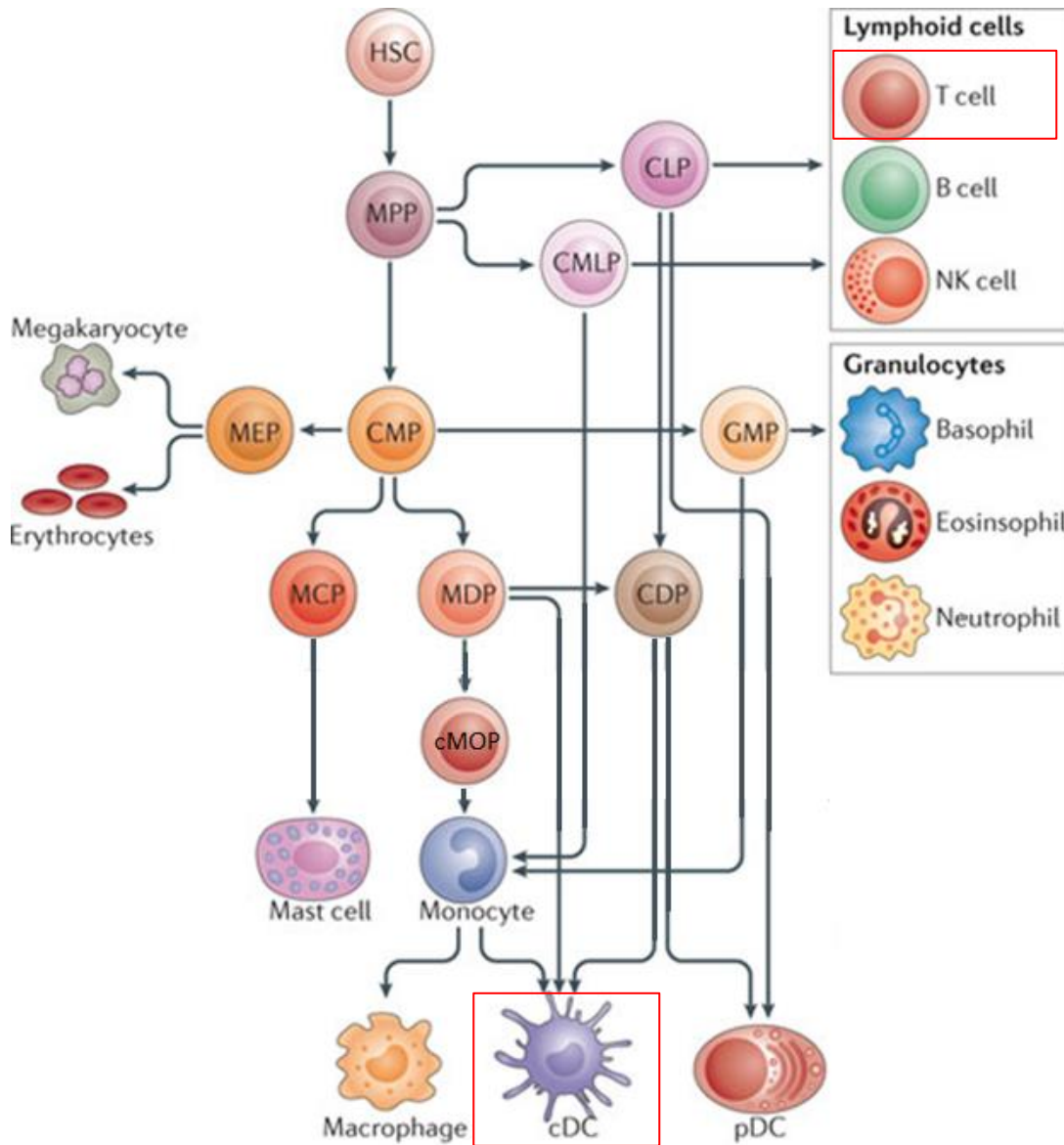
Figure 2. Leukopoiesis. Leukocytes develop from hematopoietic stem cells (HSCs) and multipotent progenitor cells (MPPs). The figure shows how progenitor cells give rise to the different hematopoietic cell lineages. Conventional DCs (cDC) arise from the common DC progenitor (CDP). Monocytes originate from a common myeloid progenitor (CMP). Lymphoid cells such as T and B cells originate from the common lymphoid progenitor (CLP). GMP granulocyte and macrophage progenitor; MCP mast cell progenitor; MDP macrophage and DC progenitor; MEP megakaryocyte and erythroid progenitor; NK natural killer; pDC, plasmacytoid DC. (Adapted from Gabrilovich *et al.*)[15]

1.2.1 Dendritic cells

Dendritic cells (from the greek work déndron, "tree") where first described in 1973 by Ralph Steinman and Zenvil A. Cohn. Both depicted DCs as large cells with branch-like projections, retractile and contorted in shape, giving them a stellate morphology (Figure

3).[16] Soon after Steinman and Cohn´s discovery, a multitude of studies exposed cells with similar phenotypic characteristics in most non-lymphoid tissues.
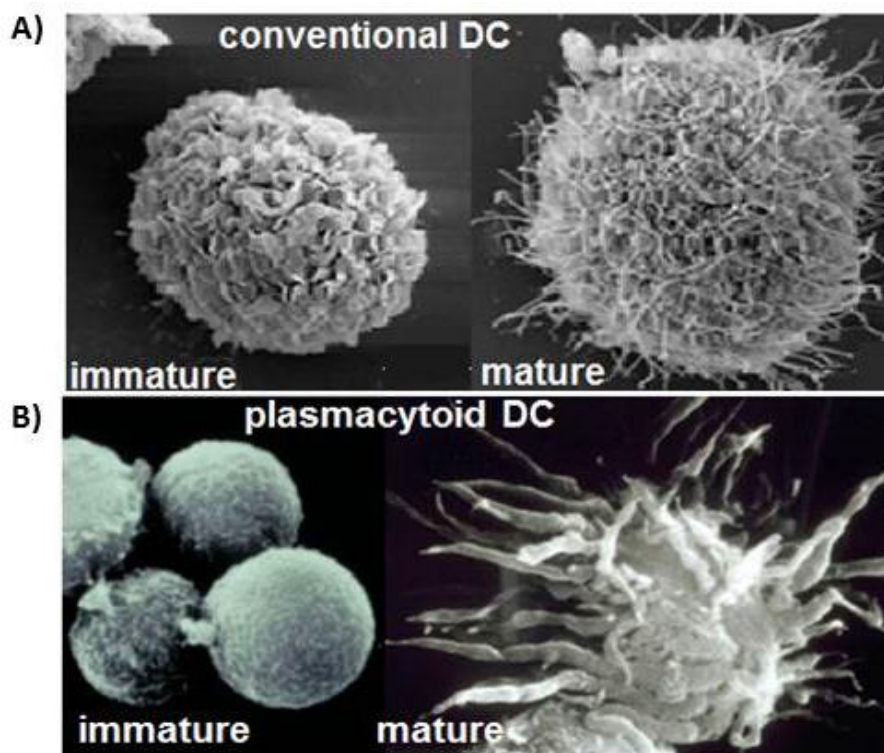
Figure 3. Conventional and plasmacytoid dendritic cells. A) Morphology of an immature-DC (left) and a CD40L activated mature DC (right) examined by scanning electron microscopy. (Adapted from Baron *et al.*).[17] **B)** Morphology of pDCs Examined by scanning electron microscopy. Resting pDCs have a spherical shape (left), whereas CD40L-activated pDCs have a dendritic cell–like morphology (right). Original magnifications, ×3,000 (adapted from Colonna *et al.*).[18]

DCs are a heterogeneous population of cells, which play a pivotal role at the border between the innate and adaptive immunity. As mentioned above DCs can originate in the bone marrow either from common myeloid progenitors (CMPs) or from common lymphoid progenitor (CLPs) and are the most potent APCs. Subsequently, CMPs develop into monocyte/macrophages and DC precursors (MDPs) and further into the monocyte precursor (cMOP) or the common DC precursor (CDP).[19] cMOP differentiates into monocytes[20] which migrate into tissues where, under certain conditions, they are able to give rise to DCs. In tissues CDPs are able to differentiate under steady state into DCs (Figure 4).[21]
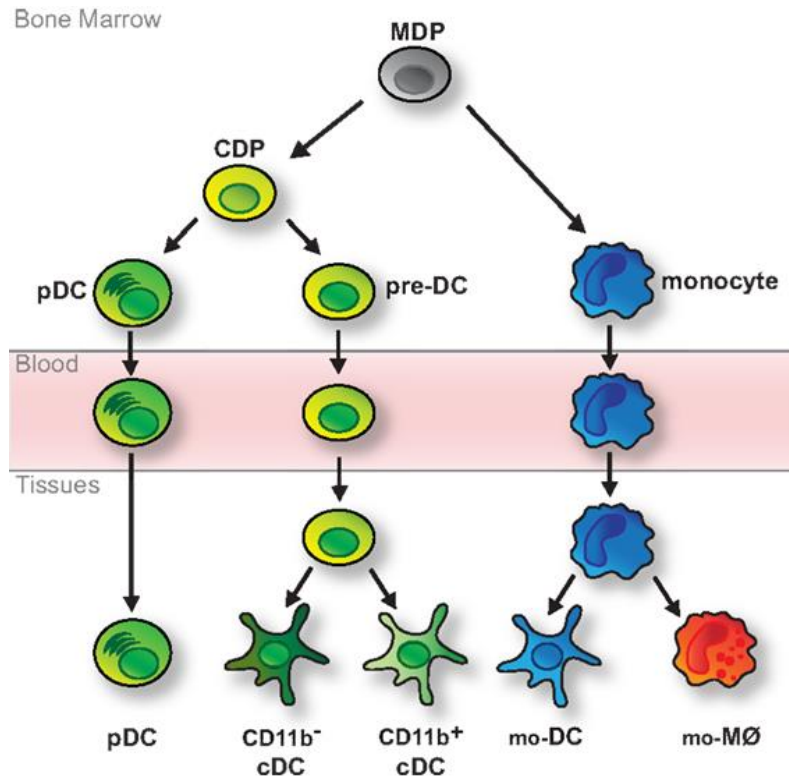
Figure 4. Classic model of DC development. DCs and monocytes develop from bi-potential MDPs residing in the bone marrow. MDPs further differentiate into monocytes and CDPs. CDPs can develop either into DCs, which fully develop in the bone marrow, or into pre-DCs, which migrate through the blood to tissues. In the tissues pre-DCs differentiate into CD11b⁻ (including CD8α⁺ cDCs in lymphoid tissue and migratory CD103⁺ cDCs in non-lymphoid tissue) and CD11b⁺ cDCs. Monocytes develop in the bone marrow and reach peripheral tissues via the bloodstream. There they further differentiate into monocyte-derived DCs (mo-DCs) or macrophages (MØs) (mo-MØs) in response to environmental cues (copied from Schraml *et al.*).[22]

Their ability to phagocyte pathogens and present their antigens by MHC, as well as their capacity to migrate from sites of inflammation to lymphoid tissues, is vital for igniting protective pro-inflammatory, as well as tolerogenic immune responses.[23] In lymphoid tissues (e.g. lymph nodes (LN)) the now-mature DCs are able to activate T cells carrying a T cell receptor being specific for the foreign-peptide–MHC complexes on the DC surface. Therefore, DCs are described as sentinels of the immune system, as they survey the peripheral tissues and instruct the adaptive immune system in response to peripheral cues.[24]

Besides their role of sampling the environment for antigens and migrating to peripheral lymphoid organs, DCs are important mediators attracting T lymphocytes to sites of antigen accumulation and exposure. Through the secretion of different constitutive and inducible chemokines DCs are able to attract T cells to sites where they are needed. Important chemokines attracting naive T cells into the T cell zone of lymphoid tissues,

are the DC-derived CC chemokine 1 (DC-CK1) (CCL18)[25] and EBV-ligand chemokine (ELC) (CCL19).[26] Inflammatory chemokines such as macrophage inflammatory protein (MIP)-1α (CCL3),[27] and macrophage-derived chemokine (MDC) (CCL22)[28] mainly recruit activated cells to sites of inflammation.

DCs can be subdivided into three distinct groups: plasmacytoid DCs (pDCs), conventional DCs (cDCs) and monocyte derived DCs (moDCs).[29] pDCs are a special subset of DCs which differentiate (dependent on the transcription factor E2-2) completely in the bone marrow and reside in lymphoid organs under steady state conditions.[30] Their main function lies in the production of high amounts of type I interferons (mainly IFN-α) upon activation of TLR7/9 signaling, after viral infections. pDCs can act as APCs, but are less efficient in antigen presentation than other DC subsets.[31] In mice, pDCs are characterized by their expression of Siglec-H, B220, Ly6C and CCR9. In humans, they are characterized as Human Leukocyte Antigen – antigen D Related positive (HLA-DR$^+$), interleukin-3 receptor positive (CD123$^+$) and blood dendritic cell antigen 2 protein positive (BDCA-2$^+$) (Figure 3).[32]

Differentiation into cDCs is regulated by the transcription factor inhibitor of DNA binding 2 (Id2).[33] There are two main populations of cDCs with distinct functions: CD11b$^+$ and CD11b$^-$cDCs. CD11c$^-$ DCs can be further divided into CD8a$^+$ DCs residing in lymphoid organs and into CD103$^+$ DCs located in non-lymphoid organs. These two subsets of CD11b$^-$cDCs, depending on the transcription factors BATF3 (Basic leucine zipper transcriptional factor ATF-like 3)[34] and IRF-8 (Interferon regulatory factor 8)[35] respectively, are the most efficient cross-presenting (naive cytotoxic CD8$^+$ T cell stimulation) DCs, characterized by high expression of MHC-I.[36] In contrast, CD11b$^+$ DCs are characterized by the expression of CD11c, CD11b and CD172a and require the transcription factors IRF4 and RbpJ (Recombining binding protein suppressor of hairless) for their differentiation and reside in lymphoid organs. CD11b$^+$ DCs are specialized in presenting antigens via MHC-II to CD4$^+$ T helper cells.[37]

moDCs are nearly absent during steady state conditions but can originate, as their name suggests, from Ly6C^{high} monocytes during inflammation, cancer and, infections.[38] They are described by the expression of MHCII, CD11b, CD11c, F4/80, Ly6C, CD206, CD115, LAMP2 (lysosomal-associated membrane protein 2), CD64, Zbtb46 (Zinc finger and BTB domain-containing protein 46) and, FcεR. The later allowing to distinguish

them from cDCs. In humans, moDCs are characterized by expression of HLA-DR, CD11c, BDCA1, CD1a, FcεRI, CD206, CD172a, CD14 and CD11b and ZBTB46.[38,39]

1.2.2 T cells

Development of T cells begins in the bone marrow, from where pluripotent progenitors migrate towards the thymus, a primary lymphoid organ, and go through a rigorous differentiation protocol.[40] Till today, it is agreed on that the thymus is responsible for the differentiation of various distinct T cell population. These include γδ T cells, αβT cells (including CD4^{+} and CD8^{+} T cells, as well as their regulatory counterparts) and Natural Killer T cells (NKT cells, as well as intraepithelial lymphocytes (IEL). The following chapters will be focusing on the development and the function of αβ T cells and their different subpopulations.[40]

After entering the thymus, early T cell progenitors (ETP) undergo extensive proliferation, which is initiated through thymic stromal cells, producing interleukin (IL)-7.[41] This proliferative state is denominated as the double negative (DN) stage 2 (**Figure 5**). At the DN2 T cell progenitors are yet not fully committed to the T cell lineage.[42] Next the T cells enter the DN3 stage, stop proliferating and undergo TCR gene rearrangements (see chapter 1.1.2.). Furthermore, they express antigen receptors consisting of only one chain (either the TCRβ chain or the TCRγ and TCRδ chain).[43] Only cells carrying appropriate pre-TCRs will survive. Cells not carrying appropriate pre-TCRs will enter apoptosis, due to lack of signal. Continuing the maturation, T cells carrying a successfully rearranged TCRβ chain undergo β-selection inducing the expression of CD4 and CD8, transforming them into double positive cells (DP).[42] In the DP stage, the T cells will undergo αTCR gene rearrangements (see chapter 1.1.2) and express the full αβTCR, which will be the basis for a specific selection program. Immature cells recognizing self-peptide-MHC molecules with their specific TCR in the thymus, but exhibit a weak affinity will further differentiate. This process is denominated positive selection.[44] If the αβTCR of the DP interacts appropriately with MHC-I/peptide complexes it differentiates into CD8^{+} single positive (SP) αβ T cells. If the αβTCR of the DP interacts appropriately with MHC-II/peptide complexes it differentiates into CD4^{+} SP αβ T cells.[45] If the TCR binds with to high affinity, the cell will undergo apoptosis

(negative selection). T cells with rearranged TCRγ and TCRδ chains will be selected as γδ T cells.[44]

At the end of the thymic selection process, the SP progenitor is no longer responsive to apoptosis. In this last stage, the SP progenitor is able to proliferate after stimulation through the TCR. The mature and naïve T cell that is able to proliferate, emigrates from the thymus.[46]
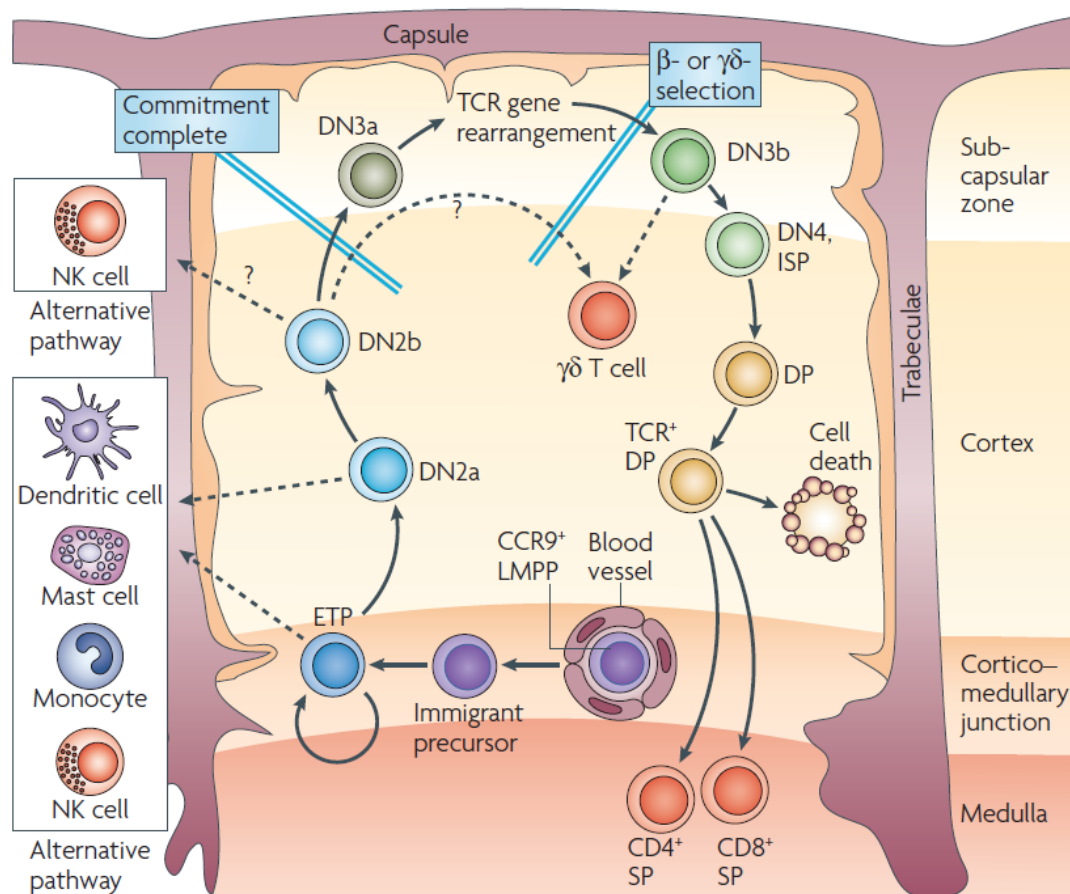
Figure 5. Cross-section through an adult thymic lobule showing the migration path of T cell precursors during development. First, T cell precursors enter the thymus through blood vessels near the cortico–medullary junction. These early T-cell precursors (ETP) migrate, and differentiate from double negative (DN) to double positive (DP) to single positive (SP) stages, through the distinct microenvironments of the thymus. ETPs can continue their expansion with minimal differentiation in the cortico–medullary junction region or differentiate into DN2 cells that begin migrating from the site of entry to the outer rim of the cortex. β-selection occurs during the accumulation of the DN3 T cells in the subcapsular zone. If the αβTCR of the DP interacts appropriately with MHC-I/peptide complexes it differentiates into CD8+ single positive (SP) αβ T cells. If the αβTCR of the DP interacts appropriately with MHC-II/peptide complexes it differentiates into CD4+ SP αβ T cells. In this last stage, the SP progenitor is able to proliferate after stimulation through the TCR. The mature and naïve T cell that is able to proliferate, emigrates from the thymus. Broken arrows depict alternative developmental pathways which are still possible for ETPs and for different subsets of DN2 cells which are likely to correspond to DN2a and DN2b cells before they complete their commitment to the T-cell-lineage. CCR9, CC-chemokine receptor 9; ISP, immature single positive; LMPP, lymphoid primed multipotent progenitor; NK, natural killer; TCR, T-cell receptor (copied from Rothenberg et al.).[40]

Mature naïve T cells express antigen receptors and co-stimulatory molecules necessary for the antigen recognition. However, these naïve cells are not capable of carrying out effector mechanisms allowing them to combat pathogens. For this purpose, naïve T cells need to be activated and differentiate into T effector cells. This process will occur in secondary lymphoid organs.[47] For homing towards LN, most naïve T cells express CCR7 as well as CXCR4 and enter the LN through high endothelial venules (HEV). The chemokine CCL21 is produced by HEV and presented on their luminal endothelium.[48,49] CCL19 and CXCL12 (the ligand for CXCR4) are produced by fibroblastic reticular cells (FRC) and transcytosed across the HEV and presented on their luminal endothelium, as already described for CCL21.[50] Similar to the DC, the T cell follows the CCL21/19 gradient in the subcapsular sinus of the LN to migrate into the T cell area of the LN, where it scans DCs for foreign antigens.[47]

The activation and differentiation of T cells can be divided into three stages: *First*, antigen recognition and co-stimulation resulting in cytokine secretion. *Second*, the clonal expansion, describing the process where a T cell clone recognizes its specific antigen and starts proliferating. *Third* and last, T cells differentiate either into CD4$^+$ or CD8$^+$ T effector cells or memory T cells.[4] CD8$^+$ cytotoxic T cells are mainly responsible for eliminating infected or damaged cells via interaction of MHCI. Almost all cells (exception of non-nucleated cells) express MHCI on the surface. When infected, these cells degrade foreign peptides and present antigens via MHCI, which in turn, can be detected by CD8$^+$ T cells. When activated CD8$^+$ T cells start proliferating and releasing cytotoxins such as perforins and granzymes which induce apoptosis of the APC.[51]

CD4$^+$ T cells, also known as T helper cells, assist in shaping the activity of macrophages, B cells and dendritic cells. Through secretion of certain cytokines and through upregulation of CD40 ligand on the surface of T cells they induce the activation of macrophages, B cells and, DCs. Thus, leading to improved phagocytosis, increased expression of co-stimulatory factors on the APC surface, and, in the case of B cells, to an augmented antibody production.[4] Mature CD4$^+$ T cells can differentiate into several subpopulations of effector cells, of which the most studied and prominent candidates are T helper type 1 (T$_H$1), T$_H$2, T$_H$17 and regulatory T cells (Tregs). The differentiation of naïve T cells into these effector subsets occurs after few days of direct contact with APCs.[52] Innumerous factors are involved during this differentiation process. These

include the affinity of the antigen, the type of signaling induced by the TCR, the set of co-receptors involved, the underlying cytokine milieu present, as well as the set of signal transducer and activator of transcription (STAT) factors expressed in the T cell. The following chapters will focus on these T helper cell subsets.[4]
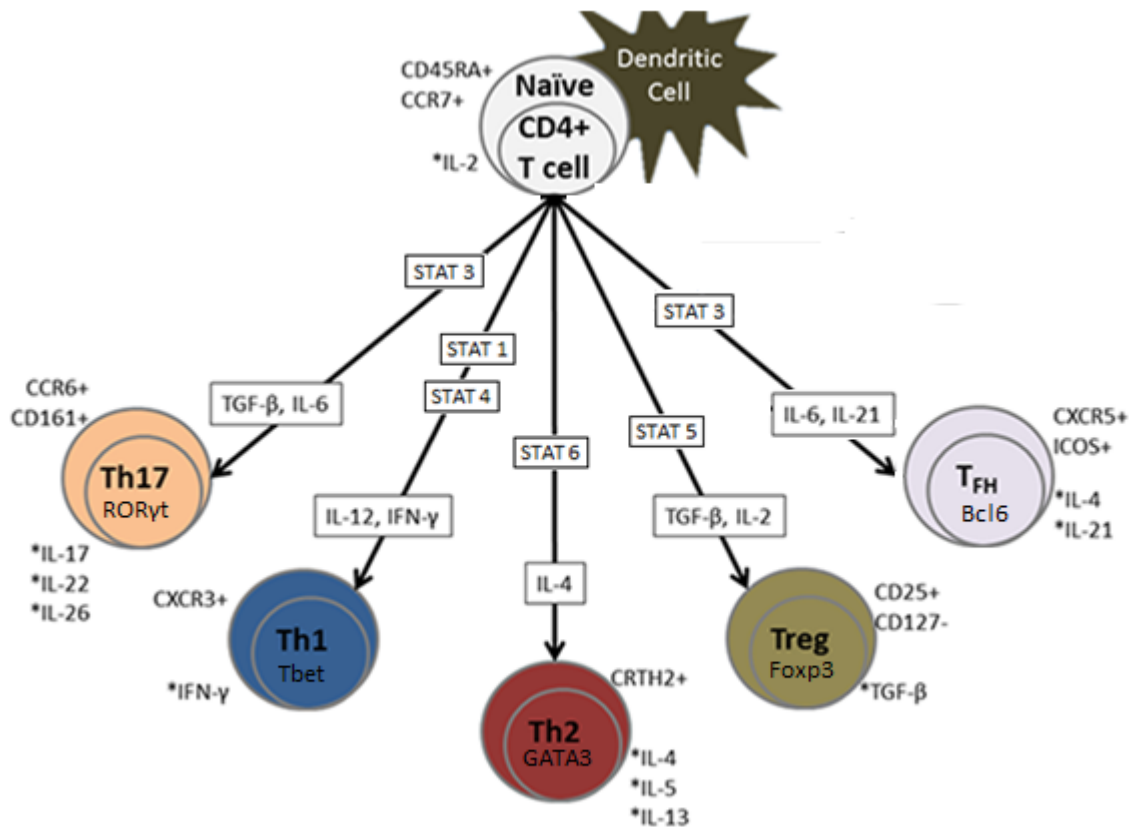
Figure 6. CD4+ T cell subsets. Depicted are the five best described CD4^{+} T helper (T$_H$) cell subsets, their immunomodulatory mediators, cell specific surface markers and transcription factors and a corresponding cytokine milieu controlling the individual T$_H$-subset differentiation. Adapted after *http://www.lonza.com/products-services/bio-research/primary-cells/hematopoietic-cells/hematopoietic-knowledge-center/cd4-t-cell-subsets.aspx*

1.2.2.1. T$_H$1 cells

T$_H$1 cells are characterized by the secretion of IFN-γ, IL-2, TNF-α and Lymphotoxin. All of these enhance pro-inflammatory cell mediated immune responses by maximizing killing efficacy of macrophages and proliferation of cytotoxic CD8[+] T cells. This increase in killing efficacy is for example initiated by stimulating antibody production, mainly opsonizing isotypes of immunoglobulin G (IgG) by B cells.[51] Naïve T cells differentiate into T$_H$1 cells when they are surrounded by an inflammatory cytokine milieu composed

13

of IL-12, and Type I Interferons (IFN-α and IFN-β) and INF-γ, among others (Figure 6). This inflammatory cytokine milieu (IL-12; Type I interferons, IFN-y) is primarily being secreted by macrophages and DCs after activation through extracellular pathogens, such as bacteria.[53] IFN-γ stimulation of naive T cells leads to activation of the Janus kinase (JAK) 1 + 2 pathway that further (downstream) activates the transcription factor STAT1. STAT1 activation induces the expression of the transcription factor *T-box expressed in T* cells (Tbet) (Figure 6). This transcription factor is responsible for remodeling the IFN-γ gene locus and therefore the expression and secretion of IFN-γ. Furthermore, Tbet maintains expression and stabilization of the IL-12 receptor on the surface of the T_H1 cell.[54]

1.2.2.2. T_H2 cells

The predominant role of T_H2 cells is their interaction with B cells. Through this interaction T_H2 cells promote the stimulation of the humoral immune system.[52] Cytokines involved during this process are IL-4, IL-5, IL-6, IL-10 and IL-13 (Figure 6). With these tools T_H2 cells promote protection against helminthic infections but are also involved in several allergic diseases.[55] The T_H2 signature cytokine IL-4 is also known as B cell stimulating factor. IL-4 is crucial for the induction of IgE synthesis by activated B lymphocytes and influences class switching to IgG1 as well.[56] IL-4 itself is a key cytokine during polarization of T_H2 cells and through binding to the IL-4 receptor on the surface of naïve T cells, IL-4 activates STAT6 signaling. STAT6 signaling on the other hand leads to the expression of the transcription factors c-Maf (musculoaponeurotic fibrosarcoma oncogene homologue) and GATA binding protein 3 (GATA3) (Figure 6). c-Maf induces high expression of IL-4, whereas GATA3 antagonizes T_H1 differentiation by inhibiting the expression of IL-2 receptor β-chain and of STAT4.[53]

1.2.2.3. T_H17 cells

With the proposition of the dichotomy of T_H1 and T_H2 cells, which was proposed by Mossman and Coffman in 1989,[57] that divided CD4^{+} T helper cells in IFN-γ producing T_H1 cells and IL-4 producing T_H2 cells it was thought to explain the tendency of T cells to act either in a cellular or a humoral immune response.[57] However, it was predicted that there must be other subsets involved that would explain STAT3-dependent CD4^{+} T cells during autoimmune diseases and infections.

In studies performed in a mouse model of experimental autoimmune encephalopathy (EAE), which at that point was thought to be dependent of T_H1 cells, it was shown that development of EAE failed in mice deficient of p40.[58,59] The subunit p40 forms together with the subunit p35 IL-12. As mentioned in chapter 1.2.2.1., IL-12 induces T_H1 cell differentiation. Nevertheless, mice deficient in the subunit of p35 still developed EAE.[60] Later it was found that p40 not only forms heteromers with p35, but is also able to form heteromers with p19, creating IL-23. Further studies in mice lacking p19 failed to develop EAE, phenocopying p40 deficiency and indicating the crucial role of IL-23 in the onset of EAE.[61] Furthermore, it was shown that IL-23 induces the secretion of IL-17 from another T_H subset, denominated T_H17 cells.[62]

IL-23 is not the sole factor driving T_H17 differentiation; it is rather a mixture of cytokines, including TGF-β and IL-6, promoting T_H17 cells (Figure 6).[63-65] IL-6 plays a pivotal role in activating STAT3. Through this activation, expression of several genes regulating T_H17 induction is induced. These include *Rorc* (encodes the transcription factor RAR-related orphan receptor gamma (RorγT)), *Il17* and *Il23r* (Figure 6).[66-68] STAT3 also inhibits TGF-β-induced expression of Forkhead-Box-Protein P3 (Foxp3), thus suppressing the generation of regulatory T cells.[69] IL-6 also induces the expression of IL-1R, a receptor for the pro-inflammatory cytokine IL-1β.[70] IL-1β induces the phosphorylation of the mechanistic Target of Rapamycin (mTOR) (a protein kinase that regulates cell growth, cell proliferation, cell motility, cell survival, protein synthesis, autophagy, and transcription) in T_H17 cells and increases proliferation of T_H17 cells during inflammation.[71] TGF-β plays a more complex role and functions either as an obligate T_H17 inducing factor or indirectly suppresses alternate cell fates by repressing Tbet and GATA3.[69]

RorγT$^+$ T_H17 cells are divided into two groups: Host protective cells expressing IL-17 and IL-10 and inflammatory cells characterized by IL-17, IL-22, IFN-γ and GM-CSF (Granulocyte-macrophage colony-stimulating factor) expression.[72] TGF-β and IL-6-induced T_H17 cells promote (via IL-10 secretion) a host protective phenotype, related to mucosal defense against microorganisms and barrier tissue integrity. IL-23 activated T_H17 cells on the other hand promote chronic tissue inflammation during infections and autoimmunity.[69]

1.2.2.4. Regulatory T cells

Regulatory T cells (Tregs) are also known as suppressor T cells and are a subpopulation of CD4$^+$ T cells. Their main responsibilities are the modulation and regulation of the immune system by ensuring the balance between immune activation and tolerance towards self-antigens.[73] In mice, Tregs are characterized as CD3$^+$CD4$^+$CD25$^+$ and the transcription factor Foxp3$^+$.[74] At least in mice Foxp3 is associated with the suppressive functions of Tregs. In humans, the expression of Foxp3 can be transient.[74] There are two distinct subtypes of Tregs. Those generated in the thymus and denominated natural Tregs (nTregs)[73] and those induced in the periphery (iTregs).[75] Tregs generated in the thymus develop similar to naïve T cells (described in chapter 1.2.2.). The affinity of interaction with self-peptide MHC complex plays a pivotal role in determining the fate of the developing T cell. T cells that encounter very strong signals will undergo apoptosis. A weak signal will induce survival programs and the cell will become an effector cell. In the case of an intermediate signal strength, the T cell will develop into a regulatory T cell.[76]

Next to the strength of the TCR stimulus, other factors contribute to the development of nTregs. These include cytokines such as IL-2, IL-15 and TGF-β, who all increase the expression of Foxp3.[74] Induced regulatory T cells (iTregs) develop from mature CD4$^+$ T cells outside of the thymus. This requires stimulation in an anti-inflammatory milieu. The cytokines TGF-β and IL-10 as well as DCs play a pivotal role in this process.[77,78]

Moreover, Tregs are classified into three distinct groups, characterized by their secretion profile. T$_H$3 cells are the predominant producers of TGF-β[79], whereas Tr1 cells are the main producers of IL-10[80] and Tr35 cells are known to secrete high amounts of IL-35.[81]

Tregs can modulate the immune response through a plethora of mechanisms. One mechanism is the inhibition of immune responses via secretion of cytokines such as TGF-β, IL-10 and IL-35. IL-10 for instance inhibits the expression of pro inflammatory cytokines such as IL-12. This leads to a reduced T$_H$1 response.[82] Another important role of IL-10 is its induction of phagocytic activity in phagocytic cells. Consequently, cellular debris at inflamed sites get removed faster and more efficient.[82]

IL-35 is an immunosuppressive cytokine known to inhibit proliferation of CD4$^+$ T helper cells and promotes the differentiation of naïve T cells into inducible Tr35 cells (iTr35).

These iTr35 cells are highly suppressive and produce again high amounts of IL-35.[83] IL-35 was further shown to be involved in the conversion of B cells into B regulatory cells.[84] The role of TGF-β in promoting anti-inflammatory immune responses is rather complex. Briefly, TGF-β is capable of regulating several immune cells. For instance, it is involved in suppressing effector T cell differentiation and driving differentiation of naïve T cells into Tregs (depending on the cytokine milieu also into T_H17 cells).[85] TGF-β has also been implicated in inhibiting the activity of macrophages, DCs and NK cells.[86]

Besides secretion of anti-inflammatory cytokines, Tregs can mediate their suppressive effects via cytolysis of pro-inflammatory cells through secretion of granzyme and perforin.[87] Tregs are also able to inhibit proliferative responses via consumption of IL-2.[88] Furthermore, cyclic adenosine monophosphate (cAMP) (an important secondary messenger used in many intracellular signal transduction pathways) mediated metabolic inhibition[89] and immunomodulation mediated via the A2 adenosine receptor,[90] are inhibitory mechanisms used by Tregs. Tregs are also capable to interact with DCs, through cytotoxic T-lymphocyte-associated Protein 4 (CTLA-4)-CD80/86 interactions, and modulate their maturation and function.[91]

Tregs are found broadly across most lymphoid and non-lymphoid tissues during homeostatic conditions.[92] In humans, expression of chemokine receptors on Tregs change with age. In neonatal cord blood Tregs are naïve and express CCR7 and CXCR4 (LN homing receptors), as conventional naïve T cells do, or they express the gut-homing receptor CCR9.[93,94] In a three year old child Tregs appear to be divided into two groups that resemble a memory phenotype. They are characterized as CCR7$^+$ L-selectin$^+$ Tregs resembling central memory T (TCM) cells or, CCR7$^-$ Tregs that resemble effector memory T (TEM) cells. This memory like Tregs downregulate CCR9 and instead express skin-, lung-, or inflammation-homing chemokine receptors such as CXCR3, CCR2, CCR4, CCR5, CCR6 and CCR8.[93,94] All of the latter are part of the chemokine-chemokine receptor system which will be described in the next section.

1.3.   The chemokine – chemokine receptor system

Chemokines belong to a superfamily of secreted chemotactic cytokines that are best known to control migration of immune cells. Chemokines are small molecules with a molecular weight of around 8-10 kDa. Today the chemokine system consists of around

50 endogenous chemokines and 20 G protein-coupled seven-transmembrane signaling receptors (see also Figure 7).[95] The chemokine system is involved in many physiological and pathological processes, such as embryogenesis, immune system development and function, inflammation, tumorigenesis and cancer metastasis.[96]
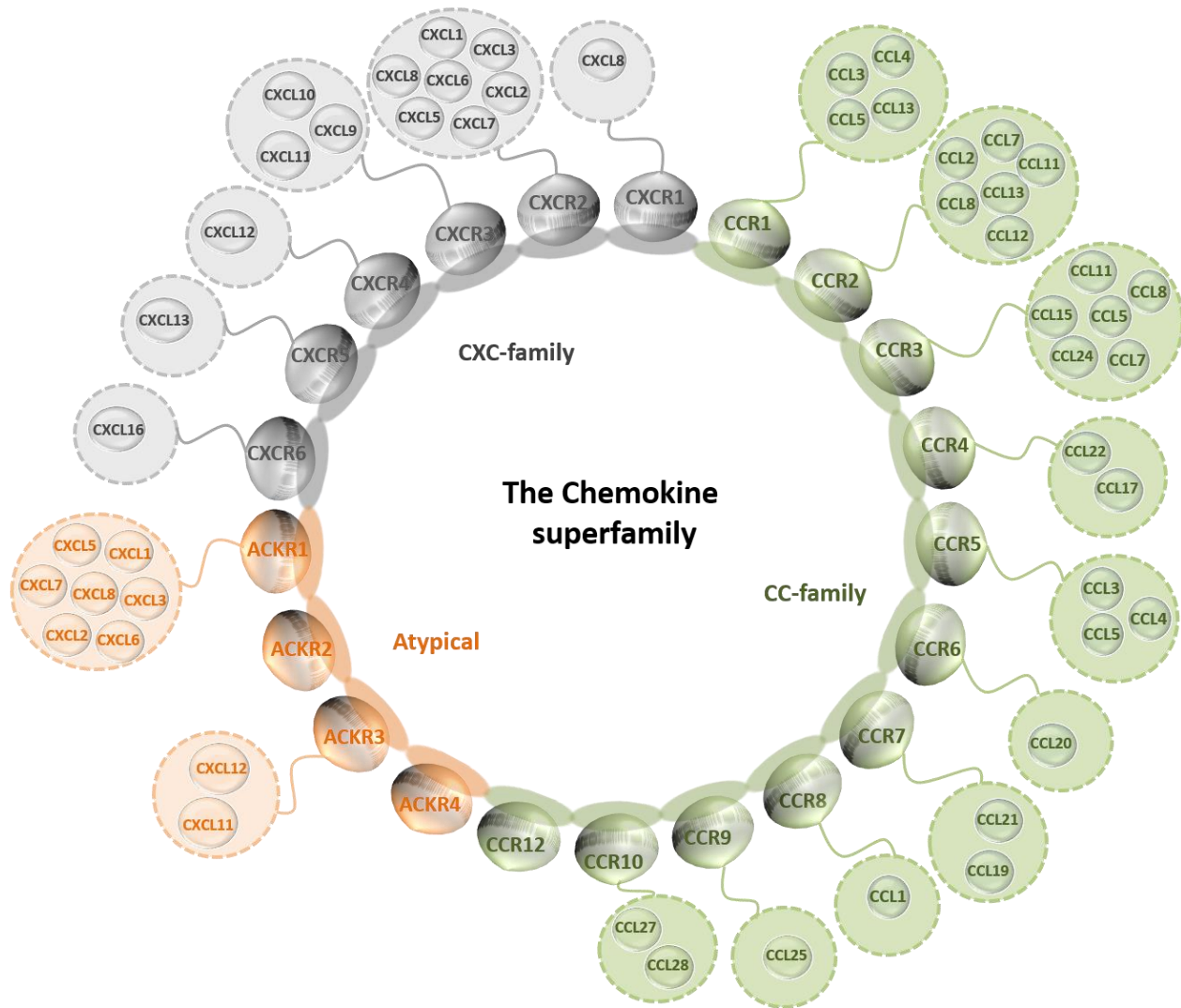
Figure 7. Chemokine superfamily. Overview of the most important chemokine receptors and their cognate chemokine ligands. (Courtesy of Yvonne Döring)

Chemokines have a highly conserved secondary structure and built up by their unique tetracysteine motif. Through this motif, the chemokine superfamily can be subdivided into four distinct groups. The majority of chemokines belongs to the CC group where the N-terminal cysteine's are next to each other. The CXC group is characterized by an amino acid that separates the first two cysteine's from each other. The CX3C group has only one member, Fraktaline (CX3CL1), and is characterized by three amino acids,

which separate the N-terminal cysteins. Chemokines belonging to the C group possess only two out of the four cysteines present in other chemokines.[97,98]
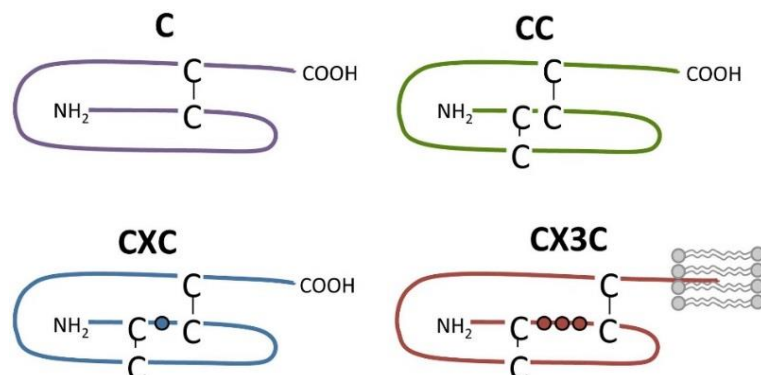
Figure 8. Chemokine subclasses. Chemokines are divided into four families according to the number and spatial organization of conserved cysteine residues in their N-terminus. Disulfide bridges are shown as black lines. The transmembrane domain of CX3CL1 is depicted by lipids (in gray) (copied from de Munnik *et al.*).[99]

The chemokine receptors are named according to the group of chemokines they bind (CC, CXC, XC, and CX3C). These G protein-coupled seven-transmembrane receptors signal through coupled heterotrimeric G proteins. In general, receptor binding induces a signal transduction cascade that leads to activation of protein kinases and increase in intracellular Ca^{2+}.[100]
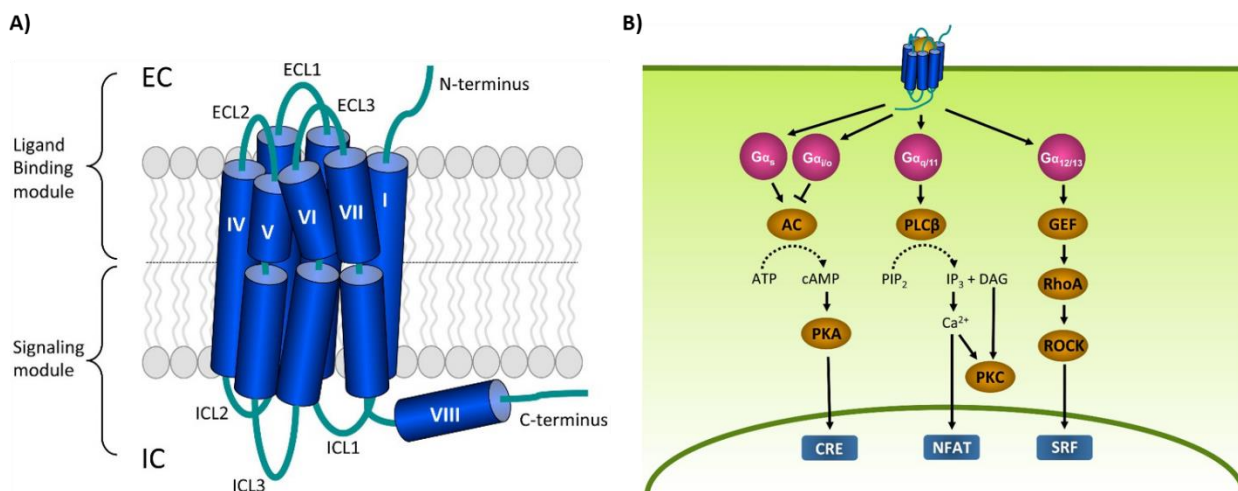
Figure 9. G protein-coupled receptors (GPCRs) and their signaling. A) Depicted are the three extracellular loops (ECL1-3) and the N-terminus in the extracellular (EC) region and the three intracellular loops (ICL1-3) and the C-terminus in the intracellular (IC) region. The seven transmembrane (TM) helices contain a number of proline-dependent kinks that divide the GPCR into the ligand binding module and the module that binds downstream effectors such as G proteins. The C-terminus of many GPCRs is folded into an eighth helix that runs parallel to the plasma membrane and is often anchored to the membrane via a palmitoylation site.[99,101] **(B)** G protein-dependent signaling: Gα proteins are divided into $G\alpha_s$, $G\alpha_i$, $G\alpha_q$, and $G\alpha_{12/13}$ protein families that regulate different effector proteins such as AC and PLC. Effector proteins produce second messengers (e.g., cAMP) that subsequently activate transcription factors such as CRE, NFAT and SRF. *Abbreviations*: AC, adenylyl cyclase; ATP, adenosine triphosphate; cAMP, cyclic

adenosine monophosphate; CRE, cAMP-responsive element; DAG, diacylglycerol; GEF, guanine nucleotide exchange factor; IP_3, inositol 1,4,5-triphosphate; NFAT, nuclear factor of activated T-cells; PIP_2, phosphatidylinositol-4,5-bisphosphate; PKA, protein kinase A; PKC, protein kinase C; PLCβ, phospholipase Cβ; RhoA, Ras homolog gene family A; ROCK, RhoA kinase; SRF, serum response factor 8copied from de Munnik *et al.*).[99]

The main function of the chemokine system lies in the control of migratory patterns and positioning of immune cells.[102] The majority of chemokines carries an overall net positive charge at neutral pH. This allows for interactions of varying affinity with different negatively charged extracellular structures like glycosaminoglycans (GAG) which are present for example on the surface of endothelial cells. This deposition allows the generation of a steeply decaying chemokine gradient, providing stable directional cues.[103,104] The chemokine gradient plays a pivotal role during the leukocyte extravasation to sites of inflammation. When endothelial cells get activated through cytokines released during inflammation of the underlying tissue, they initially start expressing P- and later E-selectins.[105] Circulating leukocytes recognize these selectins (P-selectin on endothelial cells binds for example PSGL-1 (P-selectin glycoprotein ligand 1) on leukocytes) with moderate affinity. This causes the slow down and rolling of leukocytes on the endothelial surface. Rolling leukocytes, which encounter a chemokine gradient and recognize it with a specific receptor get then activated and start expressing integrins (lymphocyte function associated antigen-1 (LFA-1) and Very Late Antigen-4 (VLA-4)) which mediate the arrest of rolling leukocytes on the endothelial surface and the transmigration into the tissue and to sites of inflammation.[106,107]

As mentioned above chemokines are not just relevant during the migration of immune cells to the site of inflammation, but are also involved in guiding cells during homeostasis. During homeostatic conditions, DCs for example use a Ccr7-dependent process to migrate via the efferent lymphatics into the draining LN, similar to that described for T cells.[108] Ccl21 is produced by lymphatic vessels in peripheral tissues and promotes migration of Ccr7$^+$ cells. The migration through lymphatic vessels does not seem to be integrin-dependent, in contrast to the migration under high shear rates in the bloodstream.[109] As soon as Ccr7$^+$ DCs arrive in the lymphatics, Ccl21 and Ccl19 appear and play an additive role in DC migration into the subcapsular sinus of the draining LN. The DC follows a gradient of Ccl21 and Ccl19, produced by fibroblastic reticular cells (FRC) in the subcapsular sinus. This gradient promotes the positioning of DCs in the T cell area of the LN.[110]

1.3.1 Ccl17 – Ccr4

Ccl17 was first discovered by Imai and Yoshida in 1996 and characterized as a CC chemokine constitutively expressed in the thymus and highly selective for T cells.[111] In a follow up study the group was able to identify the chemokine receptor 4 (Ccr4) as receptor for Ccl17.[112] Other studies point towards Ccr8 as a receptor for Ccl17[113,114] but have to be considered with caution, as they have been questioned by others and still await confirmation.[115,116] Furthermore, Ccl17 is expressed by thymic DC, LN DC and CD11c$^+$ DC in the lung of mice.[117]

Ccl17 is known to play a role in the recruitment and migration of different T cell subsets including T_H1, T_H2 and Tregs. In addition murine Ccl17 expressing DCs induce both, the production of the T_H1 cytokine IFN-γ and the T_H2 and Treg cytokine IL-10 in an antigen specific manner in T cells *in vitro.*[118] Recent work of our group revealed that the DC-derived chemokine Ccl17 promotes atherogenesis by controlling regulatory T cell (Treg) homeostasis, restraining their expansion, while its deficiency decreased plaque burden by facilitating Treg maintenance and survival. Despite a partial function of Ccr4 in acute inflammatory Treg recruitment and maintenance of Tregs, we did not observe a comparable reduction in lesion formation and infiltration in chimeric mice carrying *Ccr4$^{-/-}$* bone marrow.[119] Similar findings were obtained in a model of atopic dermatitis, where the inflammatory burden was reduced in mice lacking Ccl17 but not Ccr4[120], giving rise to the conclusion that Ccl17 is required for sensitizing Ccr7$^-$ and Cxcr4-dependent DC migration to the LN and subsequent T cell priming. Accordingly, *Ccr7$^{-/-}$Ldlr$^{-/-}$* mice exhibit less plaque formation attributed to a critical involvement of Ccr7 in recirculation of T cells between lymphoid organs and sites of inflammation.[121] Furthermore, and consistent with data obtained in our lab, Heisseke *et al.* were able to demonstrate that lack of Ccl17 protects from intestinal inflammation due to a reduced inflammatory cytokine milieu of DC origin, which facilitates Treg expansion. Again, Ccl17 seemed to promote inflammation independently of Ccr4-mediated T cell recruitment, suggesting an autocrine mechanism stimulated by the Ccl17-Ccr4 axis in DCs, involving other cytokines.[122] In contrast, others have shown that expression of Ccr4 on Treg is crucial to secure Treg recruitment to sites of inflammation[123,124] and facilitates Treg-dependent graft survival.[125]

1.3.2 Ccl5 and its receptors

Ccl5 or RANTES (Regulated upon Activation, Normal T cell Expressed, and Secreted) was first identified in the 1980s as a CC-chemokine expressed by T cells.[126] It was described to recruit T cells, eosinophils and macrophages to sites of inflammation.[127] Its expression is regulated by Kruppel-like factor 13.[128] It is not only expressed by T cells, but also by macrophages, platelets, synovial fibroblasts, tubular epithelium and certain types of tumor cells. Further studies also revealed an upregulation of Ccl5 in activated vascular smooth muscle cells (VSMC).[129-131] Ccl5 is involved in a variety of diseases including atherosclerosis, asthma, Acquired Immune Deficiency Syndrome (AIDS), graft versus host disease and autoimmune diseases such as arthritis and diabetes.

Further, Ccl5 has been shown to bind to the receptors Ccr1, Ccr3 and Ccr5. Through binding to Ccr1 and Ccr5, Ccl5 induces leukocyte arrest and transmigration.[132] In a mouse model of atherosclerosis Braunersreuther and co-workers could show in 2007 that, Ccr5 deficiency but not Ccr1 deficiency protected from atherosclerotic lesion development, due to a reduction in monocyte recruitment.[133] However, while various groups could confirm the data of Ccr5 deficiency, including ours, data regarding Ccr1 deficiency has to be considered with caution. Söhnlein and Drechsler *et al.* did not find an increase of lesion size in the absence of Ccr1. The authors show that Ccr1 deficiency reduced atherosclerotic lesion formation at least in early stage lesions.[134] Hence, further studies are required to clearly address the role of Ccr1 during atherosclerotic lesion formation.

1.3.3 Chemokine heterodimerization

Chemokines are small secreted proteins that are best known for their specialized roles in cell trafficking and cell positioning and increasing evidence supports an emerging role of chemokines in modulating immune mechanisms beyond cell trafficking and positioning. They not just appear in a monomeric form but are also able to form dimers and even higher order oligomers, based on two modes to support interfaces.[135] On the one side, CC chemokines are able to form dimeric structures via interaction of the flexible N-termini. This leads to the formation of a two-stranded anti-paralleled β-sheet. On the other side, CXC chemokines form homodimers through antiparallel extension of preformed β-strands.[135] CC-dimers are also able to form higher order oligomers,

consisting of up to 50 units and more. Through this the chemokine CCL3 (Macrophage inflammatory protein 1 alpha (MIP1-α)) for instance, is able to form rod-like structures.[136] This multimeric structures would allow the creation of soluble gradients (compared with stable gradients bound to GAGs) if dimers and monomers would be released from the multimeric structure in a constant rate.[137] Chemokines are not just able to form homodimeric structures, but taking into account the structural similarities of this group, allows them to form unique heterodimers. These heterodimeric structures modify and fine-tune the overall signaling response of their receptors and with this open up a further dimension of biological versatility.

Molecular dynamic simulation (MDS) for selected chemokine homo- and heterodimer pairs suggest that CC-Chemokines preferably form pairs with other CC-chemokines and that CXC chemokines interact preferably with CXC-chemokines.[138] But it was also shown that CC-CXC heterodimerization occurs. A prominent member of the CC-CXC heteromers was identified by nuclear magnetic resonance (NMR) analysis and consists of CCL5 and CXCL4. In the case of CCL5-CXCL4 heterodimerization, our group was able to demonstrate that disruption of the CCL5-CXCL4 heterodimer reduced monocyte recruitment, thereby ameliorating the disease outcome after induced lung injury as well as atherosclerosis in mouse models.[138] Inflammation and in particular chronic inflammation is characterized by marked vascular changes, including vasodilation, increased permeability and increased blood flow, which are induced by the actions of various inflammatory mediators. During inflammatory processes blood cells including T cells and DCs migrate to sites of inflammation where they play an important role in the maintenance of inflammation. To reach the site of inflammation but also for cell-cell communications chemokines and chemokine receptors have emerged major players. In the following section atherosclerosis as a chronic inflammation of the arterial wall and the role of T cells and DCs (and their secreted chemokines) in the pathophysiology of this disease will be further described.

1.4. Atherosclerosis

Atherosclerosis is a disease affecting mid-sized to large arteries. Atherosclerotic lesion formation takes place at sites of disturbed flow. In these areas endothelial dysfunction and sub-endothelial lipoprotein retention will occur, which will lastly lead to a non-

resolving inflammatory response. As a consequence, intimal destruction, thrombosis and end-organ ischemia may occur.[139]

The term 'Atherosclerosis' is derived from the two Greek words "athera" (gruel) and "sclerosis" (induration) and was first introduced by Johann Friedrich Lobstein in 1829. Atherosclerotic lesions are described by multiple atheromatous plaques within the arteries. Atheromatous plaques are nodular accumulations of a soft, yellowish material at the center of large plaques, composed of macrophages nearest the lumen of the artery.[140,141]

In the later mid-19th century, researchers such as Carl von Rokitansky and Rudolph Virchow proposed two opposing views on the pathology of atherosclerosis. Rokitansky postulated that a trauma, caused by mechanical stress, would initially injure the vessel wall. This initial injury then would lead to endothelial dysfunction. Virchow on the other hand emphasized on the critical role of the immune system during atherosclerotic lesion development. He recognized atherosclerotic lesions as an irritation at the vessel wall, that preceded the fatty metamorphosis and compared that to swelling, cloudiness and general enlargement, as seen in other inflamed parts of the body.[142] In the early 20th century Nikolai N. Anitschkow described the "cholesterinesterphagozyten" which derived from macrophages.[140] These cells are known today as foam cells. This discovery elucidated the leading role of cholesterol in atherosclerotic lesion development. In the 1970s Russell Ross established the "response to injury" hypothesis complementing Rokitansky's hypothesis which he had postulated more than 100 years earlier. Russell brought together the importance of hyperlipidemia and inflammation and suggested that vascular accumulation of lipids triggers an inflammatory response.[143-145] This hypothesis was further strengthened in the 1990s, when Daniel Steinberg and others proposed altered lipoprotein compositions and modified low density lipoprotein (LDL) (mainly oxidized LDL) as disease triggers being taken up by macrophages which would eventually turn into foam cells.[146]

But, even to date – despite the intensive research in this field, the concordant acceptance of hyperlipidemia as the main risk factor and growing evidence that atherogenesis is strongly regulated by immunological mechanisms – the initial reason unbalancing the system remains vague.[139]

1.4.1 Pathomechanisms of atherosclerosis

The normal artery is build up by three layers. The tunica intima is lined by a monolayer of endothelial cells, which is in contact with the blood stream. The tunica media contains smooth muscle cells (SMCs) embedded in a complex extracellular matrix and the adventitia contains mast cells, nerve endings and micro vessels[147] (Figure10A). The main underlying cause for atherosclerotic lesion formation is endothelial dysfunction.[148] Endothelial dysfunction is caused by pro-inflammatory conditions putatively arising during long-term hyperlipidemic exposure.[149] The activated endothelium upregulates adhesion molecules e.g., Selectin's and Integrin's, which will trigger the leukocyte adhesion cascade leading to infiltration of leukocytes into the intimal space. This infiltration will cause asymmetrical thickening of the intima.[150] (Figure10B) Hyperlipidemia together with other risk factors allows for ongoing leukocyte infiltration leading to plaque growth and chronic inflammation.[151] This inflammation will not be resolved, resulting in an increase of apoptotic cells and an accumulation of apoptotic bodies and cholesterol crystals. This will ultimately form a mature plaque, also known as atheroma.[152,153] Atheromas consist of a necrotic core (containing lipids), surrounded by foam cells and other immune cells overall covered by a cap of smooth muscle cells and collagen rich matrix (Figure 10C).[154,155] Furthermore, the secretion of pro-inflammatory cytokines and proteases limits collagen formation causing thinning of the fibrous cap. Weakening of the fibrous cap makes the plaque more vulnerable to rupture. Rupture of the fibrous cap results in thrombus formation possibly causing acute ischemia, manifesting as myocardial infarction or stroke (Figure10D).[156,157]

Figure 10. shown on page 26. The normal muscular artery and changes that occur during atherosclerotic lesion progression as well as thrombus formation after plaque rupture. **A)** The normal artery is build up by three layers. The tunica intima is lined by a monolayer of endothelial cells which is in direct contact with the blood stream. The tunica media contains vascular SMCs embedded in a complex extracellular matrix. The third layer, called adventitia contains mast cells, nerve endings and microvessels. **B)** Atherosclerotic lesion development begins with endothelial dysfunction and subsequent adhesion of blood leukocytes to the activated endothelial monolayer, transmigration of the bound leukocytes into the intima, maturation of monocytes into macrophages taking up lipids thereby transforming into foam cells. **C)** As the lesion progresses SMCs migrate from the media into the intima, resident intimal SMCs and media-derived SMCs start proliferating, and increase the synthesis of extracellular matrix macromolecules. Plaque macrophages and SMCs may undergo apoptosis in progressing lesions. Extracellular lipids derived from dead and dying cells can accumulate in the central region of a plaque, often denoted the lipid or necrotic core. Advancing plaques also contain cholesterol crystals and microvessels. **D)** Thrombosis, often complicates a physical disruption of the atherosclerotic plaque. Shown is a fracture of the plaque's fibrous cap, which has enabled blood coagulation components to come into contact with tissue factors in the plaque's interior, triggering the thrombus that extends into the vessel lumen, where it can impede blood flow (copied from Libby *et al.*).[158]
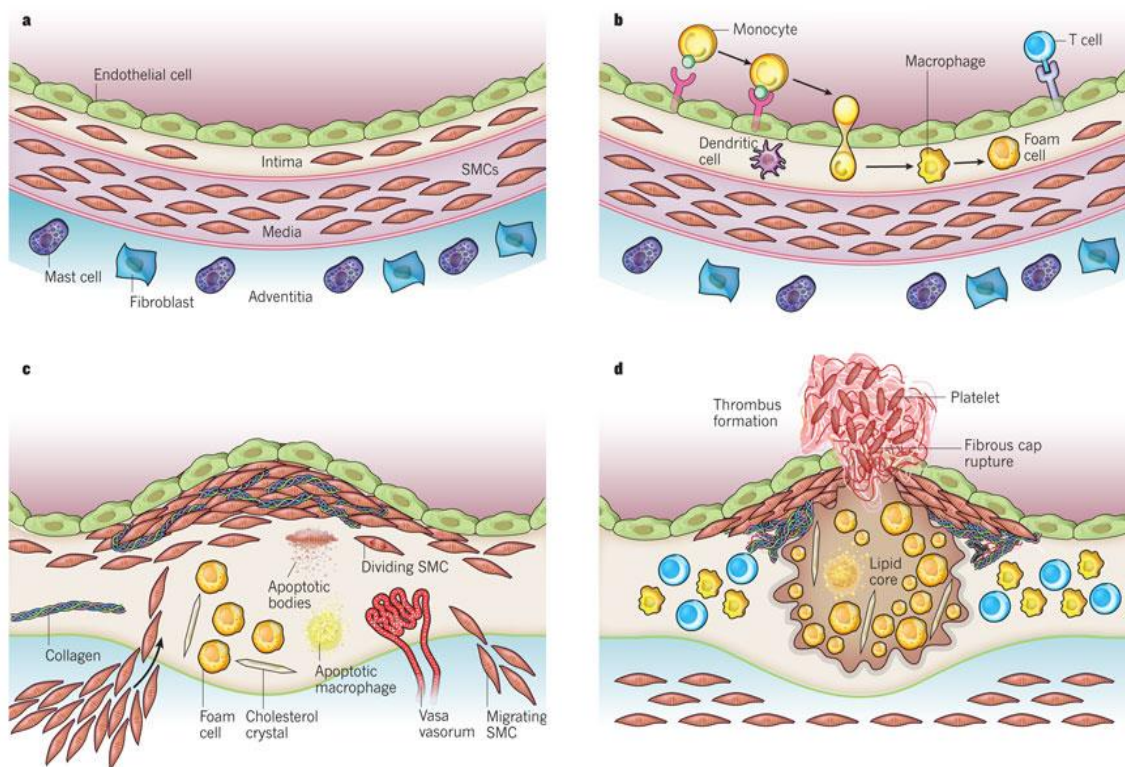
1.4.2 Dendritic cells in atherosclerosis

DCs are known to be present in the atherosclerotic lesion, as well as in the adventitia. In mice, an intimal network of CD11c$^+$ MHCII$^+$ DCs has been described at sites prone to develop atherosclerotic lesion. This network of DCs consist of fms like tyrosine kinase 3 (Flt3)/Flt3L-dependent CD103$^+$ and CD11b$^+$CD172a$^+$ conventional DCs. A large portion of DCs found in atherosclerotic lesions is monocyte-derived and express CD11b. Further, these cells depend on macrophage colony-stimulating-factor (M-CSF) or express CD64.[159-161] Upon stimulation DCs mature and upregulate co-stimulatory molecules such as CD80 (B7-1) and CD86 (B7-2) as well as MHC-II, which are required for an appropriate stimulation of T cells (see chapter 1.1.2). DCs in atherosclerotic lesion mainly express the costimulatory molecules CD80 and CD86 indicating their activated state. *Ldlr$^{-/-}$m*ice deficient for both CD80 and CD86 showed reduced early and to some extent advanced atherosclerotic lesions. Furthermore, these mice showed decreased levels of MHCII$^+$, as well as CD3$^+$ cells in atherosclerotic lesions. Splenic T cells isolated from these *Ldlr$^{-/-}$Cd80$^{-/-}$Cd86$^{-/-}$* mice showed reduced production of IFN-γ in response to

stimulation with heat shock protein 60. These results suggest that absence of co-stimulatory molecules inhibits priming of an adequate T_H1 response.[162]

Although DCs can be found in marginal parts of the plaque core, they mostly localize in the plaque shoulder and regions prone to rupture.[163,164] Rohm *et al.* performed an immunohistochemical analysis of human carotid specimens, comparing stable and unstable plaques. The group found in unstable plaques an 1.6 fold increase in both fascin^{+} mDCs and S100^{+} DCs and a 5.9-fold increase of mature CD83^{+} mDCs.[164] Furthermore, Weyand, *et al.* demonstrated that 53% of endarterectomy samples contained CD123^{+} pDCs and CD11c^{+} DC-sign^{+}fascin^{+} mDCs.[165] But pDC numbers are very low compared to cDC numbers.[166,167] Furthermore, DCs are present in the adventitia and in tertiary lymphoid organs (TLOs) that form in the adventitia of aged *Apoe^{-/-}* mice.[168] In humans, the presence of TLOs in atherosclerotic regions remains controversial but a recent study performed by Akhavanpoor *et al.* demonstrates that adventitial cellular accumulations show characteristics of highly organized TLOs.[169] As mentioned coronary artery disease (CAD) patients show increased numbers of DCs in the atherosclerotic vascular wall. However, interestingly Yilmaz *et al.* were able to show that CAD patients have decreased levels of circulating pDCs and mDCs and total DCs in the blood.[170,171]

DCs are able to modulate atherosclerotic lesion development in many different ways (Figure 11). For instance, DCs invade the vascular wall stimulated by oxLDL, TNF-α and hypoxia, which are commonly found in atherosclerotic lesions.[172,173] Other atherogenic factors such as, oxLDL[174], advanced glycation end products (AGE),[175] nicotine,[176] insulin[177] and angiotensin II[178] lead to further maturation of DCs. Furthermore, during hyperlipidemic conditions, vascular DCs are known to accumulate lipids, adopting a foam cell-like appearance.[179] Moreover, it was shown that DCs play an important role in cholesterol homeostasis. In DC depletion studies, using the CD11c-DTR *Apoe^{-/-}* mouse model, loss of DCs induced higher cholesterol levels in plasma of these mice. These effects were not observed in *CD11b-DTR Apoe^{-/-}* mice with a depletion of monocytes/macrophages, neutrophils, and CD11b^{+} DCs indicating that CD11c^{+} DCs mostly control cholesterol metabolism.[179,180] One of the major roles DCs play in the immune system is antigen presentation and priming of T cells. DCs may interact with T cells in the plaque or in the adventitia. However, it is also possible that they emigrate

27

from the vessel wall towards lymphoid organs and prime T cells there.[181] Studies have shown the importance of DC-T cell interactions in the context of atherosclerosis. For example, a study performed in *Ldlr*^{-/-} mice deficient for the invariant chain of MHCII showed protection against atherosclerosis. This was due to a reduction in activated T cells in the plaque.[182] Furthermore, it was shown that different DC subtypes could control regulatory T cell responses. For instance, the Ccl17 expressing $CD11b^+CD11c^+MHCII^+$ DC subset restrains regulatory T cells, thereby aggravating atherosclerosis.[119] Importantly, patients with CAD show an increased level of serum Ccl17[183] and reduced numbers of peripheral Treg numbers.[184] Using Flt3-deficient mice it was shown that $CD103^+$ cDC numbers where reduced in aortas, that diminished systemic and local regulatory T cell numbers and worsened atherosclerotic burden. This study indicates, that the Flt3-dependent $CD103^+CD11c^+MHCII^+$ cDC subset promotes regulatory T cells and acts anti-atherogenic.[159] pDCs are also able to interfere in atherosclerotic lesion development, but results obtained in different studies came to different conclusions. For instance, in a study using *Ldlr*^{-/-} deficient mice treated with pDC depleting antibodies (PDCA1 neutralizing antibody) in a carotid artery cuff model, mice developed more atherosclerotic lesions.[185] Moreover, in an *Apoe*^{-/-} mouse model reduced atherosclerotic lesions where observed.[166,167] More recently, Sage *et al.* were able to demonstrate that by using CD11c-restricted deletion of the transcription factor Tcf4/E2-2 (required for pDC development and maintenance), pDC deficiency reduced atherosclerotic lesion formation in *Ldlr*^{-/-} chimeras[186]. This phenotype was confirmed in chimeras lacking the pIII and IV promoters of MHC-II transactivator (CIITA) in pDCs, leading to MHC-II-restricted antigen presentation defects in pDCs.[187] Together these findings point towards a pro-atherogenic role for pDCs in experimental atherosclerosis. However, a study performed by Yun *et al.* suggested that pDCs might act tolerogenic and protective in experimental atherosclerosis, decreasing plaque progression *via* induction of Tregs.[188] The authors generated atherosclerotic chimeric mice by transplanting bone marrow from *BDCA2-DTR* mice into *Ldlr*^{-/-} mice. In these mice, the simian diphtheria toxin receptor (DTR) is expressed under the transcriptional control of the human pDC gene promoter BDCA-2.[189] This model allows pDCs to be successfully and selectively depleted 24 h after diphtheria toxin (DT) treatment. Atherosclerotic plaque formation significantly increased in the sinus of pDC-depleted animals.[188]

Interestingly, the authors found that mouse and human aortic pDCs expressed the tolerogenic enzyme indoleamine 2,3-dioxygenase (IDO)-1, suggesting an activated/matured pDC phenotype. Moreover, they showed an interesting correlation between aortic pDCs and Treg numbers with disease progression and proposed a direct functional link between the presence of Indolamin-2,3-Dioxygenase (IDO-1)[+] pDCs and Treg generation in the diseased vessel.[188] However, in a study performed by Mandl *et al.* the authors used *Apoe*^{−/−} *BDCA2-DTR* mice to further investigate the role of pDCs in atherosclerosis.[190] In this study, DT administration to induce pDC depletion for 4 weeks during high-fat diet (HFD) did not affect lesion formation in the aortic sinus. Importantly and surprisingly, a detailed analysis of depletion efficiency demonstrated complete pDC depletion for 1 week only. After 4 weeks of continuous DT administration, pDCs failed to express Diphtheria toxin receptor (DTR) anymore and therefore, could not be depleted.[190] It is possible that crossing of *BDCA2-DTR* mice to *Apoe*^{−/−} mice may have led to altered pDC depletion. However, the results presented by Mandl *et al.* demonstrate that long-term experiments with *BDCA2-DTR* mice have to be evaluated carefully.
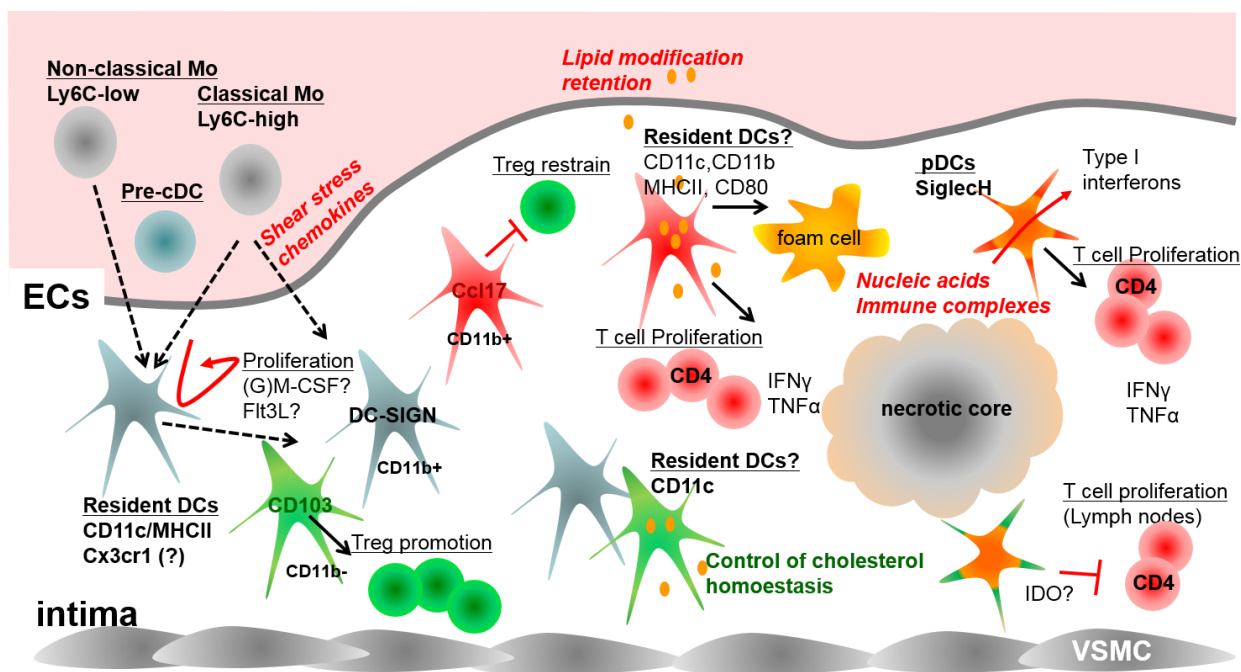
Figure 11. Dendritic cells (DCs) in atherosclerosis. CD11c^{+} DCs can be found in atherosclerotic lesions, and exert different pro-atherogenic and protective functions in disease development. DCs can engulf lipids to adopt a foam cell-like appearance that may constitute the earliest stages of plaque formation. In addition, DCs regulate cholesterol homeostasis and decrease serum very low–density

lipoprotein (VLDL) and low-density lipoprotein (LDL) levels by yet unknown mechanisms. Plasmacytoid DCs (pDCs) promote atherosclerosis by a MHCII-dependent activation of TH1 cell responses and secretion of interferon (IFN) α; a subset of CCL17-expressing CD11b$^+$ DCs restrains Treg responses and drives atherosclerosis; CD103$^+$ classical DCs promote Treg responses and protect from atherosclerosis. (Courtesy of Yvonne Döring)

1.4.3 T cells in atherosclerosis

T cells are an abundantly present leukocyte population in atherosclerotic plaques. Considering their plasticity though, deciphering the role of various T cell subsets in the development of atherosclerosis is not an easy task. Focusing on CD3$^+$CD4$^+$ T helper cells the most abundant subsets present in atherosclerotic plaques is the T$_H$1 cell.[191,192] Differentiation into T$_H$1 subsets requires the transcription factor Tbet and a cytokine milieu containing IL-12 and IL-18 as well as IFN-y (all mainly produced by macrophages; see chapter 1.2.2.1).[193] Studies performed in *Ifn-γR$^{-/-}$Apoe$^{-/-}$* mice showed a 60% reduction in lesion size compared to *Apoe$^{-/-}$* control mice.[194] Furthermore, studies in which A*poe$^{-/-}$* mice where either lacking IL-12[195,196] or IL-18[197,198] showed reduced atherosclerosis compared with control animals, which was accompanied by reduced IFN-γ levels. Consistent with these studies, mice deficient for the transcription factor Tbet showed also reduction of atherosclerotic lesion size by 30%. These results were accompanied by an increase in T$_H$2 cytokine production (IL-4, IL-5 and IL-10) and an increase in IgM natural antibodies.[199]

Since Tbet deficiency increased T$_H$2 cytokine production and T$_H$2 cells are thought to oppose differentiation of T$_H$1 cells it was assumed that T$_H$2 cells ought to be athero-protective. However, studies revealed that defining the role of T$_H$2 cells during atherosclerotic lesion development might be more challenging than for T$_H$1 cells. For instance, the T$_H$2 signature cytokine IL-4 leads to upregulation of CD36 (scavenger receptor class B member 3, important for scavenging oxLDL)[200,201] and class A scavenger receptor (important for scavenging oxLDL and collagens) on macrophages,[202] as well as upregulation of vascular cell adhesion molecule 1 (VCAM-1)[203,204] and matrix metalloproteinase (MMP) 1,[205] which would all indicate an atherogenic phenotype. On the other hand, studies performed on *Il4$^{-/-}$Apoe$^{-/-}$* mice have shown no difference in plaque burden. Regarding one other T$_H$2 signature cytokine, IL-5, it could be shown that bone marrow transplantation studies, where *Ldlr$^{-/-}$* mice were reconstituted with *Il5$^{-/-}$* bone marrow had increased plaque size compared to control

mice. This was due to reduced amounts of plasma natural IgMs. Natural IgMs act as blocking antibodies against modified lipoproteins such as oxLDL.[206]

The role of T_H17 cells in atherosclerosis is still controversial. As mentioned before, T_H17 cells are induced in the presence of IL-6 and TGF-β and are known to secret IL-17 and IL-22. In general IL-17 signaling leads to the production of TNF, IL-1β,[207,208] IFN-γ[209] as well as G-CSF (Granulocyte-colony stimulating factor).[210] All together these are pro-inflammatory mediators that would suggest that T_H17 cells play an atherogenic role. Animal models of atherosclerosis show conflicting results. For instance, studies performed in *Apoe*^{-/-} mice using a rat-anti mouse IL-17A antibody show 50% reduction in aortic root lesions. Interestingly, this study did not show any evidence of reduced IL-17A signaling, which could explain a reduction in atherosclerotic lesion formation.[207,211] In another experiment performed by Cheng *et al.*, the authors used a mouse-anti mouse IL-17A. In this study, the authors did not observe any changes in atherosclerotic lesion size, although they found reduced levels of IL-17A.[211] Results obtained from *knock out* studies showed also conflicting results depending on the mouse model used to study atherosclerotic lesion development. *Il17a*^{-/-}*Ldlr*^{-/-} mice displayed no difference in atherosclerotic lesion size compared to their controls,[209] whereas *Il17a*^{-/-}*Apoe*^{-/-} mice showed a reduction of 35 % compared to the control group.[212] Regarding human studies, patient data revealed a possible atherogenic role of T_H17 cells since patients with unstable angina have increased levels of IL-17A as well as IL-6 and IL-23.[213,214] Thus, the role of T_H17 cells and its signature cytokine IL-17 in the development of atherosclerosis has to be further elucidated.

Tregs are known as immune suppressor cells and are a subpopulation of $CD4^+$ T helper cells. They are characterized as $CD3^+CD4^+CD25^+$ and $Foxp3^+$. Tregs are able to negatively regulate pro-inflammatory immune effects through a variety of mechanisms, e.g. via secretion of their signature cytokines IL-10, IL-35 and TGF-β (Figure 12). Antibody depletion of TGF-β (targeting TGFβ-1, -2 and -3) promotes atherosclerotic lesion formation through increased numbers in pro-inflammatory cells. For instance, the lesion cross-sectional area occupied by $MOMA-2^+$ macrophages increased in anti-TGF-β-treated mice when compared to control mice. Furthermore, reduction of collagen content in the plaque was observed in the anti–TGF-β–treated mice when compared to the control group. [215,216] IL-10 is known to have a protective role in atherogenesis. IL-10-

deficiency in mice results in three fold increased atherosclerotic lesions, accompanied by a 2.5 fold increase in CD3^{+} T-cell infiltration, strong IFN-γ expression, and decreased collagen content. Furthermore, *in vivo*, transfer of murine IL-10 achieved 60% reduction in lesion size.[217,218,219] The Treg cytokine IL-35 is known to suppress T effector cell mechanisms and induces the secretion of IL-10 thereby acting protective during atherogenesis[220]. *In vitro* studies also revealed that Tregs are able to inhibit foam cell formation and skewed macrophages into an M2-like, anti-inflammatory phenotype.[221,222] Furthermore, Tregs are known to suppress B cell responses (Figure 12).[223] B cell depletion in *Apoe*^{−/−} mice using anti-CD20 neutralizing antibodies reduced atherosclerosis lesion formation. Furthermore, adoptive transfer of conventional B2 B cells but not B1 B cells to an *Apoe*^{−/−}*Rag-2*^{−/−} deficient (lymphocyte deficient) mouse that was fed a high-fat diet increased atherosclerosis by 72%.[224] In this study levels of IgG, IgM and total Ig´s did not differ. The increased size of atherosclerotic lesions in mice which received adoptively transferred B2 B cells was attributed to elevated levels of TNF-α in these mice. Though, the inhibition of B cells by Tregs might be one mechanism underlying the protective effect of Tregs during atherosclerosis.[225] Tregs show anti-inflammatory effects on endothelial cells leading to a decrease in expression of adhesion molecules and recovery of endothelial function (Figure 12).[226] Other studies also revealed beneficial effects of Tregs regarding foam cell formation, showing that Tregs reduced macrophage and lipid content in atherosclerotic plaques and increased smooth muscle cell numbers. These findings were accompanied by higher levels of collagen as well as reduced expression of pro-inflammatory cytokines and MMPs in the lesion.[227] Interestingly, Tregs are of very low abundance in atherosclerotic plaques (1-5 % of all T cells) compared to other chronically inflamed tissues (approx. 25% of all T cells in eczema or psoriasis).[228,229] A study performed on a prospective cohort consisting of a random sample of participants (n=700), aged 68 to 73 years, in Sweden showed low numbers of circulating regulatory T cells correlated with development of myocardial infarction and for coronary events in general.[230]
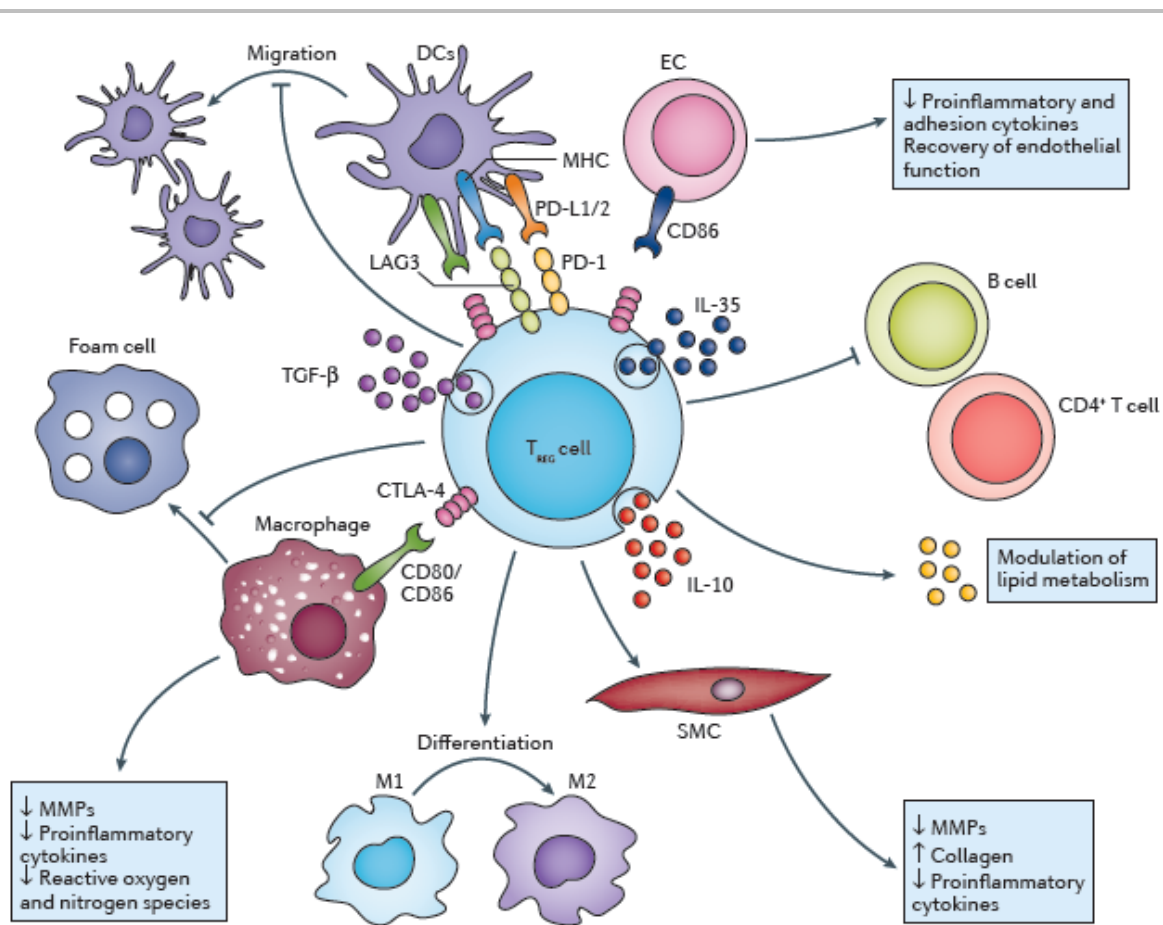
Figure 12. Mechanisms of Treg cell-mediated suppression and the implicative pathways. The mechanisms by which Tregs mediate their suppression can be classified into two major categories: cell-contact-independent mechanisms (production of inhibitory cytokines, deprivation of IL-2 and ATP/ADP) and cell-contact-dependent mechanisms (induction of cytolysis, modulation of APCs). CTLA-4, cytotoxic T lymphocyte-associated antigen-4; DC, dendritic cell; ITAM, immunoreceptor tyrosine-based activation motif; LAG3, lymphocyte activation gene 3; MHC, major histocompatibility complex; TGF, transforming growth factor; TREG cell, regulatory T cell (copied from Meng *et al.*).[225]

2. Materials and methods

2.1. Materials

2.1.1 General equipment

Table 1: General equipment

equipment	source
autoclave	Systec 2540EL (Systec, Wettenberg, Germany)
balance	Analytical Plus, (Ohaus, Pine Brook, NJ, USA)
centrifuges	Eppendorf 5427R (Eppendorf, Hamburg, Germany), Heraeus Laborfuge 400 and Heraeus Multifuge 3 S-R (Heraeus, Osterode,Germany) Eppendorf 5920R (Eppendorf, Hamburg, Germany)
flow cytometers	FACSCantoII, FACSAria (BD Biosciences, San Jose, CA, USA)
fluorescence plate reader	SpectraFluor Plus (Tecan, Crailsheim, Germany)
laminar flow hood	Herasafe (Heraeus, Osterode, Germany)
microscopes	Olympus IX71 and BX51 (Olympus Optical, Hamburg, Germany), Leica DMLB (Leica, Wetzlar, Germany)
pH-meter	InoLab level 1 (WTW, Weilheim, Germany)
spectrometer	NanoDrop (Peqlab, Erlangen, Germany)
Irradiator	Faxitron (Tucson, USA)
Incubator	Thermo Fisher Scientific (Waltham, USA)
BIAcore	GE - BIAcore, AB (Uppsala, Sweden)
Luminex ™ xMAP	Luminex Corp. (Austin, USA)

2.1.2 Consumables

Table 2: Consumables

consumables	source
96well plates flat, round bottom	Corning, New York, USA
cannulas 23G, 27G	BD, Franklin Lakes, USA
cell strainer	BD, Franklin Lakes, USA
disposable scalpel	Feather Safety Razor Co., Osaka, Japan

FACS-tubes	BD, Franklin Lakes, USA
microscope slides	Thermo Scientific, Braunschweig, Germany
microtubes EDTA, with clot activator for sera	Sarstedt, Nümbrecht, Germany
glassware	Schott, Mainz, Germany
reaction cups 1,5ml, 2,0ml	Eppendorf, Hamburg, Germany
reaction tubes 15ml, 50ml	Sarstedt, Nümbrecht, Germany
serological pipettes 5ml, 10ml, 25ml	Sarstedt, Nümbrecht, Germany
sterile filter-tips	Starlab, Ahrensburg, Germany
syringes 2ml, 5ml, 10ml, 20ml	BD, Franklin Lakes, USA
syringes 1ml	Braun, Melsungen, Germany

2.1.3 Buffers, chemicals, media, solutions

If not mentioned otherwise, protocols were adapted from standard protocols [ref 159]. Solutions were prepared with Millipore water (Milli-Q Plus ultrapure purification, Millipore, MA). If not stated otherwise, chemical reagents were obtained either from Fulka (Buchs, Switzerland), Sigma-Aldrich (Deisenhofen, Germany) or Roth (Karlsruhe, Germany).

Table 3: Buffers chemicals, media and solutions

Buffer/Solution/Medium	Composition
FACS staining buffer	2% mouse serum; 2% rabbit serum (both Sigma-Aldrich, St. Louis, USA); 2% human serum (Innovative Research, Novi, USA); 2% bovine serum albumin (BSA) (Serva, Heidelberg, Germany); dissolved in PBS
Hank´s complete	HBSS (Thermo Fisher Scientific (Gibco) Waltham, USA), 0,3mM diNaEDTA, 0,1% BSA
Lysis buffer	150mM NH_4Cl; 10mM $KHCO_3$; 0,1mM diNaEDTA, pH 7,4
Phosphate buffered saline (PBS)	w/o Ca^{2+} and Mg^{2+}, sterile (Thermo Fisher Scientific (Gibco) Waltham, USA), pH 7,4
RPMI Medium	RPMI1640 (Thermo Fisher Scientific (Gibco) Waltham, USA); 10% fetal calf serum (FCS) (Thermo Fisher Scientific (Gibco) Waltham, USA)
Paraformaldehyde	4% Paraformaldehyde, 5% Sucrose, 0,02M EDTA, pH 7,4
ELISA Stop	2N sulfuric acid
ELISA Wash	10 mM phosphate buffer pH 7.4, 150 mM NaCl, 0.05% Tween 20
MACS Buffer	phosphate-buffered saline (PBS), 2% fetal calf serum

	(FCS) (Thermo Fisher Scientific (Gibco) Waltham, USA), 1 mM EDTA
DEMEM Medium	DEMEM (Thermo Fisher Scientific (Gibco) Waltham, USA); 10% fetal calf serum (FCS) (Thermo Fisher Scientific (Gibco) Waltham, USA)

2.1.4 Peptides, antagonists and antibodies

Peptides, antagonists and antibodies used for different experimental setups are listed below in tables 4-8. Antagonists were all obtained from Tocris bioscience (Bristol, United Kingdom). If not stated otherwise, all antibodies used (table 5) were reactive to mouse.

Table 4: Peptides

Peptide	Manufacturer
rmCcl17 (TARC)	BioLegend, San Diego, USA
rmTgf-ß	BioLegend, San Diego, USA
rmCcl3	Peprotech, Hamburg, Germany
rmCcl1	Peprotech, Hamburg, Germany
rmCcl18	Peprotech, Hamburg, Germany
rmCcl20	Peprotech, Hamburg, Germany
CCR8 (Human) Proteoliposome	Abnova, Taipei City, Taiwan

Table 5: Antagonists

Antagonist	Type	Specific against
C021 Dihydrochloride	Small molecule	Chemokine (C- C motif) receptor 4
DAPTA	Peptide	Chemokine (C-C motif) receptor 5
J113863	Small molecule	Chemokine (C-C motif) receptor 1

Table 6: Primary antibodies

Antibody	Specificity	Conjugate	Application	Manufacturer
Anti-Mac-2	Mouse/Human Mac-2 (Galectin-3)	unconjugated	IHC	Cedarlane, Burlington, Canada
Anti-Actin, α-Smooth Muscle	Mouse Actin, α-Smooth Muscle	FITC	IHC	Sigma-Aldrich, St. Louis, US
Anti-FoxP3	mouse Foxp3	unconjugated	IHC	Abcam, Cambridge, UK
Anti-Ccl3	mouse Ccl3/Mip-	unconjugated	IHC	Abcam,

Anti- Ccl5	1a mouse Ccl5/RANTES	unconjugated	IHC	Cambridge, UK BioTechne, Minneapolis, US
Anti-Ccl17	mouse Ccl17/TARC	unconjugated	IHC	R&D System, Minneapolis, US
Anti-Ccl1	mouse Ccl1	unconjugated	IHC	Biorbyt, Cambridge, UK
Anti-Ccl3	mouse Ccl3	unconjugated	IHC	R&D Systems, Minneapolis, US
Anti-Ccr8	mouse Ccr8	unconjugated	IHC	GeneTex, Irvine, USA
Anti-Ccr5	mouse Ccr5	unconjugated	IHC	Santa Cruz Biotechnology, Dallas, USA
Anti-Ccr4	mouse Ccr4	unconjugated	IHC	Thermo Fisher Scientific Waltham, USA

IHC: Immunohistochemistry

Table 7: Primary antibodies

Antibody	Specificity	Conjugate	Application	Manufacturer
Anti-CD25	Regulatory T cells	APC	FC	Thermo Fisher Scientific (eBioscience)
Anti-CD115	Monocytes, Macrophages	PE	FC	Thermo Fisher Scientific (eBioscience)
Anti-CD11b	Neutrophils, Monocytes, Macro-phages	PerCP, PE-Cy7	FC	Thermo Fisher Scientific (eBioscience)
Anti-CD11c	Dendritic cells	PE-Cy7	FC	Thermo Fisher Scientific (eBioscience)
Anti-B220	B-cells, Plasmacytoid DCs	PerCP, PE-Cy7	FC	Thermo Fisher Scientific (eBioscience)

Anti-CD3	T-cells	FITC	FC	Thermo Fisher Scientific (eBioscience)
Anti-CD45	All Leukocytes	APC-Cy7	FC	Thermo Fisher Scientific (eBioscience)
Anti-CD4	T helper cells	V500	FC	BD Biosciences, Franklin Lakes, USA
Anti-CD8	Cytotoxic T cells	eF450	FC	Thermo Fisher Scientific (eBioscience)
Anti-FoxP3	Regulatory T cells	PE	FC	Thermo Fisher Scientific (eBioscience)
Anti-MHC-II	Dendritic Cells, Macrophages, B cells	V500	FC	BD Biosciences, Franklin Lakes, USA
Anti-PDCA-1	Plasmacytoid DCs	PE	FC	BD Biosciences, Franklin Lakes, USA
Anti-F4/80	Macrophages	PE	FC	Thermo Fisher Scientific (eBioscience)
Anti-Gr-1 (Ly6C and Ly6G)	Neutrophils and one subset of mouse Monocytes	APC	FC	Thermo Fisher Scientific (eBioscience)
Anti-SiglecH	Plasmacytoid DCs	eF450	FC	Thermo Fisher Scientific (eBioscience)
Anti-CD301	M2 Macrophages	APC	FC	Biorad, Hercules, USA

FC: Flow Cytometry

Table 8: Secondary antibodies

Antibody	Specificity	Conjugate	Application	Manufacturer
Anti- Rabbit IgG	Rabbit	FITC	IHC	Dianova, Hamburg

Anti- Rat IgG	Rat	Cy3	IHC	Sigma-Aldrich, St. Louis, US

IHC: Immunohistochemistry

2.1.5 Reagent kits and miscellaneous

Table 9: Reagent kits and miscellaneous

Kit	Purpose	Manufacturer
Cytokine & Chemokine 26-Plex Mouse ProcartaPlex™ Panel 1	assessing multiple protein biomarkers in a single sample	Thermo Fisher Scientific (eBioscience) Waltham, USA)
Ccl3 Mouse Uncoated ELISA Kit with Plates	accurate and precise measurement of mouse Ccl3 protein levels	Thermo Fisher Scientific (eBioscience) Waltham, USA
Mouse Ccl17 Quantikine ELISA Kit	accurate and precise measurement of mouse Ccl3 protein levels	R&D Systems, Minneapolis, US
CD11c MicroBeads UltraPure, mouse	isolation of mouse DCs from single-cell suspensions from lymphoid tissues	Miltenyi Biotec GmbH, Bergisch Gladbach, Germany
CD4$^+$CD62L$^+$ T Cell Isolation Kit II, mouse	isolation of mouse CD4$^+$CD62L$^+$ T helper cells from spleen and lymph nodes	Miltenyi Biotec GmbH, Bergisch Gladbach, Germany
CD4$^+$ T Cell Isolation Kit, mouse	isolation of mouse CD4$^+$ T cells from spleen and lymph nodes	Miltenyi Biotec GmbH, Bergisch Gladbach, Germany
CD4$^+$CD25$^+$ Regulatory T Cell Isolation Kit, mouse	solation of CD4$^+$CD25$^+$ regulatory T cells (Treg) from single-cell suspensions of mouse spleen and lymph nodes	Miltenyi Biotec GmbH, Bergisch Gladbach, Germany
Monocyte Isolation Kit mouse	isolation of monocytes from single-cell suspensions of mouse spleens	Miltenyi Biotec GmbH, Bergisch Gladbach, Germany
Duolink® In Situ Red Goat/Rabbit	Detection and quantification of protein interactions and their	Sigma-Aldrich, St. Louis, US

	modifications	
Foxp3 / Transcription Factor Staining Buffer Set	staining with antibodies to transcription factors and nuclear proteins	Thermo Fisher Scientific (eBioscience) Waltham, USA)
CountBright™ Absolute Counting Beads, for flow cytometry	Calculation of absolute cell numbers in flow cytometry	Thermo Fisher Scientific (life technologies) Waltham, USA)

2.1.6 Mice

Wild-type (*wt*) C57BL/6 and Apolipoprotein E-deficient (*Apoe*$^{-/-}$) mice were obtained from the local animal breeding facility (Zentrale Versuchstierhaltung Innenstadt (ZVH), Klinikum der Universität München) or purchased at Charles River, England or Janvier, Belgium. Mice deficient for different chemokine receptors and ligands were all received from the in-house animal facility of the Clinic of the University of Munich. All strains used are summarized in table 10 and were backcrossed for at least ten generations in their stated genetic background. All mouse strains deficient for a chemokine receptor or ligand are furthermore deficient for Apolipoprotein E.

Table 10: Mouse strains

Gene Name	Abbreviation	Background	Mutation	Origin
Wildtype	*Bl6 wt*	C57/Bl6	None	Jackson Laboratories (Bar Harbor, USA)
Apolipo-protein E	*Apoe*	C57/Bl6	Targeted mutation (Knock-out)	Jackson Laboratories (Bar Harbor, USA)
Chemokine (C-C motif) receptor 1	*Ccr1*	C57/Bl6	Targeted mutation (Knock-out)	Gao *et al.* *J Exp Med.* 1997 PMID: 9166425
Chemokine (C-C motif) receptor 4	*Ccr4*	C57/Bl6	Targeted mutation (Knock-out)	Chvatchko *et al.* *J Exp Med.* 2000 PMID: 10811868
Chemokine (C-C motif) receptor 5	*Ccr5*	C57/Bl6	Targeted mutation (Knock-out)	Kuziel *et al.* *Atherosclerosis.* 2003 PMID: 12618265
Chemokine (C-C) ligand	*Ccl17*	C57/Bl6	Targeted mutation	Lieberam, Förstner *Eur J Immunol.* 1999

17			(GFP reporter Knock-in)	PMID: 12615900
Chemokine (C-C) ligand 3	*Ccl3*	C57/Bl6	Targeted mutation (Knock-out)	Cook *et al. Science.* 1995 PMID: 7667639
Chemokine (C-C) ligand 5	*Ccl5*	C57/Bl6	Targeted mutation (Knock-out)	Makino *et al. Clin Immunol.* 2002 PMID: 11890717

2.2. Methods

2.2.1. *In vivo* experiments

2.2.1.1. Mouse models

Ccr4$^{-/-}$ mice were kindly provided by PD Dr. med. David Anz (Ludwig-Maximilians-Universität, München, Germany), whereas the *Ccl17*$^{e/e}$ mice were generously provided by I. Förstner (Universität Bonn, Germany). *Ccl3*$^{-/-}$ mice were purchased from the Jackson Laboratories (Bar Harbor, USA). *Ccr1*$^{-/-}$ mice and *Ccr5*$^{-/-}$ mice were bread in house. *Ccr4*$^{-/-}$, *Ccr1*$^{-/-}$, *Ccr5*$^{-/-}$, *Ccl17*$^{e/e}$ and *Ccl3*$^{-/-}$ mice were crossed with *Apoe*$^{-/-}$ mice, purchased from the Jackson Laboratories (all C57BL/6J background). *Apoe*$^{-/-}$, *Apoe*$^{-/-}$ *Ccr4*$^{-/-}$, *Apoe*$^{-/-}$*Ccl17*$^{e/e}$, *Apoe*$^{-/-}$*Ccl3*$^{-/-}$ were fed normal chow.

2.2.1.2. Mouse models of atherosclerosis

For atherosclerosis studies, mice were fed an atherogenic high-fat diet (HFD) containing 21% fat and 0.15-0.2% cholesterol (Altromin 132010, Sniff TD88137), starting at 8-10 weeks of age for 12 weeks, after which they were sacrificed. Experiments were approved by local authorities and complied with German animal protection law. Every effort was made to minimize suffering. Hearts, aortic arches, aortas, blood, bone marrow, lymph nodes (axillar, mesenteric, inguinal and para-aortic), and spleens were harvested. Hearts, aortic arches and aortas were fixed in 4 % PFA for further histological and immunohistological analysis of atherosclerotic lesion size and composition.

2.2.1.3. Bone marrow transplantation

Bone marrow cells (3×10^6/mouse) from C57BL/6 *Apoe*$^{-/-}$ mice or from *Apoe*$^{-/-}$ *Ccr4*$^{-/-}$ mice were flushed from femur and tibia cavities and subsequently administered to

C57BL/6 *Apoe*$^{-/-}$ recipient mice by lateral tail vein injection one day after a lethal dose of whole-body irradiation (2x 6.5 Gy). After four weeks of recovery, the mice were placed on HFD for up to 12 weeks as mentioned under 2.2.2.

2.2.1.4. Cell culture

Cell culture was performed under sterile conditions in a laminar flow hood. Cells were maintained in a CO_2-incubator at 37°C and a humidified 5% CO_2 atmosphere. Cells were cultured in growth medium (RPMI 1640) supplemented with 10% (v/v) fetal calf serum (FCS), 2 mM L-glutamine and penicillin (100 U/mL)/streptomycin (100 µg/mL) (Thermo Fisher Scientific (Gibco) Waltham, USA) to avoid contamination with bacteria. FCS was incubated at 56°C for 30 min to inactivate the complement system and stored at -20°C until use. All media and solutions used for cell culture were from Gibco if not stated otherwise and purchased sterile or sterilized through a 0.2 µm filter. Cultured cells were regularly tested to be mycoplasma free by the VenorGeM Mycoplasma detection kit (Minerva Biolabs, Berlin, Germany).

2.2.1.5. Preparation of primary cell suspensions

For flow cytometric analysis of **lymph nodes** (axillary, inguinal, para-aortic, and mesenteric) or **spleen** organs were pressed through a 70-µM cell strainer. Cells isolated from spleen were lysed with red blood cell lysis buffer for 5 min. **Bone marrow (BM)** cells were extracted from the tibia and femur with Hank's complete solution using a 1 ml syringe and 23-gauge needle. The single cell suspension was centrifuged and the pellet resuspended in about 1 ml RBC lysis buffer for 5 min. Whole **blood** obtained from the retro-orbital plexus of mice was EDTA-buffered and subjected to red-cell lysis for 15 min in 5 ml RBC lysis buffer, followed by 2 wash steps in Hank's complete solution. Cells were then used for further analysis

2.2.1.6. Isolation of CD4$^+$ T cells

CD4$^+$T cells were isolated from secondary lymphoid organs via depletion of non-CD4$^+$T cells. For this purpose, the CD4$^+$T cell Isolation Kit (containing a cocktail of biotin-conjugated Abs against CD8a, CD45R, CD11b, CD49b and Ter-119, as well as magnetic anti-biotin MicroBeads) and a separation column (all Miltenyi Biotec) were used according to the recommended protocol, allowing a negative selection of CD4$^+$T

cells. Briefly, the freshly isolated secondary lymphoid organ cells were mixed with the cocktail of biotin-conjugated antibodies (Abs) and incubated for 10 min at 4°C. After washing with MACSbuffer, the cells were mixed with magnetic anti-biotin microbeads, incubated for 15 min at 4°C, washed and loaded onto the separation column. The magnetically labeled cells were retained in a separation column placed in a magnetic field, whereas cells were recovered in the eluate and cultured in cell culture medium for further analysis.

2.2.1.7. Isolation of CD4$^+$CD25$^+$ regulatory T cells

The isolation is performed in a two-step procedure. At first, non-CD4$^+$ are indirectly magnetically labeled with a cocktail of biotin-conjugated antibodies against CD8, CD11b, CD45R, CD49b, Ter-119 and Anti-Biotin MicroBeads as mentioned under **2.2.1.6.** The labeled cells are subsequently depleted over a separation column. The flow-through fraction contains pre-enriched CD4$^+$ T cells which in a second step, can be labeled with CD25 MicroBeads (all Miltenyi Biotec) for subsequent positive selection of CD4$^+$CD25$^+$ regulatory T cells (Tregs).

2.2.1.8. Isolation of CD4$^+$CD62L$^+$ naive T cells

Mouse naive CD4$^+$ T cells are isolated by depletion of memory CD4$^+$ T cells and non-CD4$^+$ T cells. Single-cell suspensions of mouse spleen or lymph nodes are indirectly magnetically labeled with a cocktail of biotinylated monoclonal antibodies, and anti-biotin MicroBeads, as secondary labeling reagent as mentioned under **2.2.1.6.** Subsequently, CD4$^+$CD62L$^+$ T cells are positively selected from the enriched CD4$^+$ T helper cell fraction with CD62L (L-selectin) MicroBeads (all Miltenyi Biotec).

2.2.1.9. Isolation of CD11c$^+$ dendritic cells

For the isolation of CD11c$^+$ DCs cells from spleens and LN of *wt* mice cell suspensions were incubated with CD11c MicroBeads (Miltenyi) for 15 min at 4°C, washed and loaded onto the separation column. The CD11c$^+$ DCs retained in the separation column and could be eluted after the column was removed from the magnetic field. Furthermore, eGFP$^+$*Ccl17$^{e/+}$* and eGFP$^+$*Ccl17$^{e/e}$* DCs were sorted using a BD FACSAria (BD). For this purpose single-cell suspensions of mouse (either *Apoe$^{-/-}$Ccl17$^{e/e}$* or *Apoe$^{-/-}$*

Ccl17^{e/+}) lymph nodes were stained with Antibodies against CD45, CD11c, MHCII and eGFP.

2.2.1.10. Isolation of monocytes

Using the Monocyte Isolation Kit mouse (all Miltenyi Biotec), monocytes are isolated by depletion of non-target cells. Non-target cells are indirectly magnetically labeled with a cocktail of biotin-conjugated monoclonal antibodies, as primary labeling reagent, and anti-biotin monoclonal antibodies conjugated to MicroBeads as secondary labeling reagent. The unwanted cells are depleted by retaining them within a separation Column in a magnetic field, while the unlabeled monocytes pass through the column.

2.2.1.11. Isolation of neutrophils

Neutrophils are isolated by depletion of non-target cells using the Miltenyi Neutrophil isolation kit. Non-target cells are indirectly magnetically labeled with a cocktail of biotin-conjugated monoclonal antibodies, as primary labeling reagent, and anti-biotin monoclonal antibodies conjugated to MicroBeads as secondary labeling reagent. The unwanted cells are depleted by retaining them within a separation Column in a magnetic field, while the unlabeled monocytes pass through the column.

2.2.2. Protein assays

2.2.2.1. Analysis of atherosclerotic lesion using histology

For analysis of mouse atherosclerotic lesions, the aortic root and the thoraco-abdominal aorta were stained for lipid depositions with Oil-Red-O. In brief, hearts with aortic root were fixed with 4% paraformaldehyde and embedded in Tissue-Tek O.C.T. compound (Sakura) for cryo-sectioning. Atherosclerotic lesions were quantified in 4 μm transverse plane sections and averages were calculated from 3 sections. The thoraco-abdominal aorta was fixed with 4% paraformaldehyde and opened longitudinally, mounted on glass slides and *en face*-stained with Oil-Red-O. The aortich arch was stained using Haematoxylin-Eosin (HE) staining. Aortic arches with main branch points (brachiocephalic artery left subclavian artery and left common carotid artery) were fixed with 4% paraformaldehyde and embedded in paraffin. Lesion size was quantified after HE-staining of 4 coronal plane sections.

2.2.2.2. Analysis of the cellular composition of atherosclerotic lesion using immunohistochemistry

For analysis of the cellular composition or inflammation of atherosclerotic lesions, aortic root sections were stained with an antibody to Mac2 (AbD Serotec) and SMA (Dako). Nuclei were counter-stained by 4',6-Diamidino-2-phenylindol (DAPI). After incubation with a secondary FITC- or Cy3-conjugated antibody (Life Technologies), sections were analyzed using a Leica DMLB fluorescence microscope and charge-coupled device (CCD) camera. Blinded image analysis was performed using Diskus, Leica Qwin Imaging (Leica Lt.) or Image J software. For each mouse and staining, 3 root sections were analyzed and data were averaged.

2.2.2.3. Laboratory parameters and flow cytometry

Leukocyte counts in blood were determined using a Celltac Automated Hematology Analyzer (Nihon Kohden) or counting beads (Invitrogen) during flow cytometry analysis. Differential white blood cell counts were performed by flow cytometric analysis. For flow cytometry analysis primary cell suspensions from lymph nodes, spleen, bone marrows and whole blood were made as described under 2.2.1.5 Leukocyte subsets were analyzed using the following combination of surface markers: neutrophils ($CD45^+CD11b^+CD115^-Gr1^{high}$), monocytes ($CD45^+CD11b^+CD115^+$), classical monocytes (GR1high monocytes), non-classical monocytes ($GR1^{low}$ monocytes), conventional dendritic cells ($CD45^+CD11c^+MHCII^+$) plasmacytoid dendritic cells ($CD45^+B220^+SigH^+$), B-cells ($CD45^+B220^+$), T-cells ($CD45^+CD3^+$), cytotoxic T cells ($CD45^+CD3^+CD8^+$), T helper cells ($CD45^+CD3^+CD4^+$). Regulatory T cells (Tregs) were classified as $CD45^+CD3^+CD4^+CD25^+Foxp3^+$, whereas Foxp3 was stained using the Foxp3/ Transcription Factor Staining Buffer Set (eBioscience). Cell populations and marker expression were analyzed using a FACSCanto-II, FACSDiva software (BD Biosciences) and the FlowJo analysis program (Treestar). Cholesterol and triglyceride levels in mouse plasma or serum were measured using enzymatic assays (Roche).

2.2.2.4. Enzyme-Linked Immunosorbent Assay (ELISA)

The enzyme-linked immunosorbent assay (ELISA) is an easy method to detect and quantify an antigen (e.g. proteins such as cytokines or chemokines) within nearly every

type of biological fluid e.g. serum, cell culture supernatant or lavage. All Kits used during this thesis were based on the principle of a sandwich ELISA.

The mechanism of a sandwich ELISA is based on a purified Ab specific for the antigen of interest (capture antibody) which is pre-coated onto a microplate. Samples and standards are added onto and bind the plate bound capture antibody. After several washing steps the detection antibody is added, and also binds to the antigen. After further washing steps an enzyme-linked secondary antibody is added which binds the detecting antibody. After adding a specific substrate the enzyme reaction leads to a blue product that turns yellow when the 2 N sulfuric acid stop solution is added. The intensity of the color measured is in proportion to the amount of antigen bound in the initial step. The sample values are then read of a standard curve. Mouse plasma and cell culture supernatants were analyzed using the "Ccl3 Mouse Uncoated ELISA Kit with Plates" (Thermo Fisher Scientific (eBioscience) Waltham, USA).

2.2.2.5. ProcartaPlex Bead assays

ProcartaPlex Bead assays enable assessing multiple targets in a single biological sample (cell/tissue culture supernatants, serum, and plasma). The ProcartaPlex assays use the Luminex™ xMAP technology for multi-analyte detection of secreted proteins including cytokines, chemokines, growth factors and other proteins. Cell culture supernatants and mouse plasma were analyzed for various cytokines using the "Cytokine & Chemokine 26-Plex Mouse ProcartaPlex™ Panel 1" (Thermo Fisher Scientific (eBioscience) Waltham, USA), sample preparation and analysis was performed according to the manufacturer's protocol. The kit allows the simultaneous detection and quantification of soluble murine IFN gamma; IL-12p70; IL-13; IL-1 beta; IL-2; IL-4; IL-5; IL-6; TNF alpha; GM-CSF; IL-18; IL-10; IL-17A; IL-22; IL-23; IL-27; IL-9; GRO alpha; IP-10; MCP-1; MCP-3; MIP-1 alpha; MIP-1 beta; MIP-2; RANTES; Eotaxin. The bead-based assay follows the principles of a sandwich immunoassay. Fluorescent magnetic beads are coupled with antibodies specific to the analytes to be detected. Beads are differentiated by their sizes and distinct spectral signature (color-coded) by flow cytometry using the Luminex™ xMAP.

2.2.2.6. Surface plasmon resonance (SPR)

SPR was performed on a BIAcore X100 instrument (GE Healthcare Europe GmbH, Freiburg, Germany) using neutravidin-modified C1 sensor chips.[231] Biotinylated chemokine CCL17 was immobilized on flow cells to $0.3-1.3 \times 10^3$ response units (RU). Screening of chemokine receptor binding with CCR8 proteoliposomes was performed starting at a concentration of 100 nM in HBS-EP+ buffer at 90 µl/min after 20 s. Apparent affinities were calculated from on and off rates after fitting of the curves obtained from increasing analyte concentrations using a 1:1 Langmuir interaction model (BIAevaluation software, GE Healthcare).

2.2.2.7. Proximity ligation assay

Proximity ligation was carried out using the Duolink In Situ Red Kit Goat/Rabbit on PFA fixated mouse dendritic cells cultured on collagen-coated cover slips which were pre-incubated with mouse Ccl1 and Ccl17 (BioLegend) alone using primary polyclonal antibodies to mouse Ccl17 (R&D, AF529), mouse Ccl1 (Acris, AP20618PU-N), mouse Ccr1 (Biorbyt), mouse Ccr4 (Thermo Scientific) and mouse Ccr8 (Abcam) according to the manufacturer's instructions. Imaging was performed using fluorescence microscopy (Leica DM4000, Germany) after which deconvolution algorithms for wide field microscopy were applied to improve overall image quality (Huygens professional 16.10; SVI, the Netherlands). The number of Duolink detected interactions was determined in the processed images using the Leica LAS 4.2 analyses software. In order to more accurately resolve the interactions detected with Duolink, representative dendritic cell samples of each condition were also visualized with a Leica SP8 3X microscope (Germany) using a combination of 3D confocal microscopy (DAPI) and 3D STED nanoscopy (Duolink Red). Image processing and deconvolution of the resultant 3D datasets was performed using the Leica LAS X and Huygens professional software packages.

2.2.3. Functional assays

2.2.3.1. Transmigration assays

Transmigration assays were performed using Transwell-96 Permeable Support plates (Corning) with a 3.0 µm pore size. Murine rCcl17 (BioLegend) was added to bottom

chambers at a concentration of 100 ng/mL in RPMI-1640 medium containing 0.5% BSA. Naïve CD4$^+$ spleen and LN T cells were obtained by immunomagnetic isolation (Miltenyi Biotec) (refer to 2.2.1.6.) and activated via plate bound α-CD3 (10 µg/ml, 50 µl per well, 4 °C overnight) and soluble α-CD28 (1 µg/ml) (both eBioscience). Activated CD4$^+$ T cells (2x10^5) were allowed to migrate for 2 h from the top chamber. Ccr4 receptor antagonist C021 Dihydrochloride (Tocris) was added at a concentration of 0,5 µM to top chambers. The number of cells migrated was analyzed by flow cytometry (FACSCanto II, BD Biosciences) and FlowJo v.10 software (Tree Star Inc.). The chemotactic index was calculated as the ratio of chemokine-stimulated to unstimulated migration.

2.2.3.2. T effector polarization assays

Naive CD62L$^+$CD4$^+$ spleen and LN cells were obtained by immunomagnetic isolation (Miltenyi Biotec) (refer to 2.2.1.8). CD4$^+$T cells (1 × 10^5) were cultured in 96-well tissue round bottom culture plates in the presence of 3 µg/ml anti-CD3e, α-CD28 (1 µg/ml) and supplemented with TGF-β (5 ng/ml) in the presence or absence of Ccl3 (100 ng/mL) for 3 days. The number of regulatory T cells was analyzed by flow cytometry (FACSCanto II, BD Biosciences) and FlowJo v.10 software (Tree Star Inc.).

2.2.3.3. Co culture experiments

Isolated *wt,* EGFP$^+$ *Ccl17$^{e/e}$, Ccr4$^{-/-}$* , *Apoe$^{-/-}$*, *Apoe$^{-/-}$Ccl3$^{-/-}$,* EGFP$^+$ *Apoe$^{-/-}$Ccl17$^{e/+}$* and EGFP$^+$ *Apoe$^{-/-}$Ccl17$^{e/e}$* DCs (refer to 2.1.1.9.) (5 ×10^4) were co cultured for 3 days in 96-well tissue flat bottom culture plates with naïve CD4$^+$ LN T cells (1 × 10^5) obtained by immunomagnetic isolation (Miltenyi Biotec refer to 2.1.1.8) from different genetic backgrounds (*wt*, *Apoe$^{-/-}$Ccr4$^{-/-}$, Apoe$^{-/-}$Ccr1$^{-/-}$, Apoe$^{-/-}$Ccr5$^{-/-}$*). The number of regulatory T cells was analyzed by flow cytometry (FACSCanto II, BD Biosciences) and FlowJo v.10 software (Tree Star Inc.).

2.2.3.4. Cyclic AMP signaling

The GloSensor cAMP (cyclic adenosine monophosphate) assay (Promega) provides a sensitive format for the interrogation of overexpressed or endogenous GPCRs that signal via changes in the intracellular concentration of cAMP. The assay uses genetically encoded biosensor variants with cAMP binding domains fused to mutant forms of *Photinus pyralis* luciferase. Upon binding to cAMP, conformational changes

occur that promote large increases in light output. The magnitude of the luminescence increase is directly proportional to the amount of analyte or protease activity present. Levels of cAMP were measured in confluent HEK293 transfected with either Ccr4 or Ccr8, after stimulation with chemokines over up to 30 min. After incubation with luciferin-EF (2.5 mM) at RT for 2 h, cells were stimulated with PBS control, Ccl17 (100 ng/ml), Ccl1 (100 ng/ml) or Ccl18 (100 ng/ml) and luminescence indicating the reduction of cAMP was recorded.

2.2.4. Statistical analysis

Data are expressed as mean ± standard error of the mean (SEM) unless otherwise specified. If D'Agostino & Pearson omnibus and/or Shapiro-Wilk normality test indicated Gaussian distribution, an unpaired t-test for side-by-side comparisons or one-way ANOVA with Newman-Keuls post-test for multiple comparisons were performed. Otherwise, Mann-Whitney-tests for side-by-side comparison and Kruskal-Wallis-test for multiple comparisons were performed using GraphPad Prism for Windows (GraphPad Software, San Diego, USA). For animal studies, a power analysis was performed using BiAS software (version 11.02). We assumed a detectable biological difference of at least 50% among up to four groups with a standard deviation < 15%, an α of 0.05, and a resultant power of 0.8. The number of biological replicates for each data point is included in the figure legends.

3. Results

As described before, recent work performed in our group revealed that the DC-derived chemokine Ccl17 promotes atherogenesis by controlling regulatory T cell (Treg) homeostasis, restraining their expansion, while its deficiency decreased plaque burden by facilitating Treg maintenance and survival. During this study, we did not observe a comparable reduction in lesion formation and infiltration in chimeric mice carrying *Ccr4*$^{-/-}$ bone marrow.[119] Using a reporter mouse model, which allows tracking of Ccl17-expressing cells, as well as mice deficient for various chemokine receptors including Ccr4-, Ccr5-, and Ccr1-deficient mice, we investigated the role of Ccl17 during the onset of atherosclerotic lesion formation and its involvement in restraining Treg homeostasis.

The following section will explain and display the experimental results, which were obtained throughout this thesis.

The first part will detail on differences observed between Ccl17- deficient mice and Ccr4-deficient mice, as seen in atherosclerotic plaque development and describe experiments and subsequent conclusions drawn, to further unravel the role of Ccl17 and Ccl17-producing DCs during the onset of atherosclerosis (Figure 13).

The second part illustrates the experimental setup chosen to gain insight in how Ccl17 promotes lesion development and through which alternative receptors Ccl17 might be able to signal. Furthermore, this part will highlight pro-inflammatory mediators which are key players in mediating Ccl17-dependent promotion of atherosclerosis and restrain of regulatory T cell homeostasis (Figure 13).

The third part will briefly introduce the concept of chemokine heterodimerization, using Ccl5-Ccl17 heterodimer as an example. Further, this section will explore possible actions of this heterodimeric structure on T cell and DC function, possible receptor interactions and the potential role heterodimeric structures, in particular Ccl5-Ccl17, have on atherosclerotic lesion development (Figure 13).
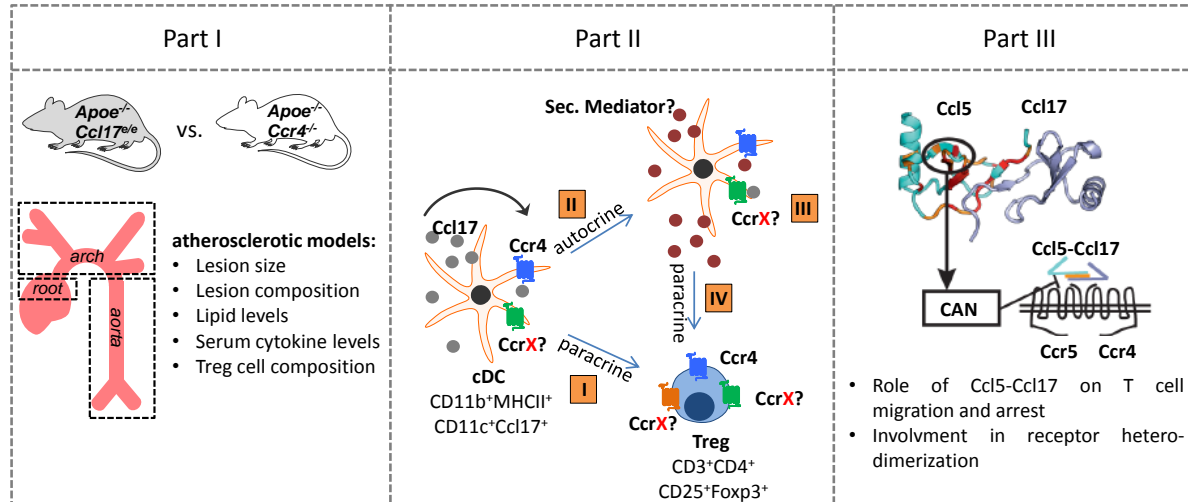
Figure 13. Experimental setup. Part I. Comparison between Ccl17 and Ccr4 deficiency. Evaluation of atherosclerotic lesion size and composition (12 weeks HFD), lipid levels and serum cytokine titers, followed by subsequent monitoring of Treg numbers in blood, spleen, and lymph nodes. **Part II. How does Ccl17 affect Treg maintenance and homeostasis?** Evaluation of direct autocrine Ccl17 stimulation on Tregs. Analysing effects of Ccl17 and Ccl17-producing DCs, as well as Ccr4 involvement, on T cell migration and Treg polarization/differentiation **(I)**. Evaluation of autocrine Ccl17 stimulation on DCs and subsequent release of secondary mediators by DCs **(II)** and involvement of alternative Ccl17 recpetors **(III)**. Analysis of the role of a possible secondary mediator on Treg polarization/differentiation **(IV) Part III. Ccl5-Ccl17 heterodimers.** Analysis of Ccl5-Ccl17 heterodimers and their role on T cell migration and arrest, as well as their chemokine receptor binding behavior.

3.1. Discrepancy between Ccl17 deficiency and Ccr4 deficiency

3.1.1. Deficiency of Ccl17 reduces atherosclerosis in $Apoe^{-/-}$ mice by restraining Tregs

To investigate the role of the Thymus- and activation-regulated chemokine (TARC) or Ccl17 during the onset of atherosclerosis we used $Apoe^{-/-}Ccl17^{e/e}$ mice and fed them a high fat diet (HFD) for 12 weeks. We analyzed atherosclerotic lesion formation in the aortic root, the aortic arch and in the thoraco-abdominal aorta (Figure 14A). A significant reduction in atherosclerotic lesion formation was observed in $Apoe^{-/-}Ccl17^{e/e}$ mice in comparison to $Apoe^{-/-}$ control mice, as visible after Oil-red-O staining in the aortic root and the *en face* prepared thoracoabdominal aorta (Figure 14B and D), as well as after HE staining in the aortic arch (Figure 14C). Body weight, cholesterol and triglyceride plasma levels did not reveal any differences comparing $Apoe^{-/-}$ and $Apoe^{-/-}Ccl17^{e/e}$ mice (Figure 14E-G).

Figure 14. Deficiency of Ccl17 reduces atherosclerosis. (A) Experimental scheme depicting the type of animals used, duration of diet feeding and endpoint analysis performed**. B-D)** Atherosclerotic lesions were quantified in $Apoe^{-/-}$ and $Apoe^{-/-}Ccl17^{e/e}$ mice after 12 weeks of HFD. **(B)** Representative images (left) and quantification (right) of Oil-red-O+ area in aortic root sections are shown. **(C)** Representative images (left) and quantification of lesion size in HE-stained aortic arches are depicted. **(D)** Representative images (left) and quantification of Oil-red-O+ area in *en face* prepared thoracoabdominal aortas are shown. **(E-G)** Bodyweight **(E)**, plasma cholesterol levels **(F)**, and plasma triglyceride levels **(G)** of $Apoe^{-/-}$ and $Apoe^{-/-}Ccl17^{e/e}$ mice after 12 weeks of HFD are depicted. **(A-G)** Data represent mean±SEM with *$P < 0.05$; **$P < 0.005$ as analyzed by Student's t-test with Welsh correction (n=10-11 per group).

Quantitative immunostaining revealed that the reduction in atherosclerotic lesion size observed in $Apoe^{-/-}Ccl17^{e/e}$ mice, was accompanied by a significant decrease in the absolute numbers of Dapi+ cells and MAC2+ macrophages, whereas the relative content of macrophages was unaltered, when compared to $Apoe^{-/-}$ control mice (Figure 15 A,B,D). Furthermore, the relative content in SMA+ smooth muscle cells was significantly

increased in $Apoe^{-/-}Ccl17^{e/e}$ mice, whereas the total counts of SMA$^+$ smooth muscle cells showed a tendency towards higher counts (Figure 15A+C). This data indicates a shift towards a more stable plaque phenotype in $Apoe^{-/-}Ccl17^{e/e}$ mice.

Figure 15. Deficiency of Ccl17 influences plaque composition. Atherosclerotic lesion composition was analyzed using immunohistochemistry. **(A)** Representative images of macrophage (**red**) and smooth muscle cell (**green**) staining, in the aortic root of $Apoe^{-/-}$(upper picture) and $Apoe^{-/-}Ccl17^{e/e}$ mice (lower picture) after 12 weeks of HFD are shown; cell nuclei are counterstained by DAPI (**blue**); scale bars: 200 µm. **(B-D)** The relative (left) and absolute quantification (right) of MAC-2$^+$ macrophages **(B)** and SMA$^+$ smooth muscle cells **(C)** and the absolute number of DAPI$^+$ cells **(D)** per plaque area are depicted. **(B-D)** Data represent mean±SEM, Student t test with Welch correction. (n=10-11) *$P < 0.05$.

To determine the differences in plaque size and plaque composition between $Apoe^{-/-}$ versus $Apoe^{-/-}Ccl17^{e/e}$, we performed Fluorescence-activated Cell Sorting (FACS) analysis of blood, as well as of single cell suspensions of bone marrow, spleen and para-aortic-, axillar-, inguinal- and mesenteric lymph nodes. Analyzing the distribution of different CD45$^+$ leukocyte populations as described in chapter 2.2.2.3. in the above mentioned organs, we only observed higher frequencies and an expansion of CD4$^+$CD25$^+$Foxp3$^+$ Tregs in $Apoe^{-/-}Ccl17^{e/e}$ mice when compared to $Apoe^{-/-}$ control mice (Figure 16A-G and Supplemental table 1-4). CD45$^+$CD3$^+$CD4$^+$CD25$^+$Foxp3$^+$ Tregs were

significantly increased in spleen, para-aortic-, axillary-, inguinal- and mesenteric lymph nodes of *Apoe*$^{-/-}$*Ccl17*$^{e/e}$ mice when compared to *Apoe*$^{-/-}$ control mice but where not altered in the circulation of these mice.

Figure 16. Ccl17 deficiency affects regulatory T cell populations. (A) Representative dot plots of Flow cytometric analysis of CD3$^+$CD4$^+$CD25$^+$Foxp3$^+$ Tregs in para-aortic LNs of *Apoe*$^{-/-}$ and *Apoe*$^{-/-}$*Ccl17*$^{e/e}$ mice after 12 weeks of HFD; numbers in dot plots are percentage of CD4$^+$ events. **(B-G)** Flow cytometric analysis of CD3$^+$CD4$^+$CD25$^+$Foxp3$^+$ Tregs **(B)** in Blood **(C)** Spleen **(D)** para-aortic LNs **(E)** axillar LNs **(F)** inguinal LNs and **(G)** mesenteric LNs of *Apoe*$^{-/-}$ and *Apoe*$^{-/-}$*Ccl17*$^{e/e}$ mice after 12 weeks of HFD employing indicated surface and intracellular markers. Data **(B-G)** represent mean±SEM, Student t test with Welch correction. (n=10-11) *P < 0.05; **P < 0.005; **P < 0.001.

3.1.2. Deficiency of Ccr4 does not reduce atherosclerosis in *Apoe*$^{-/-}$ mice and has no effect on regulatory T cell populations

To clarify the mechanisms of Ccl17 action, namely a potential involvement of its *bona fide* receptor Ccr4, during the progression of atherosclerosis, we used *Apoe*$^{-/-}$*Ccr4*$^{-/-}$ mice and fed them a HFD for 12 weeks. We analyzed atherosclerotic lesion formation in the aortic root, the aortic arch and in the thoraco-abdominal aorta (Figure 17A). No changes in atherosclerotic lesion formation were observed in *Apoe*$^{-/-}$*Ccr4*$^{-/-}$ mice in comparison to *Apoe*$^{-/-}$ control mice, as visible after Oil-red-O staining in the aortic root and the *en face* prepared thoraco-abdominal aorta (Figure 17B and D), as well as after HE staining in the aortic arch (Figure 17C). Body weight, cholesterol and triglyceride plasma levels did

also not differ between Ccr4-deficient and control animals (Figure 17E-G).
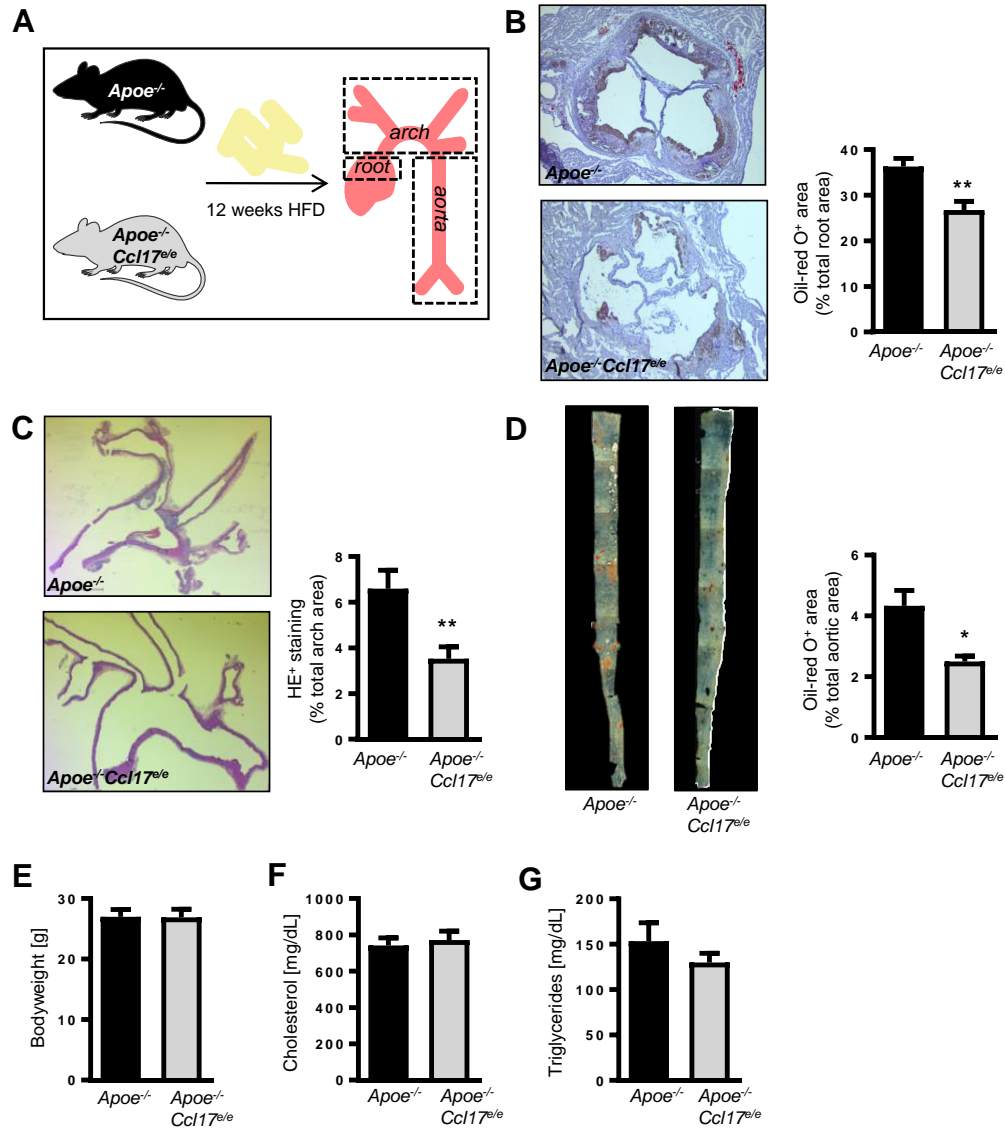

Figure 17. Deficiency of Ccr4 does not reduce atherosclerosis. (A) Experimental scheme depicting the type of animals used, duration of diet feeding and endpoint analysis performed. (**B-D**) Atherosclerotic lesions were quantified in *Apoe*^{-/-} and *Apoe*^{-/-}*Ccr4*^{-/-} mice after 12 weeks of HFD. **(B)** Representative images (left) and quantification (right) of Oil-red-O[+] area in aortic root sections are shown. **(C)** Representative images (left) and quantification of lesion size in HE-stained aortic arches are depicted. **(D)** Representative images (left) and quantification of Oil-red-O[+] area in *en face* prepared thoraco-abdominal aortas are shown. **(E-G):** Bodyweight **(E)**, plasma cholesterol levels **(F)**, and plasma triglyceride levels **(G)** of *Apoe*^{-/-} and *Apoe*^{-/-}*Ccr4*^{-/-} mice after 12 weeks of HFD are depicted. (**A-G**) Data represent mean±SEM with *P < 0.05; **P < 0.005 as analyzed by Student's t-test with Welsh correction (n=16-20).

Quantitative immunostaining could not show any differences in absolute numbers of Dapi^{+} cells nor MAC2^{+} macrophages per plaque when comparing *Apoe*^{-/-}*Ccr4*^{-/-} mice to *Apoe*^{-/-} control mice. Interestingly, there was a decrease in SMA[+] smooth muscle cell

frequency in lesions of *Apoe⁻/⁻Ccr4⁻/⁻* mice compared to *Apoe⁻/⁻* control mice (Figure 18A-D).
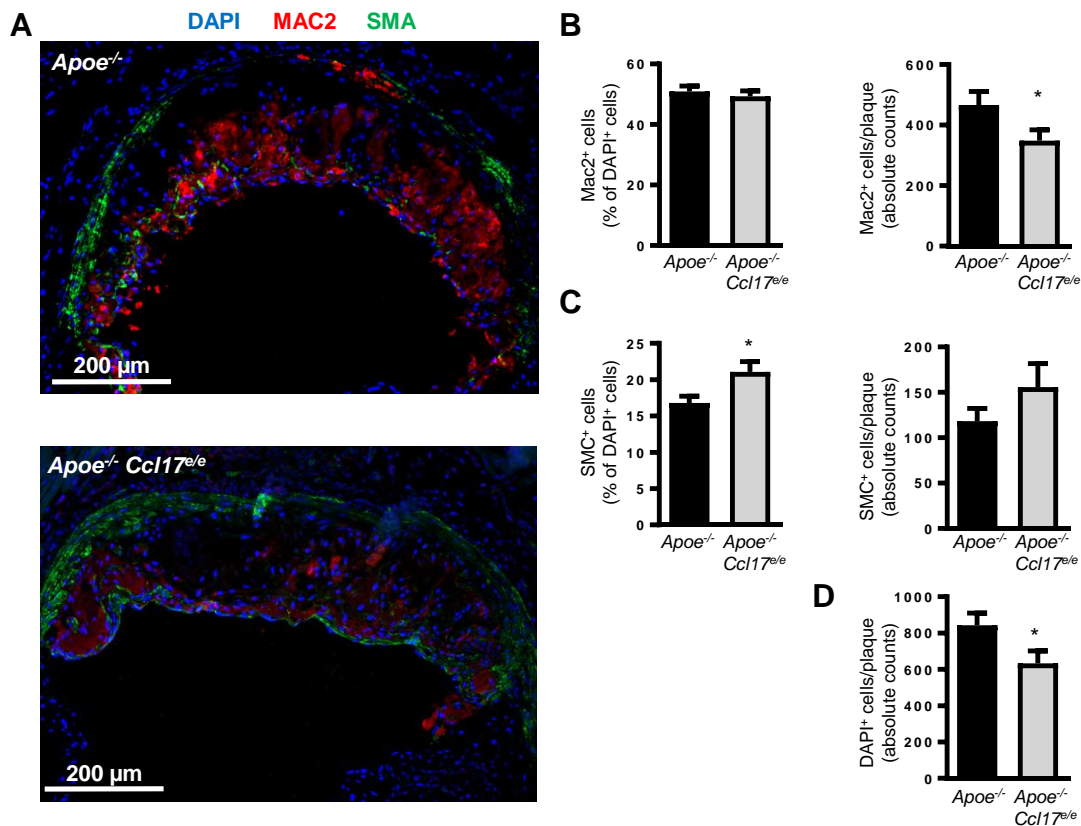

Figure 18. Deficiency of Ccr4 does not influence plaque composition. Atherosclerotic lesion composition was analyzed using immunohistochemistry. **(A)** Representative images of macrophage (**red**) and smooth muscle cell (**green**) staining, in the aortic root of *Apoe⁻/⁻* (upper picture) and *Apoe⁻/⁻Ccr4⁻/⁻* mice (lower picture) after 12 weeks of HFD are shown; cell nuclei are counterstained by DAPI (**blue**); scale bars: 200 µm. **(B-D)** The relative (left) and absolute quantification (right) of MAC-2⁺ macrophages **(B)** and SMA⁺ smooth muscle cells **(C)** and the absolute number of DAPI⁺ cells **(D)** per plaque area are depicted. **(B-D)** Data represent mean±SEM, Student t test with Welch correction. (n=10-11) *$P < 0.05$. (n=9-10).

To unravel why Ccr4 deficiency does not phenocopy the results obtained in Ccl17-deficient animals and to explain the different outcomes in atherosclerotic lesion sizes between *Apoe⁻/⁻Ccl17^e/e^* and *Apoe⁻/⁻Ccr4⁻/⁻* we again performed flow cytometric analysis of blood, as well as of single cell suspensions from bone marrow, spleen and para-aortic-, axillar-, inguinal- and mesenteric lymph nodes. Analyzing the distribution of different CD45⁺ leukocyte populations, as mentioned in 2.2.2.3 in the above mentioned organs we observed a significant decrease of neutrophils (CD45⁺Gr1⁺CD115⁻) in the bone marrow of *Apoe⁻/⁻Ccr4⁻/⁻* mice when compared to *Apoe⁻/⁻* control mice (Supplemental table 5-9). No differences in the CD4⁺CD25⁺Foxp3⁺ Treg population was

observed in blood, spleen, para-aortic-, axillar-, inguinal- and mesenteric lymph nodes of *Apoe^-/-Ccr4^-/-* mice in comparison to *Apoe^-/-* control mice (Figure 19A-G).
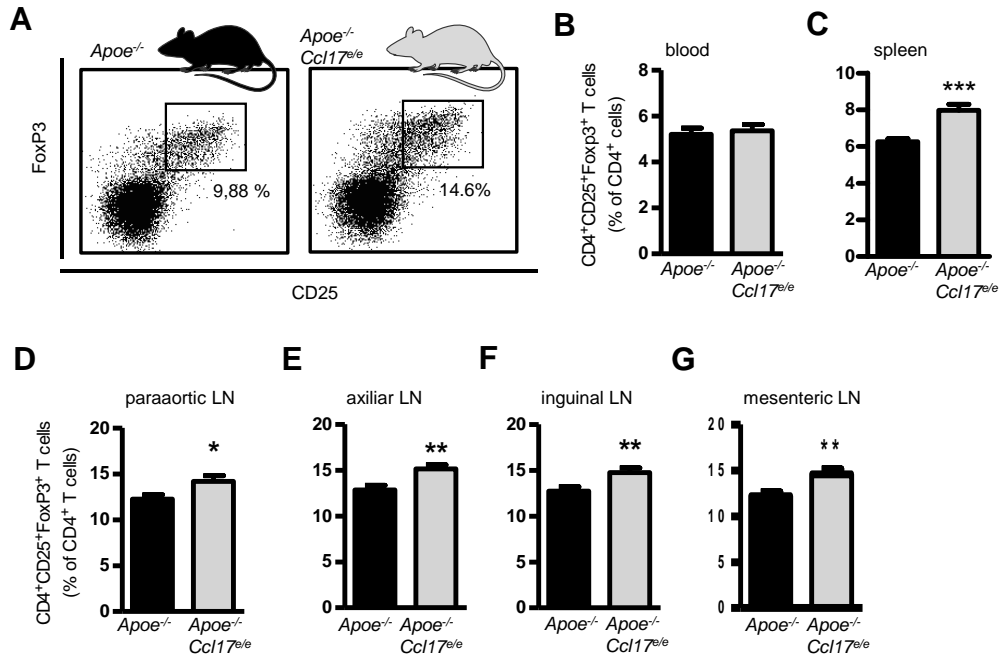

Figure 19. Ccr4 deficiency does not affect regulatory T cell populations. (A) Representative dot plots of Flow cytometric analysis of CD3^+CD4^+CD25^+Foxp3^+ Tregs in para-aortic LNs of *Apoe^-/-* and *Apoe^-/-Ccr4^-/-* mice after 12 weeks of HFD; numbers in dot plots are percentage of CD4^+ events. **(B-G)** Flow cytometric analysis of CD3^+CD4^+CD25^+Foxp3^+ Tregs **(B)** in Blood **(C)** Spleen **(D)** para-aortic LNs **(E)** axillar LNs **(F)** inguinal LNs and **(G)** mesenteric LNs of *Apoe^-/-* and *Apoe^-/-Ccr4^-/-* mice after 12 weeks of HFD employing indicated surface and intracellular markers. Data **(B-G)** represent mean±SEM, Student t test with Welch correction. (n=16-20) *$P < 0.05$; **$P < 0.005$; **$P < 0.001$.

3.1.3. Hematopoietic deficiency of Ccr4 increases atherosclerotic lesions in *Apoe^-/-* mice through hypocholesteremia

To further investigate a potential involvement of the Ccl17 receptor Ccr4 during the onset of atherosclerosis and to rule out possible side effects of a full body *knock out*, we wanted to concentrate on the role of hematopoietic Ccr4 expression during atherosclerotic lesion development. For this purpose, we performed a bone marrow transplantation of either *Apoe^-/-Ccr4^-/-* bone marrow into *Apoe^-/-* mice (*Apoe^-/-Ccr4^-/-* ►*Apoe^-/-*) or *Apoe^-/-* control bone marrow into *Apoe^-/-* animals (*Apoe^-/-*►*Apoe^-/-*). After one month of recovery, we fed them a HFD for 12 weeks. We quantified the extend of atherosclerotic lesion formation in the aortic root, the aortic arch and in the thoraco-abdominal aorta (Figure 20A). No changes in atherosclerotic lesion size in the aortic root was observed in *Apoe^-/-Ccr4^-/-*►*Apoe^-/-* mice in comparison to *Apoe^-/-*►*Apoe^-/-* control

mice, as visible after Oil-red-O staining in the aortic root (Figure 20B). When analyzing atherosclerotic lesions in the HE stained aortic arch as well as in the *en face* prepared and oil-red-O stained thoracoabdominal aorta we observed a significant increase in lesion size in the $Apoe^{-/-}Ccr4^{-/-} \blacktriangleright Apoe^{-/-}$ animals when compared to the $Apoe^{-/-} \blacktriangleright Apoe^{-/-}$ control mice (Figure 20C and D). These findings were in line with higher levels of plasma cholesterol in the $Apoe^{-/-}Ccr4^{-/-} \blacktriangleright Apoe^{-/-}$ mice in comparison to the $Apoe^{-/-} \blacktriangleright Apoe^{-/-}$ control mice (Figure 20G). Body weight and triglyceride plasma levels were not altered in both groups (Figure 20E and F).
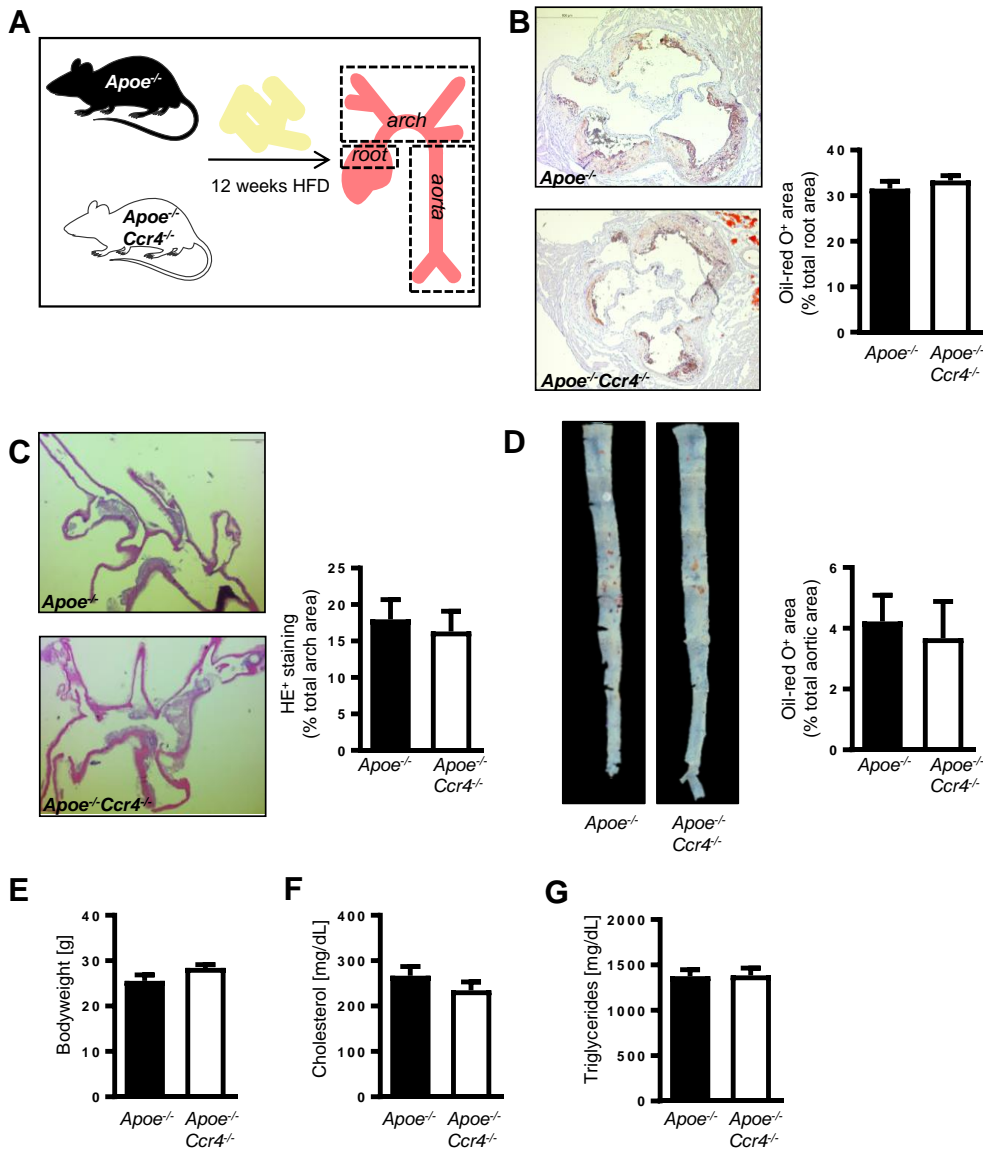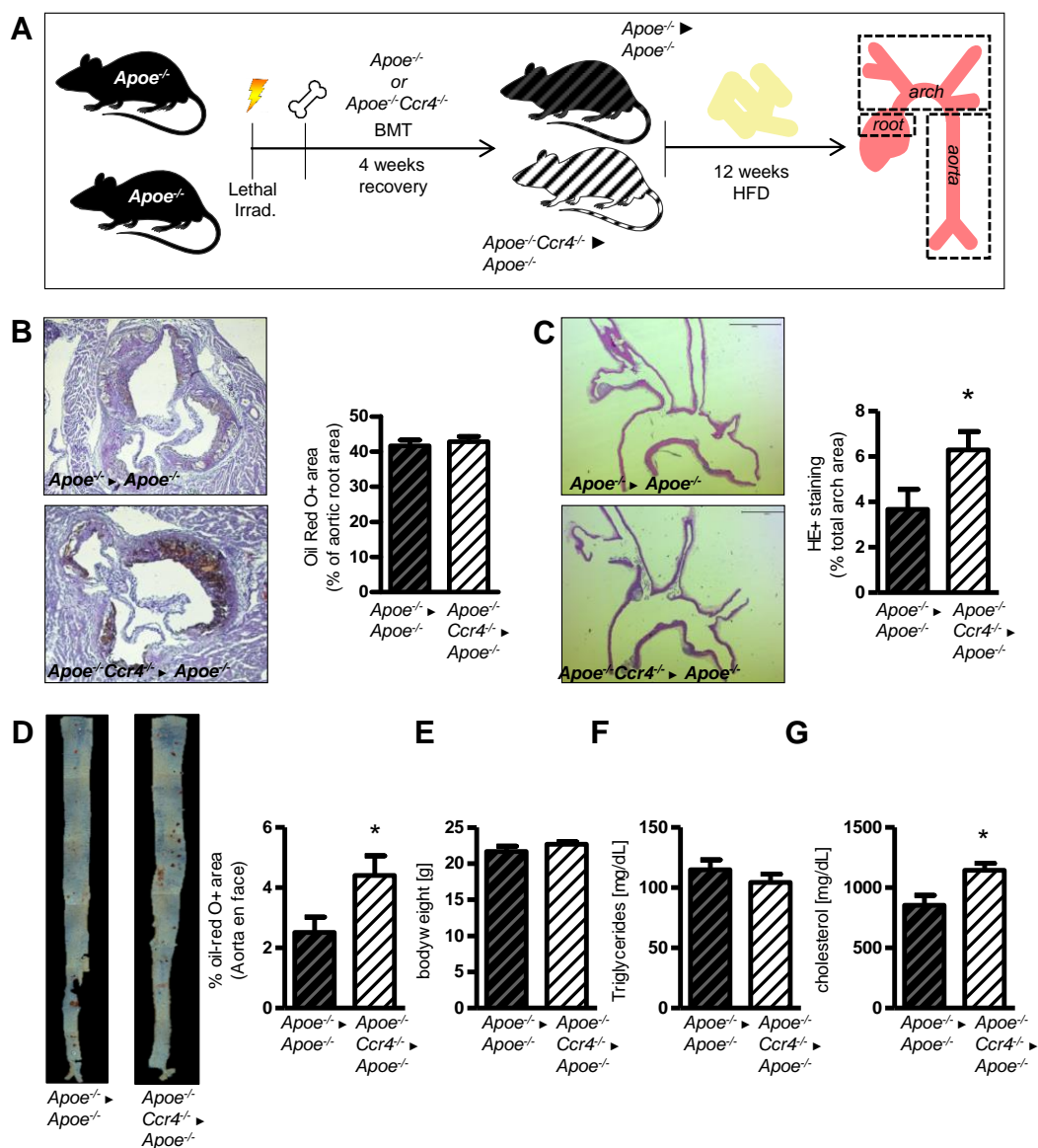

Figure 20. Hematopoietic deficiency of Ccr4 does not reduce atherosclerosis. (A) Experimental scheme depicting the type of animals used, the procedure performed for bone marrow transplantation as well as duration of diet feeding and endpoint analysis performed. **(B-D)** Atherosclerotic lesions were

quantified in *Apoe*^{-/-} ►*Apoe*^{-/-} or *Apoe*^{-/-}*Ccr4*^{-/-} ►*Apoe*^{-/-} mice after 12 weeks of HFD. **(B)** Representative images (left) and quantification (right) of Oil-red-O[+] area in aortic root sections are shown. **(C)** Representative images (left) and quantification of lesion size in HE-stained aortic arches are depicted. **(D)** Representative images (left) and quantification of Oil-red-O[+] area in *en face* prepared thoracoabdominal aortas are shown. **(E-G):** Bodyweight **(E)**, plasma triglyceride levels **(F)**, and plasma cholesterol levels **(G)** of *Apoe*^{-/-} ►*Apoe*^{-/-} or *Apoe*^{-/-}*Ccr4*^{-/-} ►*Apoe*^{-/-} mice after 12 weeks of HFD are depicted. **(A-G)** Data represent mean±SEM with *$P < 0.05$; **$P < 0.005$ as analyzed by Student's t-test with Welsh correction (n=9-10 per group).

Quantitative immunofluorescence staining's of aortic root sections did not reveal any differences in absolute numbers of Dapi^{+} cells nor in the number of MAC2^{+} macrophages per plaque comparing *Apoe*^{-/-}*Ccr4*^{-/-}►*Apoe-/-* mice to *Apoe*^{-/-}►*Apoe*^{-/-} control mice. There were also no differences observed in the SMA[+] smooth muscle cell content per plaque in *Apoe*^{-/-}*Ccr4*^{-/-}►*Apoe-/-*mice in comparison to *Apoe*^{-/-}►*Apoe*^{-/-} control animals (Figure 21A-D).
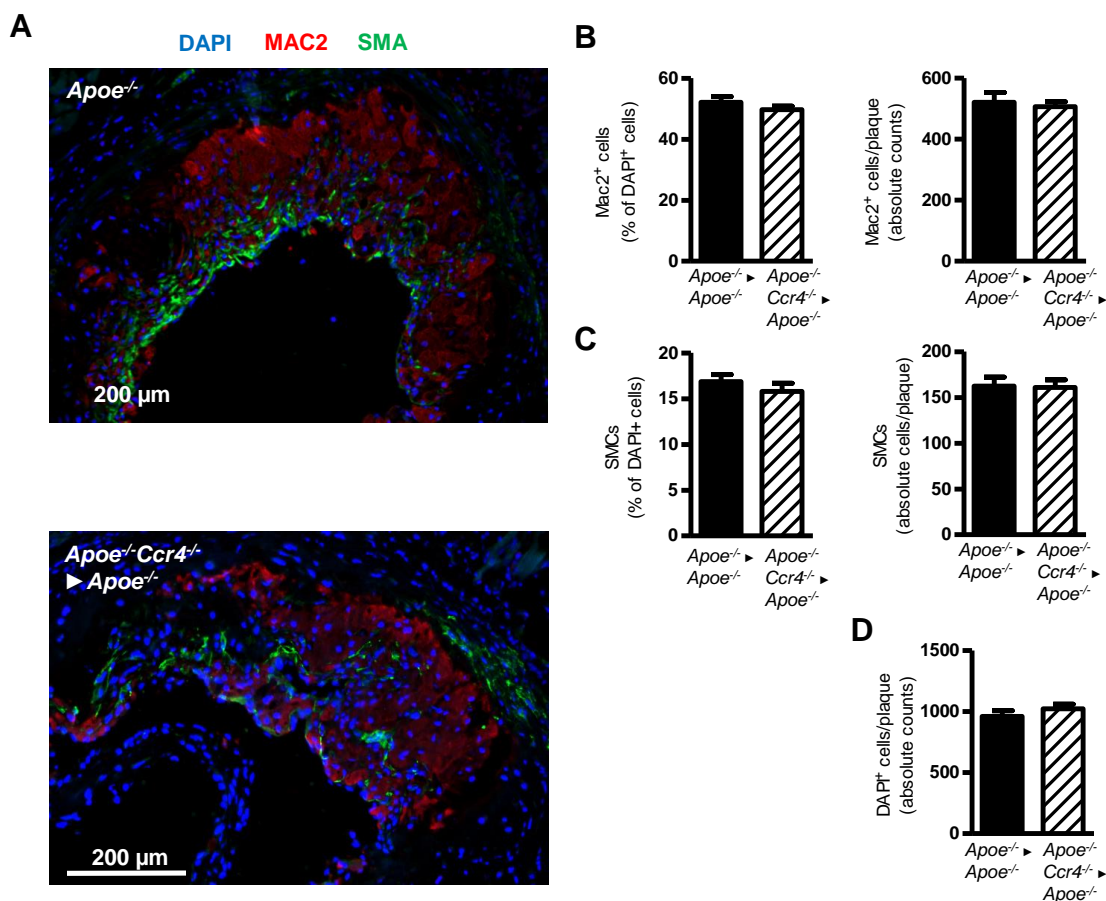
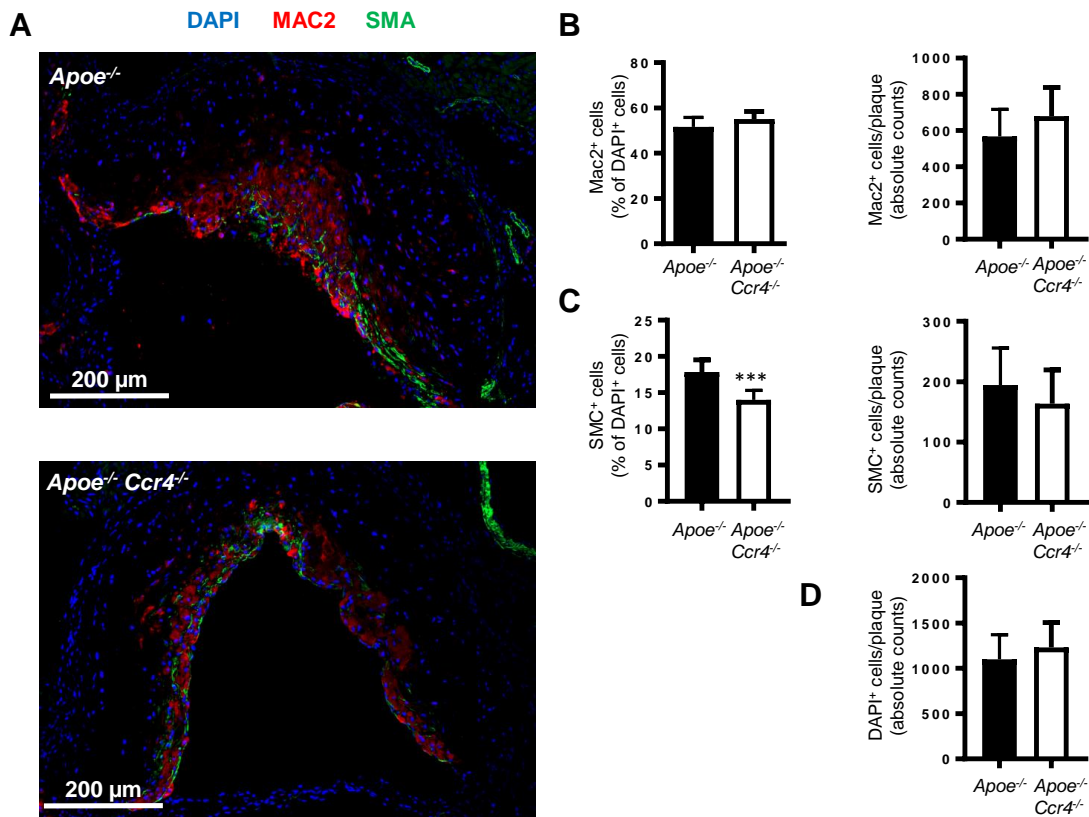**Figure 21. Hematopoietic deficiency of Ccr4 does not influence plaque composition.** Atherosclerotic lesion composition was analyzed using immunohistochemistry. **(A)** Representative images of macrophage (red) and smooth muscle cell (green) staining, in the aortic root of *Apoe*^{-/-}►*Apoe*^{-/-} (upper picture) and *Apoe*^{-/-}*Ccr4*^{-/-}►*Apoe*^{-/-} mice (lower picture) after 12 weeks of HFD are shown; cell nuclei are counterstained by DAPI (blue); scale bars: 200 µm. **(B-D):** The relative (left) and absolute quantification (right) of MAC-2^{+} macrophages **(B)** and SMA[+] smooth muscle cells **(C)** and the absolute number of DAPI[+]

cells **(D)** per plaque area are depicted. **(B-D)** Data represent mean±SEM, Student t test with Welch correction. (n=9-10) *P < 0.05.

FACS analysis of different leukocyte subsets (see methods chapter 2.2.2.3.) revealed a significant increase of CD45$^+$Gr1$^+$CD115$^-$ neutrophils and a reduction in classical monocytes (CD45$^+$Gr1$^+$CD115$^+$) in the blood of *Apoe$^{-/-}$Ccr4$^{-/-}$►Apoe$^{-/-}$* mice compared to *Apoe$^{-/-}$►Apoe$^{-/-}$* mice. Furthermore, we saw a significant increase of neutrophils and macrophages in the bone marrow of *Apoe$^{-/-}$Ccr4$^{-/-}$►Apoe$^{-/-}$* mice when compared to *Apoe$^{-/-}$►Apoe$^{-/-}$* mice. The spleen of the *Apoe$^{-/-}$Ccr4$^{-/-}$►Apoe$^{-/-}$* mice contained significant lower numbers of CD45$^+$Gr1$^-$CD115$^+$ non-classical monocytes, T cells, cytotoxic T cells and T helper cells in comparison to *Apoe$^{-/-}$►Apoe$^{-/-}$* mice. The para-aortic LN of the *Apoe$^{-/-}$Ccr4$^{-/-}$►Apoe$^{-/-}$* mice contained increased numbers of classical monocytes, non-classical monocytes and CD45$^+$CD11c$^+$MHCII$^+$ cDCs. (Supplemental table 9-12) No differences in the CD4$^+$CD25$^+$Foxp3$^+$ Treg population was observed in blood, spleen, para-aortic-, axillar-, inguinal- and mesenteric lymph nodes of *Apoe$^{-/-}$Ccr4$^{-/-}$►Apoe$^{-/-}$* comparing them with *Apoe$^{-/-}$►Apoe$^{-/-}$* control mice (Figure 22A-G).
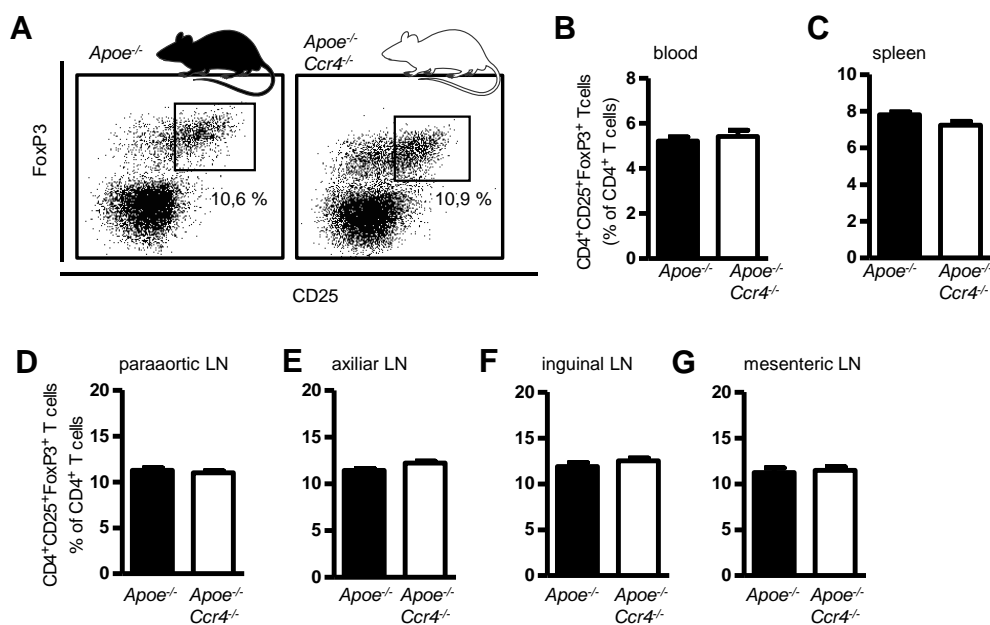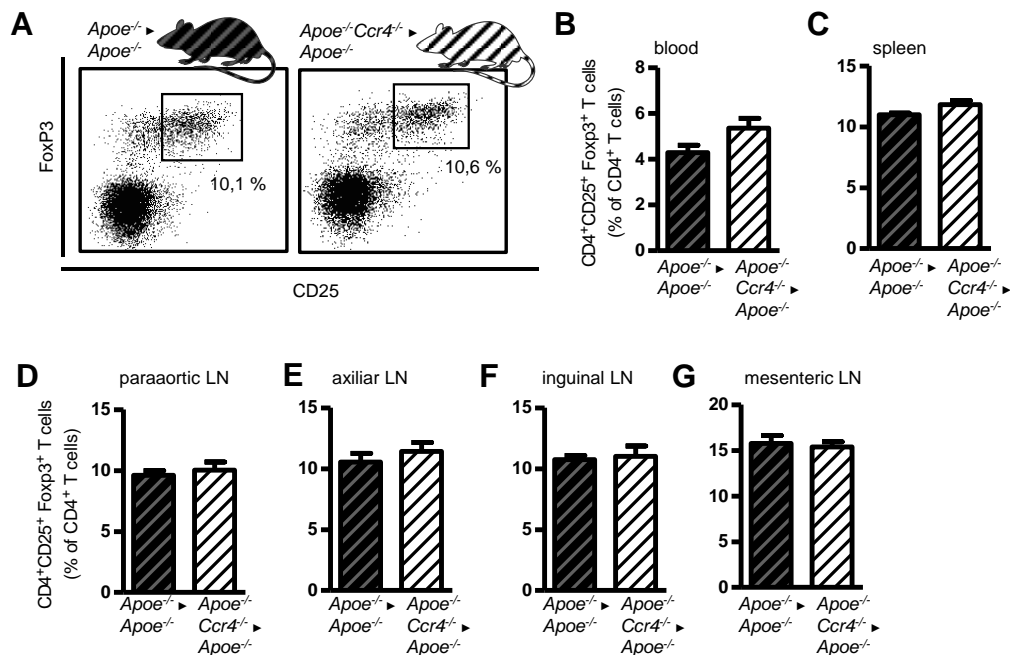

Figure 22. Hematopoietic Ccr4 deficiency does not affect regulatory T cell populations. (A) Representative dot plots of Flow cytometric analysis of CD3$^+$CD4$^+$CD25$^+$Foxp3$^+$ Tregs in para-aortic LNs of *Apoe$^{-/-}$►Apoe$^{-/-}$* and *Apoe$^{-/-}$Ccr4$^{-/-}$►Apoe$^{-/-}$* mice after 12 weeks of HFD; numbers in dot plots are percentage of CD4$^+$ events. **(B-G)** Flow cytometric analysis of CD3$^+$CD4$^+$CD25$^+$Foxp3$^+$ Tregs **(B)** in Blood **(C)** Spleen **(D)** para-aortic LNs **(E)** axillar LNs **(F)** inguinal LNs and **(G)** mesenteric LNs of *Apoe$^{-/-}$►Apoe$^{-/-}$* and *Apoe$^{-/-}$Ccr4$^{-/-}$►Apoe$^{-/-}$* mice after 12 weeks of HFD employing indicated surface and intracellular

markers. Data **(B-G)** represent mean±SEM, Student t test with Welch correction. (n=9-10) *P < 0.05; **P < 0.005; **P < 0.001.

3.1.4. Ccl17 induces T cell migration via Ccr4 but does not affect Tregs directly

Ccl17 is known to be a chemoattractant for T cells. To confirm that this chemoattraction is mediated via Ccr4 we performed *in vitro* transwell assays (see methods 2.2.3.1.). CD4$^+$ T cells were isolated from spleen and LNs of *wt* mice and were allowed to transmigrate towards recombinant murine (rm) Ccl17 in the presence or absence of the Ccr4 inhibitor C 021 dihydrochloride, which was placed in the lower chamber of transwell-migration plates. Transmigrated cells were monitored using flow cytometry. We observed that CD4$^+$ cells did migrate towards rmCcl17 and that this migration was impaired in the presence of the Ccr4 inhibitor C 021 dihydrochloride (Figure 23).
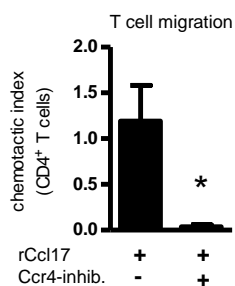
Figure 23. Ccl17 attracts CD4$^+$ T cells via Ccr4. Transwell migration of CD4$^+$ T cells towards recombinant murine Ccl17, in the presence or absence of the Ccr4 inhibitor C 021 dihydrochloride was quantified by FACS analysis (n=3-6). Data represents mean±SEM, Student t test with Welch correction. *P<0.05.

To investigate if Ccl17 is directly involved in mechanisms of Treg expansion, we studied whether Ccl17 affects the polarization of naive T cells toward Tregs (see methods 2.2.3.2.). In *in vitro* T cell polarization assays using TGF-β, addition of Ccl17 did not alter the frequencies of Foxp3$^+$ Tregs among CD4$^+$ T cells (Figure 24). Implying that Ccl17 has no direct effect on restraining Treg polarization.
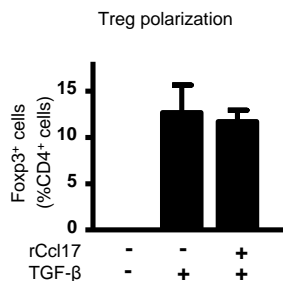
Treg polarization

Figure 24. Ccl17 does not affect Treg polarization directly. Naïve CD4$^+$ CD62L$^+$ T cells were cultured under Treg polarization conditions using TGF-β in the presence or absence of recombinant murine Ccl17. Frequencies of CD4$^+$CD25$^+$Foxp3$^+$ Tregs among CD4$^+$ T cells were analyzed by flow cytometry (n=5). Data represents mean±SEM. 1-way analysis of variance (ANOVA) with, Kruskal-Wallis test with Dunn posttest were used. P values <0.05 were considered statistically significant.

Since Ccl17 appears not to directly affect Treg maintenance, we thought that Ccl17 producing DCs might limit Treg expansion and differentiation, through secretion of unknown mediators. To further study the mechanisms by which Ccl17 producing DCs affect Tregs and to elucidate a potential involvement of Ccr4, we performed co-culture experiments employing *wt* T cells and DCs isolated either from *wt*, *Ccl17*$^{e/e}$ or *Ccr4*$^{-/-}$ mice (see methods 2.2.3.3.). Notably, the frequency of CD4$^+$Foxp3$^+$ Tregs obtained in co-culture with wild-type DCs was significantly higher than that obtained in co-cultures with *Ccr4*$^{-/-}$ DCs or *wt* DCs (Figure 25). This implies that Ccr4 on DCs is not involved in mediating effects of Ccl17 on Treg maintenance, at least *in vitro*, but that the Ccl17 producing DC might secrete an unknown mediator influencing Treg development.

iTreg differentiation
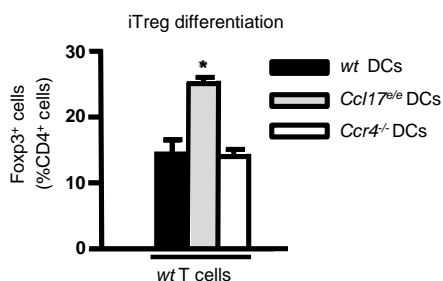
Figure 25. Ccl17-deficient DCs induce iTreg differentiation. DCs isolated via flow cytometric sorting from either *wt*, *Ccl17*$^{e/e}$ or *Ccr4*$^{-/-}$ mice were cultured together with *wt* naïve CD4$^+$ CD62L$^+$ T cells for three days. Frequencies of CD4$^+$CD25$^+$Foxp3$^+$ Tregs among CD4$^+$ T cells were analyzed by flow cytometry. Data represent three independent experiments depicted as mean±SEM. One-way analysis of variance (ANOVA) with Kruskal-Wallis test with Dunn posttest were used. P values <0.05 were considered statistically significant. *P<0.05.

3.1.5. Summary and hypothesis

As mentioned in the results above *Apoe*$^{-/-}$*Ccl17*$^{e/e}$ mice show reduced atherosclerotic lesion size after 12 weeks HFD accompanied by higher frequencies of CD3$^+$CD4$^+$Cd25$^+$Foxp3$^+$ Treg cells in spleen, para-aortic LN, axillar LN, inguinal LN and mesenteric LN, when compared to *Apoe*$^{-/-}$ control mice. Although, so far Ccr4 is the only known *bona fide* receptor for Ccl17, *Apoe*$^{-/-}$*Ccr4*$^{-/-}$ mice do not phenocopy observations made in mice lacking Ccl17, instead *Apoe*$^{-/-}$*Ccr4*$^{-/-}$ mice show no differences in atherosclerotic lesion size nor in Treg frequencies. Hematopoietic deficiency in Ccr4 does also not phenocopy Ccl17 deficiency but rather increases lesion size after 12 weeks HFD, when compared to *Apoe*$^{-/-}$ control mice. These results suggest an alternative mechanism through which Ccl17 engages its atherogenic functions. Further experiments concluded that recombinant murine Ccl17 induces migration of CD4$^+$ T cells via Ccr4 but does not affect polarization of naïve CD62L$^+$CD4$^+$ T cells towards Tregs. Ccl17-deficient DCs do promote iTreg differentiation independent of Ccr4, since Ccr4-deficient DCs do not promote iTreg differentiation. These results suggest that, instead of acting directly upon Tregs, Ccl17 binds via an alternative receptor (not Ccr4), in an autocrine fashion to (specific) DCs and induces the release of a secondary mediator restraining Treg homeostasis (Figure 26).
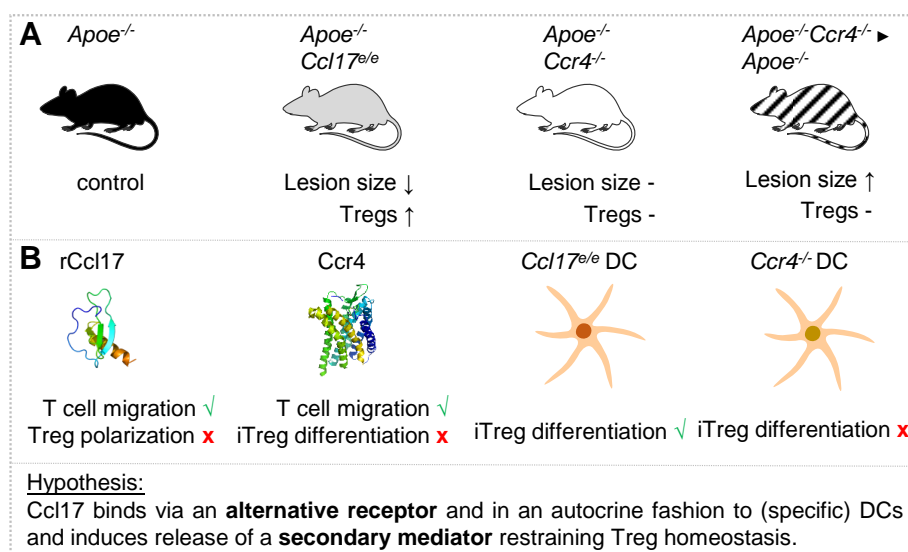
Figure 26. Summary and hypothesis. A) *Apoe*$^{-/-}$*Ccl17*$^{e/e}$ mice show reduced atherosclerotic lesion size after 12 weeks HFD accompanied by higher frequencies of CD3$^+$CD4$^+$Cd25$^+$Foxp3$^+$ Treg cells in spleen, para-aortic LN, axillar LN, inguinal LN and mesenteric LN, when compared to *Apoe*$^{-/-}$ control mice. Although, Ccr4 is the only known *bona fide* receptor for Ccl17, *Apoe*$^{-/-}$ *Ccr4*$^{-/-}$ mice do not phenocopy

Ccl17 deficiency, showing no differences in atherosclerotic lesion size or Treg frequencies. Hematopoietic deficiency in Ccr4 also does not phenocopy Ccl17 deficiency but rather increases lesion size after 12 weeks HFD. **B)** Recombinant murine Ccl17 induces migration of CD4$^+$ T cells dependent on Ccr4, but does not affect polarization of naïve CD62L$^+$CD4$^+$ T cells towards Tregs. Ccl17-deficient DCs do promote iTreg differentiation independent of Ccr4 since Ccr4-deficient DCs do not promote iTreg differentiation.

3.2. Searching for a secondary mediator

3.2.1. Ccl17-dependent secretion of Ccl3 and Cxcl10 by DCs

Since previous results indicate that Ccl17 does not directly act upon Tregs, but rather binds an alternative receptor (not Ccr4) in an autocrine fashion on DCs, and this leads to the secretion of a secondary mediator, which is responsible for restraining Treg homeostasis, we thought to investigate the secretion profile of DCs upon Ccl17 stimulation. For this purpose, CD11b$^+$CD11c$^+$MHCII$^+$ DCs were cultured for 4h at 37°C in the presence or absence of Ccl17 and with or without the Ccr4 inhibitor C 021 dihydrochloride. The supernatant of these cells was analyzed using a Luminex multiplex-bead-array measuring protein concentrations of 26 different cytokines and chemokines (see methods 2.2.2.5) (Figure 27). Out of the 26 cytokines and chemokines analyzed, only two showed differences after stimulation with Ccl17. Concentrations of the chemokines Ccl3 and Cxcl10 were significantly increased in supernatants of DCs which had been treated with rmCcl17 (Figure 27B-C). Using the Ccr4 inhibitor C 021 dihydrochloride, we observed a reduction in Cxcl10 in the supernatants after stimulation with rmCcl17, when compared to the untreated control group (Figure 27C). The Ccr4 inhibitor did not affect Ccl3 levels after Ccl17 stimulation (Figure 27B). Taken together these results indicate that, Ccl3 secretion by DCs after stimulation with Ccl17 is independent of Ccr4, whereas Cxcl10 secretion from DCs after Ccl17 stimulation depends on Ccr4. This makes Ccl3 a promising candidate for studying its effects on regulatory T cells.
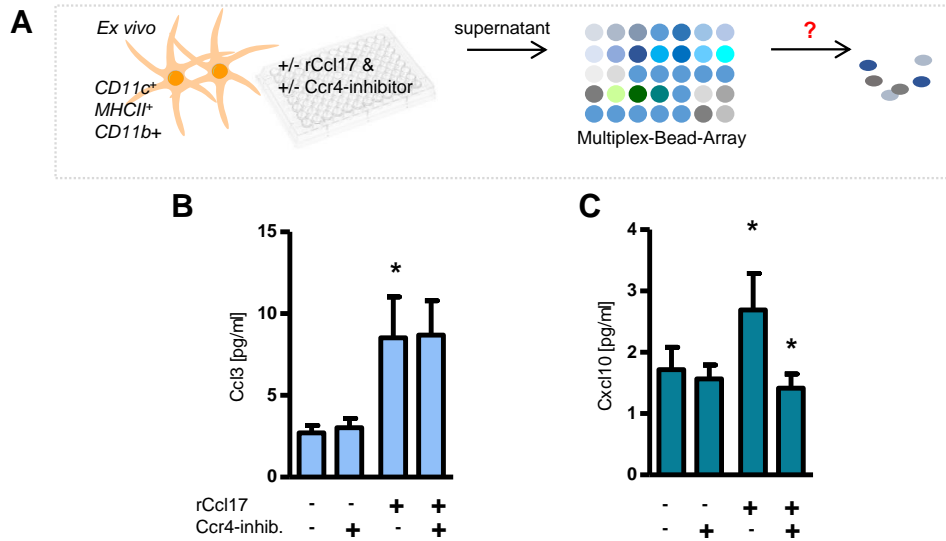
Figure 27. Ccl17-dependent secretion of Ccl3 and Cxcl10. (A) Sorted CD11b⁺CD11c⁺MHCII⁺ DCs were cultured for 4h at 37°C in the presence or absence of rmCcl17 and with or without the Ccr4 inhibitor C 021 dihydrochloride. Subsequently the supernatant was subjected to a Luminex multiplex-bead-array measuring protein concentrations of 26 different cytokines and chemokines. **(B)** Ccl3 concentrations (pg/ml) and **(C)** Cxcl10 concentrations (pg/ml) in supernatants of stimulated DCs. Data **(B+C)** represent mean±SEM, Student t test with Welch correction (n=4-5). P values <0.05 were considered statistically significant. *P<0.05.

Following the discovery that Ccl3 secretion by DCs is mediated by Ccl17 we analyzed Ccl3 concentrations using ELISA in plasma samples obtained either from *Apoe⁻/⁻* or *Apoe⁻/⁻Ccl17ᵉ/ᵉ* mice under steady state conditions and observed a reduction in Ccl3 plasma levels in Ccl17-deficient mice compared to the wild type control (Figure 28A). These findings were also seen in *Apoe⁻/⁻* and *Apoe⁻/⁻Ccl17ᵉ/ᵉ* mice after 12 weeks HFD (Figure 28B). In line with our hypothesis that Ccl17 induces secretion of Ccl3 by DCs we could not observe any differences in Ccl3 plasma levels when comparing *Apoe⁻/⁻* ►*Apoe⁻/⁻* and *Apoe⁻/⁻*►*Apoe⁻/⁻ Ccl17ᵉ/ᵉ* mice (hematopoietic system is Ccl17 competent) after 12 weeks HFD (Figure 28C). Furthermore, and as expected we could not observe any differences in Ccl3 plasma levels when comparing Apoe⁻/⁻ and *Apoe⁻/⁻Ccr4⁻/⁻* mice after 12 weeks HFD (Figure 28D).
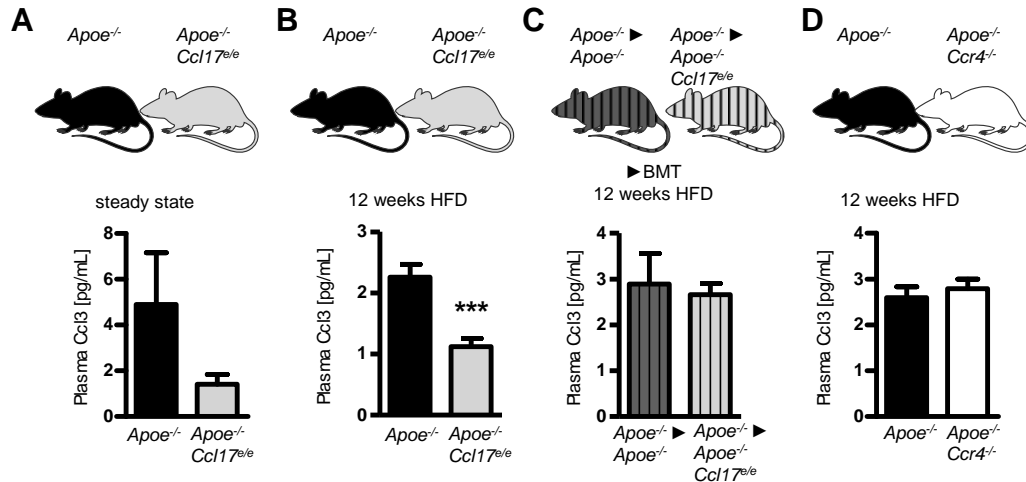
Figure 28. Ccl3 plasma levels are reduced in Ccl17-deficient mice. (A-D) Ccl3 concentrations were measured using ELISA in plasma obtained either from **(A)** *Apoe*$^{-/-}$ *and Apoe*$^{-/-}$*Ccl17*$^{e/e}$ mice under steady state conditions (n=10); **(B)** *Apoe*$^{-/-}$ and *Apoe*$^{-/-}$*Ccl17*$^{e/e}$ mice after 12 weeks HFD (n=10-15); **(C)** *Apoe*$^{-/-}$ ►*Apoe*$^{-/-}$ and *Apoe*$^{-/-}$►*Apoe*$^{-/-}$ *Ccl17*$^{e/e}$ mice after 12 weeks HFD (n=5); **(D)** in *Apoe*$^{-/-}$ and *Apoe*$^{-/-}$*Ccr4*$^{-/-}$ mice after 12 weeks HFD (n=27). Data **(A-D)** represent mean±SEM, Student t test with Welch correction. P values <0.05 were considered statistically significant. *P<0.05, **P<0.01, ***P<0.001.

To elucidate the role of Ccl3 in Treg maintenance we performed flow cytometric analysis of blood, as well as of single cell suspensions of spleen and para-aortic-, axillar-, inguinal- and mesenteric lymph nodes, isolated from *Ccl3*$^{-/-}$ mice under steady state conditions. Analyzing the distribution of CD4^{+}CD25^{+}Foxp3^{+} Tregs in the above mentioned organs, we observed significant increases in the CD4^{+}CD25^{+}Foxp3^{+} Treg populations in the para-aortic-, axillar-, inguinal- and mesenteric lymph nodes of *Ccl3*$^{-/-}$ mice when compared to *C57BL/6* control mice (Figure 29A-G).

Figure 29. shown at page 68. Ccl3 deficiency affects regulatory T cell populations. (A) Representative dot plots of Flow cytometric analysis of CD3^{+}CD4^{+}CD25^{+}Foxp3^{+} Tregs in para-aortic LNs of *Ccl3*$^{-/-}$ and *C57BL/6* mice under steady state conditions; numbers in dot plots are percentage of CD4^{+} events. **(B-G)** Flow cytometric analysis of CD3^{+}CD4^{+}CD25^{+}Foxp3^{+} Tregs **(B)** in Blood **(C)** Spleen **(D)** para-aortic LNs **(E)** axillar LNs **(F)** inguinal LNs and **(G)** mesenteric LNs of *Ccl3*$^{-/-}$ and *C57BL/6* mice employing indicated surface markers. Data **(B-G)** represents mean±SEM, Student t test with Welch correction (n=10). P values <0.05 were considered statistically significant. *P<0.05, **P<0.01, ***P<0.001.
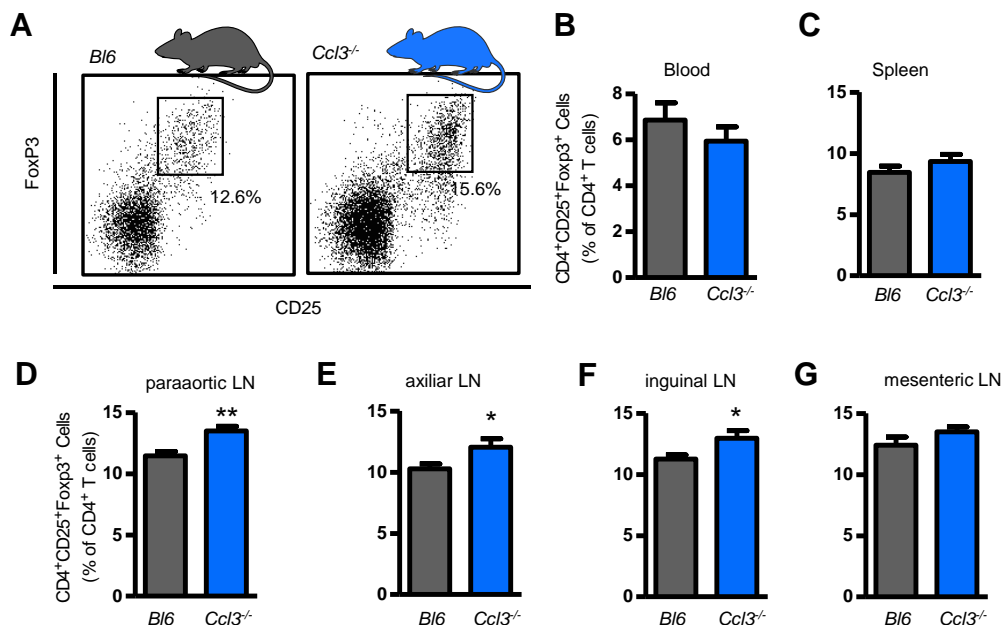
To clarify whether DCs are the only cell type that secret Ccl3 after Ccl17 stimulation, or if other leukocyte populations are also able to release Ccl3 upon rmCcl17 treatment, we isolated CD11b+CD11c+MHCII+ DCs, CD3+ T cells and B220+ B cells through flow cytometric sorting. In addition, we used positive magnetic sorting to obtain CD115+ monocytes. Furthermore, we carried out negative magnetic sorting to obtain untouched neutrophils. These cells were cultured for 4h at 37°C in the presence or absence of rmCcl17. Subsequently Ccl3 concentrations in the supernatant were measured by ELISA. Notably, DCs were the only cell population secreting considerable amounts of Ccl3 after Ccl17 stimulation, while T cells, B cells, monocytes and neutrophils did not release significant amounts of Ccl3 after stimulation with rmCcl17 (Figure 30).
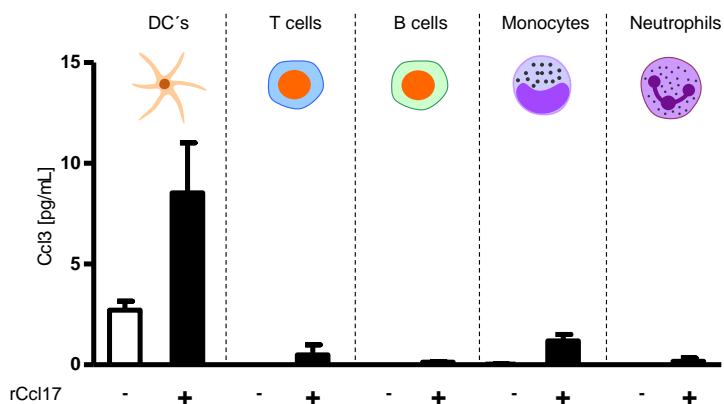
Figure 30. DCs are the main producers of Ccl3 after Ccl17 stimulation. Sorted CD11b$^+$CD11c$^+$MHCII$^+$ DCs, CD3$^+$ T cells, B220$^+$ B cells and magnetically sorted CD115$^+$ monocytes and untouched neutrophils were cultured for 4h at 37°C in the presence or absence of rmCcl17. Subsequently the supernatant was subjected to an ELISA measuring Ccl3 concentration (pg/ml). Data represents mean±SEM (n=3-6).

To further dissect the mechanism by which Ccl3 restrains Tregs, we isolated naïve CD4$^+$ CD62L$^+$ T cells from spleens of *Apoe$^{-/-}$*, *Apoe$^{-/-}$Ccr4$^{-/-}$*, *Apoe$^{-/-}$Ccr5$^{-/-}$*, or *Apoe$^{-/-}$Ccr1$^{-/-}$* mice. We cultured them under Treg polarizing conditions using TGF-β in the presence or absence of recombinant murine Ccl3 (see methods 2.2.3.2.). Frequencies of CD4$^+$CD25$^+$Foxp3$^+$ Tregs among CD4$^+$ T cells were analyzed by flow cytometry. We observed significant decreases in CD4$^+$CD25$^+$Foxp3$^+$ Treg frequencies when treating cells isolated from *Apoe$^{-/-}$*, *Apoe$^{-/-}$Ccr4$^{-/-}$*, *Apoe$^{-/-}$Ccr5$^{-/-}$* mice with Ccl3 compared to the non- treated control. Only cells isolated from *Apoe$^{-/-}$Ccr1$^{-/-}$* mice and treated with Ccl3 displayed no differences in CD4$^+$CD25$^+$Foxp3$^+$ Treg frequencies, indicating that Ccl3 signals via Ccr1 to restrain Tregs (Figure 31A). Furthermore, we investigated if Ccl3 might affect the polarization of T cells and direct them towards a more pro-inflammatory phenotype. For this purpose, we isolated again naïve CD4$^+$CD62L$^+$ T cells from spleens of *Apoe$^{-/-}$*, *Apoe$^{-/-}$Ccr4$^{-/-}$*, *Apoe$^{-/-}$Ccr5$^{-/-}$*, or *Apoe$^{-/-}$Ccr1$^{-/-}$* mice and cultured them under Treg polarizing conditions using TGF-β in the presence or absence of rmCcl3. Frequencies of either CD4$^+$Tbet$^+$ T$_H$1 cells (Figure 31B), CD4$^+$GATA3$^+$ T$_H$2 cells (Figure 31C) or CD4$^+$RorγT$^+$ T$_H$17 cells (Figure 31D), among CD4$^+$ T cells were analyzed by flow cytometry. We observed significant increases in T$_H$1 cell frequencies and T$_H$17 cell frequencies when treating cells with TGF-β in combination with Ccl3 compared to TGF-β treated cells alone. Only cells isolated from *Apoe$^{-/-}$Ccr1$^{-/-}$* mice did not reveal any differences in T$_H$1 cells frequencies nor T$_H$17 cells frequencies upon treatment with TGF-β in combination with Ccl3, indicating that Ccl3 signals via Ccr1 to induce T$_H$1 and T$_H$17 differentiation and demonstrating its strong pro-inflammatory properties. We were not able to observe any effects of Ccl3 towards differentiation into T$_H$2 cells.

Figure 31. shown on page 70. Ccl3 induces differentiation of naïve T cells into T$_H$1 and T$_H$17 cells. Naïve CD4$^+$ CD62L$^+$ T cells isolated either from spleens and LN of *Apoe$^{-/-}$*, *Apoe$^{-/-}$Ccr4$^{-/-}$*, *Apoe$^{-/-}$Ccr5$^{-/-}$*, or *Apoe$^{-/-}$Ccr1$^{-/-}$* mice were cultured under Treg polarization conditions using TGF-β in the presence or absence of rmCcl3 for 3 days. Frequencies of **(A)** CD4$^+$CD25$^+$Foxp3$^+$ Tregs (n=6) **(B)** CD4$^+$Tbet$^+$ TH1 cells (n=3) **(C)** CD4$^+$GATA3$^+$ TH2 cells (n=3) and **D)** CD4$^+$RorγT$^+$ TH17 cells (n=3), among CD4$^+$ T cells were analyzed by flow cytometry. Displayed are percentages normalized to the non-Ccl3 treated control group. **(A-D)** Data represent mean±SEM. 1-way analysis of variance (ANOVA) with, Kruskal-Wallis test with Dunn posttest were used. P values <0.05 were considered statistically significant. *P<0.05. **P<0.01. ***P<0.001.

A iTreg differentiation

B T_H1 differentiation

C T_H2 differentiation

D T_H17 differentiation
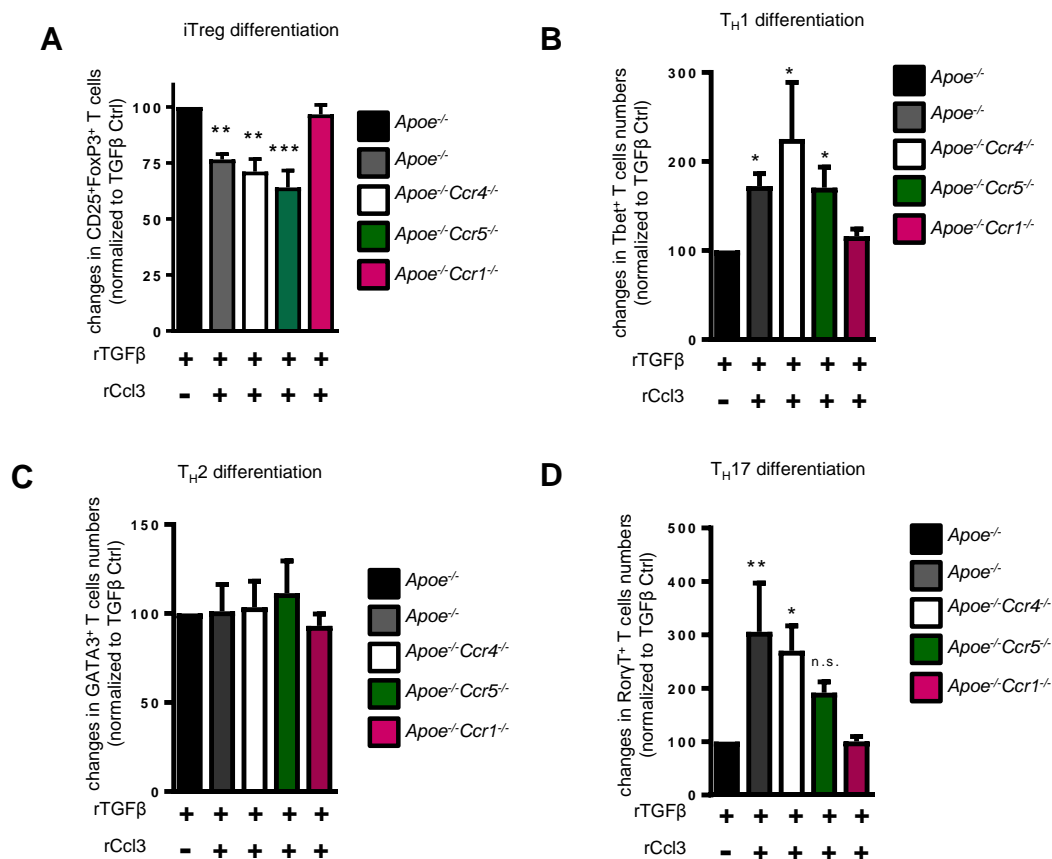
To elucidate if Ccl17 producing DCs are responsible for the secretion of Ccl3 and the subsequent restrain of Tregs, we isolated CD11b$^+$CD11c$^+$MHCII$^+$eGFP$^+$ DCs from either *Apoe$^{-/-}$Ccl17$^{e/w}$* (Ccl17 competent) or *Apoe$^{-/-}$Ccl17$^{e/e}$* (Ccl17-deficient) mice. We cultured them together with naïve CD4$^+$CD62L$^+$ T cells isolated from either *Apoe$^{-/-}$*, *Apoe$^{-/-}$Ccr4$^{-/-}$*, or *Apoe$^{-/-}$Ccr1$^{-/-}$* for three days (see methods 2.2.3.3.) (Figure 32). We analyzed the frequencies of CD4$^+$CD25$^+$Foxp3$^+$ Tregs among CD4$^+$ T cells and observed that when co-cultured with *Apoe$^{-/-}$Ccl17$^{e/w}$* DCs, *Apoe$^{-/-}$* naïve CD4$^+$CD62L$^+$ T cells differentiated less into CD4$^+$CD25$^+$Foxp3$^+$ Tregs. When *Apoe$^{-/-}$* naïve CD4$^+$CD62L$^+$ T cells were co-cultured with *Apoe$^{-/-}$Ccl17$^{e/e}$* DCs, we observed an increase in CD4$^+$CD25$^+$Foxp3$^+$ Tregs. Similar results were obtained when *Apoe$^{-/-}$Ccl17$^{e/w}$* DCs or *Apoe$^{-/-}$Ccl17$^{e/e}$* DCs were co-cultured with *Apoe$^{-/-}$Ccr4$^{-/-}$* naïve CD4$^+$CD62L$^+$ T cells respectively. Only when *Apoe$^{-/-}$Ccr1$^{-/-}$* naïve CD4$^+$CD62L$^+$ T cells where co-cultured with *Apoe$^{-/-}$Ccl17$^{e/w}$* DCs we could not observe changes in Treg frequencies when comparing them to the ones co-cultured

with *Apoe$^{-/-}$Ccl17$^{e/e}$*. These results indicate that Ccl17 producing DCs secrete a secondary mediator that restrains Tregs via the chemokine receptor Ccr1.
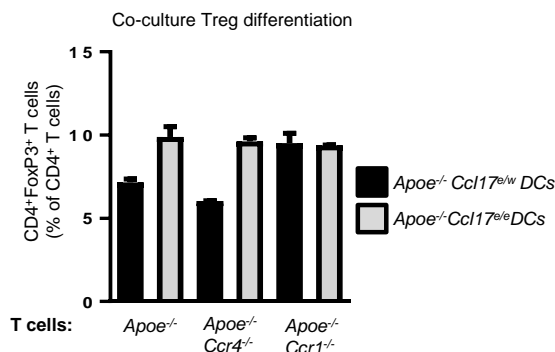
Figure 32. DC-T cell co-culture Treg differentiation. CD11b$^+$CD11c$^+$MHCII$^+$eGFP$^+$ DCs where isolated via flow cytometric sorting from either *Apoe$^{-/-}$Ccl17$^{e/w}$* or *Apoe$^{-/-}$Ccl17$^{e/e}$* mice and cultured together with naïve CD4$^+$ CD62L$^+$ T cells isolated from either *Apoe$^{-/-}$*, *Apoe$^{-/-}$Ccr4$^{-/-}$*, or *Apoe$^{-/-}$Ccr1$^{-/-}$* mice for three days. Frequencies of CD4$^+$CD25$^+$Foxp3$^+$ Tregs among CD4$^+$ T cells were analyzed by flow cytometry.

3.2.2. Deficiency of Ccl3 reduces atherosclerosis in *Apoe$^{-/-}$* mice by restraining Tregs and thereby phenocopies Ccl17 deficiency

To investigate whether Ccl3 acts as a secondary mediator for Ccl17 and if Ccl3 deficiency phenocopies Ccl17 deficiency during the onset of atherosclerosis, we used *Apoe$^{-/-}$*, Apoe$^{-/-}$Ccl3$^{-/-}$ and *Apoe$^{-/-}$Ccl17$^{e/e}$* mice and fed them a HFD for 12 weeks. We analyzed atherosclerotic lesion formation in the aortic root, the aortic arch and in the thoraco-abdominal aorta (Figure 33A). As expected we found a significant reduction in atherosclerotic lesion formation in *Apoe$^{-/-}$Ccl17$^{e/e}$* mice, as well as in *Apoe$^{-/-}$Ccl3$^{-/-}$* in comparison to *Apoe$^{-/-}$* control mice, as visible after Oil-red-O staining in the aortic root and in the *en face* prepared thoraco-abdominal aorta (Figure 33B and D). These effects were also observed after HE staining in the aortic arch (Figure 33C). No alterations were seen in terms of body weight or cholesterol or triglyceride plasma levels (Figure 33E-G).

Figure 33. shown on page 72. Deficiency of Ccl3 reduces atherosclerosis and phenocopies Ccl17 deficiency. (A) Experimental scheme depicting the type of animals used, duration of diet feeding and endpoint analysis performed. **(B-D)** Atherosclerotic lesions were quantified in *Apoe$^{-/-}$* (n=23), *Apoe$^{-/-}$Ccl3$^{-/-}$* (n=13) and *Apoe$^{-/-}$Ccl17$^{e/e}$* (n=10) mice after 12 weeks of HFD. **(B)** Representative images (left) and quantification (right) of Oil-red-O$^+$ area in aortic root sections are shown. **(C)** Representative images (left) and quantification of lesion size in HE-stained aortic arches are depicted. **(D)** Representative images (left) and quantification of Oil-red-O$^+$ area in *en face* prepared thoracoabdominal aortas are shown. **E-H)** Bodyweight **(E)**, plasma cholesterol levels **(F)**, plasma triglyceride levels **(G)**, CCL3 Plasma levels **(H)** of *Apoe$^{-/-}$* (n=23), *Apoe$^{-/-}$Ccl3$^{-/-}$* (n=13) and *Apoe$^{-/-}$Ccl17$^{e/e}$* (n=10) mice after 12 weeks of HFD. Data **(A-H)** represent mean±SEM, One-way analysis of variance (ANOVA) with, Kruskal-Wallis test with Dunn posttest were used. P values <0.05 were considered statistically significant. *P<0.05. **P<0.01.
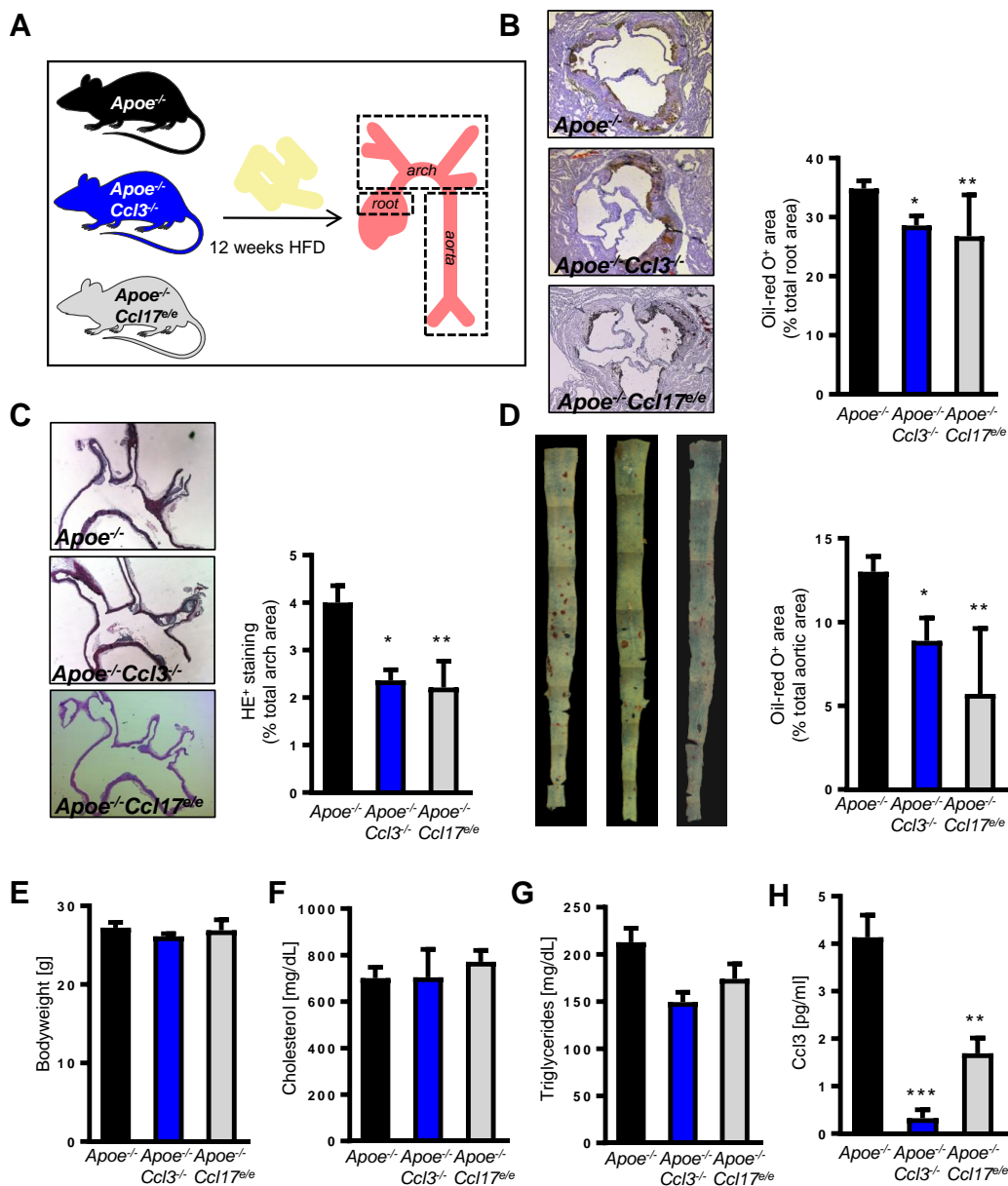
Quantitative immunostaining revealed that the reduction in atherosclerotic lesion size observed in $Apoe^{-/-}Ccl3^{-/-}$ and $Apoe^{-/-}Ccl17^{e/e}$ mice was due to different outcomes in plaque composition. While $Apoe^{-/-}Ccl3^{-/-}$ mice showed a significant reduction in the relative and absolute amount of Mac2$^+$ macrophages compared to $Apoe^{-/-}$ mice, $Apoe^{-/-}$ $Ccl17^{e/e}$ mice did not show these effects (Figure 34A,B,D). Furthermore, the relative and absolute content in SMA$^+$ smooth muscle cells was significantly increased in $Apoe^{-/-}$ $Ccl17^{e/e}$ mice, whereas $Apoe^{-/-}Ccl3^{-/-}$ mice displayed no differences in SMC content compared to control animals (Figure 34A, C).
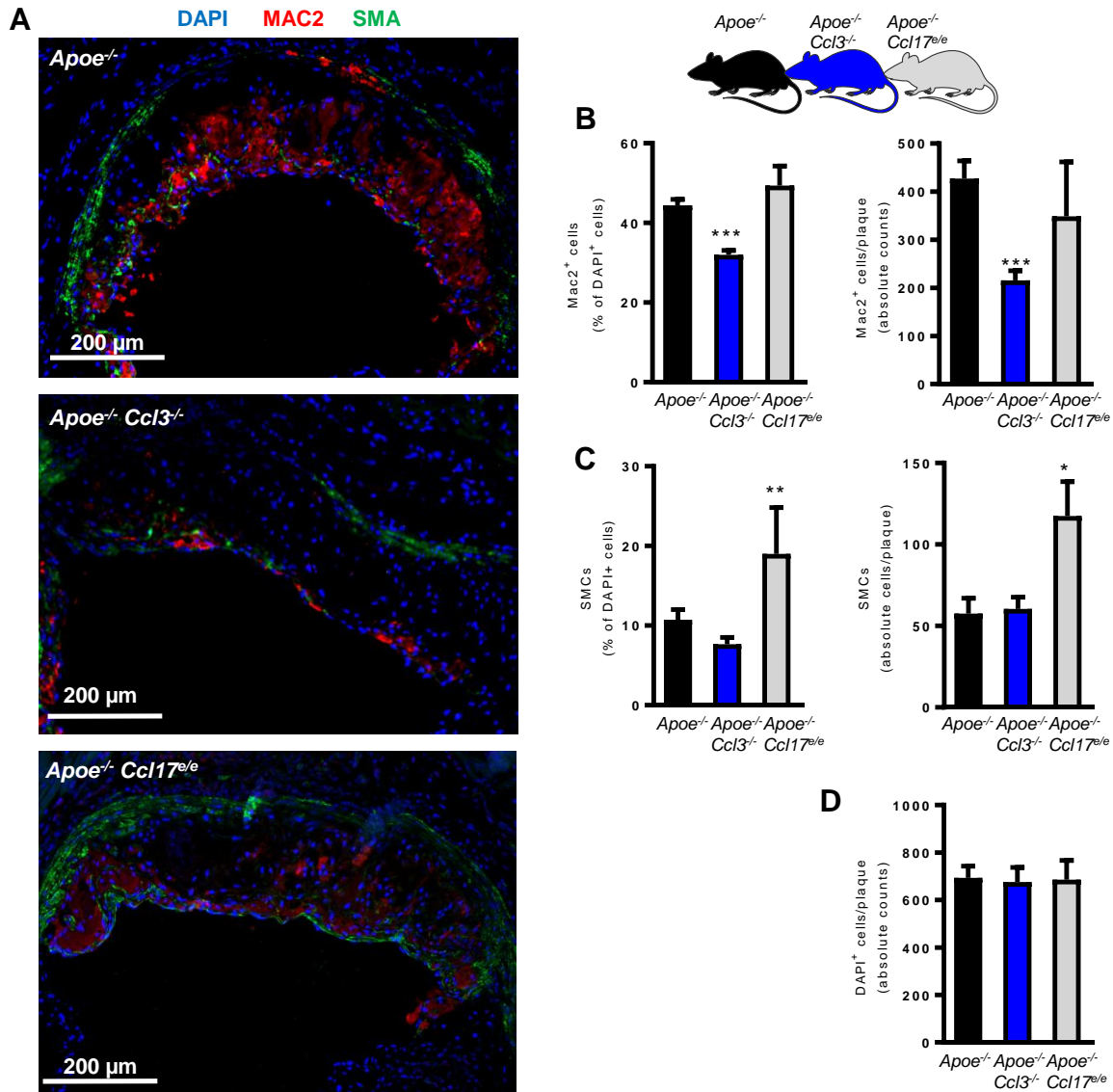
Figure 34. Ccl3- and Ccl17-deficiency differentially impact on plaque composition. Atherosclerotic lesion composition was analyzed using immunohistochemistry. **(A)** Representative images of macrophage (red) and smooth muscle cell (green) staining, in the aortic root of $Apoe^{-/-}$ (n=23; upper picture), $Apoe^{-/-}Ccl3^{-/-}$ (n=13; middle picture) and $Apoe^{-/-}Ccl17^{e/e}$ (n=10; lower picture) mice after 12 weeks of HFD, are shown; cell nuclei are counterstained by DAPI (blue); scale bars: 200 μm. **(B-D)** The relative (left) and absolute quantification (right) of MAC-2+ macrophages **(B)** and SMA+ smooth muscle cells **(C)** and the absolute number of DAPI+ cells **(D)** per plaque area was analyzed by quantitative immunofluorescence. Data **(B-D)** represent mean±SEM, One-way analysis of variance (ANOVA) with, Kruskal-Wallis test with Dunn posttest were used. P values <0.05 were considered statistically significant. *P<0.05. **P<0.01. ***P<0.001.

In order to explain the differences in plaque size and plaque composition between $Apoe^{-/-}$ versus $Apoe^{-/-}Ccl3^{-/-}$ and $Apoe^{-/-}Ccl17^{e/e}$, we performed flow cytometric analysis of blood, as well as of single cell suspensions of bone marrow, spleen and para-aortic-, axillar-, inguinal- and mesenteric lymph nodes. Analyzing the distribution of CD45+

leukocyte subsets mentioned in chapter (see methods 2.2.2.3.), we only observed higher frequencies and an expansion of CD4$^+$CD25$^+$Foxp3$^+$ Tregs in *Apoe$^{-/-}$Ccl3$^{-/-}$* and *Apoe$^{-/-}$Ccl17$^{e/e}$* mice when compared to *Apoe$^{-/-}$* control mice. These results indicate that Ccl3 deficiency induces similar effects already revealed in mice lacking Ccl17 (Figure 35 and Supplemental table 13-16). CD4$^+$CD25$^+$Foxp3$^+$ Tregs were significantly increased in spleen, para-aortic-, axillar-, inguinal- and mesenteric lymph nodes of *Apoe$^{-/-}$Ccl3$^{-/-}$* and *Apoe$^{-/-}$Ccl17$^{e/e}$* mice when compared to *Apoe$^{-/-}$* control mice but where not altered in the circulation of these animals (Figure 35).
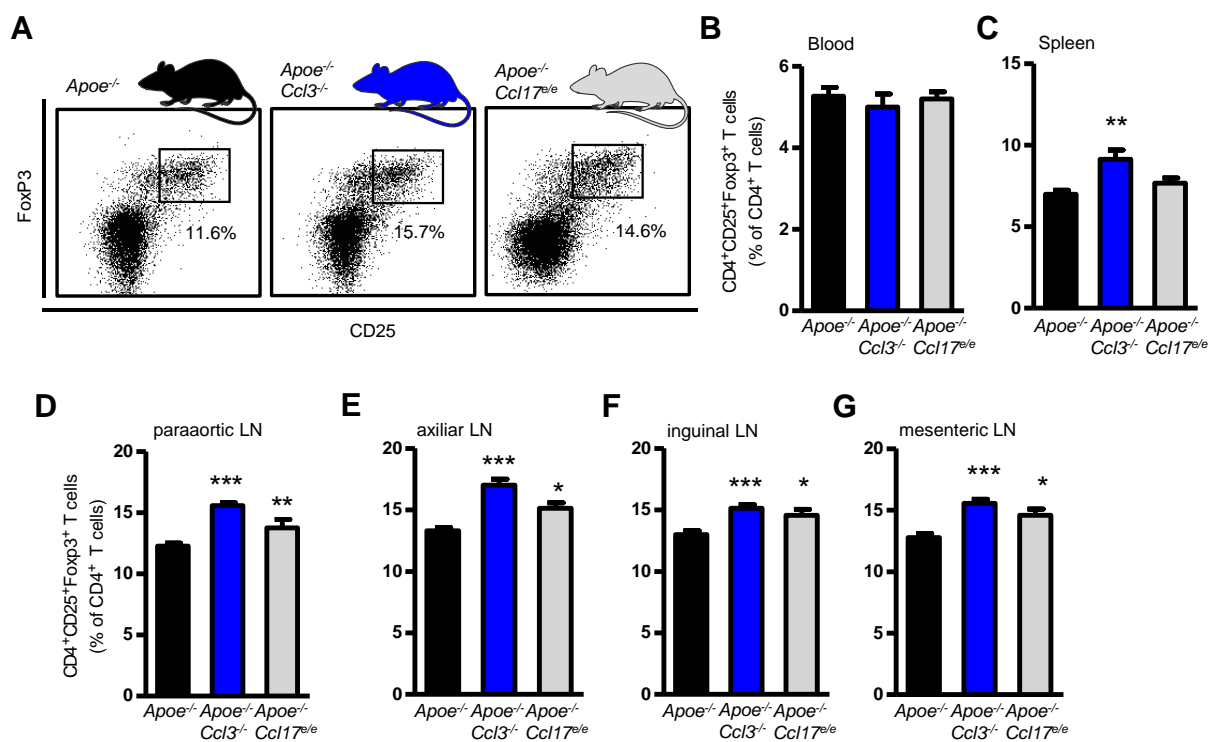
Figure 35. Ccl3 and Ccl17 deficiency affects regulatory T cell populations. (A) Representative dot plots of Flow cytometric analysis of CD3$^+$CD4$^+$CD25$^+$Foxp3$^+$ Tregs in para-aortic LNs of *Apoe$^{-/-}$* (n=23), *Apoe$^{-/-}$Ccl3$^{-/-}$* (n=13) and *Apoe$^{-/-}$Ccl17$^{e/e}$* (n=10) mice after 12 weeks of HFD; numbers in dot plots are percentage of CD4$^+$ events. **(B-G)** Flow cytometric analysis of CD3$^+$CD4$^+$CD25$^+$Foxp3$^+$ Tregs **(B)** in Blood **(C)** Spleen **(D)** para-aortic LNs **(E)** axillar LNs **(F)** inguinal LNs and **(G)** mesenteric LNs of *Apoe$^{-/-}$* (n=23), *Apoe$^{-/-}$Ccl3$^{-/-}$* (n=13) and *Apoe$^{-/-}$Ccl17$^{e/e}$* (n=10) mice after 12 weeks of HFD employing indicated surface markers. Data **(B-G)** represent mean±SEM, One-way analysis of variance (ANOVA) with, Kruskal-Wallis test with Dunn posttest were used. P values <0.05 were considered statistically significant. *P<0.05. **P<0.01. ***P<0.001.

3.2.3. Recombinant Ccl3 reverses effects of Ccl17 deficiency

To investigate if treatment with rmCcl3 could reverse the atheroprotective effects of Ccl17 deficiency, we employed *Apoe$^{-/-}$Ccl17$^{e/e}$* mice and fed a HFD for 4 weeks, while

injecting 20 µg rmCcl3 intraperitoneally three times a week. As a control, *Apoe$^{-/-}$Ccl17$^{e/e}$* and *Apoe$^{-/-}$* mice received shots of PBS three times per week, during a 4 week HFD (Figure 36A). We observed, as expected, a reduction in atherosclerotic lesion size in the *Apoe$^{-/-}$Ccl17$^{e/e}$* mice that were treated with PBS when compared with *Apoe$^{-/-}$* control mice. Analyzing the *Apoe$^{-/-}$Ccl17$^{e/e}$* treated with rmCcl3 we observed plaque sizes that were comparable in size to that of the *Apoe$^{-/-}$* control mice receiving PBS (Figure 36B+C). Moreover, CD4$^+$CD25$^+$Foxp3$^+$ Tregs significantly increased in para-aortic lymph nodes of *Apoe$^{-/-}$Ccl17$^{e/e}$* animals treated with rmCcl3 in comparison to the control group. Treg numbers in *Apoe$^{-/-}$Ccl17$^{e/e}$* mice treated with rmCcl3 were comparable to that of the *Apoe$^{-/-}$* control mice receiving PBS (Figure 36D+E).
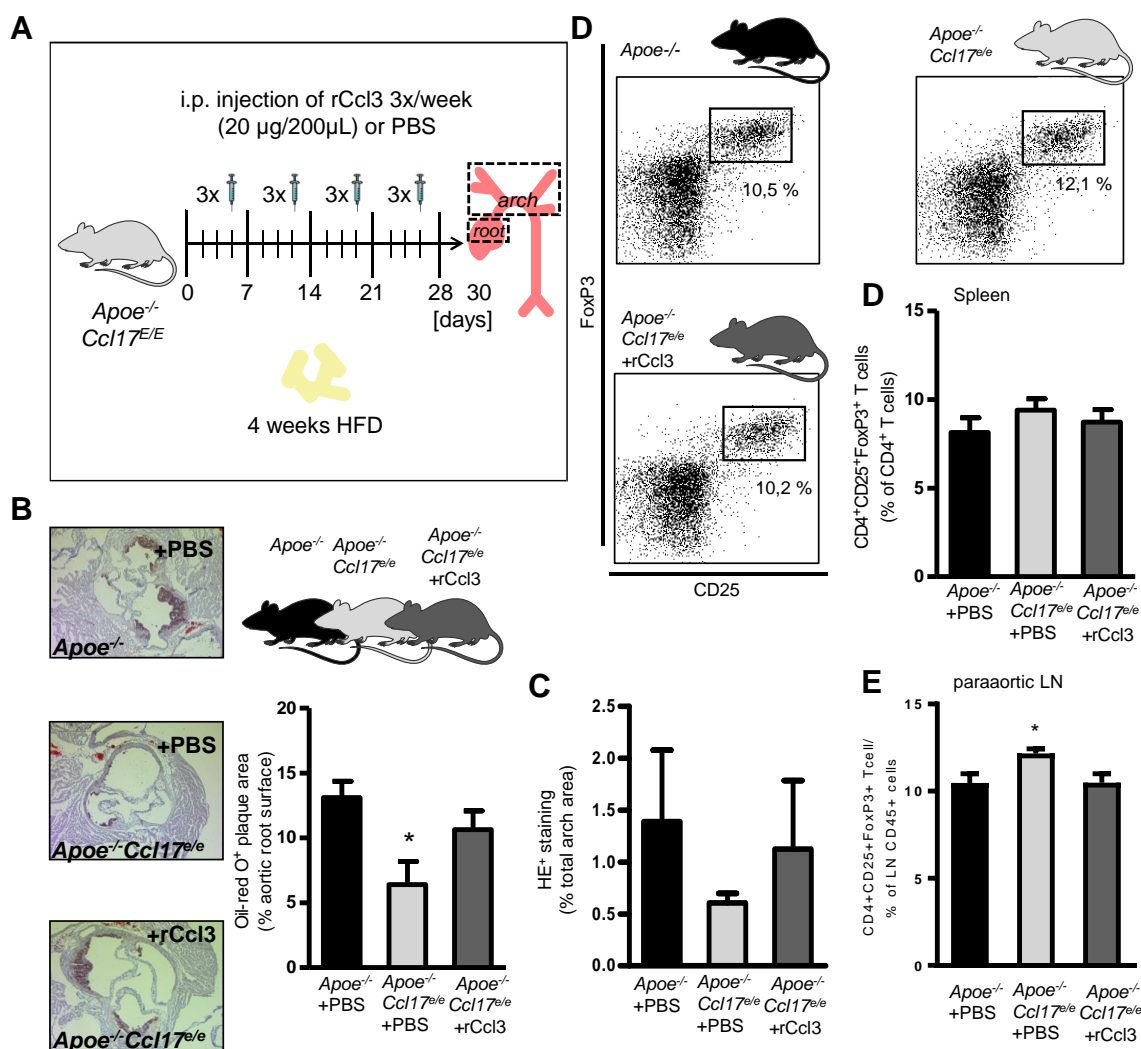
Figure 36. Recombinant Ccl3 reverses effects of Ccl17 deficiency. (A) Experimental scheme depicting the type of animals used, treatment carried out, duration of diet feeding and endpoint analysis performed. **(B+C)** Atherosclerotic lesions were quantified in *Apoe$^{-/-}$*, *Apoe$^{-/-}$Ccl17$^{e/e}$* and CCL3 treated

Apoe^{-/-}Ccl17^{e/e} (n=10) mice after 4 weeks of HFD. **(B)** Representative images (left) and quantification (right) of Oil-red-O$^+$ area in aortic root sections are shown. **(C)** Quantification of lesion size in HE-stained aortic arches is depicted. **(D)** Representative dot plots of Flow cytometric analysis of CD3$^+$CD4$^+$CD25$^+$Foxp3$^+$ Tregs in para-aortic LNs of *Apoe^{-/-}*, *Apoe^{-/-}Ccl17^{e/e}* and CCL3 treated *Apoe^{-/-}Ccl17^{e/e}* (n=10) mice after 4 weeks of HFD; numbers in dot plots are percentage of CD4$^+$ events. **(E+F)** Flow cytometric analysis of CD3$^+$CD4$^+$CD25$^+$Foxp3$^+$ Tregs **(E)** in Spleen and **(F)** para-aortic LNs. Data **(B-F)** represent mean±SEM, One-way analysis of variance (ANOVA) with, Kruskal-Wallis test with Dunn posttest were used. P values <0.05 were considered statistically significant (n=10). *P<0.05, **P<0.01, ***P<0.001.

3.2.4. Deficiency of Ccr1 reduces atherosclerosis in *Apoe^{-/-}* mice by restraining Tregs and thereby phenocopies Ccl17 and Ccl3 deficiency

Since we were able to demonstrate that Ccl3 signals via Ccr1 to restrain Tregs and to push differentiation of naïve T cells towards pro-inflammatory subtypes such as T$_H$1 and T$_H$17 we further wanted to investigate the role of Ccr1 during atherosclerosis. For this purpose, we used *Apoe^{-/-}Ccr1^{-/-}* mice and fed them a high fat diet (HFD) for 12 weeks. We analyzed the atherosclerotic lesion formation in the aortic root, the aortic arch and in the thoraco-abdominal aorta (Figure 37A). A significant reduction in atherosclerotic lesion formation was observed in *Apoe^{-/-}Ccr1^{-/-}* mice in comparison to *Apoe^{-/-}* control mice, as visible after Oil-red-O staining in the aortic root and the *en face* prepared thoraco-abdominal aorta (Figure 37B and D), as well as after HE staining in the aortic arch (Figure 37C). No alterations were observed concerning the weight of the mice, nor the cholesterol or triglyceride plasma levels, nor Ccl3 plasma levels (Figure 37E-H).

Figure 37. shown on page 77. Deficiency of Ccr1 reduces atherosclerosis. (A) Experimental scheme depicting the type of animals used, duration of diet feeding and endpoint analysis performed. **(B-D)** Atherosclerotic lesions were quantified in *Apoe^{-/-}* and *Apoe^{-/-}Ccr1^{-/-}* mice after 12 weeks of HFD. **(B)** Representative images (left) and quantification (right) of Oil-red-O$^+$ area in aortic root sections are shown. **(C)** Representative images (left) and quantification of lesion size in HE-stained aortic arches are depicted. **(D)** Representative images (left) and quantification of Oil-red-O$^+$ area in *en face* prepared thoraco-abdominal aortas are shown. **(E-H)** Bodyweight **(E)**, plasma cholesterol levels **(F)**, plasma triglyceride levels **(G)** and CCL3 plasma levels **(H)** of *Apoe^{-/-}* (n=10) and *Apoe^{-/-}Ccr1^{-/-}* (n=5) mice after 12 weeks of HFD. Data **(A-H)** represent mean±SEM, Student t test with Welch correction. *$P < 0.05$; **$P < 0.01$.
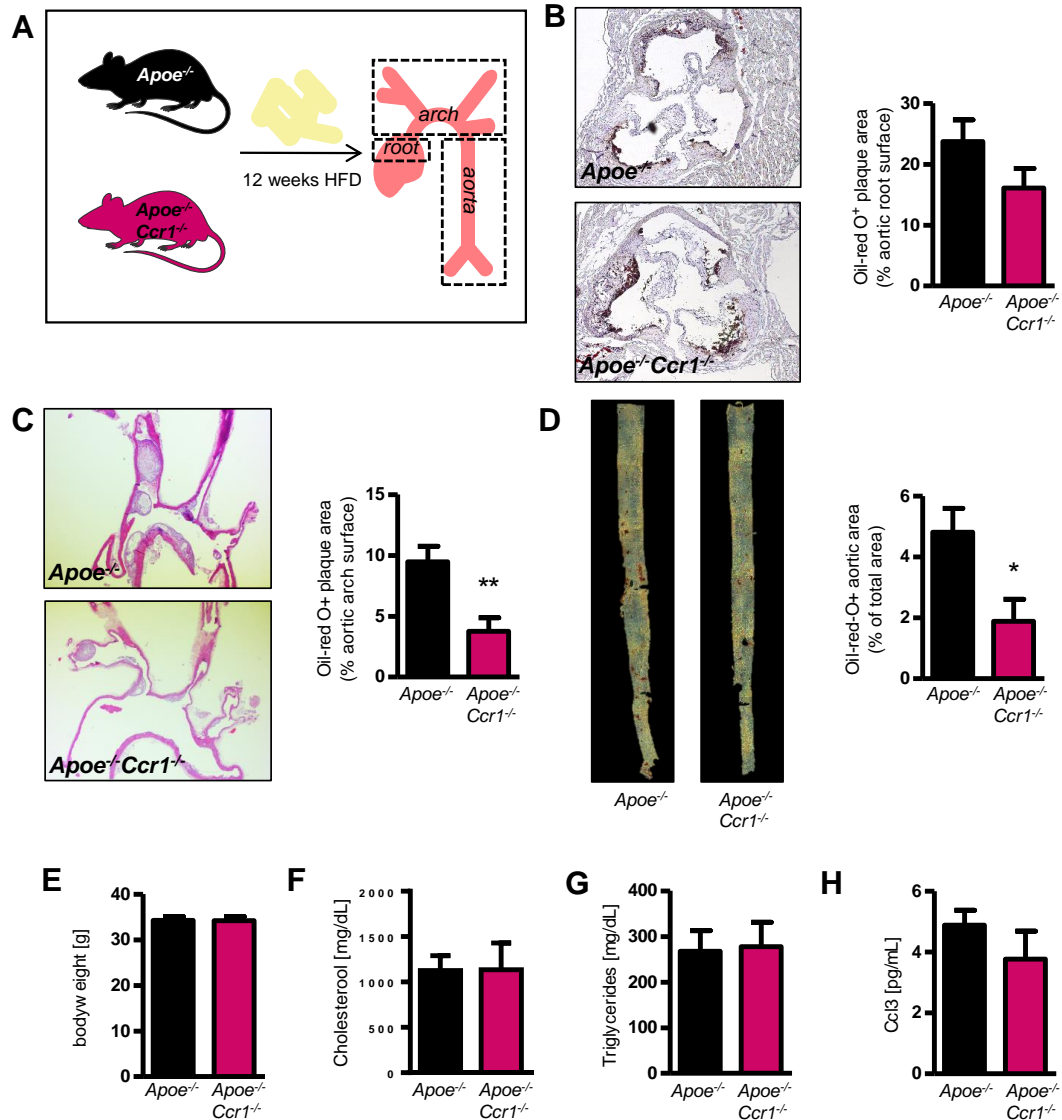
Quantitative immunostaining revealed that the reduction in atherosclerotic lesion size observed in $Apoe^{-/-}Ccr1^{-/-}$ mice, was accompanied by a significant decrease in the absolute and relative numbers of MAC2$^+$ macrophages, when compared to $Apoe^{-/-}$ control mice (Figure 38A and B). Furthermore, the absolute content of SMA$^+$ smooth muscle cells was significantly increased in lesions of $Apoe^{-/-}Ccr1^{-/-}$ mice, whereas the relative content of SMA$^+$ smooth muscle cells showed a tendency towards higher counts (Figure 38A and C). We did not observe any significant changes in DAPI$^+$ cell counts when comparing $Apoe^{-/-}Ccr1^{-/-}$ mice to $Apoe^{-/-}$ mice (Figure 38D). This data indicates a shift towards a more stable plaque phenotype in $Apoe^{-/-}Ccr1^{-/-}$ mice.
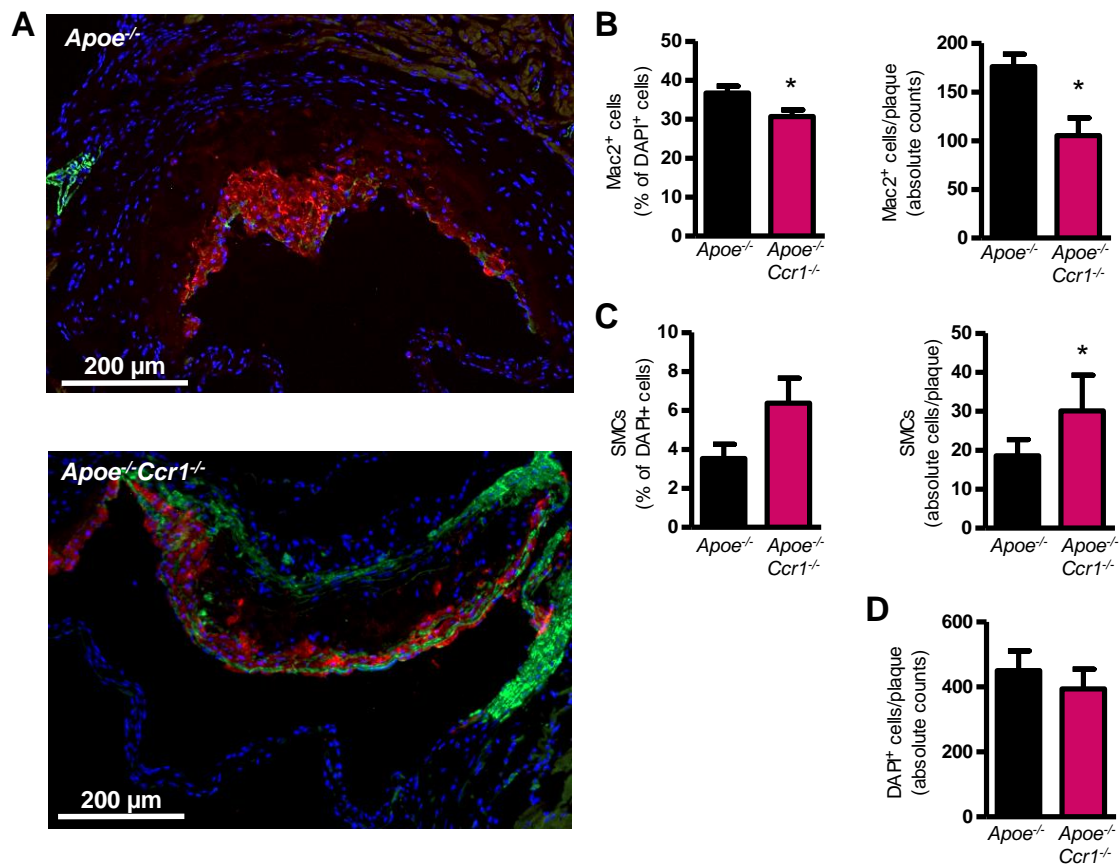
Figure 38. Deficiency of Ccr1 influences plaque composition. Atherosclerotic lesion composition was analyzed using Immunohistochemistry. **(A)** Representative images of macrophage (red) and smooth muscle cell (green) staining, in the aortic root of *Apoe*^{-/-} (n=10; upper picture) and *Apoe*^{-/-}*Ccr1*^{-/-} (n=5; lower picture) mice after 12 weeks of HFD, are shown; cell nuclei are counterstained by DAPI (blue); scale bars: 200 μm. **B-D)** The relative (left) and absolute quantification (right) of MAC-2^{+} macrophages **(B)** and SMA[+] smooth muscle cells **(C)** and the absolute number of DAPI^{+} cells **(D)** per plaque area are shown. Data **(B-D)** represent mean±SEM, Student t test with Welch correction. P values <0.05 were considered statistically significant. *P<0.05

In order to explain the differences in plaque size and plaque composition between *Apoe*^{-/-} versus *Apoe*^{-/-}*Ccr1*^{-/-}, we performed flow cytometric analysis of blood, as well as of single cell suspensions of bone marrow, spleen and para-aortic-, axillar-, inguinal- and mesenteric lymph nodes. Analyzing the distribution of different CD45^{+} leukocyte populations as mentioned in chapter (see methods chapter 2.2.2.3.), we observed higher frequencies and an expansion of CD45^{+} leukocytes in general. Furthermore, we have seen increases in Gr1^{+}CD115^{-} neutrophils, Gr1^{+}CD115^{+} monocytes, Gr1^{-}CD115^{+} monocytes CD11c^{+}MHCII^{+} cDCs and a reduction of CD11b^{+}F4/80^{+} macrophages in the bone marrow of *Apoe*^{-/-}*Ccr1*^{-/-} when compared to *Apoe*^{-/-} mice. Moreover, we observed an increase in CD45^{+}Gr1^{+}CD115^{+} monocytes, CD45^{+}Gr1^{-}CD115^{+} monocytes in the

para-aortic lymph nodes (Supplemental table 17-20). When further comparing $Apoe^{-/-}$ $Ccr1^{-/-}$ mice to $Apoe^{-/-}$ control mice, we observed Tregs being significantly increased in spleen, para-aortic-, axillar-, inguinal- and mesenteric lymph nodes of $Apoe^{-/-}Ccr1^{-/-}$ mice, but no alterations in circulating numbers of Treg in these mice (Figure 39A-G), being in line with observations made in $Apoe^{-/-}Ccl3^{-/-}$ and $Apoe^{-/-}Ccl17^{e/e}$ mice (Figure 35).
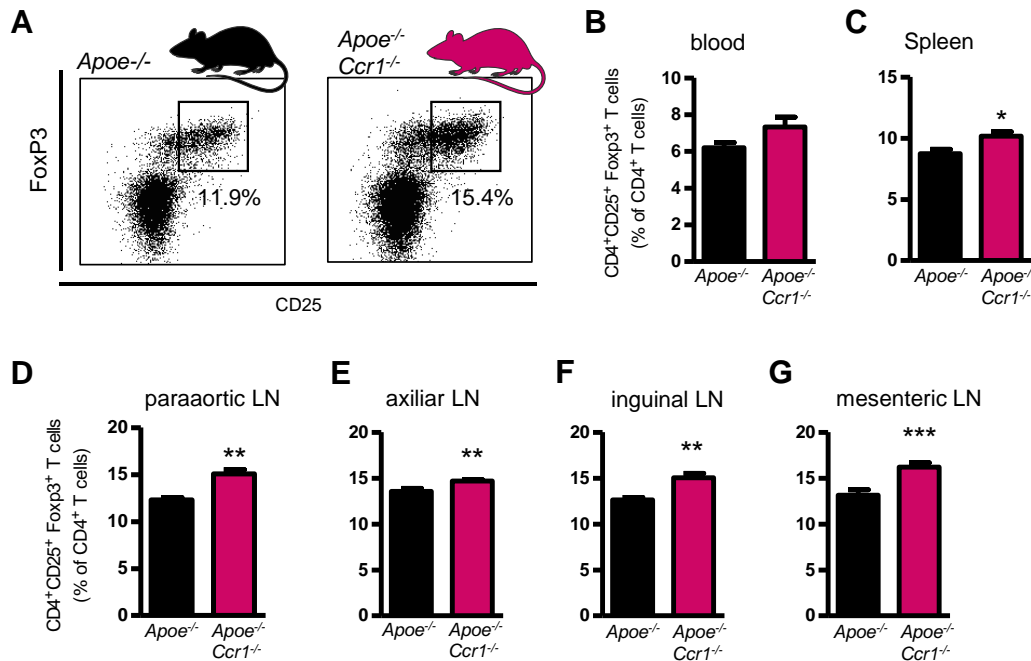
Figure 39. Ccr1 deficiency affects regulatory T cell populations. (A) Representative dot plots of Flow cytometric analysis of $CD3^{+}CD4^{+}CD25^{+}Foxp3^{+}$ Tregs in para-aortic LNs of $Apoe^{-/-}$ (n=10) and $Apoe^{-/-}Ccr1^{-/-}$ (n=5) mice after 12 weeks of HFD; numbers in dot plots are percentage of $CD4^{+}$ events. **(B-G)** Flow cytometric analysis of $CD3^{+}CD4^{+}CD25^{+}Foxp3^{+}$ Tregs **(B)** in Blood **(C)** Spleen **(D)** para-aortic LNs **(E)** axillar LNs **(F)** inguinal LNs and **(G)** mesenteric LNs of $Apoe^{-/-}$ (n=10) and $Apoe^{-/-}Ccr1^{-/-}$ (n=5) mice after 12 weeks of HFD employing indicated surface and intracellular markers. Data **(B-G)** represent mean±SEM, Student t test with Welch correction. P values <0.05 were considered statistically significant. *P<0.05, **P<0.01, ***P<0.001.

3.2.5. Identifying an alternative receptor for Ccl17

Following the discovery that Ccl3 secretion by DCs is mediated by Ccl17, we continued analyzing Ccl3 concentrations using ELISA in plasma obtained either from *C57BL/6 (Ctrl)* ► $Apoe^{-/-}$ mice (n=7); $Ccr4^{-/-}$► $Apoe^{-/-}$ mice (n=7) or $Ccr8^{-/-}$► $Apoe^{-/-}$ mice after 12 weeks HFD (n=11); (Figure 40). We observed that plasma Ccl3 levels were significantly reduced in $Ccr8^{-/-}$► $Apoe^{-/-}$ mice after 12 weeks HFD but not in *C57BL/6 (Ctrl)* ► $Apoe^{-/-}$ mice or in $Ccr4^{-/-}$► $Apoe^{-/-}$ mice after 12 weeks HFD. These results indicate that Ccr8

might be an alternative receptor for Ccl17 and encouraged us to perform further binding studies involving Ccl17 and Ccr8.
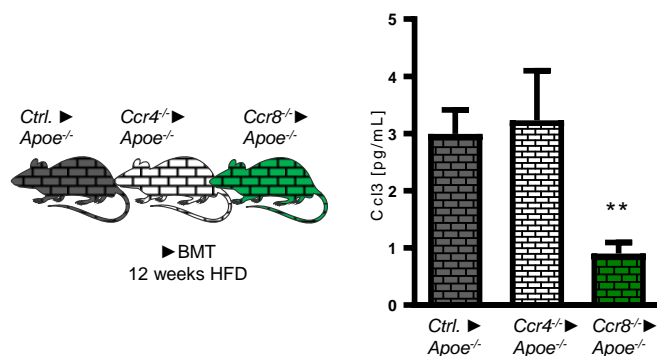
Figure 40. Using Ccl3 plasma levels as a read out to identify new Ccl17 receptors. Scheme depicting the type of animals used (left) for Ccl3 Plasma quantification (right). CCL3 plasma levels were quantified in Plasma from *C57BL/6 (Ctrl)* ▶ *Apoe$^{-/-}$* mice (n=7); *Ccr4$^{-/-}$* ▶ *Apoe$^{-/-}$* mice (n=7) or *Ccr8$^{-/-}$* ▶ *Apoe$^{-/-}$* mice after 12 weeks HFD (n=11). Data represents mean±SEM, 1-way analysis of variance (ANOVA) with, Kruskal-Wallis test with Dunn posttest were used. P values <0.05 were considered statistically significant. *$P < 0.05$; **$P < 0.01$.

To determine whether Ccl17 induces G_i signaling via Ccr8 we transfected Glosensor-HEK293 cells with either Ccr4 or Ccr8. Glosensor-HEK293 cells allow determining cAMP levels in the cell via Luciferase assay, being cAMP a readout for activated G_i signaling. GloSensor luciferase is circularly permuted, joining the wild-type N- and C-termini with a polypeptide or protein domain and creating engineered termini elsewhere within the structure. Therefore, analyte binding induces a conformational shift in the biosensor that allows large increases in luminescence activity. The magnitude of the luminescence singnal increase is proportional to the amount of analyte activity present. Using this system, we stimulated Ccr4 or Ccr8 transfected Glosensor-HEK293 cells with PBS control, Ccl17 (100 ng/ml), Ccl1 (100 ng/ml), Ccl18 (100 ng/ml) or Ccl20 (100 ng/ml). We observed that Ccl17-induced G_i signaling in the Ccr8 transfected cells as well as in the Ccr4 transfected cells indicating that Ccr8 indeed is an alternative receptor for Ccl17. Ccl1 as a positive control for Ccr8-induced, as expected, G_i signaling in the Ccr8 transfected cells, but not in the Ccr4 transfected cells. Ccl20 as a negative control for both Ccr4 and Ccr8 did not induce G_i signaling (Figure 41).
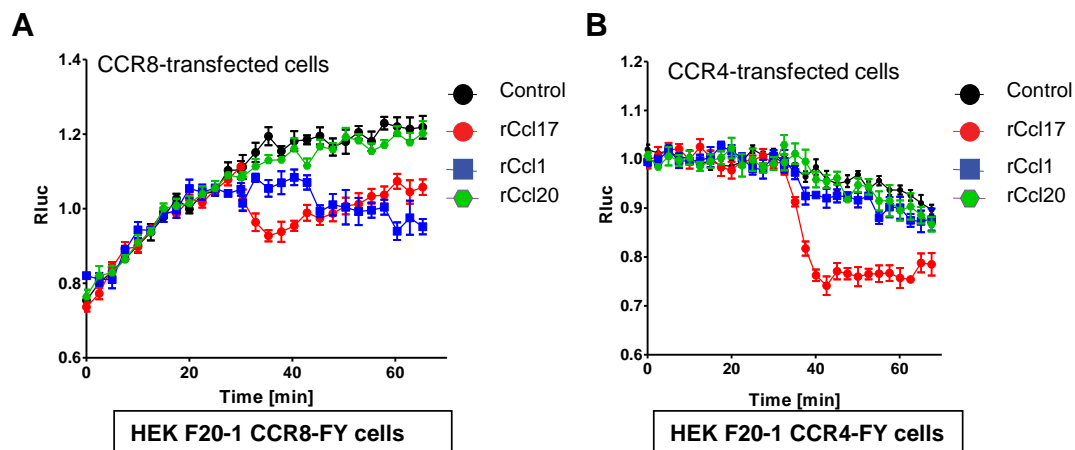
Figure 41. Ccl17 induces Gi signaling via Ccr8. Gi signaling was investigated by determining cAMP levels using Glosensor-HEK293 cells transfected with either **(A)** Ccr4 or **(B)** Ccr8 after stimulation with PBS Control, Ccl17 (100 ng/ml), Ccl1 (100 ng/ml), Ccl18 (100 ng/ml) or Ccl20 (100 ng/ml). Data represent mean±SEM from six independent experiments.

To further validate interactions between murine Ccl17 and Ccr8 we used a proximity ligation assay. Adherent DCs isolated from LNs of *Apoe$^{-/-}$* mice were incubated with Ccl17 or Ccl1 (100 ng/ml each). After stimulation, we used primary antibodies against Ccl17 or Ccl1 and either Ccr4, Ccr5 or Ccr8 to perform the proximity ligation assay according to the manufacturer's instructions. Using secondary antibodies labeled with short PLA probes and subsequent ligation and PCR amplification we generated (in case the desired molecules were in close proximity) signals (red dots) (Figure 42A). Figure 42 B and C demonstrate that when incubating DCs with Ccl17 we observe the formation of red dots when staining with anti-Ccr4 and anti-Ccr8, but not when staining with Ccr5, indicating that Ccl17 binds to Ccr8. Ccl1 on the other hand does only bind to Ccr8 and not Ccr4 or Ccr5.
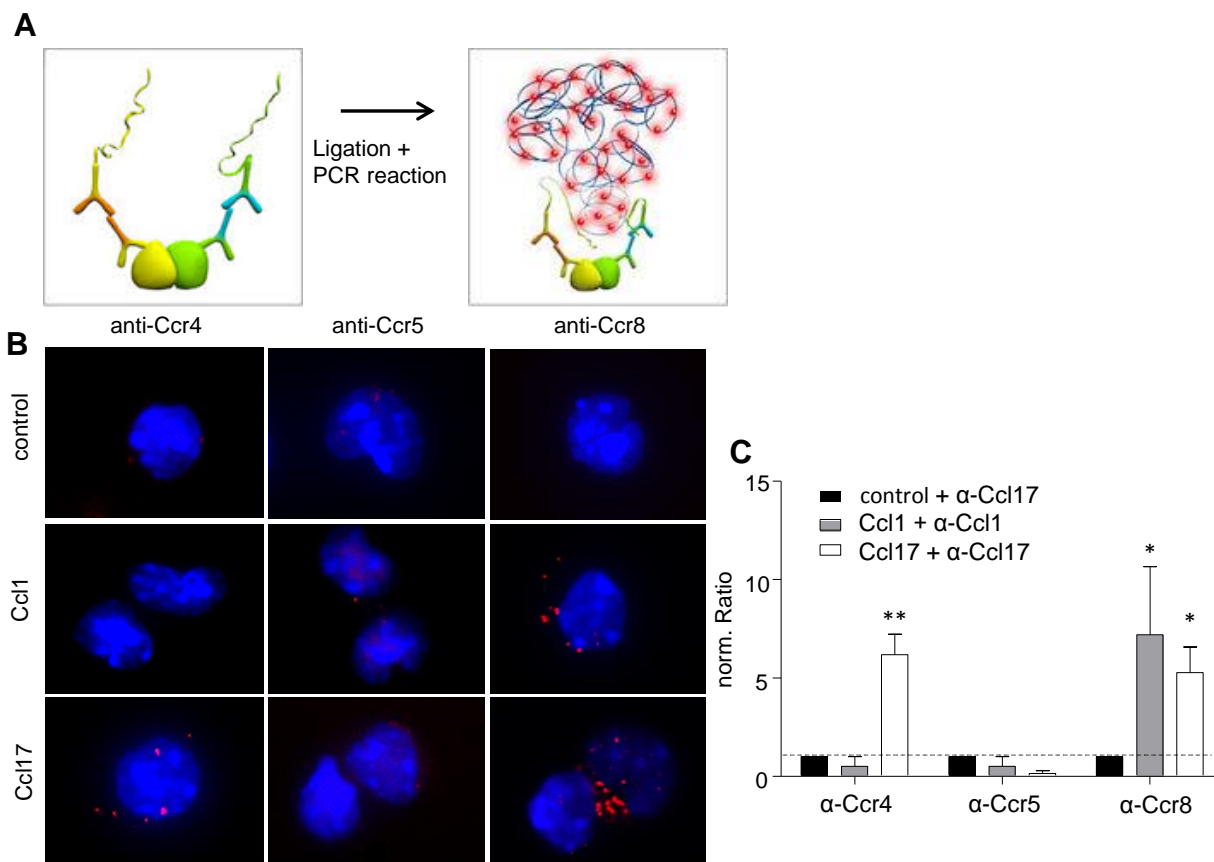
Figure 42. Ccl17 binds Ccr8 but not Ccr5 on the surface of DCs. (A) Scheme of proximity ligation reaction. Interactions between murine Ccl17 or Ccl1 and the receptors Ccr4, Ccr5 and Ccr8 were analyzed on the surface of adherent DCs using a proximity ligation assay after the cells were incubated with Ccl17 or Ccl1 (100 ng/ml each). **(B)** Representative images depict the presence of interaction between ligands and receptors (red dots) on the DC surface. **(C)** Signals generated by interactions between ligands and receptors (red dots) on the DC surface were quantified and normalized relative to the unstimulated control alone (n=3). Data represent means ± SEM. *P < 0.05, **P < 0.01, as analyzed by One-way ANOVA.

To validate CCL17-CCR8 binding, we performed kinetics analyses of their binding curves using surface plasmon resonance (SPR) (Figure 43). Apparent affinities were calculated from on-rates (ka) and off-rates (kd) obtained by fitting the curves using BIAevaluation with the 1:1 interaction model (Langmuir). CCL17 was biotinylated and immobilized onto a neutravidin-coated sensor chip C1 (BIAcore). CCR8 carrying liposomes were perfused at 62.5 ng/ml; 125 ng/ml; 250 ng/ml; 500 ng/ml; 1000 ng/ml and 2000ng/ml at 5 µl/min in running buffer (HBS-EP+, pH 7.4) and regenerated with 100 mM NaOH, 0.05% SDS and 30% acetonitrile. KD was calculated to be 1.10^{-09} M indicating a strong binding between CCL17 and CCR8.
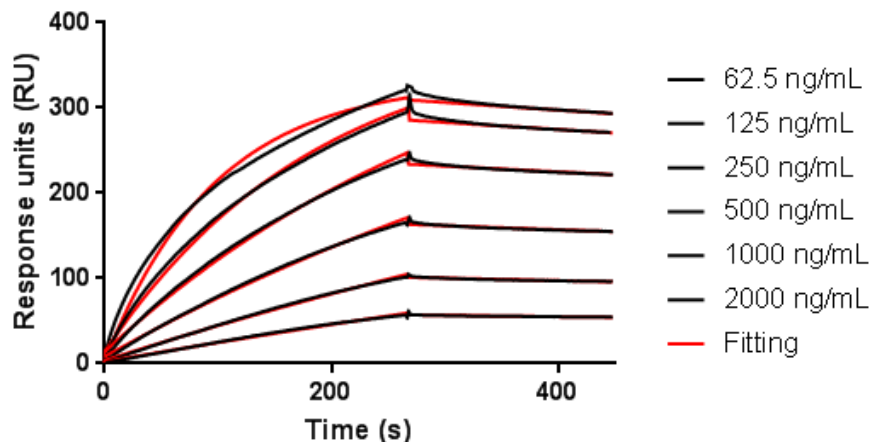
Figure 43. CCL17 binds CCR8-carrying liposomes. Binding of soluble CCR8 carrying liposomes to immobilized CCL17 was assessed by surface plasmon resonance (SPR). Apparent affinities were calculated from on-rates (ka) and off-rates (kd) obtained by fitting the curves using BIAevaluation with the 1:1 interaction model (Langmuir). KD was calculated to be 1.10^{-09} M for CCR8.

3.3.   Heteromeric complexes and their effects on Leukocyte function

Besides the possibility of Ccl17 binding by itself to an alternative receptor which enables its effect on Treg homeostasis, other mechanism may play a role in the diverse biologic functions of Ccl17. For instance, Ccl17 may engage in heterophilic interactions with other chemokines. These heterophilic interactions in a given microenvironment may amplify, inhibit, or modulate the activity of Ccl17.

3.3.1. Ccl17 forms heteromeric complexes with Ccl5

To address possible mechanisms for synergy of the Ccl5-Ccl17 heterodimer, we used an *in situ* proximity ligation assay able detect protein-protein interactions and therefore, the presence of Ccl5-Ccl17 heterodimers. On DCs, which express both Ccr4 and Ccr5, Ccl5-Ccl17 heterodimers formed on the cell surface when adding both chemokines. The increase in Ccl5-Ccl17 heterodimers was inhibited by a peptide-based inhibitor (a Ccl5-derived peptide which forms part of the heterodimer interface with Ccl17) named CAN, revealing that heterodimers can be disrupted by peptides (Figure 44A and B).[317]
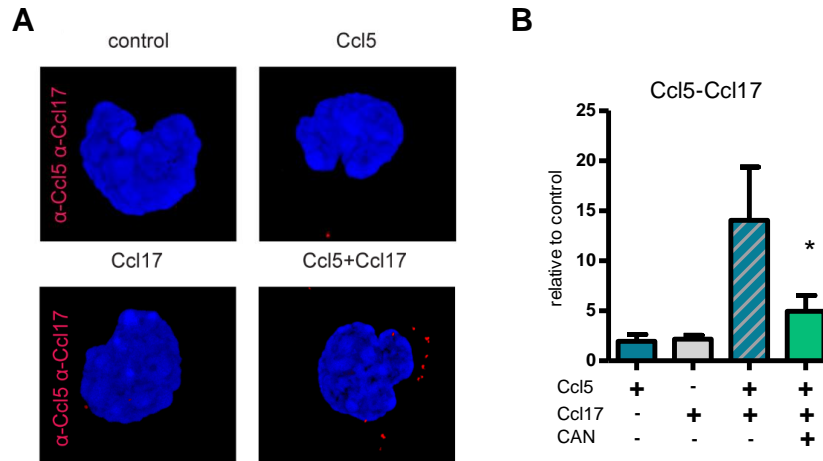
Figure 44. Ccl17 forms heteromeric complexes with Ccl5 on surface of DCs. Interactions between murine Ccl17 and Ccl5 on the surface of adherent DCs were analyzed using a proximity ligation assay after the cells were incubated with Ccl17 or Ccl5 or a combination of both (100 ng/ml each). DCs were also stimulated with Ccl17 and CCl5 in the presence of the peptide CAN (60 nM). **(A)** Representative images depict the presence of interaction Ccl17 and Ccl5 (**red dots**) on the DC surface. **(B)** signals generated by interactions between ligands and receptors (**red dots**) on the DC surface were quantified and normalized relative to the unstimulated control alone (n=5). Data represent means ± SEM. *P < 0.05, as analyzed by One-way ANOVA.[317]

Furthermore we used the *in situ* proximity ligation assay for detecting protein interactions between Ccl5 and Ccl17 and subsequently formed heterodimers on activated endothelial cells after incubation with both chemokines (Figure 45A). Endogenous heterodimers could be detected in mouse lymph nodes (Figure 45B) and in the plaque shoulder region in aortic roots of mice fed a HFD for 12 weeks (Figure 45C).[317]
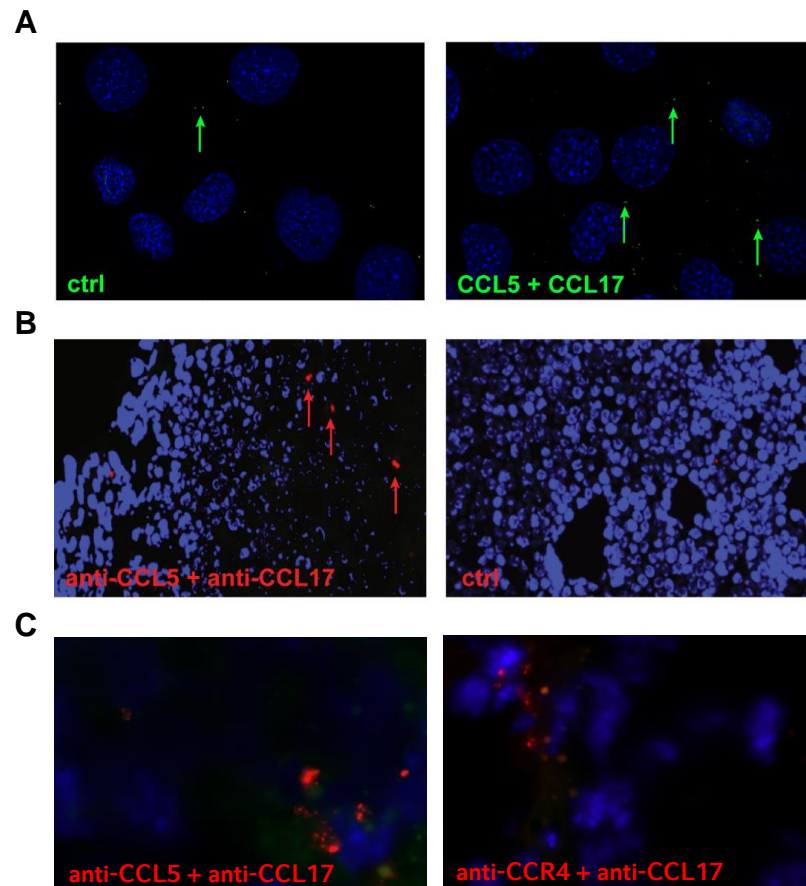
Figure 45. Ccl5-Ccl17 heterodimers are present *in vivo*. Interactions between murine Ccl17 and Ccl5 were analyzed on **(A)** the surface of adherent SVECs, **(B)** murine para-aortic LN sections, **(C)** murine aortic root sections, using a proximity ligation assay. Representative images depict the presence of interaction Ccl17 and Ccl5 (**red dots**).[317]

Furthermore, we analyzed which effects Ccl5-Ccl17 heterodimers might have on T cell biology. We performed transwell filter chemotaxis assays using CD3/CD28-activated primary mouse T cells and determined the chemotactic index as the ratio of chemokine-induced versus unstimulated migration by counting the cells in the bottom chamber. We were able to show that migration toward Ccl5-Ccl17 heterodimers was increased when compared to individually stimulated controls and was inhibited by the disruptive peptide CAN, indicating that the increase in migration is synergistically mediated by the complex rather than being an addition of the effects of both single chemokines (Figure 46).[317]
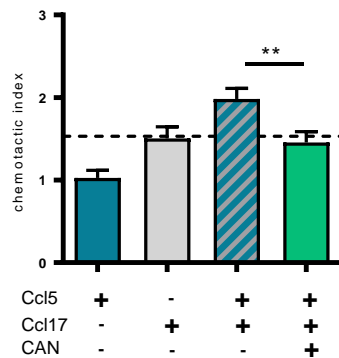
Figure 46. Ccl5-Ccl17 heterodimers induce more efficient T cell migration. Transwell filter chemotaxis assays were performed using CD3/CD28-activated primary mouse T cells (n= 8). Chemotactic index was determined as the ratio of chemokine-induced versus unstimulated migration by counting the cells in the bottom chamber. Migration toward Ccl5 and/or Ccl17 (100 ng/mL each) in the bottom chamber was analyzed in the presence/absence of CAN (60 nM) peptide. Data represent means ± SEM. *P < 0.05, **P < 0.01 as analyzed by One-way ANOVA.[317]

3.3.2. Ccl5-Ccl17 heterodimers induce more efficient T cell arrest

To further assess the functional effects of chemokine heterodimers, we studied induced T cell arrest using IL-2- and CD3/C28-activated human T cells perfused over IL-1β-stimulated human aortic endothelial cells (HAoECs). We observed that CCL5 and CCL17-induced T cell arrest with higher potency and efficacy than CCL5 or CCL17 alone (Figure 47A), establishing that heterodimers are responsible for the synergistic effects. This synergistic effect was inhibited by the disruptive peptide CAN (Figure 47B).[317]
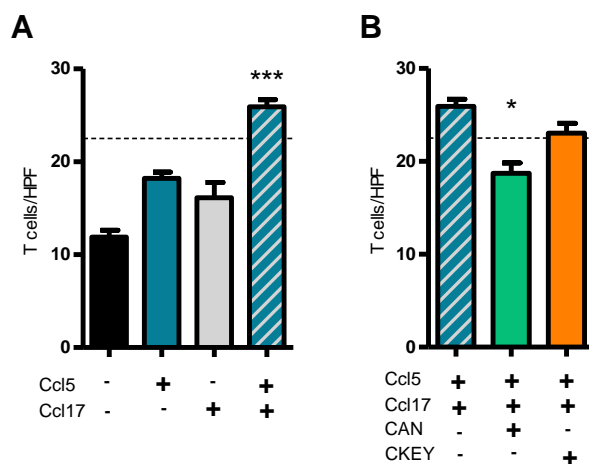
Figure 47. CCL5-CCL17 heterodimers induce more efficient T cell arrest. The firm arrest of IL-2- and CD3/C28-activated human T cells perfused over IL-1β-stimulated human aortic endothelial cells

(HAoECs) at 1.5 dyne/cm 2 was analyzed by counting high-power fields (HPF). For T-cell arrest, **(A)** CCL5 (1nM) and CCL17 (0.1nM) were immobilized on HAoECs in **(B)** combination with CAN or CKEY (both 10 nM) **(A)**, n=5; **(B)** n=3. Data represent means ± SEM. *P < 0.05, **P < 0.01 as analyzed by Kruskal-Wallis test.[317]

3.3.3. Ccl5-Ccl17 heterodimers provoke more efficient binding of Ccl17 to Ccr4

To analyze how Ccl5-Ccl17 heterodimers induce more efficient T cell migration and arrest we again performed proximity ligation assays and focused on analyzing the interactions between either Ccl17 and the receptors Ccr4 and Ccr5, or Ccl5 and the receptors Ccr4 and Ccr5. When stimulating the adherent DCs with Ccl5 and Ccl17 we first observed more efficient binding of Ccl17 to Ccr4 (Figure 48A) as well as increased ligand-receptor cross-interactions, meaning that interactions between Ccl5 and Ccr4 (Figure 48C) where detectable as well as interactions between Ccl17 and Ccr5 (Figure 48D). We did not observe increases in interactions between Ccl5 and Ccr5 when stimulating the cells with a combination of Ccl5 and Ccl17 when compared to the Ccl5 treated control (Figure 48B).[317]
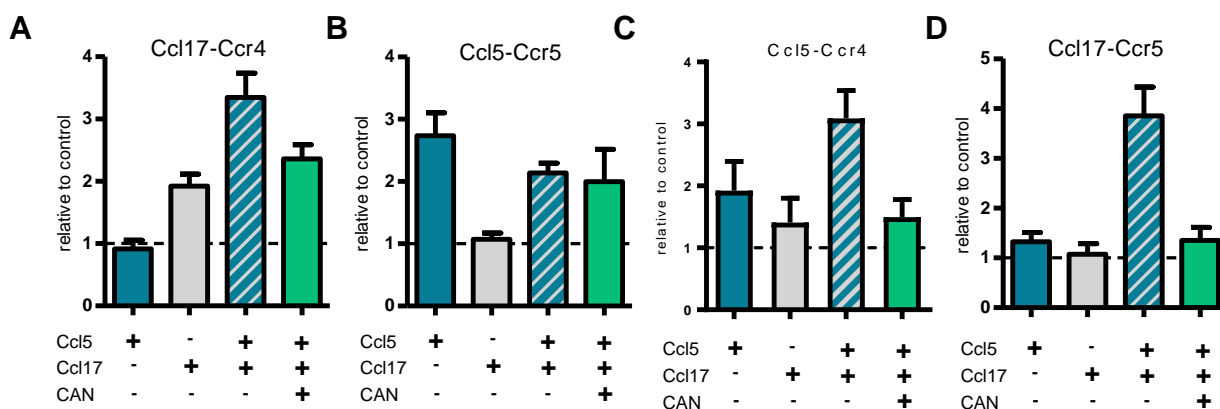
Figure 48. Ccl5-Ccl17 heterodimers bind to Ccr5 and more efficiently to Ccr4 on the surface of DCs. (A-D) Interactions between murine CCL5, CCL17, CCR4, and CCR5 were detected on the surface of adherent DCs using a proximity ligation assay after the cells were incubated with Ccl5, Ccl17, or both (100 ng/mL each) in the presence/absence of CAN (60 nM). Proximity ligation signals generated by interactions between **(A)** murine Ccl17 and the receptor Ccr4; **(B)** murine Ccl5 and the receptor Ccr5; **(C)** Ccl5 and the receptor Ccr4; **(D)** murine Ccl17 and the receptor Ccr5 were analyzed. **(A-D)** Signals generated by interactions between ligands and receptors (**red dots**) on the DC surface were quantified by IHC and normalized relative to the unstimulated control alone (n=3). Data represent mean±SEM from a number of independent experiments, as indicated. *p<0.05, **p<0.01, compared to Ccl5 and Ccl17 combined in the absence of CAN, as analyzed by Mann-Whitney-test.[317]

To further assess if CCL5-CCL17 heterodimers induce a more efficient binding of CCL17 to CCR4, we performed binding competition assays. We used CCL17–Alexa

Fluor 647 bound to CCR4-expressing human embryonic kidney (HEK) 293 transfectants and measured the rate by which the CCL17–Alexa Fluor 647 was displaced by unlabeled CCL17 in the presence or absence of CCL5 (Figure 49). We observed that in the presence of CCL5 the CCL17–Alexa Fluor 647 was displaced much more efficient then when CCL5 was absent.[317]
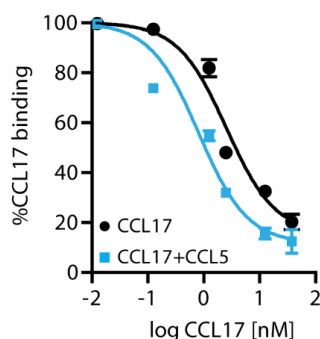
Figure 49. CCL5-CCL17 heterodimer binds more efficient to CCR4. Binding competition assay; CCL17–Alexa Fluor 647 (2.5 nM) bound to CCR4-expressing human embryonic kidney (HEK) 293 transfectants was displaced by unlabeled CCL17 in the presence or absence of CCL5 (1 nM; n = 6).[317]

3.3.4. Ccl5-Ccl17 heterodimers provoke heterodimerization of the receptors Ccr4 and Ccr5

To gain mechanistic insights on how the synergistic effects of the Ccl5-Ccl17 heterodimer work, we again used the *in situ* proximity ligation assay reporting protein interactions which this time detect the presence of Ccr4-Ccr5 heterodimers. On DCs, which express both Ccr4 and Ccr5, Ccr4-Ccr5 heterodimers assembled on the cell surface when adding Ccl5 and Ccl17 in combination. The increase in Ccr4-Ccr5 heterodimers was inhibited by the disruptive peptide CAN and by the R5-TM1/4 peptides (inhibiting heterodimerization of CCR4 and CCR5) that inhibit dimerization of Ccr4 and Ccr5 (Figure 50).[317]

Figure 50. shown on page 89. Ccl5-Ccl17 heterodimers provoke heteromerization of the receptors Ccr4 and Ccr5. Interactions between murine Ccr4 and Ccr5, were analyzed on the surface of adherent DCs using a proximity ligation assay after the cells were incubated with Ccl17 or Ccl5 or a combination of both (100 ng/ml each). DCs were also stimulated with Ccl17 and Ccl5 in the presence of the peptide CAN (60 nM) or R5-TM1/4 peptides (50mg/ml). **(A)** Representative images depict the presence of interaction between Ccr4 and Ccr5 (**red dots**) on the DC surface. **(B)** Signals generated by interactions between ligands and receptors (**red dots**) on the DC surface were quantified and normalized relative to the unstimulated control alone (n=3). Data represent means ± SEM. *P < 0.05, **P < 0.01 as analyzed by Kruskal-Wallis test.[317]
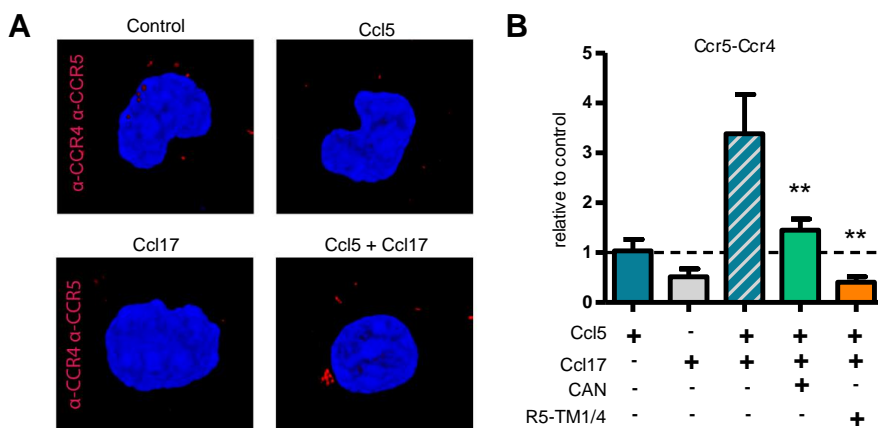
3.3.5. Synergistic effect of Ccl5-Ccl17 heterodimers in T cell transmigration is dependent on Ccr4 and Ccr5 heterodimerization.

Since we discovered that Ccl5-Ccl17 heterodimers induce stronger T cell migration and provoke heterodimerization of the receptors Ccr4 and Ccr5 we further studied if the increase in migration observed with the heterodimer is dependent on the heterodimerization of Ccr4 and Ccr5. We performed transwell filter chemotaxis assays using CD3/CD28-activated primary mouse T cells and determined the chemotactic index as the ratio of chemokine-induced versus unstimulated migration by counting the cells in the bottom chamber. We were able to show that migration toward Ccl5-Ccl17 heterodimer was increased when compared to single stimulated controls and was inhibited by the peptide CAN, indicating that the increase in migration is synergistically mediated by the complex rather than being an addition of the effects of both single chemokines. Furthermore, we treated Ccl5-Ccl17 heterodimer stimulated cells with the disruptive R5-TM1/4 peptides that inhibits dimerization of Ccr4 and Ccr5, and could also observe reduction in migration of T cells comparable to that of single stimulated controls, indicating that the increase of migration-induced by the Ccl5-Ccl17 heterodimers is indeed dependent on the heterodimerization of the receptors Ccr4 and Ccr5 (Figure 51).[317]
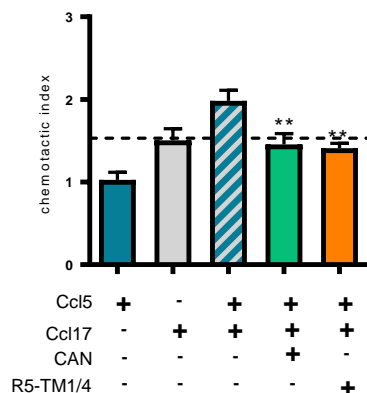
Figure 51. Ccl5-Ccl17 heterodimer induces T cell migration and blocking of Ccr4-Ccr5 heteromerisation inhibits synergistic effect. Transwell filter chemotaxis assays were performed using CD3/CD28-activated primary mouse T cells (n= 8). Chemotactic index was determined as the ratio of chemokine-induced versus unstimulated migration by counting the cells in the bottom chamber. Migration toward Ccl5 and/or Ccl17 (100 ng/mL each) in the bottom chamber was analyzed in the presence/absence of CAN (60 nM) orTM1/4 (50mg/ml) peptides. Data represent mean±SEM from the indicated numbers of independent experiments. *P < 0.05, **P <0.01 as analyzed by one-way ANOVA.[317]

To further validate the findings that the Ccl5-Ccl17 heterodimers induce synergistically a stronger migration of T cells via the heterodimerization of the receptors Ccr4 and Ccr5, we performed transwell filter chemotaxis assays using CD3/CD28-activated primary mouse T cells. We isolated the T cells either from *Apoe*^{-/-} mice and treated them with or without the Ccr4 inhibitor C 021 dihydrochloride, or isolated them from *Apoe*^{-/-}*Ccr5*^{-/-} mice. We determined the chemotactic index as the ratio of chemokine-induced versus unstimulated migration by counting the cells in the bottom chamber. We were able to show that migration toward Ccl5-Ccl17 heterodimer was increased in T cells isolated from *Apoe*^{-/-} mice that were not treated with C 021 dihydrochloride when compared to single stimulated controls. When treating the *Apoe*^{-/-} T cells with C 021 dihydrochloride we could not observe any significant increase while using Ccl5-Ccl17 heterodimer. Using *Apoe*^{-/-}*Ccr5*^{-/-} we could also not observe any significant increases in the migration behavior of the T cells while stimulating with the heterodimer. These results again illustrate that the increase of migration-induced by the Ccl5-Ccl17 heterodimers is indeed dependent on the heterodimerization of the receptors Ccr4 and Ccr5 (Figure 52).[317]
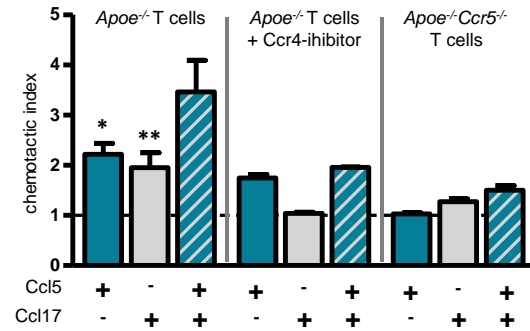
Figure 52. Ccl5-Ccl17 heterodimer induces T cell migration dependent on Ccr4-Ccr5 heteromerisation. Transwell filter chemotaxis assays were performed using CD3/CD28-activated primary mouse *Apoe*^{-/-} T cells, *Apoe*^{-/-} T cells treated with Ccr4 inhibitor, or *Apoe*^{-/-}*Ccr5*^{-/-} T cells. Chemotactic index was determined as the ratio of chemokine-induced versus unstimulated migration by counting the cells in the bottom chamber. Migration toward Ccl5 and/or Ccl17 (100 ng/mL each) in the bottom chamber was analyzed (n= 3-4). Data represent mean±SEM. *p<0.05, **p<0.01 as analyzed by two-way ANOVA.[317]

4. Discussion

4.1.   Discrepancy between Ccl17 deficiency and Ccr4 deficiency

Ccl17 was first discovered by Imai and Yoshida in 1996 and characterized as a CC chemokine constitutively expressed in the thymus and highly selective for T cells.[111] Following that study the group was able to identify the chemokine receptor 4 (Ccr4) as receptor for Ccl17.[112] Previous studies have suggested that Ccl17 is predominantly expressed in cutaneous DCs and by mucosal DCs and that it is up-regulated in Crohn's disease as well as murine experimental colitis.[232-235] The CD11c^{+}DC network found in atherosclerosis-prone regions of naive mice does not express Ccl17, but previous data obtained in our lab show increased frequencies of EGFP^{+}CD11c^{+}DCs in the aortic root of $Ccl17^{e/+}$ and $Ccl17^{e/e}Apoe^{-/-}$ mice during lesion development and an elevated Ccl17expression in advanced stages.[119] Furthermore, Ccl17 levels and myeloid DC numbers were high in advanced human plaques. In addition, Ccl17 transcripts were upregulated in human carotid endarterectomy specimens as compared with macroscopically healthy arteries.[164,236,237] We show that deficiency in the chemokine Ccl17 reduces atherosclerotic lesion formation in $Apoe^{-/-}$ mice. These findings are in line with previous data obtained in our lab that could also show that deficiency in Ccl17 reduces atherosclerosis.[119]

Ccl17 is known to play a role in the recruitment and migration of different T cell subsets including T_H1, T_H2 and Tregs.[118] We were able to show that Ccl17 deficiency protects from atherogenesis through the expansion of regulatory T cells (Tregs) in lymphoid organs. Leading not only to smaller plaque size but also to a more stable plaque phenotype, characterized by higher smooth muscle cell (SMC) levels and reduced macrophage counts in the plaque area. Similar data were observed in previously performed experiments where the increase in Foxp3 expression was also observed in the aorta of Ccl17-deficient mice after high fat diet (HFD).[119] Despite a partial function of Ccr4 in acute inflammatory Treg recruitment and maintenance of Tregs, Weber *et al.* did not observe a comparable reduction in lesion formation and infiltration in chimeric $Ldlr^{-/-}$ mice carrying $Ccr4^{-/-}$ bone marrow,[119] neither did we observe a comparable reduction in lesion formation and infiltration in chimeric $Apoe^{-/-}$ mice carrying $Apoe^{-/-}Ccr4^{-/-}$ bone marrow. On the contrary, we even observed increased plaque burden, which was

accompanied by increased cholesterol levels. Moreover, we could not observe any difference in plaque size nor in Treg numbers using $Apoe^{-/-}Ccr4^{-/-}$ full KO mice. Furthermore, in a model of atopic dermatitis, the inflammatory burden was reduced in mice lacking Ccl17 but not Ccr4.[120] Furthermore, and consistent with data obtained in our lab and by others, Heisseke *et al.* were able to show that Ccl17 deficiency protects from intestinal inflammation through a reduced inflammatory cytokine milieu of DC origin, which facilitates Treg expansion. Again, Ccl17 seemed to promote inflammation independently of Ccr4-mediated T cell recruitment, suggesting an autocrine mechanism where Ccl17 itself stimulates the DC (independent of Ccr4) leading to the secretion of other pro-inflammatory cytokines.[122] In contrast, others have shown that expression of Ccr4 on Treg is crucial to secure Treg recruitment to sites of inflammation[123,124] and facilitates Treg-dependent graft survival.[125] Studies pointing towards Ccr8 as a receptor for Ccl17[113,114] have been questioned[115], but we now show for the first time, that Ccl17 binds to Ccr8 and induces signaling.

The main function of Ccl17 might be to recruit T cells to sites of inflammation. Together with other molecules expressed in the inflamed vessel wall,[238] it is possible that Ccl17 immobilized and presented by endothelial cells[239] is involved in the recruitment of circulating T cells to atherosclerotic lesions. A similar mechanism is reported for the integrin-dependent arrest of memory T cells in chronically inflamed skin.[240] Supporting this idea Weber *et al.* who observed that CD3$^+$ T cells were reduced in lesions of $Ccl17^{e/e}Apoe^{-/-}$ mice, and adoptively transferred CD4$^+$ T cells more efficiently homed to aortas of $Ccl17^{+/+}Apoe^{-/-}$ mice than to those of $Ccl17^{e/e}Apoe^{-/-}$ mice.[119] Nevertheless, the recruitment of CD4$^+$ T cells was enhanced by Ccl17 in an air pouch model.[119] This was in line with previous studies showing that Ccl17 enhances CD4$^+$ T cell recruitment.[114,241-243] The involvement of Ccr4 in recruiting CD4$^+$ T cells in response to Ccl17 (and Ccl22) has been shown by us and others also *in vitro.*[241]

Next we were interested to know if Ccl17, besides being a potent chemoattractant, is able to directly interfere with the polarization of Tregs. Therefore, we performed *in vitro* polarization assays of naïve CD4$^+$ T cells in the presence or absence of Ccl17. We were not able to observe any changes in Treg frequencies after adding Ccl17, indicating that Ccl17 does not directly affect Treg polarization.

As mentioned above, lack of Ccr4 did not resemble the effects of Ccl17 deficiency. No increase in frequencies of CD4$^+$ T cells and Tregs in *Apoe$^{-/-}$Ccr4$^{-/-}$* mice were observed. Moreover, when culturing wild type (*wt)* T cells with either *wt, Ccr4$^{-/-}$* or *Ccl17$^{-/-}$* DCs we observed an increase in the frequency of Tregs when the DCs where lacking Ccl17 which was not observed when they lacked Ccr4. Thus, the mechanisms by which Ccl17 acts pro-inflammatory are not mediated by Ccr4, but rather through other alternative receptors that enable the complex functional profile of Ccl17. This would also explain why, unlike the deletion of Ccl17, a lack of Ccr4 did not confer protection against the formation of atherosclerotic lesions, which likely requires an attenuation of the full spectrum of Ccl17-mediated actions.

4.2.   Ccl3 as the missing secondary mediator

Our results clearly demonstrate that Ccl17 does not interfere with the polarization of Tregs. Furthermore, Heisseke *et al.* described convincingly that Ccl17 deficiency lead to a reduced inflammatory cytokine milieu of DC origin. Therefore, we hypothesized that instead of acting directly upon Tregs, Ccl17 binds via an alternative receptor (not Ccr4) and in an autocrine fashion to (specific) DCs, thereby inducing the release of a secondary mediator restraining Treg homeostasis (see Figure 26).

To test this hypothesis we isolated CD11b$^+$CD11c$^+$MHCII$^+$ DCs via flow cytometry, and stimulated them with or without recombinant Ccl17, in the presence or absence of a specific Ccr4 inhibitor. After four hours of stimulation we collected the supernatant and performed a Multiplex Bead Array, detecting 26 different cytokines and chemokines. We only observed increased levels of Ccl3 (MIP-1α) and Cxcl10 (IP-10) after stimulation with Ccl17. Interestingly secretion of Ccl3 by DCs was independent of Ccr4, whereas secretion of Cxcl10 was dependent on Ccr4 signaling.

Ccl3 belongs (as Ccl17) to the CC chemokine family. During the acute inflammatory state Ccl3 participates in the recruitment and activation of leukocytes via interacting with the receptors Ccr1, Ccr4 and Ccr5.[244] Ccl3 is known as a pyrogen, inducing monophasic fevers similar to those induced by TNFα or IL-1α and IL-1β. In contrast to TNFα, IL-1α and IL-1β, Ccl3-induced fevers are not dampened by ibuprofen (a cyclooxygenase inhibitor).[245] Its expression is known to be significantly increased during atherosclerotic

lesion formation in *Apoe*^{-/-} mice.[246] The main source of Ccl3 seems to be macrophages,[247,248] but different studies also indicate that activated platelets, neutrophils, and mast cells secrete Ccl3.[249-253] Here we demonstrated that the major source of Ccl3 after Ccl17 stimulation is the DC.

Cxcl10 is a T-cell chemokine that was identified as an abundantly induced mRNA after interferon (IFN)-γ activation of monocytic U937 cells.[254,255] Cxcl10 is constitutively expressed at low levels in thymic, splenic, and lymph node stroma. Its expression can be strongly induced by interferons in monocytes and macrophages, as well as in endothelial and smooth muscle cells.[256,257] Several studies suggest that Cxcl10 may play a role in chronic inflammatory diseases, including coronary artery disease and related manifestations of atherosclerosis.[258-260] Cxcl10 binds with a specific high-affinity, the G-protein–coupled receptor Cxcr3, which is highly expressed on activated effector T lymphocytes of the T_H1 phenotype.[261-263] Cxcl10 induces migration of monocytes/macrophages, T cells, NK cells, and dendritic cells. Furthermore, Cxcl10 is involved in antitumor activity, and inhibition of bone marrow colony formation and angiogenesis.[264,265] Heller *et al*. have demonstrated that the absence of Cxcl10 confers a reduction in early lesion formation in *Apoe*^{-/-}*Cxcl10*^{-/-} mice compared with *Apoe*^{-/-} controls, indicating an important role during atherosclerotic lesion formation.[258] These data, together with our results that Cxcl10 secretion by DCs is dependent of Ccl17 signaling, allows us to speculate that part of the pro-atherogenic effects of Ccl17 are mediated via Cxcl10.

Since Ccl17-dependent secretion of Cxcl10 by DCs is dependent on Ccr4 and secretion of Ccl3 is independent of Ccr4 we thought that Ccl3 might be the secondary mediator restraining Treg homeostasis, we were looking for. Therefore, we analyzed plasma Ccl3 levels in samples obtained during several HFD studies. We observed that Ccl3 levels were significantly lower in Ccl17-deficient mice at steady state but also after 12 weeks HFD. Interestingly in a reverse BMT approach; transplanting ApoE-deficient control bone marrow into *Apoe*^{-/-}*Ccl17*^{e/e} mice we were able to restore Ccl3 levels back to control levels. These results indicate that Ccl3 is mainly produced by the hematopoietic system. As expected Ccr4 deficiency had no effect on Ccl3 plasma levels. Furthermore, we obtained Ccl3-deficient mice and investigated the regulatory T cell pool under steady

state using flow cytometry. Already under steady state conditions, we were able to observe significant increases in Treg frequencies in para-aortic, axillar and inguinal lymph nodes, whereas we did not observe any changes in Treg frequencies in circulation, nor in spleen or mesenteric lymph nodes. These results indicate a major role of Ccl3 in negatively controlling Treg homeostasis. Since it is known that several cell types are able to secrete Ccl3 under inflammatory conditions we were interested to know which cells secrete Ccl3 after Ccl17 stimulation. We found that DCs where the major source of Ccl3 after Ccl17 stimulation. To elucidate if Ccl3 interferes with T cell polarization and restrains differentiation into Tregs, we cultured naïve T cells under Treg polarizing conditions using TGF-β in the presence or absence of recombinant murine Ccl3. We found that Ccl3 inhibits differentiation of CD25$^+$Foxp3$^+$ Tregs. Furthermore, using naïve T cells deficient either for Ccr1, Ccr4 or Ccr5 we were able to show that restriction of Treg differentiation by Ccl3 was mediated via Ccr1. Different mechanisms of gene regulation are involved in T cell plasticity. It is known that direct interactions between transcription factors may antagonize the function of opposing transcription factors.[266,267] Since we observe a downregulation in the anti-inflammatory transcription factor Foxp3, we thought to evaluate if we would observe an increase in the expression of the pro inflammatory transcription factors Tbet (T$_H$1 cells) and RoryT (T$_H$17 cells). Indeed, we observed an upregulation of Tbet and RoryT after Ccl3 stimulation that was abrogated in the absence of Ccr1. These results are in line with results obtained by Chen *et al.* where they could demonstrate that high-concentrations of Ccl3 decreased FOXP3 stability by promoting FOXP3's degradation through K48-linkage ubiquitination. This degradation was mainly dependent on upregulation of Serine 473 phosphorylation of the PKBα/Akt1 isoform, and almost independent of mTORC1 (mammalian target of rapamycin complex 1) activity.[268] These data clearly indicate that Ccl3 secreted by DCs after Ccl17 stimulation, acts via Ccr1 on Treg cells and drives their differentiation into pro inflammatory T$_H$1 and T$_H$17 cells and thereby establishing its role as a pro-inflammatory and atherogenic molecule. To further validate the Ccl17-Ccl3 axis and to address the question if the Ccl17 producing DC is responsible for the secretion of Ccl3 and the subsequent restrain of Tregs, we cultured naïve T cells deficient either in *Apoe$^{-/-}$*, *Apoe$^{-/-}$Ccr4$^{-/-}$*, or *Apoe$^{-/-}$Ccr1$^{-/-}$* for three days with DCs deficient or competent for Ccl17. We observed that when co-cultured with *Apoe$^{-/-}$Ccl17$^{e/w}$* DCs, *Apoe$^{-/-}$* naïve CD4$^+$

CD62L$^+$ T cells differentiated less into CD4$^+$CD25$^+$Foxp3$^+$ Tregs then in comparison to *Apoe$^{-/-}$* naïve CD4$^+$ CD62L$^+$ T cells co-cultured with *Apoe$^{-/-}$Ccl17$^{e/e}$* DCs. Similar results were obtained when *Apoe$^{-/-}$Ccl17$^{e/w}$* DCs or *Apoe$^{-/-}$Ccl17$^{e/e}$* DCs were co-cultured with *Apoe$^{-/-}$Ccr4$^{-/-}$* naïve CD4$^+$ CD62L$^+$ T cells respectively. Only when *Apoe$^{-/-}$Ccr1$^{-/-}$* naïve CD4$^+$ CD62L$^+$ T cells where co-cultured with *Apoe$^{-/-}$Ccl17$^{e/w}$* DCs we could not observe changes in Treg frequencies when comparing them to the ones co-cultured with *Apoe$^{-/-}$Ccl17$^{e/e}$*. These results indicate that Ccl17 producing DCs secrete a secondary mediator that restrains Tregs via the chemokine receptor Ccr1.

Several clinical studies have suggested that Ccl3 could serve as a marker of clinical atherosclerosis,[269] and studies confirmed it to be an independent marker of future ischemia.[270,271] And as mentioned above, data obtained under steady state conditions in Ccl3-deficient mice showed significant increases in Treg frequencies in para-aortic, axillar and inguinal lymph nodes indicating a major role of Ccl3 in negatively controlling Treg homeostasis. Therefore, we hypothesized that Ccl3 deficiency would protect from atherosclerotic lesion development. In this study, we therefore aimed to establish the effect of Ccl3 deficiency on atherosclerotic lesion development. We were able to show that Ccl3 deficiency protects from atherogenesis through the expansion of Tregs in lymphoid organs, leading not only to smaller plaque size but also to a more stable plaque phenotype, characterized by reduced macrophage counts in the plaque area. These results were in line with data previously obtained in Ccl17-deficient mice. Furthermore, it confirmed data obtained by de Jager *et al.* who could show that leukocyte specific deficiency of Ccl3 in an *Ldlr$^{-/-}$* mouse model of atherosclerosis was also atheroprotective.[272] The study performed by de Jager *et al.* arguments that macrophages, and to a lesser extent neutrophils, are the primary source of Ccl3 and that hematopoietic Ccl3 deficiency leads to reduced neutrophil adhesion and accumulation in the plaque. Furthermore, they show that Ccl3 deficiency affects neutrophil elimination kinetics and that the half-life of Ccl3-deficient neutrophils was almost 2-fold decreased, and apoptosis rate and activation status were increased. Apoptosis of neutrophils is known to be a protective measure to dampen acute inflammatory responses and prevent unwanted tissue damage.[273] Unfortunately, this study did not analyze the Treg compartment in lymphoid organs.[272]

To validate our assumption, that Ccl3 is the secondary mediator secreted after stimulation with Ccl17, we hypothesized that peritoneal administration of rmCcl3 could reverse the atheroprotective effects of Ccl17 deficiency. Therefore, we employed *Apoe^-/-^ Ccl17^e/e^* mice and fed a HFD for 4 weeks. We injected 20µg rmCcl3 intraperitoneally three times per week. We observed, as expected, a reduction in atherosclerotic lesion size in the *Apoe^-/-^Ccl17^e/e^* mice that were treated with PBS when compared with *Apoe^-/-^* mice. And this phenotype was reversed when treating the *Apoe^-/-^Ccl17^e/e^* mice with rmCcl3 instead of PBS. This was in line with a significant increase in the Treg population in the para-aortic lymph nodes of *Apoe^-/-^Ccl17^e/e^* mice that were treated with PBS and with a reduction in Tregs in *Apoe^-/-^Ccl17^e/e^* mice treated with rmCcl3, that were comparable in number to that of the *Apoe^-/-^* control mice receiving PBS.

4.3. Ccl3-Ccr1 axis in atherosclerosis and other chronic inflammatory disorders

Ccl3 can bind to Ccr4, Ccr1, and Ccr5, of which the latter two have been implicated in atherogenesis.[133,274-277] Interestingly, and to our surprise Potteaux, *et al.* demonstrated that a hematopoietic deficiency of the Ccl3 receptor Ccr1 led to no differences in fatty streak size or composition after 8 weeks of HFD. But after 12 weeks of HFD diet the authors observed a 70% increase in atherosclerotic lesion size in the thoracic aorta of mice transplanted with *Ccr1^-/-^* bone marrow. They explained these results with the fact, that in their hands *Ccr1^-/-^* mice showed enhanced basal and concanavalin A-stimulated IFN-γ production by splenic T cells and enhanced plaque inflammation. In their conclusion they state that, blood-borne Ccr1 alters the immuno-inflammatory response in atherosclerosis and prevents excessive plaque growth and inflammation.[274,276] In line with these findings Braunersreuther *et al.* found that lesion formation, T cell numbers, and IFN-γ content were increased in *Apoe^-/-^Ccr1^-/-^* mice after 12 weeks HFD but not after 4 weeks HFD. Furthermore the group was able to show that atherosclerotic lesion formation was reduced in *Apoe^-/-^Ccr5^-/-^* mice. They concluded that lesional macrophage content and T_H1-related Tim3 expression were reduced, and SMC content and expression of IL-10 in plaques were elevated.[133] These results are in contrast to a study performed by Söhnlein and Drechsler *et al.*, in which the authors analyzed distinct functions of chemokine receptor axes in the atherogenic mobilization and recruitment of

classical monocytes. The authors were able to demonstrate that $Apoe^{-/-}Ccr1^{-/-}$ mice developed significantly lesser atherosclerotic lesions after 4 weeks HFD, which was accompanied by an absolute reduction in macrophages and classical monocytes in the aorta of these animals when compared to the $Apoe^{-/-}$ control. Furthermore the study showed that after 8 weeks of HFD $Apoe^{-/-}Ccr1^{-/-}$ mice still had reduced atherosclerotic plaque burden but that did not reach significance, although a significant reduction in aortic classical monocytes was observed.[134]

Unfortunately, none of these studies looked into the regulatory T cell pool. Since we were able to demonstrate that Ccl3 signals via Ccr1 to restrain Tregs and to push differentiation of naïve T cells towards pro-inflammatory subtypes, such as T_H1 and T_H17, we hypothesized that Ccr1 deficiency would lead to an increase in the regulatory T cell pool and thereby reduce atherosclerotic lesion formation. Hence, we wanted to investigate the role of Ccr1 during the onset of atherosclerosis and analyze the regulatory T cell compartment. For this purpose, we used $Apoe^{-/-}Ccr1^{-/-}$ mice and fed them a HFD for 12 weeks. We analyzed the atherosclerotic lesion formation in the aortic root, the aortic arch and in the thoracoabdominal and observed, contrary to the previously mentioned studies by Potteaux, *et al.* and Braunersreuther *et al.*, a significant reduction in atherosclerotic lesion formation in $Apoe^{-/-}Ccr1^{-/-}$ mice. No alterations were observed concerning the weight of the mice, nor in the cholesterol or triglyceride plasma levels or the Ccl3 plasma levels. These results could be explained by a reduction in the plaque macrophage content and an increase in SMC in the plaque. We also observed in line with our hypothesis increased frequencies of Tregs in lymphoid tissues.

Another study performed in a different disease model was more in line with our results. The authors tested whether Ccl3, and its receptors, Ccr1 and Ccr5, can prevent radiation-induced lung inflammation and fibrosis. Irradiated mice lacking Ccl3 or its receptor, Ccr1, did not develop lung inflammation, fibrosis, and decline in lung function seen in irradiated wild-type mice. Interestingly, mice deficient for Ccr5 were not protected from radiation-induced injury and fibrosis.[278] Several studies came to similar results. For example anti-Ccr1 treatments, reduce bleomycin-induced inflammation and collagen deposition.[279-281] Other studies showed that Ccr1 deficiency protects from hepatic fibrosis[282] and renal fibrosis.[283] A number of small molecule antagonists of Ccr1

have been generated so far;[284,285] a study using a specific Ccr1 antagonist (BX-471) showed protection against acute pancreatitis-associated lung injury by modulating neutrophil recruitment.[286] Some of these small molecule antagonists even have entered into clinical trials;[287] for example BX-471 for multiple sclerosis,[288,289] CP-481715[290] for rheumatoid arthritis (RA),[291-293] AZD-4818[294] for chronic obstructive pulmonary disease,[295] and MLN-3897[296] also for RA.[297] Unfortunately, these antagonists failed to achieve their targeted clinical end points in phase 2 studies. Several scientists have discussed that failures of these mentioned studies and assumed that insufficient outcomes were due to inadequate blockade of the Ccr1 receptor over the course of the trial.[298,299]

The role of Ccr1 in chronic inflammations, especially in atherosclerosis, still remains controversial and needs further characterization. One might argue the need of the Cre-Lox recombination system for cell specific deletion of Ccr1. Placing the Cre recombinase gene after, for example the promotor of Foxp3, would allow for deletion of Ccr1 specifically in Treg cells, and therefore allowing us to study the effect of Ccr1 deficiency in Tregs during atherosclerotic lesion formation.

4.4. Ccr8 – a new receptor for Ccl17

Following the discovery that Ccl17 mediates Ccl3 secretion by DCs, and that plasma Ccl3 levels are useful read outs we continued analyzing Ccl3 concentrations using ELISA in plasma obtained from HFD studies previously performed in our lab. The results indicate that Ccr8 might be an alternative receptor for Ccl17 and led us to perform further binding studies involving Ccl17 and Ccr8. Besides classical biochemical analysis using BIAcore technology, we were also able to confirm binding of Ccl17 to Ccr8 via a proximity ligation assay and confirmed signaling in transfected Glosensor-HEK293 cells via luciferase assay. In addition, other studies pointed towards Ccr8 as a receptor for Ccl17[113,114] but till now had to be considered with caution, as they have been questioned by others.[115,116] Islam, *et al.* argued in their study that chemokine receptors typically undergo internalization upon chemokine agonist binding. Therefore, they conducted internalization assays, using *Ccr8*-transfected cells. The authors showed that surface Ccr8 expression on *Ccr8*-transfected cells was reduced after treatment with increasing concentrations of Ccl18 or Ccl1 but not Ccl17 for 20 min at 37°C. These results led to

the assumption that Ccl17 cannot be a ligand of Ccr8. This does not necessarily be true. Mariani, *et al.* performed an interesting study where they compared Ccl17- and Ccl22-dependent Ccr4 internalization as a mechanism of receptor availability and function on human Th2 cells. They demonstrated that Ccl22 is a strong inducer of Ccr4 internalization, while Ccl17 is not. Nonetheless, Ccl17 is a strong chemotactic factor for Ccr4 expressing cells.[300] Taken together we and others were able to convincingly demonstrate that Ccl17 binds to Ccr8, and indicate that Ccr8 might be involved in Ccl17-dependent secretion of Ccl3, since deficiency in Ccl17 resulted in decreased plasma Ccl3 levels. Further experiments need to be conducted, confirming the Ccl17-Ccr8-Ccl3 axis.

Ccr8 is expressed in T_H2 cells,[301] Tregs,[114] DCs,[302] monocytes[303] and macrophages[304] and is involved in various disease conditions. So far not much is known about Ccr8 and its specific role in chronic inflammatory settings. Especially its involvement in atherosclerosis has still to be clarified. Several studies attribute Ccr8 expressed on T_H2 cells to the development of allergic inflammation.[301] It was shown that Ccr8 is preferentially expressed on T_H2 cells and Ccr4, Ccr8, and Cxcr3 ligands are increased in asthma,[301,305,306] but also in atopic dermatitis.[307] These effects are mainly mediated by the expression of Ccr8 on T_H2 cells and do not explain the role of Ccr8 on the myeloid lineage. Moreover, Ccr8 expression on Tregs is implicated in sustaining their survival e.g. in graft versus host disease[308] most likely through pronounced interaction of Ccl1 with Ccr8 on Tregs underlining the pivotal role of Ccr8+ Treg cells in restraining immunity and controlling inflammation.[309] In the absence of Ccl17 interaction of Ccl1-Ccr8 might further be strengthened adding to the protective effects observed in Ccl17-deficient mice. Likewise, Ccr8 expression has been reported on DCs, which migrate towards its major ligand Ccl1.[310] To investigate the function of Ccr8 in macrophages, Oshio, *et al.* compared cytokine secretion from mouse peritoneal macrophages or bone marrow-derived macrophages stimulated with various Toll-like receptors (TLR) ligands in Ccr8-deficient and wild-type mice. They observed that *Ccr8-/-* macrophages showed attenuated secretion of TNF-α, IL-6, and IL-10 when stimulated with LPS. The authors were also able to show that Ccr8-dependent cytokine secretion was a characteristic of peritoneal macrophages but not of bone marrow-derived macrophages.[311] Therefore,

antagonism of Ccr8 may be beneficial in ameliorating or preventing inflammatory events. First attempts to identify pharmacological antagonists of Ccr8 have been made but did not yet have convincing effects.[312-314]

The role of Ccr8 in chronic inflammatory settings, especially in atherosclerosis, still needs to be elucidated. In addition, similar to Ccr1, a Cre-Lox recombination system for cell specific deletion of Ccr8 would be a helpful tool to dissect cell specific effects of Ccr8 and its involvement in chronic inflammatory disorders.

4.5.   Ccl5-Ccl17 heterodimers

Nesmelova *et al.* wrote that, the apparent complexity of biology increases, as more biomolecular interactions that mediate function become known.[315] Interactions between chemokines in a given microenvironment may amplify, inhibit, or modulate their activity. For instance, homo-oligomerization of Ccl5 is essential for its chemotactic functions. Baltus, *et al.* found that higher order Ccl5 oligomers were needed for Ccr1-mediated arrest but not for Ccr5-mediated spreading/transmigration in flow or transendothelial chemotaxis of leukocytes. They claimed that efficient leukocyte arrest in flow but not transmigration may require the presentation of Ccl5 oligomers to bridge surface-bound Ccl5 and Ccr1.[316] These data demonstrate quite nicely the level of complexity emerging in chemokine biology, as we should keep in mind that different order chemokine homo-oligomers bare potential to different modes of regulation. Recently it also came to our understanding, that chemokine heterodimerization represents an additional regulatory mechanism. A study performed by Nesmelova *et al.* was able to demonstrate that tetrameric platelet factor 4 (PF4/ Cxcl4) and dimeric IL-8 (Cxcl8), two members of the CXC chemokine family, interact. Thereby they exchange subunits and form heterodimers through extension of their antiparallel beta-sheet domains.[315] Furthermore, Hundelshausen, *et al.* demonstrated that Cxcl4 enhanced the arrest of Ccl5-stimulated monocytes on activated endothelial cells under flow conditions, while binding of Cxcl4 to the monocyte surface was increased by Ccl5. These effects were conducted via heterophilic interaction of Cxcl4 with Ccl5.[231] In a follow-up study the same authors were able to determine structural features of Ccl5-Cxcl4 heterodimers. These data led to designing stable peptide inhibitors that could specifically disrupt Ccl5-Cxcl4 interactions. The authors also showed that these peptides reduced atherosclerotic lesion formation

via reduced monocyte infiltration. These results clearly establish the *in vivo* relevance of chemokine heteromers and show the potential of targeting heteromer formation to achieve therapeutic effects.[138]

Hundelshausen *et al.* identified, in an unbiased bidirectional immunoblot chemokine screening and through surface plasmon resonance, heteromeric interactions between pairwise combinations of all known human chemokines.[317] The study found that neither CC chemokines that adopt unusual polymeric or unique monomer states (Ccl3, Ccl4, and Ccl18),[137,318] nor transmembrane chemokines (CX3CL1 and Cxcl16) formed heteromers. With the exception of Ccr7 ligands, only some non-mucosal homeostatic chemokines or plasma chemokines activated by N-terminal cleavage[319] engaged in interactions.[317] One promising heterodimer pair that was discovered by Hundelshausen *et al.* was Ccl5-Ccl17. Using an *in situ* proximity ligation assay, we were able to detect these Ccl5-Ccl17 complexes on the surface of *in vitro* activated endothelial cells, after incubation with both chemokines. Ccl5-Ccl17 heterodimers were also shown to be present in lymph node sections of wild type mice, as well as in the plaque shoulder region in aortic roots of mice fed a HFD for 12 weeks. On DCs, which express both Ccr4 and Ccr5, Ccl5-Ccl17 heterodimers were observed on the cell surface, when stimulating with both chemokines. Interestingly, we also observed Ccr4-Ccr5 complexes that were constitutively present. Using the disruptive peptide CAN, Ccl5-Ccl17 heterodimer formation could be inhibited, demonstrating that heterodimerization can be disrupted by peptides. Interestingly, we observed an increase of Ccr4-Ccr5 complexes when combining Ccl5 and Ccl17 but not by either alone. Moreover, when stimulating the DCs with Ccl5 and Ccl17 we observed increased binding of Ccl17 to Ccr4 (but not binding of Ccl5 to Ccr5), as well as increased ligand-receptor cross-interactions. This means that interactions between Ccl5 and Ccr4 where detectable as well as interactions between Ccl17 and Ccr5. This effect was impaired by CAN, thus being mediated by Ccl5-Ccl17 heterodimers, and disrupted by Ccr5-derived peptides spanning transmembrane 1 and 4 motifs as seen for Ccr5 homodimers.

Moreover, we were able to show that migration toward Ccl5-Ccl17 heterodimer was synergistically increased when compared to single stimulated controls and was inhibited

by the peptide CAN, indicating that the increase in migration is synergistically mediated by the complex rather than being an addition of the effects of both single chemokines.

In general, activation of chemokine receptors requires a two-site binding mechanism. Hereby the chemokine N-loop or core domain of the chemokine interacts with the receptor N terminus (site I). Furthermore, the chemokine N terminus interacts with the extracellular residues of the receptor (site II).[320] It is believed that dependent on their quaternary state, chemokine's are able to play different biological roles. Monomers are believed to be the receptor-binding unit, whereas dimers have been implicated in binding cell surface glycosaminoglycan's. In a study performed by Qin, *et al.* the authors were able to model the structure for binding of the atypical CC chemokine vMIP-II to Cxcr4. These models suggest and support findings that CC chemokine homodimers are not able to neither bind nor activate receptors because the dimerization interface largely overlaps with an intermediate recognition site.[321,322] However, this may not be true to all chemokine-receptor interactions because N-terminal and core structures in a CC-type heterodimers may be differently presented to receptors. Instead, binding may involve receptor complexes enabling synergy.

The idea that CC-type heterodimers can induce the formation of corresponding receptor complexes, requiring Ccr5 transmembrane regions is supported by concomitant peptide-based disruption of Ccl5-Ccl17 and Ccr4-Ccr5 formation and function.[322] The fact that chemokine N-terminal residues are crucial elements during receptor activation[320] indicates that they may also play a role in the mechanisms of action for heterodimers. For example, N-terminal sequence variations may cause differences in N-terminal orientation and/or accessibility between Ccl17-Ccl5 heterodimers and Ccl5 homodimers to affect receptor binding and activation. Jin, *et al.* for instance were able to demonstrate that in a disulfide-trapped Ccl4 variant, dissociation of Ccl4 homodimers may be required to accomplish receptor binding and activation by a monomer.[323] In this study, they showed that the disulfide-trapped Ccl4 variant binds to a heparin-sepharose column as strong as the wild type protein and stronger than monomeric variants. Nonetheless, the disulfide-trapped Ccl4 variant was not able to neither bind nor activate the Ccl4 receptor Ccr5. The group showed that the ability to activate Ccr5 was recovered after reduction of the intermolecular disulfide cross-link.[323] This work clearly

demonstrated that Ccl4 dimers are not able to bind or activate its receptor and evidenced that the CC chemokine monomer is the sole receptor-interacting unit. This may also hold true for chemokine heterodimers, namely, Ccl5-Ccl17, when addressing respective heterodimers.[323]

The rise in efficacy of Ccl5-bearing heterodimers may be explained by several aspects. For instance, Ccr5 antagonists inhibited both Ccl5-Cxcl4– and Ccl5-Ccl17–induced arrest. Therefore, CC-type heterodimers can modulate Ccr5 functionality, converting it into an arrest receptor such as Ccr1 (requiring Ccl5 oligomers and extracellular loop 3 for sensing).[132,316,324] Usage of a GAG binding–impaired Cxcl4 (GAG binding–impaired through mutation $Cxcl4^{R>Q}$), which is still able to form heterodimers with CCL5, showed that synergy with Ccl5 depends on increased cell surface presentation. This hinders Ccr1 internalization and thereby sustains its signaling activity.[317] Finally several studies support a functional role of heteromer formation in disease models. For instance, treatment of ApoE-deficient mice with the disruptive peptide CAN reduce atherosclerotic lesion formation by promoting Treg homeostasis. This shows that Ccl5-Ccl17 heterodimers can be prevented (by disruptive peptides) and this reduces atherosclerotic lesion formation.[317] Similar results were seen in studies using CKEY peptide (inhibiting formation of Ccl5-Cxcl4). In these studies CKEY limits atherosclerosis and acute lung injury by interfering with residues crucial for heterodimerization.[138,325]

5. Summary

This work focused on the understanding of the pathophysiological role of the chemokine Ccl17 in the course of atherosclerosis and its effect on the biology of regulatory T cells (Treg). Atherosclerosis is a chronic inflammation of the vessel wall. The pathomechanism of atherosclerosis involves the inflammatory recruitment of leukocytes, which play a central role in the initiation and progression of atherosclerotic lesions. In addition to monocytes/macrophages, mainly dendritic cells (DCs) and T cells are detected in atherosclerotic plaques. Moreover, the DC-derived chemokine Ccl17 is also present in atherosclerotic plaques and in addition, Ccl17 interacts with the chemokine receptor Ccr4 and induces migration of T cells.

Previous studies conducted in our group have shown that in ApoE-deficient mice, Ccl17 deficiency leads to smaller atherosclerotic lesions. This result was accompanied by elevated levels of Tregs. While Ccl17 deficiency had an atheroprotective effect, studies in Ccr4-deficient animals showed no improved clinical picture. Therefore, we investigated which Ccl17 induced mechanisms are dependent on Ccr4 and which are independent of Ccr4. We could for example show that expression of Ccl17 by DCs leads to an increased migration of CD4$^+$ T cells *in vitro* and *in vivo* and limits the expansion of Tregs by restricting their maintenance. While Ccl17-induced migration of T cells occurs via signaling through its receptor Ccr4, the Ccl17-dependent restriction of Tregs occurs independent of Ccr4. Furthermore, we discovered that Ccl17 itself, does not affect T cell polarization directly, but rather influences the phenotype of DCs through autocrine stimulation, leading to the secretion of pro-inflammatory mediators such as Cxcl10 and Ccl3. While Ccl17-dependent secretion of Cxcl10 by DCs was Ccr4-dependent, secretion of Ccl3 by DCs was independent of Ccr4, indicating that Ccl3 might be responsible for mediating restriction of Tregs. Subsequent experiments indeed confirmed that Ccl3 deficiency phenocopies the effects seen in Ccl17-deficient mice, abrogating atherosclerotic lesion development through induction of Treg.

The pro-inflammatory chemokine Ccl3 was shown to directly restrict Tregs via signaling through its chemokine receptor Ccr1. Furthermore, using T cell polarization assays we were able to demonstrate that Ccl3 not just restricted polarization of Tregs but also induced the expression of the transcription factors RorγT and Tbet, therefore inducing

T_H17 and T_H1 responses respectively. Ccr1 deficiency diminished atherosclerotic lesion formation and enhanced Treg numbers. Moreover, this study was able to proof Ccl17 binding to the chemokine receptor Ccr8 and subsequent G_i coupled signaling, introducing Ccr8 as a new alternative receptor for Ccl17.

Furthermore this work evaluated the concept of chemokine heterodimerization and gave new insight into the broad mechanisms of Ccl17 biology. This study confirmed the formation of Ccl5-Ccl17 heterodimers and revealed that chemokine activity can be enhanced by CC-type heterodimers. As an example Ccl5-Ccl17 heterodimers show synergistic effects resulting in increased migration of T cells. In addition, Ccl5-Ccl17 heterodimers induce more efficient T cell arrest and provoke more efficient binding of Ccl17 to Ccr4. Furthermore, it was demonstrated that functional synergism, seen with Ccl5-Ccl17 heterodimers, was achieved through heterodimerization of the receptors Ccr4 and Ccr5. The synergistic effects of Ccl5-Ccl17 heterodimers could be inhibited by a peptide-based inhibitor (a Ccl5-derived peptide which forms part of the heterodimer interface with Ccl17) named CAN. Thus, this study provides evidence that formation of specific chemokine heterodimers broadens their functional activity.

Since atherosclerosis is being characterized as a chronic inflammatory disease of the vessel wall, one might reason that breaking the chronic inflammatory cycle and inducing resolution of inflammation would not only stop disease progression but also induce lesion regression. Here we depicted the manifold modes of action of DC derived chemokine Ccl17 on maintaining chronic inflammation. The data presented in this thesis point at a possible mechanism to pharmacologically induce resolution of inflammation by blocking either Ccl17 or Ccl3 or inhibiting either the receptor Ccr8 (Ccl17) or Ccr1 (Ccl3), thereby enhancing Treg numbers thus supporting control of (chronic) inflammation. Furthermore, targeting the formation of specific chemokine heterodimers by peptide-based inhibitors demonstrates a new and alternative area to be exploited for therapeutic targeting.

6. Zusammenfassung

Diese Arbeit konzentriert sich auf die Klärung der pathophysiologischen Rolle des Chemokins Ccl17 im Verlauf der Atherosklerose und seine Wirkung auf die Biologie regulatorischer T Zellen (Treg). Unter Atherosklerose, ist eine chronische Entzündung der Gefäßwand zu verstehen. Der Pathomechanismus der Atherosklerose beinhaltet die inflammatorische Rekrutierung leukozytärer Zellen, welche eine zentrale Bedeutung für die Initiierung und Progression atherosklerotischer Läsionen spielen. Neben Monozyten/Makrophagen sind es vor allem dendritische Zellen und T Zellen die in atherosklerotischen Läsionen detektiert werden können. Ccl17, ein Chemokin welches von dendritischen Zellen sekretiert wird, ist ebenfalls in atheroskrostischen Läsionen vorhanden. Außerdem aktiviert Ccl17 den Chemokinrezeptor Ccr4 und induziert die Migration von T Zellen.

Frühere Studien, die in unserer Gruppe durchgeführt wurden haben gezeigt, dass in ApoE-defizienten Mäusen eine Ccl17 Defizienz zu kleineren atherosklerotischen Läsionen führt. Dieses Ergebnis ging einher mit erhöhten Werten an regulatorischen T Zellen. Während sich eine Ccl17 Defizienz atheroprotektiv auswirkt, zeigten Studien in Ccr4-defizienten Tieren kein verbessertes Krankheitsbild. Daher wurde in dieser Arbeit untersucht welche Ccl17-induzierten Mechanismen abhängig von Ccr4 ablaufen und welche unabhängig von Ccr4 verlaufen.

Diese Arbeit konnte zum Beispiel zeigen, dass Ccl17, Ccr4 abhängig, die Migration von CD4^{+} T Zellen *in vitro* und *in vivo* induziert. Andererseits limitierte Ccl17, Ccr4 unabhängig, die Expansion regulatorischer T Zellen. Dabei beeinflusste Ccl17 nicht selbst die Polarisierung naiver T Zellen, sondern stimulierte dendritische Zellen autokrin, was dazu führte, dass diese wiederum pro-inflammatorische Chemokine sekretierten, namentlich Cxcl10 (Ccr4 abhängig) und Ccl3 (Ccr4 unabhängig). Des Weiteren konnte gezeigt werden, dass eine Ccl3 Defizienz die Effekte einer Ccl17 Defizienz kopiert. Dabei wurde eine Reduktion atherosklerotischer Läsionen beobachtet, welche mit einer Erhöhung der regulatorischen T Zellzahlen einherging. Ccl3 inhibierte dabei die Treg Differenzierung abhängig von Ccr1. Eine Ccr1 Defizienz reduzierte außerdem die Bildung von atherosklerotischen Läsionen und erhöhte die Anzahl regulatorischer T Zellen. Weiterhin konnte belegt werden, dass Ccl17 an den Chemokinrezeptor Ccr8

bindet und ein G_i gekoppeltes Signal induziert. Weitere Studien müssen noch zeigen, dass die Ccl17 vermittelte Sekretion von Ccl3 über die Aktivierung von Ccr8 verläuft.

Darüber hinaus beschäftigte sich diese Arbeit mit dem Konzept der Chemokin-heterodimerisierung und ermöglichte neue Einblicke in die komplexe Biologie des Chemokins Ccl17. Diese Studie bestätigte die Bildung von Ccl5-Ccl17-Heterodimeren und zeigte, dass die Chemokinaktivität durch Heterodimere vom CC-Typ verstärkt werden konnte. Zum Beispiel zeigten sich synergistische Effekte durch Induktion einer erhöhten Migration. Desweitern zeigten unsere Ergebnisse, dass Ccl5-Ccl17-Heterodimere einen effizienteren T-Zell-Arrest induzieren und eine effizientere Bindung von Ccl17 an Ccr4 bewirken. Weiterhin konnten wir demonstrieren, dass ein funktioneller Synergismus mit Ccl5-Ccl17 Heterodimeren durch Heterodimerisierung der Rezeptoren Ccr4 und Ccr5 erreicht wird. Die synergistischen Effekte von Ccl5-Ccl17-Heterodimeren konnten außerdem durch einen peptid-basierten Inhibitor (ein von Ccl5 abgeleitetes Peptid, das einen Teil der Heterodimer-Schnittstelle mit Ccl17 bildet), genannt CAN, inhibiert werden.

Atherosklerose ist als chronisch-entzündliche Erkrankung der Gefäßwand charakterisiert, daher zielen mögliche therapeutische Ansätze auf eine Reduktion der Entzündung und eine Regression der atherosklerotischen Läsionen ab. Diese Arbeit beschreibt die vielfältigen Wirkungsweisen des Chemokins Ccl17 und dessen Rolle beim Aufrechterhalten der chronischen Entzündung. Die in dieser Arbeit präsentierten Daten zeigten einen möglichen Mechanismus um pharmakologisch die Auflösung von Entzündungsreaktionen zu induzieren, indem entweder Ccl17 oder Ccl3 blockiert oder deren Rezeptoren Ccr8 (Ccl17) oder Ccr1 (Ccl3) inhibiert werden. Darüber hinaus konnte gezeigt werden, dass die Bildung spezifischer Chemokin-Heterodimere durch peptid-basierte Inhibitoren unterbunden werden kann.

7. References

1   (WHO), W. H. O. Cardiovascular diseases (CVDs) Fact Sheet. *http://www.who.int/mediacentre/factsheets/fs317/en/* (2016).

2   Dahlof, B. Cardiovascular disease risk factors: epidemiology and risk assessment. *Am J Cardiol* **105**, 3A-9A, doi:10.1016/j.amjcard.2009.10.007 (2010).

3   Hansson, G. K. & Hermansson, A. The immune system in atherosclerosis. *Nat Immunol* **12**, 204-212, doi:10.1038/ni.2001 (2011).

4   Vollmar, A. Z., Ilse; Dingermann, Theodor. *Immunologie. Grundlagen und Wirkstoffe.* 2 edn, (Wissenschaftliche Verlagsgesellschaft Stuttgart, 2013).

5   Mruphy, K. P. *Janeways Immunobiology.* 8 edn, (Garland Science, 2012).

6   Mogensen, T. H. Pathogen recognition and inflammatory signaling in innate immune defenses. *Clin Microbiol Rev* **22**, 240-273, Table of Contents, doi:10.1128/CMR.00046-08 (2009).

7   Medzhitov, R. & Janeway, C. A., Jr. Innate immune recognition and control of adaptive immune responses. *Semin Immunol* **10**, 351-353 (1998).

8   Cooper, M. D. & Alder, M. N. The evolution of adaptive immune systems. *Cell* **124**, 815-822, doi:10.1016/j.cell.2006.02.001 (2006).

9   Hoebe, K., Janssen, E. & Beutler, B. The interface between innate and adaptive immunity. *Nat Immunol* **5**, 971-974, doi:10.1038/ni1004-971 (2004).

10   Iwasaki, A. & Medzhitov, R. Regulation of adaptive immunity by the innate immune system. *Science* **327**, 291-295, doi:10.1126/science.1183021 (2010).

11   Janeway, C. A., Jr. How the immune system protects the host from infection. *Microbes Infect* **3**, 1167-1171 (2001).

12   Dranoff, G. Cytokines in cancer pathogenesis and cancer therapy. *Nat Rev Cancer* **4**, 11-22, doi:10.1038/nrc1252 (2004).

13   Abraham, S. N. & St John, A. L. Mast cell-orchestrated immunity to pathogens. *Nat Rev Immunol* **10**, 440-452, doi:10.1038/nri2782 (2010).

14   Ardavin, C. Origin, precursors and differentiation of mouse dendritic cells. *Nat Rev Immunol* **3**, 582-590, doi:10.1038/nri1127 (2003).

15   Gabrilovich, D. I., Ostrand-Rosenberg, S. & Bronte, V. Coordinated regulation of myeloid cells by tumours. *Nat Rev Immunol* **12**, 253-268, doi:10.1038/nri3175 (2012).

16   Steinman, R. M. & Cohn, Z. A. Identification of a novel cell type in peripheral lymphoid organs of mice. I. Morphology, quantitation, tissue distribution. *J Exp Med* **137**, 1142-1162 (1973).

17   Pilon, C. *et al.* CD40 engagement strongly induces CD25 expression on porcine dendritic cells and polarizes the T cell immune response toward Th1. *Mol Immunol* **46**, 437-447, doi:10.1016/j.molimm.2008.10.014 (2009).

18   Colonna, M., Trinchieri, G. & Liu, Y. J. Plasmacytoid dendritic cells in immunity. *Nat Immunol* **5**, 1219-1226 (2004).

19   Fogg, D. K. *et al.* A clonogenic bone marrow progenitor specific for macrophages and dendritic cells. *Science* **311**, 83-87, doi:10.1126/science.1117729 (2006).

20   Hettinger, J. *et al.* Origin of monocytes and macrophages in a committed progenitor. *Nat Immunol* **14**, 821-830, doi:10.1038/ni.2638 (2013).

21   Veglia, F. & Gabrilovich, D. I. Dendritic cells in cancer: the role revisited. *Curr Opin Immunol* **45**, 43-51, doi:10.1016/j.coi.2017.01.002 (2017).

22   Poltorak, M. P. & Schraml, B. U. Fate mapping of dendritic cells. *Front Immunol* **6**, 199, doi:10.3389/fimmu.2015.00199 (2015).

23   Worbs, T., Hammerschmidt, S. I. & Forster, R. Dendritic cell migration in health and disease. *Nat Rev Immunol* **17**, 30-48, doi:10.1038/nri.2016.116 (2017).

24   Merad, M., Sathe, P., Helft, J., Miller, J. & Mortha, A. The dendritic cell lineage: ontogeny and function of dendritic cells and their subsets in the steady state and the inflamed setting. *Annu Rev Immunol* **31**, 563-604, doi:10.1146/annurev-immunol-020711-074950 (2013).

25   Vulcano, M. *et al.* Unique regulation of CCL18 production by maturing dendritic cells. *J Immunol* **170**, 3843-3849 (2003).

26   Katou, F. *et al.* Differential expression of CCL19 by DC-Lamp+ mature dendritic cells in human lymph node versus chronically inflamed skin. *J Pathol* **199**, 98-106, doi:10.1002/path.1255 (2003).

27   Thaiss, C. A., Semmling, V., Franken, L., Wagner, H. & Kurts, C. Chemokines: a new dendritic cell signal for T cell activation. *Front Immunol* **2**, 31, doi:10.3389/fimmu.2011.00031 (2011).

28   Vulcano, M. *et al.* Dendritic cells as a major source of macrophage-derived chemokine/CCL22 in vitro and in vivo. *Eur J Immunol* **31**, 812-822, doi:10.1002/1521-4141(200103)31:3<812::AID-IMMU812>3.0.CO;2-L (2001).

29   Helft, J., Ginhoux, F., Bogunovic, M. & Merad, M. Origin and functional heterogeneity of non-lymphoid tissue dendritic cells in mice. *Immunol Rev* **234**, 55-75, doi:10.1111/j.0105-2896.2009.00885.x (2010).

30   Cisse, B. *et al.* Transcription factor E2-2 is an essential and specific regulator of plasmacytoid dendritic cell development. *Cell* **135**, 37-48, doi:10.1016/j.cell.2008.09.016 (2008).

31   Swiecki, M. & Colonna, M. The multifaceted biology of plasmacytoid dendritic cells. *Nat Rev Immunol* **15**, 471-485, doi:10.1038/nri3865 (2015).

32   Swiecki, M. & Colonna, M. Unraveling the functions of plasmacytoid dendritic cells during viral infections, autoimmunity, and tolerance. *Immunol Rev* **234**, 142-162, doi:10.1111/j.0105-2896.2009.00881.x (2010).

33   Hacker, C. *et al.* Transcriptional profiling identifies Id2 function in dendritic cell development. *Nat Immunol* **4**, 380-386, doi:10.1038/ni903 (2003).

34   Hildner, K. *et al.* Batf3 deficiency reveals a critical role for CD8alpha+ dendritic cells in cytotoxic T cell immunity. *Science* **322**, 1097-1100, doi:10.1126/science.1164206 (2008).

35   Luda, K. M. *et al.* IRF8 Transcription-Factor-Dependent Classical Dendritic Cells Are Essential for Intestinal T Cell Homeostasis. *Immunity* **44**, 860-874, doi:10.1016/j.immuni.2016.02.008 (2016).

36   Schraml, B. U. & Reis e Sousa, C. Defining dendritic cells. *Curr Opin Immunol* **32**, 13-20, doi:10.1016/j.coi.2014.11.001 (2015).

37   Plantinga, M. *et al.* Conventional and monocyte-derived CD11b(+) dendritic cells initiate and maintain T helper 2 cell-mediated immunity to house dust mite allergen. *Immunity* **38**, 322-335, doi:10.1016/j.immuni.2012.10.016 (2013).

38   Segura, E. & Amigorena, S. Inflammatory dendritic cells in mice and humans. *Trends Immunol* **34**, 440-445, doi:10.1016/j.it.2013.06.001 (2013).

39   Segura, E. *et al.* Human inflammatory dendritic cells induce Th17 cell differentiation. *Immunity* **38**, 336-348, doi:10.1016/j.immuni.2012.10.018 (2013).

40   Rothenberg, E. V., Moore, J. E. & Yui, M. A. Launching the T-cell-lineage developmental programme. *Nat Rev Immunol* **8**, 9-21, doi:10.1038/nri2232 (2008).

41   Petrie, H. T. & Zuniga-Pflucker, J. C. Zoned out: functional mapping of stromal signaling microenvironments in the thymus. *Annu Rev Immunol* **25**, 649-679, doi:10.1146/annurev.immunol.23.021704.115715 (2007).

42   Allman, D. *et al.* Thymopoiesis independent of common lymphoid progenitors. *Nat Immunol* **4**, 168-174, doi:10.1038/ni878 (2003).

43   Taghon, T., Yui, M. A., Pant, R., Diamond, R. A. & Rothenberg, E. V. Developmental and molecular characterization of emerging beta- and gammadelta-selected pre-T cells in the adult mouse thymus. *Immunity* **24**, 53-64, doi:10.1016/j.immuni.2005.11.012 (2006).

44   Melichar, H. J. *et al.* Regulation of gammadelta versus alphabeta T lymphocyte differentiation by the transcription factor SOX13. *Science* **315**, 230-233, doi:10.1126/science.1135344 (2007).

45   Rothenberg, E. V. & Taghon, T. Molecular genetics of T cell development. *Annu Rev Immunol* **23**, 601-649, doi:10.1146/annurev.immunol.23.021704.115737 (2005).

46   McCaughtry, T. M., Wilken, M. S. & Hogquist, K. A. Thymic emigration revisited. *J Exp Med* **204**, 2513-2520, doi:10.1084/jem.20070601 (2007).

47   Masopust, D. & Schenkel, J. M. The integration of T cell migration, differentiation and function. *Nat Rev Immunol* **13**, 309-320, doi:10.1038/nri3442 (2013).

48   Forster, R. *et al.* CCR7 coordinates the primary immune response by establishing functional microenvironments in secondary lymphoid organs. *Cell* **99**, 23-33 (1999).

49   Nakano, H. *et al.* Genetic defect in T lymphocyte-specific homing into peripheral lymph nodes. *Eur J Immunol* **27**, 215-221, doi:10.1002/eji.1830270132 (1997).

50   Okada, T. *et al.* Chemokine requirements for B cell entry to lymph nodes and Peyer's patches. *J Exp Med* **196**, 65-75 (2002).

51   Nijkamp, F. P., Parnham, M. J. & SpringerLink (Online service).   xxxi, 728 p. (Birkhauser Basel, Basel, 2011).

52   Lafaille, J. J. The role of helper T cell subsets in autoimmune diseases. *Cytokine Growth Factor Rev* **9**, 139-151 (1998).

53   Farrar, J. D., Asnagli, H. & Murphy, K. M. T helper subset development: roles of instruction, selection, and transcription. *J Clin Invest* **109**, 431-435, doi:10.1172/JCI15093 (2002).

54   Mullen, A. C. *et al.* Role of T-bet in commitment of TH1 cells before IL-12-dependent selection. *Science* **292**, 1907-1910, doi:10.1126/science.1059835 (2001).

55   Wang, Z. Y. *et al.* Regulation of Th2 cytokine expression in NKT cells: unconventional use of Stat6, GATA-3, and NFAT2. *J Immunol* **176**, 880-888 (2006).

56   Kaplan, M. H., Schindler, U., Smiley, S. T. & Grusby, M. J. Stat6 is required for mediating responses to IL-4 and for development of Th2 cells. *Immunity* **4**, 313-319 (1996).

57   Mosmann, T. R. & Coffman, R. L. TH1 and TH2 cells: different patterns of lymphokine secretion lead to different functional properties. *Annu Rev Immunol* **7**, 145-173, doi:10.1146/annurev.iy.07.040189.001045 (1989).

58   Zhang, G. X. *et al.* Induction of experimental autoimmune encephalomyelitis in IL-12 receptor-beta 2-deficient mice: IL-12 responsiveness is not required in the pathogenesis of inflammatory demyelination in the central nervous system. *J Immunol* **170**, 2153-2160 (2003).

59   Leonard, J. P., Waldburger, K. E. & Goldman, S. J. Prevention of experimental autoimmune encephalomyelitis by antibodies against interleukin 12. *J Exp Med* **181**, 381-386 (1995).

60   Gran, B. *et al.* IL-12p35-deficient mice are susceptible to experimental autoimmune encephalomyelitis: evidence for redundancy in the IL-12 system in the induction of central nervous system autoimmune demyelination. *J Immunol* **169**, 7104-7110 (2002).

61   Cua, D. J. *et al.* Interleukin-23 rather than interleukin-12 is the critical cytokine for autoimmune inflammation of the brain. *Nature* **421**, 744-748, doi:10.1038/nature01355 (2003).

62   McGeachy, M. J. *et al.* The interleukin 23 receptor is essential for the terminal differentiation of interleukin 17-producing effector T helper cells in vivo. *Nat Immunol* **10**, 314-324, doi:10.1038/ni.1698 (2009).

63   Mangan, P. R. *et al.* Transforming growth factor-beta induces development of the T(H)17 lineage. *Nature* **441**, 231-234, doi:10.1038/nature04754 (2006).

64   Veldhoen, M., Hocking, R. J., Atkins, C. J., Locksley, R. M. & Stockinger, B. TGFbeta in the context of an inflammatory cytokine milieu supports de novo differentiation of IL-17-producing T cells. *Immunity* **24**, 179-189, doi:10.1016/j.immuni.2006.01.001 (2006).

65   Bettelli, E. *et al.* Reciprocal developmental pathways for the generation of pathogenic effector TH17 and regulatory T cells. *Nature* **441**, 235-238, doi:10.1038/nature04753 (2006).

66   Yang, X. O. *et al.* STAT3 regulates cytokine-mediated generation of inflammatory helper T cells. *J Biol Chem* **282**, 9358-9363, doi:10.1074/jbc.C600321200 (2007).

67   Ivanov, II *et al.* The orphan nuclear receptor RORgammat directs the differentiation program of proinflammatory IL-17+ T helper cells. *Cell* **126**, 1121-1133, doi:10.1016/j.cell.2006.07.035 (2006).

68   Nishihara, M. *et al.* IL-6-gp130-STAT3 in T cells directs the development of IL-17+ Th with a minimum effect on that of Treg in the steady state. *Int Immunol* **19**, 695-702, doi:10.1093/intimm/dxm045 (2007).

69   Gaffen, S. L., Jain, R., Garg, A. V. & Cua, D. J. The IL-23-IL-17 immune axis: from mechanisms to therapeutic testing. *Nat Rev Immunol* **14**, 585-600, doi:10.1038/nri3707 (2014).

70   Sutton, C., Brereton, C., Keogh, B., Mills, K. H. & Lavelle, E. C. A crucial role for interleukin (IL)-1 in the induction of IL-17-producing T cells that mediate autoimmune encephalomyelitis. *J Exp Med* **203**, 1685-1691, doi:10.1084/jem.20060285 (2006).

71   Gulen, M. F. *et al.* The receptor SIGIRR suppresses Th17 cell proliferation via inhibition of the interleukin-1 receptor pathway and mTOR kinase activation. *Immunity* **32**, 54-66, doi:10.1016/j.immuni.2009.12.003 (2010).

72   Hirota, K. *et al.* Fate mapping of IL-17-producing T cells in inflammatory responses. *Nat Immunol* **12**, 255-263, doi:10.1038/ni.1993 (2011).

73   Arce-Sillas, A. *et al.* Regulatory T Cells: Molecular Actions on Effector Cells in Immune Regulation. *J Immunol Res* **2016**, 1720827, doi:10.1155/2016/1720827 (2016).

74   Schmidt, A., Oberle, N. & Krammer, P. H. Molecular mechanisms of treg-mediated T cell suppression. *Front Immunol* **3**, 51, doi:10.3389/fimmu.2012.00051 (2012).

75   Curotto de Lafaille, M. A. & Lafaille, J. J. Natural and adaptive foxp3+ regulatory T cells: more of the same or a division of labor? *Immunity* **30**, 626-635, doi:10.1016/j.immuni.2009.05.002 (2009).

76   Josefowicz, S. Z., Lu, L. F. & Rudensky, A. Y. Regulatory T cells: mechanisms of differentiation and function. *Annu Rev Immunol* **30**, 531-564, doi:10.1146/annurev.immunol.25.022106.141623 (2012).

77   Vignali, D. A., Collison, L. W. & Workman, C. J. How regulatory T cells work. *Nat Rev Immunol* **8**, 523-532, doi:10.1038/nri2343 (2008).

78   Dhainaut, M. & Moser, M. Mechanisms of Surveillance of Dendritic Cells by Regulatory T Lymphocytes. *Prog Mol Biol Transl Sci* **136**, 131-154, doi:10.1016/bs.pmbts.2015.08.003 (2015).

79   Carrier, Y., Yuan, J., Kuchroo, V. K. & Weiner, H. L. Th3 cells in peripheral tolerance. I. Induction of Foxp3-positive regulatory T cells by Th3 cells derived from TGF-beta T cell-transgenic mice. *J Immunol* **178**, 179-185 (2007).

80   Roncarolo, M. G. *et al.* Interleukin-10-secreting type 1 regulatory T cells in rodents and humans. *Immunol Rev* **212**, 28-50, doi:10.1111/j.0105-2896.2006.00420.x (2006).

81   Collison, L. W. *et al.* IL-35-mediated induction of a potent regulatory T cell population. *Nat Immunol* **11**, 1093-1101, doi:10.1038/ni.1952 (2010).

82   Loebbermann, J. *et al.* IL-10 regulates viral lung immunopathology during acute respiratory syncytial virus infection in mice. *PLoS One* **7**, e32371, doi:10.1371/journal.pone.0032371 (2012).

83   Collison, L. W. *et al.* The composition and signaling of the IL-35 receptor are unconventional. *Nat Immunol* **13**, 290-299, doi:10.1038/ni.2227 (2012).

84   Wang, R. X. *et al.* Interleukin-35 induces regulatory B cells that suppress autoimmune disease. *Nat Med* **20**, 633-641, doi:10.1038/nm.3554 (2014).

85   Li, M. O., Wan, Y. Y. & Flavell, R. A. T cell-produced transforming growth factor-beta1 controls T cell tolerance and regulates Th1- and Th17-cell differentiation. *Immunity* **26**, 579-591, doi:10.1016/j.immuni.2007.03.014 (2007).

86   Ma, H. *et al.* TGF-beta1-induced expression of Id-1 is associated with tumor progression in gastric cancer. *Med Oncol* **31**, 19, doi:10.1007/s12032-014-0019-3 (2014).

87   Gondek, D. C., Lu, L. F., Quezada, S. A., Sakaguchi, S. & Noelle, R. J. Cutting edge: contact-mediated suppression by CD4+CD25+ regulatory cells involves a granzyme B-dependent, perforin-independent mechanism. *J Immunol* **174**, 1783-1786 (2005).

88   Bayer, A. L., Pugliese, A. & Malek, T. R. The IL-2/IL-2R system: from basic science to therapeutic applications to enhance immune regulation. *Immunol Res* **57**, 197-209, doi:10.1007/s12026-013-8452-5 (2013).

89   Almahariq, M. *et al.* Exchange protein directly activated by cAMP modulates regulatory T-cell-mediated immunosuppression. *Biochem J* **465**, 295-303, doi:10.1042/BJ20140952 (2015).

90   Borsellino, G. *et al.* Expression of ectonucleotidase CD39 by Foxp3+ Treg cells: hydrolysis of extracellular ATP and immune suppression. *Blood* **110**, 1225-1232, doi:10.1182/blood-2006-12-064527 (2007).

91   Boasso, A., Herbeuval, J. P., Hardy, A. W., Winkler, C. & Shearer, G. M. Regulation of indoleamine 2,3-dioxygenase and tryptophanyl-tRNA-synthetase by CTLA-4-Fc in human CD4+ T cells. *Blood* **105**, 1574-1581, doi:10.1182/blood-2004-06-2089 (2005).

92   Sather, B. D. *et al.* Altering the distribution of Foxp3(+) regulatory T cells results in tissue-specific inflammatory disease. *J Exp Med* **204**, 1335-1347, doi:10.1084/jem.20070081 (2007).

93   Lim, H. W., Broxmeyer, H. E. & Kim, C. H. Regulation of trafficking receptor expression in human forkhead box P3+ regulatory T cells. *J Immunol* **177**, 840-851 (2006).

94   Grindebacke, H. *et al.* Dynamic development of homing receptor expression and memory cell differentiation of infant CD4+CD25high regulatory T cells. *J Immunol* **183**, 4360-4370, doi:10.4049/jimmunol.0901091 (2009).

95   Comerford, I. & McColl, S. R. Mini-review series: focus on chemokines. *Immunol Cell Biol* **89**, 183-184, doi:10.1038/icb.2010.164 (2011).

96   Gerard, C. & Rollins, B. J. Chemokines and disease. *Nat Immunol* **2**, 108-115, doi:10.1038/84209 (2001).

97   Moser, B. & Willimann, K. Chemokines: role in inflammation and immune surveillance. *Ann Rheum Dis* **63 Suppl 2**, ii84-ii89, doi:10.1136/ard.2004.028316 (2004).

98   Weber, C., Schober, A. & Zernecke, A. Chemokines: key regulators of mononuclear cell recruitment in atherosclerotic vascular disease. *Arterioscler Thromb Vasc Biol* **24**, 1997-2008, doi:10.1161/01.ATV.0000142812.03840.6f (2004).

99   de Munnik, S. M., Smit, M. J., Leurs, R. & Vischer, H. F. Modulation of cellular signaling by herpesvirus-encoded G protein-coupled receptors. *Front Pharmacol* **6**, 40, doi:10.3389/fphar.2015.00040 (2015).

100   Horuk, R. Chemokine receptors. *Cytokine Growth Factor Rev* **12**, 313-335 (2001).

101   Katritch, V., Cherezov, V. & Stevens, R. C. Diversity and modularity of G protein-coupled receptor structures. *Trends Pharmacol Sci* **33**, 17-27, doi:10.1016/j.tips.2011.09.003 (2012).

102   Charo, I. F. & Taubman, M. B. Chemokines in the pathogenesis of vascular disease. *Circ Res* **95**, 858-866, doi:10.1161/01.RES.0000146672.10582.17 (2004).

103   Middleton, J., Patterson, A. M., Gardner, L., Schmutz, C. & Ashton, B. A. Leukocyte extravasation: chemokine transport and presentation by the endothelium. *Blood* **100**, 3853-3860, doi:10.1182/blood.V100.12.3853 (2002).

104   Weber, C. & Noels, H. Atherosclerosis: current pathogenesis and therapeutic options. *Nat Med* **17**, 1410-1422, doi:10.1038/nm.2538 (2011).

105   Ley, K., Laudanna, C., Cybulsky, M. I. & Nourshargh, S. Getting to the site of inflammation: the leukocyte adhesion cascade updated. *Nat Rev Immunol* **7**, 678-689, doi:10.1038/nri2156 (2007).

106 Ley, K. Arrest chemokines. *Microcirculation* **10**, 289-295, doi:10.1038/sj.mn.7800194 (2003).

107 Laudanna, C. & Alon, R. Right on the spot. Chemokine triggering of integrin-mediated arrest of rolling leukocytes. *Thromb Haemost* **95**, 5-11 (2006).

108 Randolph, G. J., Ochando, J. & Partida-Sanchez, S. Migration of dendritic cell subsets and their precursors. *Annu Rev Immunol* **26**, 293-316, doi:10.1146/annurev.immunol.26.021607.090254 (2008).

109 Lammermann, T. *et al.* Rapid leukocyte migration by integrin-independent flowing and squeezing. *Nature* **453**, 51-55, doi:10.1038/nature06887 (2008).

110 Gunn, M. D. *et al.* Mice lacking expression of secondary lymphoid organ chemokine have defects in lymphocyte homing and dendritic cell localization. *J Exp Med* **189**, 451-460 (1999).

111 Imai, T. *et al.* Molecular cloning of a novel T cell-directed CC chemokine expressed in thymus by signal sequence trap using Epstein-Barr virus vector. *J Biol Chem* **271**, 21514-21521 (1996).

112 Imai, T. *et al.* The T cell-directed CC chemokine TARC is a highly specific biological ligand for CC chemokine receptor 4. *J Biol Chem* **272**, 15036-15042 (1997).

113 Bernardini, G. *et al.* Identification of the CC chemokines TARC and macrophage inflammatory protein-1 beta as novel functional ligands for the CCR8 receptor. *Eur J Immunol* **28**, 582-588, doi:10.1002/(SICI)1521-4141(199802)28:02<582::AID-IMMU582>3.0.CO;2-A (1998).

114 Iellem, A. *et al.* Unique chemotactic response profile and specific expression of chemokine receptors CCR4 and CCR8 by CD4(+)CD25(+) regulatory T cells. *J Exp Med* **194**, 847-853 (2001).

115 Fox, J. M. *et al.* Structure/function relationships of CCR8 agonists and antagonists. Amino-terminal extension of CCL1 by a single amino acid generates a partial agonist. *J Biol Chem* **281**, 36652-36661, doi:10.1074/jbc.M605584200 (2006).

116 Islam, S. A., Ling, M. F., Leung, J., Shreffler, W. G. & Luster, A. D. Identification of human CCR8 as a CCL18 receptor. *J Exp Med* **210**, 1889-1898, doi:10.1084/jem.20130240 (2013).

117 Lieberam, I. & Forster, I. The murine beta-chemokine TARC is expressed by subsets of dendritic cells and attracts primed CD4+ T cells. *Eur J Immunol* **29**, 2684-2694 (1999).

118 Alferink, J. *et al.* Compartmentalized production of CCL17 in vivo: strong inducibility in peripheral dendritic cells contrasts selective absence from the spleen. *J Exp Med* **197**, 585-599 (2003).

119 Weber, C. *et al.* CCL17-expressing dendritic cells drive atherosclerosis by restraining regulatory T cell homeostasis in mice. *J Clin Invest* **121**, 2898-2910, doi:10.1172/JCI44925 (2011).

120 Stutte, S. *et al.* Requirement of CCL17 for CCR7- and CXCR4-dependent migration of cutaneous dendritic cells. *Proc Natl Acad Sci U S A* **107**, 8736-8741, doi:10.1073/pnas.0906126107 (2010).

121 Luchtefeld, M. *et al.* Chemokine receptor 7 knockout attenuates atherosclerotic plaque development. *Circulation* **122**, 1621-1628, doi:10.1161/CIRCULATIONAHA.110.956730 (2010).

122   Heiseke, A. F. *et al.* CCL17 promotes intestinal inflammation in mice and counteracts regulatory T cell-mediated protection from colitis. *Gastroenterology* **142**, 335-345, doi:10.1053/j.gastro.2011.10.027 (2012).

123   Oo, Y. H. *et al.* Distinct roles for CCR4 and CXCR3 in the recruitment and positioning of regulatory T cells in the inflamed human liver. *J Immunol* **184**, 2886-2898, doi:10.4049/jimmunol.0901216 (2010).

124   Pere, H. *et al.* A CCR4 antagonist combined with vaccines induces antigen-specific CD8+ T cells and tumor immunity against self antigens. *Blood* **118**, 4853-4862, doi:10.1182/blood-2011-01-329656 (2011).

125   Yu, K., Chen, Z., Khatri, I. & Gorczynski, R. M. CCR4 dependent migration of Foxp3+ Treg cells to skin grafts and draining lymph nodes is implicated in enhanced graft survival in CD200tg recipients. *Immunol Lett* **141**, 116-122, doi:10.1016/j.imlet.2011.09.002 (2011).

126   Schall, T. J. *et al.* A human T cell-specific molecule is a member of a new gene family. *J Immunol* **141**, 1018-1025 (1988).

127   Schall, T. J., Bacon, K., Toy, K. J. & Goeddel, D. V. Selective attraction of monocytes and T lymphocytes of the memory phenotype by cytokine RANTES. *Nature* **347**, 669-671, doi:10.1038/347669a0 (1990).

128   Song, A., Nikolcheva, T. & Krensky, A. M. Transcriptional regulation of RANTES expression in T lymphocytes. *Immunol Rev* **177**, 236-245 (2000).

129   Pattison, J. M., Nelson, P. J., Huie, P., Sibley, R. K. & Krensky, A. M. RANTES chemokine expression in transplant-associated accelerated atherosclerosis. *J Heart Lung Transplant* **15**, 1194-1199 (1996).

130   Jordan, N. J. *et al.* Chemokine production by human vascular smooth muscle cells: modulation by IL-13. *Br J Pharmacol* **122**, 749-757, doi:10.1038/sj.bjp.0701433 (1997).

131   von Hundelshausen, P. *et al.* RANTES deposition by platelets triggers monocyte arrest on inflamed and atherosclerotic endothelium. *Circulation* **103**, 1772-1777 (2001).

132   Weber, C. *et al.* Specialized roles of the chemokine receptors CCR1 and CCR5 in the recruitment of monocytes and T(H)1-like/CD45RO(+) T cells. *Blood* **97**, 1144-1146 (2001).

133   Braunersreuther, V. *et al.* Ccr5 but not Ccr1 deficiency reduces development of diet-induced atherosclerosis in mice. *Arterioscler Thromb Vasc Biol* **27**, 373-379, doi:10.1161/01.ATV.0000253886.44609.ae (2007).

134   Soehnlein, O. *et al.* Distinct functions of chemokine receptor axes in the atherogenic mobilization and recruitment of classical monocytes. *EMBO Mol Med* **5**, 471-481, doi:10.1002/emmm.201201717 (2013).

135   Fernandez, E. J. & Lolis, E. Structure, function, and inhibition of chemokines. *Annu Rev Pharmacol Toxicol* **42**, 469-499, doi:10.1146/annurev.pharmtox.42.091901.115838 (2002).

136   Salanga, C. L. & Handel, T. M. Chemokine oligomerization and interactions with receptors and glycosaminoglycans: the role of structural dynamics in function. *Exp Cell Res* **317**, 590-601, doi:10.1016/j.yexcr.2011.01.004 (2011).

137   Ren, M. *et al.* Polymerization of MIP-1 chemokine (CCL3 and CCL4) and clearance of MIP-1 by insulin-degrading enzyme. *EMBO J* **29**, 3952-3966, doi:10.1038/emboj.2010.256 (2010).

138   Koenen, R. R. *et al.* Disrupting functional interactions between platelet chemokines inhibits atherosclerosis in hyperlipidemic mice. *Nat Med* **15**, 97-103, doi:10.1038/nm.1898 (2009).

139   Galkina, E. & Ley, K. Immune and inflammatory mechanisms of atherosclerosis (*). *Annu Rev Immunol* **27**, 165-197, doi:10.1146/annurev.immunol.021908.132620 (2009).

140   S.S, A. N. N. C. Ueber experimentelle Cholesterinsteatose und ihre Bedeutung für die Entstehung einiger pathologischer Prozesse. *Zbl. allg. Path. path. Anat.*, 1-9 (1913).

141   A., W. Über den Gehalt normaler und atheromatöser Aorten an Cholesterin und Cholesterinestern. *Zeitschrift für Physiologische Chemie* **67**, 174-176 (1910).

142   Mayerl, C. *et al.* Atherosclerosis research from past to present--on the track of two pathologists with opposing views, Carl von Rokitansky and Rudolf Virchow. *Virchows Arch* **449**, 96-103, doi:10.1007/s00428-006-0176-7 (2006).

143   Ross, R. & Glomset, J. A. Atherosclerosis and the arterial smooth muscle cell: Proliferation of smooth muscle is a key event in the genesis of the lesions of atherosclerosis. *Science* **180**, 1332-1339 (1973).

144   Ross, R. & Glomset, J. A. The pathogenesis of atherosclerosis (first of two parts). *N Engl J Med* **295**, 369-377, doi:10.1056/NEJM197608122950707 (1976).

145   Ross, R. & Glomset, J. A. The pathogenesis of atherosclerosis (second of two parts). *N Engl J Med* **295**, 420-425, doi:10.1056/NEJM197608192950805 (1976).

146   Steinberg, D. Role of oxidized LDL and antioxidants in atherosclerosis. *Adv Exp Med Biol* **369**, 39-48 (1995).

147   Davis, C., Fischer, J., Ley, K. & Sarembock, I. J. The role of inflammation in vascular injury and repair. *Journal of thrombosis and haemostasis : JTH* **1**, 1699-1709 (2003).

148   Davignon, J. & Ganz, P. Role of endothelial dysfunction in atherosclerosis. *Circulation* **109**, III27-32, doi:10.1161/01.CIR.0000131515.03336.f8 (2004).

149   Lee, I. K., Kim, H. S. & Bae, J. H. Endothelial dysfunction: its relationship with acute hyperglycaemia and hyperlipidemia. *International journal of clinical practice. Supplement*, 59-64 (2002).

150   Swirski, F. K. *et al.* Monocyte accumulation in mouse atherogenesis is progressive and proportional to extent of disease. *Proc Natl Acad Sci U S A* **103**, 10340-10345, doi:10.1073/pnas.0604260103 (2006).

151   Ridker, P. M. Hyperlipidemia as an instigator of inflammation: inaugurating new approaches to vascular prevention. *Journal of the American Heart Association* **1**, 3-5, doi:10.1161/JAHA.112.000497 (2012).

152   Tabas, I. Macrophage apoptosis in atherosclerosis: consequences on plaque progression and the role of endoplasmic reticulum stress. *Antioxidants & redox signaling* **11**, 2333-2339, doi:10.1089/ARS.2009.2469 (2009).

153   Martinet, W., Schrijvers, D. M. & De Meyer, G. R. Necrotic cell death in atherosclerosis. *Basic Res Cardiol* **106**, 749-760, doi:10.1007/s00395-011-0192-x (2011).

154   Oh, J. *et al.* Endoplasmic reticulum stress controls M2 macrophage differentiation and foam cell formation. *J Biol Chem* **287**, 11629-11641, doi:10.1074/jbc.M111.338673 (2012).

155   Lusis, A. J. Atherosclerosis. *Nature* **407**, 233-241, doi:10.1038/35025203 (2000).

156   Falk, E. Why do plaques rupture? *Circulation* **86**, III30-42 (1992).

157   Weber, C., Zernecke, A. & Libby, P. The multifaceted contributions of leukocyte subsets to atherosclerosis: lessons from mouse models. *Nat Rev Immunol* **8**, 802-815, doi:10.1038/nri2415 (2008).

158   Libby, P., Ridker, P. M. & Hansson, G. K. Progress and challenges in translating the biology of atherosclerosis. *Nature* **473**, 317-325, doi:10.1038/nature10146 (2011).

159   Choi, J. H. *et al.* Flt3 signaling-dependent dendritic cells protect against atherosclerosis. *Immunity* **35**, 819-831, doi:10.1016/j.immuni.2011.09.014 (2011).

160   Galkina, E. *et al.* Lymphocyte recruitment into the aortic wall before and during development of atherosclerosis is partially L-selectin dependent. *J Exp Med* **203**, 1273-1282, doi:10.1084/jem.20052205 (2006).

161   Busch, M., Westhofen, T. C., Koch, M., Lutz, M. B. & Zernecke, A. Dendritic cell subset distributions in the aorta in healthy and atherosclerotic mice. *PLoS One* **9**, e88452, doi:10.1371/journal.pone.0088452 (2014).

162   Buono, C. *et al.* B7-1/B7-2 costimulation regulates plaque antigen-specific T-cell responses and atherogenesis in low-density lipoprotein receptor-deficient mice. *Circulation* **109**, 2009-2015, doi:10.1161/01.CIR.0000127121.16815.F1 (2004).

163   Erbel, C. *et al.* Functional profile of activated dendritic cells in unstable atherosclerotic plaque. *Basic Res Cardiol* **102**, 123-132, doi:10.1007/s00395-006-0636-x (2007).

164   Yilmaz, A. *et al.* Emergence of dendritic cells in rupture-prone regions of vulnerable carotid plaques. *Atherosclerosis* **176**, 101-110, doi:10.1016/j.atherosclerosis.2004.04.027 (2004).

165   Niessner, A. *et al.* Pathogen-sensing plasmacytoid dendritic cells stimulate cytotoxic T-cell function in the atherosclerotic plaque through interferon-alpha. *Circulation* **114**, 2482-2489, doi:10.1161/CIRCULATIONAHA.106.642801 (2006).

166   Doring, Y. *et al.* Auto-antigenic protein-DNA complexes stimulate plasmacytoid dendritic cells to promote atherosclerosis. *Circulation* **125**, 1673-1683, doi:10.1161/CIRCULATIONAHA.111.046755 (2012).

167   Macritchie, N. *et al.* Plasmacytoid dendritic cells play a key role in promoting atherosclerosis in apolipoprotein E-deficient mice. *Arterioscler Thromb Vasc Biol* **32**, 2569-2579, doi:10.1161/ATVBAHA.112.251314 (2012).

168   Mohanta, S. K. *et al.* Artery tertiary lymphoid organs contribute to innate and adaptive immune responses in advanced mouse atherosclerosis. *Circ Res* **114**, 1772-1787, doi:10.1161/CIRCRESAHA.114.301137 (2014).

169   Akhavanpoor, M. *et al.* Adventitial tertiary lymphoid organ classification in human atherosclerosis. *Cardiovascular pathology : the official journal of the Society for Cardiovascular Pathology* **32**, 8-14, doi:10.1016/j.carpath.2017.08.002 (2018).

170   Yilmaz, A. *et al.* Predictive value of the decrease in circulating dendritic cell precursors in stable coronary artery disease. *Clinical science* **116**, 353-363, doi:10.1042/CS20080392 (2009).

171   Yilmaz, A. *et al.* Decrease in circulating myeloid dendritic cell precursors in coronary artery disease. *Journal of the American College of Cardiology* **48**, 70-80, doi:10.1016/j.jacc.2006.01.078 (2006).

172   Weis, M., Schlichting, C. L., Engleman, E. G. & Cooke, J. P. Endothelial determinants of dendritic cell adhesion and migration: new implications for vascular diseases. *Arterioscler Thromb Vasc Biol* **22**, 1817-1823 (2002).

173   Hansson, G. K. Inflammation, atherosclerosis, and coronary artery disease. *N Engl J Med* **352**, 1685-1695, doi:10.1056/NEJMra043430 (2005).

174   Alderman, C. J. *et al.* Effects of oxidised low density lipoprotein on dendritic cells: a possible immunoregulatory component of the atherogenic micro-environment? *Cardiovasc Res* **55**, 806-819 (2002).

175   Ge, J. *et al.* Advanced glycosylation end products might promote atherosclerosis through inducing the immune maturation of dendritic cells. *Arterioscler Thromb Vasc Biol* **25**, 2157-2163, doi:10.1161/01.ATV.0000181744.58265.63 (2005).

176   Aicher, A. *et al.* Nicotine strongly activates dendritic cell-mediated adaptive immunity: potential role for progression of atherosclerotic lesions. *Circulation* **107**, 604-611 (2003).

177   Lu, H. *et al.* Insulin enhances dendritic cell maturation and scavenger receptor-mediated uptake of oxidised low-density lipoprotein. *Journal of diabetes and its complications* **29**, 465-471, doi:10.1016/j.jdiacomp.2015.03.005 (2015).

178   Nie, W. *et al.* Angiotensin II Promotes Atherogenesis through upregulating the Expression of Connexin 43 in Dendritic Cells. *Cellular and molecular biology* **61**, 96-101 (2015).

179   Gautier, E. L. *et al.* Conventional dendritic cells at the crossroads between immunity and cholesterol homeostasis in atherosclerosis. *Circulation* **119**, 2367-2375, doi:10.1161/CIRCULATIONAHA.108.807537 (2009).

180   Stoneman, V. *et al.* Monocyte/macrophage suppression in CD11b diphtheria toxin receptor transgenic mice differentially affects atherogenesis and established plaques. *Circ Res* **100**, 884-893, doi:10.1161/01.RES.0000260802.75766.00 (2007).

181   Zernecke, A. Dendritic cells in atherosclerosis: evidence in mice and humans. *Arterioscler Thromb Vasc Biol* **35**, 763-770, doi:10.1161/ATVBAHA.114.303566 (2015).

182   Sun, J. *et al.* Deficiency of antigen-presenting cell invariant chain reduces atherosclerosis in mice. *Circulation* **122**, 808-820, doi:10.1161/CIRCULATIONAHA.109.891887 (2010).

183   Ye, Y. *et al.* Serum chemokine CCL17/thymus activation and regulated chemokine is correlated with coronary artery diseases. *Atherosclerosis* **238**, 365-369, doi:10.1016/j.atherosclerosis.2014.12.047 (2015).

184   Han, S. F. *et al.* The opposite-direction modulation of CD4+CD25+ Tregs and T helper 1 cells in acute coronary syndromes. *Clin Immunol* **124**, 90-97, doi:10.1016/j.clim.2007.03.546 (2007).

185   Daissormont, I. T. *et al.* Plasmacytoid dendritic cells protect against atherosclerosis by tuning T-cell proliferation and activity. *Circ Res* **109**, 1387-1395, doi:10.1161/CIRCRESAHA.111.256529 (2011).

186   Sage, A. P. *et al.* MHC Class II-restricted antigen presentation by plasmacytoid dendritic cells drives proatherogenic T cell immunity. *Circulation* **130**, 1363-1373, doi:10.1161/CIRCULATIONAHA.114.011090 (2014).

187   Maffia, P., Doring, Y., Biessen, E. A. & Mallat, Z. Commentary: Indoleamine 2,3-Dioxygenase-Expressing Aortic Plasmacytoid Dendritic Cells Protect against Atherosclerosis by Induction of Regulatory T Cells. *Front Immunol* **8**, 140, doi:10.3389/fimmu.2017.00140 (2017).

188   Yun, T. J. *et al.* Indoleamine 2,3-Dioxygenase-Expressing Aortic Plasmacytoid Dendritic Cells Protect against Atherosclerosis by Induction of Regulatory T Cells. *Cell metabolism* **23**, 852-866, doi:10.1016/j.cmet.2016.04.010 (2016).

189   Swiecki, M., Gilfillan, S., Vermi, W., Wang, Y. & Colonna, M. Plasmacytoid dendritic cell ablation impacts early interferon responses and antiviral NK and CD8(+) T cell accrual. *Immunity* **33**, 955-966, doi:10.1016/j.immuni.2010.11.020 (2010).

190   Mandl, M. *et al.* Evaluation of the BDCA2-DTR Transgenic Mouse Model in Chronic and Acute Inflammation. *PLoS One* **10**, e0134176, doi:10.1371/journal.pone.0134176 (2015).

191   Laurat, E. *et al.* In vivo downregulation of T helper cell 1 immune responses reduces atherogenesis in apolipoprotein E-knockout mice. *Circulation* **104**, 197-202 (2001).

192   Mallat, Z., Taleb, S., Ait-Oufella, H. & Tedgui, A. The role of adaptive T cell immunity in atherosclerosis. *J Lipid Res* **50 Suppl**, S364-369, doi:10.1194/jlr.R800092-JLR200 (2009).

193   Elhage, R. *et al.* Reduced atherosclerosis in interleukin-18 deficient apolipoprotein E-knockout mice. *Cardiovasc Res* **59**, 234-240 (2003).

194   Whitman, S. C., Ravisankar, P., Elam, H. & Daugherty, A. Exogenous interferon-gamma enhances atherosclerosis in apolipoprotein E-/- mice. *Am J Pathol* **157**, 1819-1824 (2000).

195   Davenport, P. & Tipping, P. G. The role of interleukin-4 and interleukin-12 in the progression of atherosclerosis in apolipoprotein E-deficient mice. *Am J Pathol* **163**, 1117-1125, doi:10.1016/S0002-9440(10)63471-2 (2003).

196   Hauer, A. D. *et al.* Blockade of interleukin-12 function by protein vaccination attenuates atherosclerosis. *Circulation* **112**, 1054-1062, doi:10.1161/CIRCULATIONAHA.104.533463 (2005).

197   Mallat, Z. *et al.* Interleukin-18/interleukin-18 binding protein signaling modulates atherosclerotic lesion development and stability. *Circ Res* **89**, E41-45 (2001).

198   Mallat, Z. *et al.* Expression of interleukin-18 in human atherosclerotic plaques and relation to plaque instability. *Circulation* **104**, 1598-1603 (2001).

199   Buono, C. *et al.* T-bet deficiency reduces atherosclerosis and alters plaque antigen-specific immune responses. *Proc Natl Acad Sci U S A* **102**, 1596-1601, doi:10.1073/pnas.0409015102 (2005).

200   Feng, J. *et al.* Induction of CD36 expression by oxidized LDL and IL-4 by a common signaling pathway dependent on protein kinase C and PPAR-gamma. *J Lipid Res* **41**, 688-696 (2000).

201   Huang, J. T. *et al.* Interleukin-4-dependent production of PPAR-gamma ligands in macrophages by 12/15-lipoxygenase. *Nature* **400**, 378-382, doi:10.1038/22572 (1999).

202   Cornicelli, J. A., Butteiger, D., Rateri, D. L., Welch, K. & Daugherty, A. Interleukin-4 augments acetylated LDL-induced cholesterol esterification in macrophages. *J Lipid Res* **41**, 376-383 (2000).

203   Barks, J. L., McQuillan, J. J. & Iademarco, M. F. TNF-alpha and IL-4 synergistically increase vascular cell adhesion molecule-1 expression in cultured vascular smooth muscle cells. *J Immunol* **159**, 4532-4538 (1997).

204   Lee, Y. W., Kuhn, H., Hennig, B., Neish, A. S. & Toborek, M. IL-4-induced oxidative stress upregulates VCAM-1 gene expression in human endothelial cells. *J Mol Cell Cardiol* **33**, 83-94, doi:10.1006/jmcc.2000.1278 (2001).

205   Sasaguri, T. *et al.* A role for interleukin 4 in production of matrix metalloproteinase 1 by human aortic smooth muscle cells. *Atherosclerosis* **138**, 247-253 (1998).

206   Binder, C. J. *et al.* Natural antibodies in murine atherosclerosis. *Curr Drug Targets* **9**, 190-195 (2008).

207   Erbel, C. *et al.* Inhibition of IL-17A attenuates atherosclerotic lesion development in apoE-deficient mice. *J Immunol* **183**, 8167-8175, doi:10.4049/jimmunol.0901126 (2009).

208   Jovanovic, D. V. *et al.* IL-17 stimulates the production and expression of proinflammatory cytokines, IL-beta and TNF-alpha, by human macrophages. *J Immunol* **160**, 3513-3521 (1998).

209   Madhur, M. S. *et al.* Role of interleukin 17 in inflammation, atherosclerosis, and vascular function in apolipoprotein e-deficient mice. *Arterioscler Thromb Vasc Biol* **31**, 1565-1572, doi:10.1161/ATVBAHA.111.227629 (2011).

210   Ley, K., Smith, E. & Stark, M. A. IL-17A-producing neutrophil-regulatory Tn lymphocytes. *Immunol Res* **34**, 229-242, doi:10.1385/IR:34:3:229 (2006).

211   Cheng, X. *et al.* Inhibition of IL-17A in atherosclerosis. *Atherosclerosis* **215**, 471-474, doi:10.1016/j.atherosclerosis.2010.12.034 (2011).

212   Butcher, M. J., Gjurich, B. N., Phillips, T. & Galkina, E. V. The IL-17A/IL-17RA axis plays a proatherogenic role via the regulation of aortic myeloid cell recruitment. *Circ Res* **110**, 675-687, doi:10.1161/CIRCRESAHA.111.261784 (2012).

213   Cheng, X. *et al.* The Th17/Treg imbalance in patients with acute coronary syndrome. *Clin Immunol* **127**, 89-97, doi:10.1016/j.clim.2008.01.009 (2008).

214   Li, Q. *et al.* Treg/Th17 ratio acts as a novel indicator for acute coronary syndrome. *Cell Biochem Biophys* **70**, 1489-1498, doi:10.1007/s12013-014-9993-5 (2014).

215   Mallat, Z. *et al.* Inhibition of transforming growth factor-beta signaling accelerates atherosclerosis and induces an unstable plaque phenotype in mice. *Circ Res* **89**, 930-934 (2001).

216   Robertson, A. K. *et al.* Disruption of TGF-beta signaling in T cells accelerates atherosclerosis. *J Clin Invest* **112**, 1342-1350, doi:10.1172/JCI18607 (2003).

217   Mallat, Z. *et al.* Protective role of interleukin-10 in atherosclerosis. *Circ Res* **85**, e17-24 (1999).

218   Pinderski Oslund, L. J. *et al.* Interleukin-10 blocks atherosclerotic events in vitro and in vivo. *Arterioscler Thromb Vasc Biol* **19**, 2847-2853 (1999).

219   Caligiuri, G. *et al.* Interleukin-10 deficiency increases atherosclerosis, thrombosis, and low-density lipoproteins in apolipoprotein E knockout mice. *Mol Med* **9**, 10-17 (2003).

220   Bobryshev, Y. V., Sobenin, I. A., Orekhov, A. N. & Chistiakov, D. A. Novel anti-inflammatory interleukin-35 as an emerging target for antiatherosclerotic therapy. *Curr Pharm Des* **21**, 1147-1151 (2015).

221   Lin, J. *et al.* The role of CD4+CD25+ regulatory T cells in macrophage-derived foam-cell formation. *J Lipid Res* **51**, 1208-1217, doi:10.1194/jlr.D000497 (2010).

222   Liu, G. *et al.* Phenotypic and functional switch of macrophages induced by regulatory CD4+CD25+ T cells in mice. *Immunol Cell Biol* **89**, 130-142, doi:10.1038/icb.2010.70 (2011).

223   Iikuni, N., Lourenco, E. V., Hahn, B. H. & La Cava, A. Cutting edge: Regulatory T cells directly suppress B cells in systemic lupus erythematosus. *J Immunol* **183**, 1518-1522, doi:10.4049/jimmunol.0901163 (2009).

224   Kyaw, T. *et al.* Conventional B2 B cell depletion ameliorates whereas its adoptive transfer aggravates atherosclerosis. *J Immunol* **185**, 4410-4419, doi:10.4049/jimmunol.1000033 (2010).

225   Meng, X. *et al.* Regulatory T cells in cardiovascular diseases. *Nat Rev Cardiol* **13**, 167-179, doi:10.1038/nrcardio.2015.169 (2016).

226   He, S., Li, M., Ma, X., Lin, J. & Li, D. CD4+CD25+Foxp3+ regulatory T cells protect the proinflammatory activation of human umbilical vein endothelial cells. *Arterioscler Thromb Vasc Biol* **30**, 2621-2630, doi:10.1161/ATVBAHA.110.210492 (2010).

227   Meng, X. *et al.* Regulatory T cells prevent plaque disruption in apolipoprotein E-knockout mice. *Int J Cardiol* **168**, 2684-2692, doi:10.1016/j.ijcard.2013.03.026 (2013).

228   Lahoute, C., Herbin, O., Mallat, Z. & Tedgui, A. Adaptive immunity in atherosclerosis: mechanisms and future therapeutic targets. *Nat Rev Cardiol* **8**, 348-358, doi:10.1038/nrcardio.2011.62 (2011).

229   de Boer, O. J., van der Meer, J. J., Teeling, P., van der Loos, C. M. & van der Wal, A. C. Low numbers of FOXP3 positive regulatory T cells are present in all developmental stages of human atherosclerotic lesions. *PLoS One* **2**, e779, doi:10.1371/journal.pone.0000779 (2007).

230   Wigren, M. *et al.* Low levels of circulating CD4+FoxP3+ T cells are associated with an increased risk for development of myocardial infarction but not for stroke. *Arterioscler Thromb Vasc Biol* **32**, 2000-2004, doi:10.1161/ATVBAHA.112.251579 (2012).

231   von Hundelshausen, P. *et al.* Heterophilic interactions of platelet factor 4 and RANTES promote monocyte arrest on endothelium. *Blood* **105**, 924-930, doi:10.1182/blood-2004-06-2475 (2005).

232   Kristensen, N. N., Brudzewsky, D., Gad, M. & Claesson, M. H. Chemokines involved in protection from colitis by CD4+CD25+ regulatory T cells. *Inflammatory bowel diseases* **12**, 612-618, doi:10.1097/01.ibd.0000225342.44850.d5 (2006).

233   Scheerens, H., Hessel, E., de Waal-Malefyt, R., Leach, M. W. & Rennick, D. Characterization of chemokines and chemokine receptors in two murine models of inflammatory bowel disease: IL-10-/- mice and Rag-2-/- mice reconstituted with CD4+CD45RBhigh T cells. *Eur J Immunol* **31**, 1465-1474, doi:10.1002/1521-4141(200105)31:5<1465::AID-IMMU1465>3.0.CO;2-E (2001).

234   Jugde, F. *et al.* Quantitation of chemokines (MDC, TARC) expression in mucosa from Crohn's disease and ulcerative colitis. *European cytokine network* **12**, 468-477 (2001).

235   Pabst, O. *et al.* Chemokine receptor CCR9 contributes to the localization of plasma cells to the small intestine. *J Exp Med* **199**, 411-416, doi:10.1084/jem.20030996 (2004).

236 Bobryshev, Y. V. Dendritic cells in atherosclerosis: current status of the problem and clinical relevance. *European heart journal* **26**, 1700-1704, doi:10.1093/eurheartj/ehi282 (2005).

237 Greaves, D. R. *et al.* Linked chromosome 16q13 chemokines, macrophage-derived chemokine, fractalkine, and thymus- and activation-regulated chemokine, are expressed in human atherosclerotic lesions. *Arterioscler Thromb Vasc Biol* **21**, 923-929 (2001).

238 Zernecke, A., Shagdarsuren, E. & Weber, C. Chemokines in atherosclerosis: an update. *Arterioscler Thromb Vasc Biol* **28**, 1897-1908, doi:10.1161/ATVBAHA.107.161174 (2008).

239 D'Ambrosio, D. *et al.* Quantitative differences in chemokine receptor engagement generate diversity in integrin-dependent lymphocyte adhesion. *J Immunol* **169**, 2303-2312 (2002).

240 Campbell, J. J. *et al.* The chemokine receptor CCR4 in vascular recognition by cutaneous but not intestinal memory T cells. *Nature* **400**, 776-780, doi:10.1038/23495 (1999).

241 Sallusto, F., Mackay, C. R. & Lanzavecchia, A. The role of chemokine receptors in primary, effector, and memory immune responses. *Annu Rev Immunol* **18**, 593-620, doi:10.1146/annurev.immunol.18.1.593 (2000).

242 Andrew, D. P. *et al.* C-C chemokine receptor 4 expression defines a major subset of circulating nonintestinal memory T cells of both Th1 and Th2 potential. *J Immunol* **166**, 103-111 (2001).

243 Hirahara, K. *et al.* The majority of human peripheral blood CD4+CD25highFoxp3+ regulatory T cells bear functional skin-homing receptors. *J Immunol* **177**, 4488-4494 (2006).

244 Wolpe, S. D. *et al.* Macrophages secrete a novel heparin-binding protein with inflammatory and neutrophil chemokinetic properties. *J Exp Med* **167**, 570-581 (1988).

245 Davatelis, G. *et al.* Macrophage inflammatory protein-1: a prostaglandin-independent endogenous pyrogen. *Science* **243**, 1066-1068 (1989).

246 Sarosdy, M. F., Lamm, D. L., Radwin, H. M. & Von Hoff, D. D. Clonogenic assay and in vitro chemosensitivity testing of human urologic malignancies. *Cancer* **50**, 1332-1338 (1982).

247 Kasama, T., Strieter, R. M., Standiford, T. J., Burdick, M. D. & Kunkel, S. L. Expression and regulation of human neutrophil-derived macrophage inflammatory protein 1 alpha. *J Exp Med* **178**, 63-72 (1993).

248 Harrison, L. M., van den Hoogen, C., van Haaften, W. C. & Tesh, V. L. Chemokine expression in the monocytic cell line THP-1 in response to purified shiga toxin 1 and/or lipopolysaccharides. *Infection and immunity* **73**, 403-412, doi:10.1128/IAI.73.1.403-412.2005 (2005).

249 Weber, C. Platelets and chemokines in atherosclerosis: partners in crime. *Circ Res* **96**, 612-616, doi:10.1161/01.RES.0000160077.17427.57 (2005).

250 Saraswathi, V. & Hasty, A. H. The role of lipolysis in mediating the proinflammatory effects of very low density lipoproteins in mouse peritoneal macrophages. *J Lipid Res* **47**, 1406-1415, doi:10.1194/jlr.M600159-JLR200 (2006).

251 Ying, S., Meng, Q., Barata, L. T. & Kay, A. B. Macrophage inflammatory protein-1alpha and C-C chemokine receptor-1 in allergen-induced skin late-phase

reactions: relationship to macrophages, neutrophils, basophils, eosinophils and T lymphocytes. *Clinical and experimental allergy : journal of the British Society for Allergy and Clinical Immunology* **31**, 1724-1731 (2001).

252   Montecucco, F. *et al.* Tumor necrosis factor-alpha (TNF-alpha) induces integrin CD11b/CD18 (Mac-1) up-regulation and migration to the CC chemokine CCL3 (MIP-1alpha) on human neutrophils through defined signalling pathways. *Cellular signalling* **20**, 557-568, doi:10.1016/j.cellsig.2007.11.008 (2008).

253   Miyazaki, D. *et al.* Macrophage inflammatory protein-1alpha as a costimulatory signal for mast cell-mediated immediate hypersensitivity reactions. *J Clin Invest* **115**, 434-442, doi:10.1172/JCI18452 (2005).

254   Luster, A. D., Unkeless, J. C. & Ravetch, J. V. Gamma-interferon transcriptionally regulates an early-response gene containing homology to platelet proteins. *Nature* **315**, 672-676 (1985).

255   Luster, A. D. & Ravetch, J. V. Biochemical characterization of a gamma interferon-inducible cytokine (IP-10). *J Exp Med* **166**, 1084-1097 (1987).

256   Gattass, C. R., King, L. B., Luster, A. D. & Ashwell, J. D. Constitutive expression of interferon gamma-inducible protein 10 in lymphoid organs and inducible expression in T cells and thymocytes. *J Exp Med* **179**, 1373-1378 (1994).

257   Gottlieb, A. B., Luster, A. D., Posnett, D. N. & Carter, D. M. Detection of a gamma interferon-induced protein IP-10 in psoriatic plaques. *J Exp Med* **168**, 941-948 (1988).

258   Heller, E. A. *et al.* Chemokine CXCL10 promotes atherogenesis by modulating the local balance of effector and regulatory T cells. *Circulation* **113**, 2301-2312, doi:10.1161/CIRCULATIONAHA.105.605121 (2006).

259   Segers, D. *et al.* Atherosclerotic Plaque Stability Is Affected by the Chemokine CXCL10 in Both Mice and Humans. *International journal of inflammation* **2011**, 936109, doi:10.4061/2011/936109 (2011).

260   van den Borne, P., Quax, P. H., Hoefer, I. E. & Pasterkamp, G. The multifaceted functions of CXCL10 in cardiovascular disease. *BioMed research international* **2014**, 893106, doi:10.1155/2014/893106 (2014).

261   Loetscher, M. *et al.* Chemokine receptor specific for IP10 and mig: structure, function, and expression in activated T-lymphocytes. *J Exp Med* **184**, 963-969 (1996).

262   Loetscher, M., Loetscher, P., Brass, N., Meese, E. & Moser, B. Lymphocyte-specific chemokine receptor CXCR3: regulation, chemokine binding and gene localization. *Eur J Immunol* **28**, 3696-3705, doi:10.1002/(SICI)1521-4141(199811)28:11<3696::AID-IMMU3696>3.0.CO;2-W (1998).

263   Lu, B. *et al.* Structure and function of the murine chemokine receptor CXCR3. *Eur J Immunol* **29**, 3804-3812, doi:10.1002/(SICI)1521-4141(199911)29:11<3804::AID-IMMU3804>3.0.CO;2-9 (1999).

264   Dufour, J. H. *et al.* IFN-gamma-inducible protein 10 (IP-10; CXCL10)-deficient mice reveal a role for IP-10 in effector T cell generation and trafficking. *J Immunol* **168**, 3195-3204 (2002).

265   Angiolillo, A. L. *et al.* Human interferon-inducible protein 10 is a potent inhibitor of angiogenesis in vivo. *J Exp Med* **182**, 155-162 (1995).

266   Murphy, K. M. & Stockinger, B. Effector T cell plasticity: flexibility in the face of changing circumstances. *Nat Immunol* **11**, 674-680, doi:10.1038/ni.1899 (2010).

267 Oestreich, K. J. & Weinmann, A. S. Master regulators or lineage-specifying? Changing views on CD4+ T cell transcription factors. *Nat Rev Immunol* **12**, 799-804, doi:10.1038/nri3321 (2012).

268 Chen, L., Wu, J., Pier, E., Zhao, Y. & Shen, Z. mTORC2-PKBalpha/Akt1 Serine 473 phosphorylation axis is essential for regulation of FOXP3 Stability by chemokine CCL3 in psoriasis. *The Journal of investigative dermatology* **133**, 418-428, doi:10.1038/jid.2012.333 (2013).

269 Ardigo, D. *et al.* Circulating chemokines accurately identify individuals with clinically significant atherosclerotic heart disease. *Physiological genomics* **31**, 402-409, doi:10.1152/physiolgenomics.00104.2007 (2007).

270 de Jager, S. C. *et al.* CCL3 (MIP-1 alpha) levels are elevated during acute coronary syndromes and show strong prognostic power for future ischemic events. *J Mol Cell Cardiol* **45**, 446-452, doi:10.1016/j.yjmcc.2008.06.003 (2008).

271 de Jager, S. C. *et al.* Chemokines CCL3/MIP1alpha, CCL5/RANTES and CCL18/PARC are independent risk predictors of short-term mortality in patients with acute coronary syndromes. *PLoS One* **7**, e45804, doi:10.1371/journal.pone.0045804 (2012).

272 de Jager, S. C. *et al.* Leukocyte-specific CCL3 deficiency inhibits atherosclerotic lesion development by affecting neutrophil accumulation. *Arterioscler Thromb Vasc Biol* **33**, e75-83, doi:10.1161/ATVBAHA.112.300857 (2013).

273 Luo, H. R. & Loison, F. Constitutive neutrophil apoptosis: mechanisms and regulation. *American journal of hematology* **83**, 288-295, doi:10.1002/ajh.21078 (2008).

274 Potteaux, S. *et al.* Role of bone marrow-derived CC-chemokine receptor 5 in the development of atherosclerosis of low-density lipoprotein receptor knockout mice. *Arterioscler Thromb Vasc Biol* **26**, 1858-1863, doi:10.1161/01.ATV.0000231527.22762.71 (2006).

275 Kuziel, W. A. *et al.* CCR5 deficiency is not protective in the early stages of atherogenesis in apoE knockout mice. *Atherosclerosis* **167**, 25-32 (2003).

276 Potteaux, S. *et al.* Chemokine receptor CCR1 disruption in bone marrow cells enhances atherosclerotic lesion development and inflammation in mice. *Mol Med* **11**, 16-20, doi:10.2119/2005-00028.Potteaux (2005).

277 Veillard, N. R. *et al.* Antagonism of RANTES receptors reduces atherosclerotic plaque formation in mice. *Circ Res* **94**, 253-261, doi:10.1161/01.RES.0000109793.17591.4E (2004).

278 Yang, X. *et al.* The chemokine, CCL3, and its receptor, CCR1, mediate thoracic radiation-induced pulmonary fibrosis. *American journal of respiratory cell and molecular biology* **45**, 127-135, doi:10.1165/rcmb.2010-0265OC (2011).

279 Tokuda, A. *et al.* Pivotal role of CCR1-positive leukocytes in bleomycin-induced lung fibrosis in mice. *J Immunol* **164**, 2745-2751 (2000).

280 Ishida, Y. *et al.* Essential roles of the CC chemokine ligand 3-CC chemokine receptor 5 axis in bleomycin-induced pulmonary fibrosis through regulation of macrophage and fibrocyte infiltration. *Am J Pathol* **170**, 843-854, doi:10.2353/ajpath.2007.051213 (2007).

281 Smith, R. E. *et al.* Production and function of murine macrophage inflammatory protein-1 alpha in bleomycin-induced lung injury. *J Immunol* **153**, 4704-4712 (1994).

282   Seki, E. *et al.* CCR1 and CCR5 promote hepatic fibrosis in mice. *J Clin Invest* **119**, 1858-1870 (2009).

283   Eis, V. *et al.* Chemokine receptor CCR1 but not CCR5 mediates leukocyte recruitment and subsequent renal fibrosis after unilateral ureteral obstruction. *Journal of the American Society of Nephrology : JASN* **15**, 337-347 (2004).

284   Cheng, J. F. & Jack, R. CCR1 antagonists. *Molecular diversity* **12**, 17-23, doi:10.1007/s11030-008-9076-x (2008).

285   Gladue, R. P., Brown, M. F. & Zwillich, S. H. CCR1 antagonists: what have we learned from clinical trials. *Current topics in medicinal chemistry* **10**, 1268-1277 (2010).

286   He, M., Horuk, R. & Bhatia, M. Treatment with BX471, a nonpeptide CCR1 antagonist, protects mice against acute pancreatitis-associated lung injury by modulating neutrophil recruitment. *Pancreas* **34**, 233-241, doi:10.1097/mpa.0b013e31802e7598 (2007).

287   Carter, P. H. & Hynes, J. N-aryl pyrazoles, indazoles and azaindazoles as antagonists of CC chemokine receptor 1: patent cooperation treaty applications WO2010/036632, WO2009/134666 and WO2009/137338. *Expert opinion on therapeutic patents* **20**, 1609-1618, doi:10.1517/13543776.2010.518144 (2010).

288   Liang, M. *et al.* Identification and characterization of a potent, selective, and orally active antagonist of the CC chemokine receptor-1. *J Biol Chem* **275**, 19000-19008, doi:10.1074/jbc.M001222200 (2000).

289   Zipp, F. *et al.* Blockade of chemokine signaling in patients with multiple sclerosis. *Neurology* **67**, 1880-1883, doi:10.1212/01.wnl.0000244420.68037.86 (2006).

290   Gladue, R. P. *et al.* CP-481,715, a potent and selective CCR1 antagonist with potential therapeutic implications for inflammatory diseases. *J Biol Chem* **278**, 40473-40480, doi:10.1074/jbc.M306875200 (2003).

291   Merritt, J. R. *et al.* Novel pyrrolidine heterocycles as CCR1 antagonists. *Bioorganic & medicinal chemistry letters* **20**, 5477-5479, doi:10.1016/j.bmcl.2010.07.082 (2010).

292   Haringman, J. J., Kraan, M. C., Smeets, T. J., Zwinderman, K. H. & Tak, P. P. Chemokine blockade and chronic inflammatory disease: proof of concept in patients with rheumatoid arthritis. *Ann Rheum Dis* **62**, 715-721 (2003).

293   Borregaard, J. *et al.* Evaluation of the effect of the specific CCR1 antagonist CP-481715 on the clinical and cellular responses observed following epicutaneous nickel challenge in human subjects. *Contact dermatitis* **59**, 212-219, doi:10.1111/j.1600-0536.2008.01365.x (2008).

294   Norman, P. AZD-4818, a chemokine CCR1 antagonist: WO2008103126 and WO2009011653. *Expert opinion on therapeutic patents* **19**, 1629-1633, doi:10.1517/13543770903118996 (2009).

295   Kerstjens, H. A., Bjermer, L., Eriksson, L., Dahlstrom, K. & Vestbo, J. Tolerability and efficacy of inhaled AZD4818, a CCR1 antagonist, in moderate to severe COPD patients. *Respiratory medicine* **104**, 1297-1303, doi:10.1016/j.rmed.2010.04.010 (2010).

296   Lu, C. *et al.* Quantitative prediction and clinical observation of a CYP3A inhibitor-based drug-drug interactions with MLN3897, a potent C-C chemokine receptor-1 antagonist. *The Journal of pharmacology and experimental therapeutics* **332**, 562-568, doi:10.1124/jpet.109.161893 (2010).

297 Vergunst, C. E. *et al.* MLN3897 plus methotrexate in patients with rheumatoid arthritis: safety, efficacy, pharmacokinetics, and pharmacodynamics of an oral CCR1 antagonist in a phase IIa, double-blind, placebo-controlled, randomized, proof-of-concept study. *Arthritis and rheumatism* **60**, 3572-3581, doi:10.1002/art.24978 (2009).

298 Schall, T. J. & Proudfoot, A. E. Overcoming hurdles in developing successful drugs targeting chemokine receptors. *Nat Rev Immunol* **11**, 355-363, doi:10.1038/nri2972 (2011).

299 Lebre, M. C. *et al.* Why CCR2 and CCR5 blockade failed and why CCR1 blockade might still be effective in the treatment of rheumatoid arthritis. *PLoS One* **6**, e21772, doi:10.1371/journal.pone.0021772 (2011).

300 Mariani, M., Lang, R., Binda, E., Panina-Bordignon, P. & D'Ambrosio, D. Dominance of CCL22 over CCL17 in induction of chemokine receptor CCR4 desensitization and internalization on human Th2 cells. *Eur J Immunol* **34**, 231-240, doi:10.1002/eji.200324429 (2004).

301 D'Ambrosio, D. *et al.* Selective up-regulation of chemokine receptors CCR4 and CCR8 upon activation of polarized human type 2 Th cells. *J Immunol* **161**, 5111-5115 (1998).

302 Qu, C. *et al.* Role of CCR8 and other chemokine pathways in the migration of monocyte-derived dendritic cells to lymph nodes. *J Exp Med* **200**, 1231-1241, doi:10.1084/jem.20032152 (2004).

303 Tiffany, H. L. *et al.* Identification of CCR8: a human monocyte and thymus receptor for the CC chemokine I-309. *J Exp Med* **186**, 165-170 (1997).

304 Devi, S., Laning, J., Luo, Y. & Dorf, M. E. Biologic activities of the beta-chemokine TCA3 on neutrophils and macrophages. *J Immunol* **154**, 5376-5383 (1995).

305 Bonecchi, R. *et al.* Differential expression of chemokine receptors and chemotactic responsiveness of type 1 T helper cells (Th1s) and Th2s. *J Exp Med* **187**, 129-134 (1998).

306 Panina-Bordignon, P. *et al.* The C-C chemokine receptors CCR4 and CCR8 identify airway T cells of allergen-challenged atopic asthmatics. *J Clin Invest* **107**, 1357-1364, doi:10.1172/JCI12655 (2001).

307 Islam, S. A. *et al.* Mouse CCL8, a CCR8 agonist, promotes atopic dermatitis by recruiting IL-5+ T(H)2 cells. *Nat Immunol* **12**, 167-177, doi:10.1038/ni.1984 (2011).

308 Coghill, J. M. *et al.* CC chemokine receptor 8 potentiates donor Treg survival and is critical for the prevention of murine graft-versus-host disease. *Blood* **122**, 825-836, doi:10.1182/blood-2012-06-435735 (2013).

309 Barsheshet, Y. *et al.* CCR8(+)FOXp3(+) Treg cells as master drivers of immune regulation. *Proc Natl Acad Sci U S A* **114**, 6086-6091, doi:10.1073/pnas.1621280114 (2017).

310 Connolly, S., Skrinjar, M. & Rosendahl, A. Orally bioavailable allosteric CCR8 antagonists inhibit dendritic cell, T cell and eosinophil migration. *Biochemical pharmacology* **83**, 778-787, doi:10.1016/j.bcp.2011.12.021 (2012).

311 Oshio, T. *et al.* Chemokine receptor CCR8 is required for lipopolysaccharide-triggered cytokine production in mouse peritoneal macrophages. *PLoS One* **9**, e94445, doi:10.1371/journal.pone.0094445 (2014).

312 Karlsson, A. K. *et al.* Small molecule antagonists of CCR8 inhibit eosinophil and T cell migration. *Biochem Biophys Res Commun* **407**, 764-771, doi:10.1016/j.bbrc.2011.03.097 (2011).

313 Jenkins, T. J. *et al.* Design, synthesis, and evaluation of naphthalene-sulfonamide antagonists of human CCR8. *Journal of medicinal chemistry* **50**, 566-584, doi:10.1021/jm061118e (2007).

314 Wang, L. *et al.* Antagonism of chemokine receptor CCR8 is ineffective in a primate model of asthma. *Thorax* **68**, 506-512, doi:10.1136/thoraxjnl-2012-203012 (2013).

315 Nesmelova, I. V. *et al.* Platelet factor 4 and interleukin-8 CXC chemokine heterodimer formation modulates function at the quaternary structural level. *J Biol Chem* **280**, 4948-4958, doi:10.1074/jbc.M405364200 (2005).

316 Baltus, T., Weber, K. S., Johnson, Z., Proudfoot, A. E. & Weber, C. Oligomerization of RANTES is required for CCR1-mediated arrest but not CCR5-mediated transmigration of leukocytes on inflamed endothelium. *Blood* **102**, 1985-1988, doi:10.1182/blood-2003-04-1175 (2003).

317 von Hundelshausen, P. *et al.* Chemokine interactome mapping enables tailored intervention in acute and chronic inflammation. *Science translational medicine* **9**, doi:10.1126/scitranslmed.aah6650 (2017).

318 Liang, W. G., Ren, M., Zhao, F. & Tang, W. J. Structures of human CCL18, CCL3, and CCL4 reveal molecular determinants for quaternary structures and sensitivity to insulin-degrading enzyme. *Journal of molecular biology* **427**, 1345-1358, doi:10.1016/j.jmb.2015.01.012 (2015).

319 Zlotnik, A. & Yoshie, O. The chemokine superfamily revisited. *Immunity* **36**, 705-716, doi:10.1016/j.immuni.2012.05.008 (2012).

320 Kufareva, I., Salanga, C. L. & Handel, T. M. Chemokine and chemokine receptor structure and interactions: implications for therapeutic strategies. *Immunol Cell Biol* **93**, 372-383, doi:10.1038/icb.2015.15 (2015).

321 Qin, L. *et al.* Structural biology. Crystal structure of the chemokine receptor CXCR4 in complex with a viral chemokine. *Science* **347**, 1117-1122, doi:10.1126/science.1261064 (2015).

322 Drury, L. J. *et al.* Monomeric and dimeric CXCL12 inhibit metastasis through distinct CXCR4 interactions and signaling pathways. *Proc Natl Acad Sci U S A* **108**, 17655-17660, doi:10.1073/pnas.1101133108 (2011).

323 Jin, H., Shen, X., Baggett, B. R., Kong, X. & LiWang, P. J. The human CC chemokine MIP-1beta dimer is not competent to bind to the CCR5 receptor. *J Biol Chem* **282**, 27976-27983, doi:10.1074/jbc.M702654200 (2007).

324 Kramp, B. K. *et al.* Exchange of extracellular domains of CCR1 and CCR5 reveals confined functions in CCL5-mediated cell recruitment. *Thromb Haemost* **110**, 795-806, doi:10.1160/TH13-05-0420 (2013).

325 Grommes, J. *et al.* Disruption of platelet-derived chemokine heteromers prevents neutrophil extravasation in acute lung injury. *American journal of respiratory and critical care medicine* **185**, 628-636, doi:10.1164/rccm.201108-1533OC (2012).

8. Supplement

Supplemental table 1: Circulating leukocyte subpopulations of *Apoe*^{-/-} and *Apoe*^{-/-}*Ccl17*[e/e] mice.
Peripheral blood leukocyte subsets were measured by flow cytometry. All values are displayed as mean ± SEM (n=10-11).

12 weeks HFD	Blood		
	Apoe^{-/-}	*Apoe*^{-/-}*Ccl17*[e/e]	p-Value
Leukocytes/ml	$2,6 \times 10^{06}$ ± $1,7 \times 10^{05}$	$2,9 \times 10^{06}$ ± $2,4 \times 10^{05}$	0,28
Gr1[+] monocytes/ml	$6,5 \times 10^{04}$ ± $6,7 \times 10^{03}$	$6,1 \times 10^{04}$ ± $7,1 \times 10^{03}$	0,68
Gr1[-] monocytes/ml	$3,4 \times 10^{04}$ ± $4,3 \times 10^{03}$	$4,3 \times 10^{04}$ ± $7,5 \times 10^{03}$	0,33
Neutrophils/ml	$5,1 \times 10^{05}$ ± $3,6 \times 10^{04}$	$7,2 \times 10^{05}$ ± $1,3 \times 10^{05}$	0,14
B cells/ml	$1,4 \times 10^{06}$ ± $1,0 \times 10^{05}$	$1,4 \times 10^{06}$ ± $1,5 \times 10^{05}$	0,63
CD3^{+} T cells/ml	$1,9 \times 10^{05}$ ± $1,9 \times 10^{04}$	$1,9 \times 10^{05}$ ± $1,0 \times 10^{04}$	0,83
CD4^{+} T cells/ml	$1,1 \times 10^{05}$ ± $1,3 \times 10^{04}$	$1,3 \times 10^{05}$ ± $6,4 \times 10^{03}$	0,18
CD8^{+} T cells/ml	$4,0 \times 10^{04}$ ± $5,6 \times 10^{03}$	$4,5 \times 10^{04}$ ± $3,5 \times 10^{03}$	0,49
Platelets/ml	$2,6 \times 10^{06}$ ± $1,7 \times 10^{05}$	$2,9 \times 10^{06}$ ± $2,4 \times 10^{05}$	0,28

Supplemental table 2: Bone Marrow leukocyte subpopulations of *Apoe*^{-/-} and *Apoe*^{-/-}*Ccl17*[e/e] mice.
Bone Marrow leukocyte subsets were measured by flow cytometry. All values are displayed as mean ± SEM (n=10-11).

12 weeks HFD	BM		
	Apoe^{-/-}	*Apoe*^{-/-}*Ccl17*[e/e]	p-Value
Leukocytes/ml	$7,09 \times 10^{06}$ ± $1,07 \times 10^{06}$	$8,31 \times 10^{06}$ ± $5,92 \times 10^{05}$	0,367
Gr1[+] monocytes/ml	$4,76 \times 10^{05}$ ± $5,93 \times 10^{04}$	$6,44 \times 10^{05}$ ± $7,02 \times 10^{04}$	0,098
Gr1[-] monocytes/ml	$1,54 \times 10^{05}$ ± $1,27 \times 10^{04}$	$1,74 \times 10^{05}$ ± $1,60 \times 10^{04}$	0,351
Neutrophils/ml	$2,67 \times 10^{06}$ ± $4,95 \times 10^{05}$	$3,36 \times 10^{06}$ ± $3,44 \times 10^{05}$	0,295
B cells/ml	$1,25 \times 10^{07}$ ± $1,37 \times 10^{06}$	$1,61 \times 10^{07}$ ± $1,39 \times 10^{06}$	0,094
cDCs/ml	$1,63 \times 10^{05}$ ± $1,68 \times 10^{04}$	$1,48 \times 10^{05}$ ± $1,55 \times 10^{04}$	0,530
pDCs/ml	$4,53 \times 10^{05}$ ± $4,56 \times 10^{04}$	$5,10 \times 10^{05}$ ± $5,26 \times 10^{04}$	0,440
Macrophages/ml	$9,05 \times 10^{04}$ ± $1,42 \times 10^{04}$	$7,45 \times 10^{04}$ ± $5,21 \times 10^{03}$	0,347

Supplemental table 3: Splenic leukocyte subpopulations of *Apoe$^{-/-}$* and *Apoe$^{-/-}$Ccl17$^{e/e}$* mice. Splenic leukocyte subsets were measured by flow cytometry. All values are displayed as mean ± SEM (n=10-11).

Spleen			
12 weeks HFD	***Apoe$^{-/-}$***	***Apoe$^{-/-}$Ccl17$^{e/e}$***	**p-Value**
Leukocytes/ml	5,12x10^{07} ± 5,40x10^{06}	6,62x10^{07} ± 7,69x10^{06}	0,120
Gr1$^+$ monocytes/ml	6,75x10^{05} ± 8,77x10^{04}	1,15x10^{06} ± 8,20x10^{05}	0,077
Gr1$^-$ monocytes/ml	4,84x10^{05} ± 7,33x10^{04}	8,20x10^{05} ± 1,62x10^{05}	0,067
Neutrophils/ml	1,21x10^{06} ± 1,32x10^{05}	2,31x10^{06} ± 6,36x10^{05}	0,091
B cells/ml	2,12x10^{07} ± 2,48x10^{06}	2,99x10^{07} ± 3,91x10^{06}	0,070
CD3$^+$ T cells/ml	1,20x10^{07} ± 1,38x10^{06}	1,67x10^{07} ± 2,07x10^{06}	0,068
CD4$^+$ T cells/ml	8,64x10^{06} ± 9,68x10^{05}	1,67x10^{07} ± 1,50x10^{06}	0,068
CD8$^+$ T cells/ml	2,31x10^{06} ± 2,81x10^{05}	3,35x10^{06} ± 4,94x10^{05}	0,079
cDCs/ml	1,80x10^{06} ± 2,04x10^{05}	1,63x10^{06} ± 3,31x10^{05}	0,670
pDCs/ml	3,97x10^{05} ± 1,41x10^{05}	4,94x10^{05} ± 7,99x10^{04}	0,568
Macrophages/ml	1,81x10^{06} ± 3,20x10^{05}	2,01x10^{06} ± 3,82x10^{05}	0,696

Supplemental table 4: Para-aortic lymph node leukocyte subpopulations of *Apoe$^{-/-}$* and *Apoe$^{-/-}$Ccl17$^{e/e}$* mice. Para-aortic lymph node leukocyte subsets were measured by flow cytometry. All values are displayed as mean ± SEM (n=10-11).

para-aortic Lymph Node			
12 weeks HFD	***Apoe$^{-/-}$***	***Apoe$^{-/-}$Ccl17$^{e/e}$***	**p-Value**
Leukocytes/ml	2,13x10^{06} ± 3,83x10^{05}	1,67x10^{06} ± 1,04x10^{06}	0,385
Gr1$^+$ monocytes/ml	6,70x10^{03} ± 1,40x10^{03}	4,18x10^{03} ± 2,49x10^{03}	0,147
Gr1$^-$ monocytes/ml	3,42x10^{04} ± 5,22x10^{03}	1,80x10^{04} ± 1,27x10^{04}	0,044
B cells/ml	6,97x10^{05} ± 1,17x10^{05}	5,48x10^{05} ± 4,05x10^{05}	0,412
CD3$^+$ T cells/ml	8,83x10^{05} ± 1,87x10^{05}	7,60x10^{05} ± 5,04x10^{05}	0,632
CD4$^+$ T cells/ml	6,24x10^{05} ± 1,24x10^{05}	5,66x10^{05} ± 3,75x10^{05}	0,746
CD8$^+$ T cells/ml	2,13x10^{05} ± 5,47x10^{04}	1,69x10^{05} ± 1,17x10^{05}	0,532
cDCs/ml	1,75x10^{04} ± 3,45x10^{03}	1,54x10^{04} ± 1,10x10^{04}	0,690
pDCs/ml	5,50x10^{03} ± 1,10x10^{03}	4,30x10^{03} ± 3,01x10^{03}	0,436

Supplemental table 5: Circulating leukocyte subpopulations of *Apoe*^{-/-} and *Apoe*^{-/-}*Ccr4*^{-/-} mice.
Peripheral blood leukocyte subsets were measured by flow cytometry. All values are displayed as mean ± SEM (n=9-10).

	Blood		
12 weeks HFD	***Apoe*^{-/-}**	***Apoe*^{-/-}*Ccr4*^{-/-}**	**p-Value**
Leukocytes/ml	$4{,}60 \times 10^{06}$ $\pm\, 5{,}02 \times 10^{05}$	$3{,}31 \times 10^{06}$ $\pm\, 1{,}87 \times 10^{05}$	0,062
Gr1$^+$ monocytes/ml	$2{,}40 \times 10^{05}$ $\pm\, 2{,}60 \times 10^{04}$	$1{,}87 \times 10^{05}$ $\pm\, 2{,}41 \times 10^{04}$	0,155
Gr1$^-$ monocytes/ml	$2{,}23 \times 10^{05}$ $\pm\, 3{,}48 \times 10^{04}$	$1{,}40 \times 10^{05}$ $\pm\, 2{,}17 \times 10^{04}$	0,065
Neutrophils/ml	$1{,}12 \times 10^{06}$ $\pm\, 1{,}12 \times 10^{05}$	$8{,}43 \times 10^{05}$ $\pm\, 7{,}53 \times 10^{04}$	0,073
B cells/ml	$1{,}80 \times 10^{06}$ $\pm\, 1{,}91 \times 10^{05}$	$1{,}37 \times 10^{06}$ $\pm\, 2{,}019 \times 10^{05}$	0,143
CD3$^+$ T cells/ml	$5{,}24 \times 10^{05}$ $\pm\, 7{,}95 \times 10^{04}$	$3{,}62 \times 10^{05}$ $\pm\, 3{,}55 \times 10^{04}$	0,071
CD4+ T cells/ml	$2{,}64 \times 10^{05}$ $\pm\, 4{,}07 \times 10^{04}$	$1{,}87 \times 10^{05}$ $\pm\, 1{,}70 \times 10^{04}$	0,094
CD8+ T cells/ml	$2{,}06 \times 10^{05}$ $\pm\, 3{,}35 \times 10^{04}$	$1{,}32 \times 10^{05}$ $\pm\, 1{,}34 \times 10^{04}$	0,064
Platelets/ml	$6{,}19 \times 10^{05}$ $\pm\, 1{,}25 \times 10^{05}$	$7{,}49 \times 10^{05}$ $\pm\, 4{,}60 \times 10^{04}$	0,285

Supplemental table 6: Bone marrow leukocyte subpopulations of *Apoe*^{-/-} and *Apoe*^{-/-}*Ccr4*^{-/-} mice.
Bone marrow leukocyte subsets were measured by flow cytometry. All values are displayed as mean ± SEM (n=9-10).

	Bone Marrow		
12 weeks HFD	***Apoe*^{-/-}**	***Apoe*^{-/-}*Ccr4*^{-/-}**	**p-Value**
Leukocytes/ml	$1{,}2 \times 10^{07}$ $\pm\, 6{,}57 \times 10^{05}$	$9{,}76 \times 10^{06}$ $\pm\, 9{,}18 \times 10^{05}$	0,055
Gr1$^+$ monocytes/ml	$1{,}02 \times 10^{06}$ $\pm\, 1{,}06 \times 10^{05}$	$8{,}10 \times 10^{05}$ $\pm\, 1{,}41 \times 10^{05}$	0,235
Gr1$^-$ monocytes/ml	$3{,}97 \times 10^{05}$ $\pm\, 4{,}03 \times 10^{04}$	$3{,}26 \times 10^{05}$ $\pm\, 4{,}12 \times 10^{04}$	0,237
Neutrophils/ml	$4{,}92 \times 10^{06}$ $\pm\, 2{,}20 \times 10^{05}$	$3{,}00 \times 10^{06}$ $\pm\, 6{,}28 \times 10^{05}$	0,009
B cells/ml	$2{,}92 \times 10^{06}$ $\pm\, 2{,}31 \times 10^{05}$	$2{,}20 \times 10^{06}$ $\pm\, 6{,}12 \times 10^{05}$	0,288
cDCs/ml	$7{,}22 \times 10^{04}$ $\pm\, 6{,}48 \times 10^{03}$	$9{,}75 \times 10^{04}$ $\pm\, 1{,}99 \times 10^{04}$	0,265
pDCs/ml	$2{,}57 \times 10^{05}$ $\pm\, 1{,}95 \times 10^{04}$	$1{,}87 \times 10^{05}$ $\pm\, 1{,}70 \times 10^{04}$	0,061
Macrophages/ml	$2{,}06 \times 10^{05}$ $\pm\, 3{,}35 \times 10^{04}$	$3{,}87 \times 10^{05}$ $\pm\, 5{,}33 \times 10^{04}$	0,092

Supplemental table 7: Splenic leukocyte subpopulations of *Apoe*$^{-/-}$ and *Apoe*$^{-/-}$*Ccr4*$^{-/-}$ mice. Splenic leukocyte subsets were measured by flow cytometry. All values are displayed as mean ± SEM (n=9-10).

	Spleen		
12 weeks HFD	***Apoe*$^{-/-}$**	***Apoe*$^{-/-}$*Ccr4*$^{-/-}$**	**p-Value**
Leukocytes/ml	1,12x10^{08} ± 5,69x10^{05}	1,00x10^{08} ± 1,27x10^{06}	0,335
Gr1$^+$ monocytes/ml	1,54x10^{06} ± 9,55x10^{04}	1,14x10^{06} ± 2,37x10^{05}	0,116
Gr1$^-$ monocytes/ml	8,46x10^{05} ± 1,31x10^{05}	4,87x10^{05} ± 1,26x10^{05}	0,068
Neutrophils/ml	2,02x10^{06} ± 2,16x10^{05}	2,20x10^{06} ± 3,57x10^{05}	0,674
B cells/ml	5,49x10^{07} ± 2,66x10^{06}	4,54x10^{07} ± 5,20x10^{06}	0,143
CD3$^+$ T cells/ml	2,89x10^{07} ± 1,36x10^{06}	2,86x10^{07} ± 4,77x10^{06}	0,975
CD4$^+$ T cells/ml	1,79x10^{07} ± 8,02x10^{05}	1,65x10^{07} ± 2,24x10^{06}	0,718
CD8$^+$ T cells/ml	5,56x10^{06} ± 3,02x10^{05}	5,17x10^{06} ± 9,77x10^{05}	0,733
cDCs/ml	8,60x10^{06} ± 5,95x10^{05}	9,91x10^{06} ± 8,03x10^{05}	0,148
pDCs/ml	2,59x10^{05} ± 4,05x10^{04}	2,89x10^{05} ± 3,37x10^{04}	0,687
Macrophages/ml	5,63x10^{05} ± 4,78x10^{04}	4,55x10^{05} ± 5,01x10^{04}	0,207

Supplemental table 8: Para-aortic lymph node leukocyte subpopulations of *Apoe*$^{-/-}$ and *Apoe*$^{-/-}$*Ccr4*$^{-/-}$ mice. Para-aortic lymph node leukocyte subsets were measured by flow cytometry. All values are displayed as mean ± SEM (n=9-10).

	Para-aortic Lymph Node		
12 weeks HFD	***Apoe*$^{-/-}$**	***Apoe*$^{-/-}$*Ccr4*$^{-/-}$**	**p-Value**
Leukocytes/ml	5,27x10^{06} ±7,72x10^{05}	3,22x10^{06} ± 7,34x10^{05}	0,072
Gr1$^+$ monocytes/ml	5,04x10^{03} ± 7,28x10^{02}	2,71x10^{03} ± 4,98x10^{02}	0,023
Gr1$^-$ monocytes/ml	1,23x10^{04} ± 2,11x10^{03}	1,03x10^{04} ± 1,76x10^{03}	0,467
B cells/ml	2,24x10^{06} ± 3,97x10^{05}	1,39x10^{06} ± 4,03x10^{05}	0,125
CD3$^+$ T cells/ml	1,57x10^{06} ± 1,57x10^{05}	1,20x10^{06} ± 1,86x10^{05}	0,085
CD4$^+$ T cells/ml	8,57x10^{05} ± 8,41x10^{04}	6,56x10^{05} ± 1,05x10^{05}	0,100
CD8$^+$ T cells/ml	4,81x10^{05} ± 8,41x10^{04}	3,48x10^{05} ± 5,31x10^{04}	0,060
cDCs/ml	2,04x10^{05} ± 2,00x10^{04}	1,52x10^{05} ± 2,46x10^{04}	0,039
pDCs/ml	7,76x10^{03} ± 9,06x10^{02}	8,34x10^{03} ± 2,52x10^{03}	0,882
Macrophages/ml	4,97x10^{03} ± 1,08x10^{03}	3,00x10^{03} ± 2,83x10^{02}	0,022

Supplemental table 9: Circulating leukocyte subpopulations of $Apoe^{-/-}$ ► $Apoe^{-/-}$ and $Apoe^{-/-}Ccr4^{-/-}$ ► $Apoe^{-/-}$ mice. Peripheral blood leukocyte subsets were measured by flow cytometry. All values are displayed as mean ± SEM (n=9-10).

12 weeks HFD	Blood		
	$Apoe^{-/-}$ ► $Apoe^{-/-}$	$Apoe^{-/-}Ccr4^{-/-}$ ► $Apoe^{-/-}$	p-Value
Leukocytes/ml	$4,02 \times 10^{06}$ ± $4,47 \times 10^{05}$	$4,30 \times 10^{06}$ ± $6,32 \times 10^{05}$	0,779
Gr1$^+$ monocytes/ml	$1,03 \times 10^{05}$ ± $2,44 \times 10^{04}$	$2,24 \times 10^{05}$ ± $1,48 \times 10^{04}$	0,002
Gr1$^-$ monocytes/ml	$1,06 \times 10^{05}$ ± $2,28 \times 10^{04}$	$1,41 \times 10^{05}$ ± $2,58 \times 10^{04}$	0,554
Neutrophils/ml	$3,17 \times 10^{05}$ ± $7,44 \times 10^{04}$	$5,83 \times 10^{05}$ ± $5,21 \times 10^{04}$	0,009
B cells/ml	$2,11 \times 10^{06}$ ± $2,13 \times 10^{05}$	$1,98 \times 10^{06}$ ± $3,43 \times 10^{05}$	0,697
CD3$^+$ T cells/ml	$2,63 \times 10^{05}$ ± $2,33 \times 10^{04}$	$1,06 \times 10^{05}$ ± $1,78 \times 10^{04}$	0,498
CD4$^+$ T cells/ml	$1,22 \times 10^{05}$ ± $1,15 \times 10^{04}$	$1,06 \times 10^{05}$ ± $1,78 \times 10^{04}$	0,508
CD8$^+$ T cells/ml	$1,19 \times 10^{05}$ ± $1,04 \times 10^{04}$	$1,03 \times 10^{05}$ ± $1,81 \times 10^{04}$	0,378
Platelets/ml	$6,69 \times 10^{05}$ ± $6,19 \times 10^{04}$	$4,89 \times 10^{05}$ ±$9,75 \times 10^{04}$	0,138

Supplemental table 10: Bone marrow leukocyte subpopulations of $Apoe^{-/-}$ ► $Apoe^{-/-}$ and $Apoe^{-/-}Ccr4^{-/-}$ ► $Apoe^{-/-}$ mice. Bone marrow leukocyte subsets were measured by flow cytometry. All values are displayed as mean ± SEM (n=9-10).

12 weeks HFD	Bone Marrow		
	$Apoe^{-/-}$ ► $Apoe^{-/-}$	$Apoe^{-/-}Ccr4^{-/-}$ ► $Apoe^{-/-}$	p-Value
Leukocytes/ml	$1,13 \times 10^{07}$ ± $4,66 \times 10^{05}$	$8,99 \times 10^{06}$ ± $1,14 \times 10^{06}$	0,072
Gr1$^+$ monocytes/ml	$5,49 \times 10^{05}$ ± $3,39 \times 10^{04}$	$6,28 \times 10^{05}$ ± $9,71 \times 10^{05}$	0,425
Gr1$^-$ monocytes/ml	$1,36 \times 10^{05}$ ± $7,56 \times 10^{03}$	$1,28 \times 10^{05}$ ± $2,17 \times 10^{04}$	0,704
Neutrophils/ml	$1,99 \times 10^{06}$ ± $3,01 \times 10^{05}$	$2,62 \times 10^{06}$ ± $4,36 \times 10^{05}$	0,010
B cells/ml	$9,09 \times 10^{05}$ ± $5,95 \times 10^{04}$	$7,05 \times 10^{05}$ ± $1,22 \times 10^{05}$	0,169
cDCs/ml	$1,50 \times 10^{05}$ ± $1,70 \times 10^{04}$	$1,92 \times 10^{05}$ ± $1,95 \times 10^{04}$	0,060
pDCs/ml	$2,77 \times 10^{05}$ ± $1,15 \times 10^{04}$	$2,58 \times 10^{05}$ ± $3,73 \times 10^{04}$	0,676
Macrophages/ml	$3,69 \times 10^{05}$ ± $4,57 \times 10^{04}$	$5,41 \times 10^{05}$ ± $5,43 \times 10^{04}$	0,030

Supplemental table 11: Splenic leukocyte subpopulations of *Apoe*$^{-/-}$ ► *Apoe*$^{-/-}$ and *Apoe*$^{-/-}$*Ccr4*$^{-/-}$ ► *Apoe*$^{-/-}$ mice. Splenic leukocyte subsets were measured by flow cytometry. All values are displayed as mean ± SEM (n=9-10).

12 weeks HFD	Spleen *Apoe*$^{-/-}$ ► *Apoe*$^{-/-}$	*Apoe*$^{-/-}$*Ccr4*$^{-/-}$ ► *Apoe*$^{-/-}$	p-Value
Leukocytes/ml	$9{,}34 \times 10^{07}$ ± $5{,}98 \times 10^{06}$	$7{,}77 \times 10^{07}$ ± $5{,}04 \times 10^{04}$	0,082
Gr1$^+$ monocytes/ml	$4{,}10 \times 10^{05}$ ± $4{,}95 \times 10^{04}$	$3{,}52 \times 10^{05}$ ± $5{,}04 \times 10^{04}$	0,355
Gr1$^-$ monocytes/ml	$1{,}98 \times 10^{06}$ ± $1{,}23 \times 10^{04}$	$1{,}04 \times 10^{06}$ ± $3{,}01 \times 10^{04}$	0,015
Neutrophils/ml	$8{,}18 \times 10^{05}$ ± $1{,}25 \times 10^{05}$	$9{,}41 \times 10^{05}$ ± $1{,}12 \times 10^{05}$	0,569
B cells/ml	$3{,}38 \times 10^{07}$ ± $4{,}18 \times 10^{06}$	$2{,}43 \times 10^{07}$ ± $2{,}71 \times 10^{06}$	0,067
CD3$^+$ T cells/ml	$1{,}46 \times 10^{07}$ ± $7{,}56 \times 10^{05}$	$9{,}23 \times 10^{06}$ ± $1{,}81 \times 10^{06}$	0,017
CD4$^+$ T cells/ml	$9{,}95 \times 10^{06}$ ± $5{,}39 \times 10^{05}$	$6{,}33 \times 10^{06}$ ± $1{,}13 \times 10^{06}$	0,015
CD8$^+$ T cells/ml	$3{,}69 \times 10^{06}$ ± $1{,}90 \times 10^{05}$	$1{,}94 \times 10^{06}$ ± $4{,}47 \times 10^{05}$	0,005
cDCs/ml	$8{,}73 \times 10^{06}$ ± $6{,}95 \times 10^{05}$	$8{,}18 \times 10^{06}$ ± $6{,}36 \times 10^{05}$	0,472
pDCs/ml	$1{,}48 \times 10^{05}$ ± $2{,}11 \times 10^{04}$	$1{,}02 \times 10^{05}$ ± $1{,}65 \times 10^{04}$	0,16
Macrophages/ml	$1{,}55 \times 10^{06}$ ± $1{,}23 \times 10^{05}$	$1{,}03 \times 10^{06}$ ± $2{,}93 \times 10^{04}$	0,128

Supplemental table 12: Para aortic lymph node leukocyte subpopulations of _Apoe_^{-/-} ► _Apoe_^{-/-} and _Apoe_^{-/-}_Ccr4_^{-/-} ► _Apoe_^{-/-} mice. Para aortic lymph node leukocyte subsets were measured by flow cytometry. All values are displayed as mean ± SEM (n=9-10).

12 weeks HFD	_Apoe_$^{-/-}$ ► _Apoe_$^{-/-}$	_Apoe_$^{-/-}$_Ccr4_$^{-/-}$ ► _Apoe_$^{-/-}$	p-Value
	Para-aortic Lymph Node		
Leukocytes/ml	$1{,}42 \times 10^{06}$ ± $3{,}28 \times 10^{05}$	$2{,}24 \times 10^{06}$ ± $2{,}97 \times 10^{05}$	0,060
Gr1$^+$ monocytes/ml	$1{,}49 \times 10^{03}$ ± $4{,}71 \times 10^{02}$	$3{,}13 \times 10^{03}$ ± $1{,}93 \times 10^{02}$	0,027
Gr1$^-$ monocytes/ml	$9{,}35 \times 10^{04}$ ± $2{,}38 \times 10^{03}$	$1{,}94 \times 10^{05}$ ± $1{,}02 \times 10^{04}$	0,004
B cells/ml	$1{,}95 \times 10^{05}$ ± $1{,}57 \times 10^{05}$	$5{,}36 \times 10^{05}$ ± $4{,}15 \times 10^{04}$	0,053
CD3$^+$ T cells/ml	$3{,}27 \times 10^{05}$ ± $6{,}47 \times 10^{04}$	$4{,}56 \times 10^{05}$ ± $8{,}85 \times 10^{04}$	0,191
CD4$^+$ T cells/ml	$2{,}42 \times 10^{05}$ ± $4{,}79 \times 10^{04}$	$3{,}43 \times 10^{05}$ ± $6{,}76 \times 10^{04}$	0,181
CD8$^+$ T cells/ml	$7{,}03 \times 10^{04}$ ± $1{,}50 \times 10^{04}$	$8{,}35 \times 10^{04}$ ± $1{,}79 \times 10^{04}$	0,488
cDCs/ml	$9{,}10 \times 10^{04}$ ± $4{,}93 \times 10^{04}$	$2{,}42 \times 10^{05}$ ± $2{,}03 \times 10^{04}$	0,012
pDCs/ml	$1{,}62 \times 10^{03}$ ± $6{,}19 \times 10^{02}$	$2{,}93 \times 10^{03}$ ± $4{,}60 \times 10^{02}$	0,082
Macrophages/ml	$2{,}52 \times 10^{03}$ ± $1{,}31 \times 10^{03}$	$5{,}44 \times 10^{03}$ ± $7{,}15 \times 10^{02}$	0,070

Supplemental table 13: Circulating leukocyte subpopulations of *Apoe*⁻ᐟ⁻ and *Apoe*⁻ᐟ⁻*Ccl3*⁻ᐟ⁻ mice.
Peripheral blood leukocyte subsets were measured by flow cytometry. All values are displayed as mean ± SEM (n=8-10).

Blood			
12 weeks HFD	***Apoe*⁻ᐟ⁻**	***Apoe*⁻ᐟ⁻*Ccl3*⁻ᐟ⁻**	**p-Value**
Leukocytes/ml	$1{,}64 \times 10^{06}$ $\pm 1{,}34 \times 10^{05}$	$1{,}92 \times 10^{06}$ $\pm 2{,}94 \times 10^{05}$	0,3,64
Gr1⁺ monocytes/ml	$9{,}54 \times 10^{04}$ $\pm 1{,}40 \times 10^{04}$	$1{,}25 \times 10^{05}$ $\pm 2{,}00 \times 10^{04}$	0,233
Gr1⁻ monocytes/ml	$3{,}97 \times 10^{04}$ $\pm 4{,}44 \times 10^{03}$	$5{,}97 \times 10^{04}$ $\pm 1{,}08 \times 10^{04}$	0,083
Neutrophils/ml	$3{,}96 \times 10^{05}$ $\pm 4{,}98 \times 10^{04}$	$3{,}94 \times 10^{05}$ $\pm 6{,}27 \times 10^{04}$	0,981
B cells/ml	$6{,}41 \times 10^{05}$ $\pm 8{,}76 \times 10^{04}$	$8{,}00 \times 10^{05}$ $\pm 1{,}20 \times 10^{05}$	0,291
CD3⁺ T cells/ml	$1{,}38 \times 10^{05}$ $\pm 1{,}25 \times 10^{04}$	$1{,}36 \times 10^{05}$ $\pm 2{,}18 \times 10^{04}$	0,936
CD4+ T cells/ml	$7{,}35 \times 10^{04}$ $\pm 7{,}72 \times 10^{03}$	$7{,}38 \times 10^{04}$ $\pm 1{,}19 \times 10^{04}$	0,986
CD8+ T cells/ml	$4{,}05 \times 10^{04}$ $\pm 4{,}43 \times 10^{03}$	$3{,}50 \times 10^{04}$ $\pm 5{,}14 \times 10^{03}$	0,426
Platelets/ml	$9{,}81 \times 10^{05}$ $\pm 1{,}35 \times 10^{05}$	$9{,}63 \times 10^{05}$ $\pm 5{,}65 \times 10^{04}$	0,911

Supplemental table 14: Bone marrow leukocyte subpopulations of *Apoe*⁻ᐟ⁻ and *Apoe*⁻ᐟ⁻*Ccl3*⁻ᐟ⁻ mice.
Bone marrow leukocyte subsets were measured by flow cytometry. All values are displayed as mean ± SEM (n=8-10).

Bone Marrow			
12 weeks HFD	***Apoe*⁻ᐟ⁻**	***Apoe*⁻ᐟ⁻*Ccl3*⁻ᐟ⁻**	**p-Value**
Leukocytes/ml	$5{,}54 \times 10^{06}$ $\pm 1{,}83 \times 10^{06}$	$8{,}20 \times 10^{06}$ $\pm 7{,}98 \times 10^{05}$	0,227
Gr1⁺ monocytes/ml	$4{,}76 \times 10^{05}$ $\pm 1{,}84 \times 10^{05}$	$7{,}26 \times 10^{05}$ $\pm 7{,}40 \times 10^{04}$	0,267
Gr1⁻ monocytes/ml	$7{,}14 \times 10^{04}$ $\pm 8{,}62 \times 10^{03}$	$9{,}45 \times 10^{04}$ $\pm 6{,}91 \times 10^{03}$	0,062
Neutrophils/ml	$1{,}99 \times 10^{06}$ $\pm 1{,}05 \times 10^{06}$	$3{,}27 \times 10^{06}$ $\pm 7{,}36 \times 10^{05}$	0,308
B cells/ml	$8{,}58 \times 10^{05}$ $\pm 9{,}53 \times 10^{04}$	$7{,}36 \times 10^{05}$ $\pm 1{,}49 \times 10^{05}$	0,485
cDCs/ml	$2{,}32 \times 10^{05}$ $\pm 2{,}06 \times 10^{04}$	$2{,}91 \times 10^{05}$ $\pm 2{,}20 \times 10^{04}$	0,072
pDCs/ml	$2{,}42 \times 10^{05}$ $\pm 1{,}92 \times 10^{04}$	$2{,}92 \times 10^{05}$ $\pm 3{,}61 \times 10^{04}$	0,213
Macrophages/ml	$1{,}96 \times 10^{05}$ $\pm 1{,}51 \times 10^{04}$	$2{,}31 \times 10^{05}$ $\pm 2{,}34 \times 10^{04}$	0,211

Supplemental table 15: Splenic leukocyte subpopulations of *Apoe*$^{-/-}$ and *Apoe*$^{-/-}$*Ccl3*$^{-/-}$ mice. Splenic leukocyte subsets were measured by flow cytometry. All values are displayed as mean ± SEM (n=8-10).

Spleen			
12 weeks HFD	*Apoe*$^{-/-}$	*Apoe*$^{-/-}$*Ccl3*$^{-/-}$	p-Value
Leukocytes/ml	6,211x10^{07} ± 4,00x10^{06}	5,01x10^{07} ± 3,91x10^{06}	0,052
Gr1$^+$ monocytes/ml	1,18x10^{06} ± 4,16x10^{05}	4,60x10^{05} ± 2,63x10^{05}	0,147
Gr1$^-$ monocytes/ml	3,08x10^{05} ± 6,85x10^{04}	1,55x10^{05} ± 1,82x10^{04}	0,064
Neutrophils/ml	4,04x10^{06} ± 2,22x10^{06}	1,20x10^{06} ± 8,55x10^{05}	0,272
B cells/ml	2,10x10^{07} ± 1,54x10^{06}	1,75x10^{07} ± 1,76x10^{06}	0,144
CD3$^+$ T cells/ml	1,03x10^{07} ± 1,84x10^{06}	7,98x10^{06} ± 8,63x10^{05}	0,303
CD4$^+$ T cells/ml	8,76x10^{06} ± 6,61x10^{05}	6,57x10^{06} ± 7,44x10^{05}	0,049
CD8$^+$ T cells/ml	2,23x10^{06} ± 2,49x10^{05}	1,70x10^{06} ± 1,23x10^{05}	0,088
cDCs/ml	6,59x10^{04} ± 5,38x10^{03}	7,60x10^{04} ± 1,35x10^{04}	0,462
pDCs/ml	6,56x10^{03} ± 4,95x10^{02}	8,15x10^{03} ± 1,32x10^{03}	0,244
Macrophages/ml	2,33x10^{04} ± 2,12x10^{04}	4,87x10^{04} ± 1,48x10^{04}	0,072

All values are displayed as mean ± SEM and P-value (n= 8-10).

Supplemental table 16: Para-aortic lymph node leukocyte subpopulations of *Apoe*$^{-/-}$ and *Apoe*$^{-/-}$*Ccl3*$^{-/-}$ mice. Para-aortic lymph node leukocyte subsets were measured by flow cytometry. All values are displayed as mean ± SEM (n=8-10).

para-aortic Lymph Node			
12 weeks HFD	*Apoe*$^{-/-}$	*Apoe*$^{-/-}$*Ccl3*$^{-/-}$	p-Value
Leukocytes/ml	2,81x10^{06} ± 8,78x10^{05}	1,68x10^{06} ± 5,31x10^{05}	0,317
Gr1$^+$ monocytes/ml	6,41x10^{03} ± 2,04x10^{03}	5,88x10^{03} ± 2,07x10^{03}	0,859
Gr1$^-$ monocytes/ml	6,21x10^{03} ± 2,37x10^{03}	1,03x10^{03} ± 1,51x10^{02}	0,07
B cells/ml	1,35x10^{06} ± 5,24x10^{05}	6,41x10^{05} ± 1,97x10^{05}	0,267
CD3$^+$ T cells/ml	5,81x10^{05} ± 1,41x10^{05}	4,99x10^{05} ± 1,91x10^{05}	0,731
CD4$^+$ T cells/ml	4,70x10^{05} ± 1,14x10^{05}	3,46x10^{05} ± 1,12x10^{05}	0,457
CD8$^+$ T cells/ml	3,60x10^{05} ± 5,92x10^{04}	2,85x10^{05} ± 5,66x10^{04}	0,381
cDCs/ml	4,93x10^{05} ± 2,58x10^{05}	2,25x10^{04} ±4,78x10^{04}	0,374
pDCs/ml	2,91x10^{04} ± 2,27x10^{05}	1,27x10^{05} ± 3,60x10^{04}	0,363

All values are displayed as mean ± SEM and P-value (n= 8-10).

Supplemental table 17: Circulating leukocyte subpopulations of *Apoe*^{-/-} and *Apoe*^{-/-}*Ccr1*^{-/-} mice.
Peripheral blood leukocyte subsets were measured by flow cytometry. All values are displayed as mean ± SEM (n=5-10).

12 weeks HFD	Blood		
	Apoe^{-/-}	*Apoe*^{-/-}*Ccr1*^{-/-}	p-Value
Leukocytes/ml	$1{,}68 \times 10^{06}$ ± $1{,}48 \times 10^{05}$	$2{,}02 \times 10^{06}$ ± $5{,}25 \times 10^{05}$	0,474
Gr1+ monocytes/ml	$1{,}06 \times 10^{05}$ ± $1{,}16 \times 10^{04}$	$1{,}32 \times 10^{05}$ ± $3{,}09 \times 10^{04}$	0,369
Gr1- monocytes/ml	$1{,}46 \times 10^{06}$ ± $2{,}48 \times 10^{05}$	$2{,}02 \times 10^{06}$ ± $5{,}25 \times 10^{05}$	0,208
Neutrophils/ml	$4{,}94 \times 10^{05}$ ± $1{,}11 \times 10^{05}$	$7{,}28 \times 10^{05}$ ± $1{,}92 \times 10^{05}$	0,279
B cells/ml	$6{,}15 \times 10^{05}$ ± $7{,}54 \times 10^{04}$	$6{,}86 \times 10^{05}$ ± $1{,}94 \times 10^{05}$	0,698
CD3+ T cells/ml	$8{,}36 \times 10^{04}$ ± $1{,}33 \times 10^{04}$	$6{,}65 \times 10^{04}$ ± $2{,}65 \times 10^{04}$	0,534
CD4+ T cells/ml	$4{,}79 \times 10^{04}$ ± $8{,}69 \times 10^{03}$	$3{,}91 \times 10^{04}$ ± $1{,}66 \times 10^{04}$	0,614
CD8+ T cells/ml	$1{,}83 \times 10^{04}$ ± $3{,}54 \times 10^{03}$	$1{,}70 \times 10^{04}$ ± $7{,}30 \times 10^{03}$	0,858
Platelets/ml	$1{,}16 \times 10^{06}$ ± $1{,}36 \times 10^{05}$	$8{,}90 \times 10^{05}$ ± $1{,}23 \times 10^{05}$	0,295

Supplemental table 18: Bone marrow leukocyte subpopulations of *Apoe*^{-/-} and *Apoe*^{-/-}*Ccr1*^{-/-} mice.
Bone marrow leukocyte subsets were measured by flow cytometry. All values are displayed as mean ± SEM (n=5-10).

12 weeks HFD	Bone Marrow		
	Apoe^{-/-}	*Apoe*^{-/-}*Ccr1*^{-/-}	p-Value
Leukocytes/ml	$4{,}91 \times 10^{06}$ ± $1{,}53 \times 10^{06}$	$1{,}13 \times 10^{07}$ ± $2{,}91 \times 10^{06}$	0,002
Gr1+ monocytes/ml	$4{,}68 \times 10^{05}$ ± $1{,}51 \times 10^{05}$	$1{,}45 \times 10^{06}$ ± $3{,}78 \times 10^{05}$	0,001
Gr1- monocytes/ml	$2{,}58 \times 10^{06}$ ± $4{,}33 \times 10^{04}$	$6{,}56 \times 10^{06}$ ± $7{,}66 \times 10^{04}$	0,001
Neutrophils/ml	$2{,}11 \times 10^{06}$ ± $6{,}41 \times 10^{05}$	$3{,}55 \times 10^{06}$ ± $1{,}48 \times 10^{06}$	0,001
B cells/ml	$1{,}11 \times 10^{06}$ ± $3{,}20 \times 10^{05}$	$1{,}34 \times 10^{06}$ ± $1{,}97 \times 10^{05}$	0,606
cDCs/ml	$1{,}24 \times 10^{05}$ ± $3{,}06 \times 10^{04}$	$3{,}29 \times 10^{05}$ ± $3{,}27 \times 10^{04}$	0,002
pDCs/ml	$3{,}15 \times 10^{05}$ ± $6{,}27 \times 10^{04}$	$2{,}92 \times 10^{05}$ ± $3{,}96 \times 10^{04}$	0,789
Macrophages/ml	$7{,}37 \times 10^{04}$ ± $1{,}10 \times 10^{04}$	$1{,}83 \times 10^{05}$ ± $1{,}75 \times 10^{04}$	0,001

Supplemental table 19: Splenic leukocyte subpopulations of *Apoe$^{-/-}$* and *Apoe$^{-/-}$Ccr1$^{-/-}$* mice. Splenic leukocyte subsets were measured by flow cytometry. All values are displayed as mean ± SEM (n=5-10).

12 weeks HFD	Spleen *Apoe$^{-/-}$*	*Apoe$^{-/-}$Ccr1$^{-/-}$*	p-Value
Leukocytes/ml	5,26x10^{07} ± 7,09x10^{06}	6,81x10^{07} ± 6,26x10^{06}	0,161
Gr1$^+$ monocytes/ml	1,33x10^{06} ± 3,54x10^{05}	1,79x10^{06} ± 2,44x10^{05}	0,370
Gr1$^-$ monocytes/ml	1,41x10^{06} ± 3,82x10^{05}	1,19x10^{06} ± 1,81x10^{05}	0,672
Neutrophils/ml	3,32x10^{06} ± 1,01x10^{06}	4,09x10^{06} ± 1,10x10^{06}	0,627
B cells/ml	9,57x10^{06} ± 1,48x10^{06}	1,07x10^{07} ± 1,17x10^{06}	0,078
CD3$^+$ T cells/ml	5,940x10^{06} ± 1,48x10^{06}	1,07x10^{07} ± 1,17x10^{06}	0,589
CD4$^+$ T cells/ml	5,94x10^{06} ± 8,92x10^{05}	6,84x10^{06} ± 8,44x10^{05}	0,510
CD8$^+$ T cells/ml	1,36x10^{06} ± 1,98x10^{05}	1,52x10^{06} ± 1,96x10^{05}	0,611
cDCs/ml	3,84x10^{06} ± 9,79x10^{05}	3,06x10^{06} ± 5,33x10^{05}	0,563
pDCs/ml	5,41x10^{05} ± 9,77x10^{04}	6,98x10^{05} ± 1,61x10^{05}	0,392
Macrophages/ml	1,76x10^{05} ± 4,09x10^{04}	1,31x10^{05} ± 2,39x10^{04}	0,442

Supplemental table 20: Para-aortic lymph node leukocyte subpopulations of *Apoe$^{-/-}$* and *Apoe$^{-/-}$Ccr1$^{-/-}$* mice. Para-aortic lymph node leukocyte subsets were measured by flow cytometry. All values are displayed as mean ± SEM (n=5-10).

12 weeks HFD	para-aortic Lymph Node *Apoe$^{-/-}$*	*Apoe$^{-/-}$Ccr1$^{-/-}$*	p-Value
Leukocytes/ml	1,18x10^{06} ± 3,47x10^{05}	3,42x10^{06} ± 1,01x10^{06}	0,092
Gr1$^+$ monocytes/ml	9,95x10^{03} ± 2,51x10^{03}	1,97x10^{04} ± 5,93x10^{03}	0,019
Gr1$^-$ monocytes/ml	2,26x10^{03} ± 8,72x10^{02}	4,95x10^{04} ± 1,57x10^{04}	0,079
B cells/ml	5,28x10^{05} ± 1,80x10^{05}	1,83x10^{06} ± 5,47x10^{05}	0,066
CD3$^+$ T cells/ml	3,01x10^{05} ± 6,73x10^{04}	6,30x10^{05} ± 2,03x10^{05}	0,119
CD4$^+$ T cells/ml	2,4x10^{05} ± 4,86x10^{04}	4,37x10^{05} ± 1,51x10^{05}	0,118
CD8$^+$ T cells/ml	7,76x10^{04} ± 1,69x10^{04}	1,42x10^{05} ± 4,48x10^{04}	0,141
cDCs/ml	6,02x10^{04} ± 1,29x10^{04}	8,82x10^{04} ± 2,25x10^{04}	0,265
pDCs/ml	5,05x10^{03} ± 1,18x10^{03}	1,10x10^{04} ± 3,42x10^{03}	0,190

9. Acknowledgements

Herrn Prof. Dr. Christian Weber möchte ich besonders für die Möglichkeit danken an seinem Institut promovieren zu dürfen. Ich bedanke mich für die Finanzierung meiner Doktorarbeit, die wissenschaftliche Unterstützung, die erstklassige Laborausstattung und die schönen Institutsausflüge sowie Oktoberfestbesuche.

Prof. Dr. Jürgen Bernhagen danke ich an dieser Stelle für die Übernahme der Zweitkorrektur dieser Arbeit und für die anregenden Diskussionen während meiner TAC Meetings. Prof. Dr. Anne Krug möchte ich ebenfalls für die Teilnahme an meinem TAC Meetings danken.

Ich danke den Sonderforschungsbereichen 1054 und 1123, sowie dem Deutschem Zentrum für Herz-Kreislauf-Forschung eV., durch welche diese Dissertation finanziell unterstützt wurde und dank derer es mir möglich war an wissenschaftlichen Kongressen und an Veranstaltungen der IRTG teilzunehmen.

Ganz besonders bedanken möchte ich mich bei Dr. Yvonne Döring für die Betreuung meiner Doktorarbeit, den konstruktiven wissenschaftlichen Austausch und für die Möglichkeit auch eigene Ideen verwirklichen zu können. Danke Yvonne, dass du dir immer Zeit für mich genommen hast und mir gegenüber immer Geduld bewiesen hast. Danke dass du mich frei hast arbeiten lassen, aber mich nie allein gelassen hast. Neben deiner hervorragenden wissenschaftlichen Betreuung waren es auch die spontanen Gespräche in den Kaffeepausen, die ich sehr schätzte. Danke für dein mir entgegengebrachtes Vertrauen.

Des Weiteren möchte ich mich bei Yvonne Jansen für die hervorragende Unterstützung und Betreuung im Labor bedanken. Yvonne, mit deiner ruhigen und besonnenen Art hast du mir stets beigestanden und mich tatkräftig bei meinen Experimenten unterstützt (besonders wenn es um die MAC2 Auswertung ging – entschuldige dafür ☺). Danke für deine Geduld, für die zahlreichen Überstunden und für die Methoden, Tipps und Tricks im Labor, die du mir beigebracht hast. Einen besonderen Dank auch für deine Freundschaft in den letzten vier Jahren.

Ganz besonders möchte ich mich auch bei meiner Kollegin und Mitstreiterin Manuela Mandl bedanken. Du hast dich während meiner Anfangszeit und darüber hinaus hervorragend um mich gekümmert und mich bestens in das Team integriert. Ich konnte während unserer gesamten gemeinsamen Zeit immer auf dich bauen und mich auf dich

10.   Publications

Publications

2018   **Neideck C**, van der Vorst E, Mandl M, Jansen Y , Blanchet X, Faussner A, Megens RT, Drechsler M, Weber C, Döring Y. "**Ccl17-dependent release of Ccl3 restrains regulatory T cells thereby aggravating atherosclerosis.**" *(in preparation)*

2018   Osório L, Wu X, **Neideck C**, Sheng G, Zhou Z. (2018) **"ISM1 inhibits NODAL signaling by compromising NODAL-ACVR1 interaction."** Journal of Cell Biology (*under review*).

2017   Döring Y*, Noels H*, van der Vorst E[#], **Neideck C[#],** Egea V, Drechsler M, Mandl M, Pawig L, Jansen Y, Schröder K, Bidzhekov K, Megens R, Theelen W , Klinkhammer B, Boor P, Schurgers L, van Gorp R, Ries C, Kusters P , van der Wal A, Hackeng TM, Gäbel G, Brandes R, Soehnlein O, Lutgens E, Vestweber D, Teupser D, Holdt L, Rader D, Saleheen D, Weber C. (2017) **"Vascular CXCR4 limits atherosclerosis by maintaining vascular integrity."** *Circulation 136(4):388-403.*
*,[#] denotes equal contribution

2017   von Hundelshausen P, Agten S*, Eckardt V*, Schmitt M*, Blanchet X*, Ippel H*, **Neideck C***, Bidzhekov K*, Wichapong K*, Faussner A, Drechsler M, Grommes J, van Geffen J, Li H, Leberzammer J, Naumann R, Dijkgraaf I, Nicolaes G, Döring Y, Soehnlein O, Lutgens E, Heemskerk J, Koenen R, Mayo K, Hackeng T, Weber C. (2017) **"Chemokine interactome mapping enables tailored intervention in acute and chronic inflammation."** *Science Translational Medicine* 9(384):eaah6650.
* denotes equal contribution

2016   Viola JR, Lemnitzer P, Jansen Y, Csaba G, Winter C, **Neideck C**, Silvestre-Roig C, Dittmar G, Döring Y, Drechsler M, Weber C, Zimmer R, Cenac N, Soehnlein O. (2016). **"Resolving Lipid Mediators Maresin 1 and Resolvin D2 Prevent Atheroprogression in Mice."** *Circulation Research* 119(9):1030-1038.

2015   Mandl M, Drechsler M, Jansen Y, **Neideck C**, Noels H, Faussner A, Soehnlein O, Weber C, Döring Y. (2015). **"Evaluation of the BDCA2-DTR Transgenic Mouse Model in Chronic and Acute Inflammation."** *PLoS One* 10(8):e0134176

2014 | Döring Y, Noels H, Mandl M, Kramp B, **Neideck C**, Lievens D, Drechsler M, Megens RT, Tilstam PV, Langer M, Hartwig H, Theelen W, Marth JD, Sperandio M, Soehnlein O, Weber C. (2014). **"Deficiency of the sialyltransferase St3Gal4 reduces Ccl5-mediated myeloid cell recruitment and arrest: short communication."** *Circulation Research* 114(6):976-81.